

Inaugural dissertation

submitted to

the Combined Faculty of Natural Sciences and Mathematics

of the Ruperto Carola University Heidelberg, Germany

for the degree

of Doctor of Natural Sciences

Presented by

Ombretta Colasanti (M.Sc.)

born in Bari, Italy

Oral examination: 16/10/2023

**Exploring innate immune induction and interference
mechanisms of Hepatitis A and C Viruses in human
hepatocytes: a comparative analysis**

Referees: Prof. Dr. Ralf Bartenschlager

Prof. Dr. Volker Lohmann

Declaration

The applicant, Ombretta Colasanti, declares that she is the sole author of the submitted dissertation and no other sources for help apart from those specifically referred to have been used. Additionally, the applicant declares that he has not applied for permission to enter the examination procedure at another institution, that this dissertation has not been presented to other faculty and has not been used in its current or in any other form in another examination.

Date

Ombretta Colasanti

Signature

Table of Contents

| | |
|--|----|
| Declaration | 5 |
| Summary..... | 11 |
| Zusammenfassung | 13 |
| List of figures | 15 |
| List of tables..... | 19 |
| Abbreviations..... | 20 |
| Introduction | 25 |
| 1.1 <i>The human liver</i> | 25 |
| 1.2 <i>Immune responses in the liver</i> | 27 |
| 1.3 <i>Hepatitis and viral hepatitis</i> | 31 |
| 1.4 <i>Innate immunity within the hepatocytes: from Pattern Recognition Receptors...</i> | 32 |
| 1.5 <i>...to IFN signaling and induction of ISGs</i> | 39 |
| 1.6 <i>Hepatitis C Virus (HCV)</i> | 43 |
| 1.7 <i>Hepatitis A Virus (HAV)</i> | 48 |
| 1.8 <i>HCV and immunity</i> | 54 |
| 1.9 <i>HAV and immunity</i> | 59 |
| 1.10 <i>Models to study HCV and HAV replication</i> | 61 |
| 1.11 <i>Comparison of immune responses by HAV and HCV</i> | 67 |
| <i>Aims of the thesis</i> | 71 |
| Materials..... | 72 |
| <i>Reagents and other products</i> | 72 |
| <i>Buffers and solutions</i> | 74 |
| <i>Kits</i> | 75 |
| <i>Cell lines used in this study</i> | 75 |
| <i>Bacteria</i> | 77 |
| <i>Culture media</i> | 77 |
| Bacterial culture media | 77 |
| Cell line culture media..... | 77 |
| <i>Viruses</i> | 77 |
| <i>Primary antibodies</i> | 79 |
| <i>Secondary antibodies</i> | 80 |
| <i>Chimeric mice</i> | 81 |
| <i>Infection of chimeric mice</i> | 81 |

| | |
|--|-------------------------------------|
| <i>Plasmid vectors</i> | Error! Bookmark not defined. |
| Standard vectors..... | Error! Bookmark not defined. |
| <i>Plasmid constructs</i> | 84 |
| <i>Oligonucleotides used for plasmid cloning</i> | 85 |
| Table 15. Cloning oligonucleotides used in this study. | 86 |
| <i>Oligonucleotides and probes used for qPCR</i> | 86 |
| Table 16. qPCR oligos used in this study. | 87 |
| Table 17. qPCR probes used in this study. | 88 |
| <i>Instruments</i> | 88 |
| Table 17. Instruments used in this study. | 88 |
| <i>Enzymes</i> | 89 |
| <i>Software</i> | 89 |
| <i>Other (e.g. drugs, proteins, etc.)</i> | 90 |
| Methods | 91 |
| <i>Handling, culturing and storing cells</i> | 91 |
| Production of Lentiviral Vectors and Selection of Stable Cell Lines | 92 |
| DNA transfection..... | 92 |
| Infection of cells | 93 |
| Immunostimulation..... | 94 |
| Immunostimulation of infected cells | 94 |
| Cell Viability Assay..... | 95 |
| Protease inhibitor treatment | 95 |
| <i>Manipulation of DNA and RNA</i> | 96 |
| Plasmid Constructs..... | 96 |
| Bacterial transformation | 97 |
| DNA extraction from bacteria | 98 |
| Polymerase Chain Reaction (PCR) | 98 |
| Agarose gel separation..... | 99 |
| DNA endonuclease digestion | 99 |
| In vitro transcription and virus stock production..... | 100 |
| <i>Analytical procedures</i> | 102 |
| HAV purification from stool samples | 102 |
| RNA Extraction from livers of uPA-SCID mice with humanized liver..... | 102 |
| Immunofluorescence analysis and microscopy..... | 102 |
| FACS analysis | 103 |
| Quantitative Real-Time PCR (RT-qPCR) | 104 |
| Immunoblotting | 105 |
| Statistics | 106 |
| TRIF protein structures predictions..... | 106 |
| 4. Results | 107 |
| 4.1 <i>Potential role of TLR3 in HAV and HCV infections</i> | 107 |
| 4.2 <i>Impact of TRIF cleavage on innate immune induction</i> | 122 |
| 4.3 <i>Enhancing the robustness: investigating the interplay of HAV and HCV infections</i> | 137 |
| 4.4 <i>Impact of MAVS cleavage on innate immune induction</i> | 141 |
| 4.5 <i>Redefining the model: immunocompetence and permissiveness in vitro</i> | 154 |

| | | |
|-----|--|-------------------------------------|
| 4.6 | <i>Moving the perspective towards a small in vivo model : Alb/uPa SCID mice with humanized livers</i> | 170 |
| 5. | Discussion | 180 |
| 5.1 | <i>Potential role of TLR3 in HAV and HCV infections</i> | 180 |
| 5.2 | <i>Enhancing the robustness: investigating RLRs upon HAV and HCV infections</i> | 186 |
| 5.3 | <i>HAV induces ISGs in vitro in immunocompetent cell culture models</i> | 188 |
| 5.4 | <i>Innate immune responses in vivo upon HAV or HCV have a comparable breadth</i> | 192 |
| 5.5 | <i>Future directions</i> | 197 |
| | Appendix..... | 201 |
| | Supervised projects | 201 |
| 1. | <i>Validation of a CRISPR-Cas9 KO library for potential TLR3 interactors</i> | 201 |
| 2. | <i>Identification of RBM39 as a novel factor contributing to TLR3 signaling</i> | 202 |
| 3. | <i>Impact of HAV 3C proteolytical cleavage of NEMO on the innate immune response in human hepatocytes</i> | 203 |
| 4. | <i>The contribution of IRF3 to innate immune response in human hepatocytes</i> | 204 |
| | Side projects | 205 |
| 1) | <i>Secretion of HCV replication intermediates reduces activation of Toll-Like Receptor 3 in Hepatocytes</i> | 205 |
| 2) | <i>Biochemical and structural characterization of Hepatitis A Virus 2C reveals an unusual ribonuclease activity on single-stranded RNA</i> | 206 |
| 3) | <i>Extrahepatic sites of HAV replication</i> | 207 |
| | Acknowledgements | Error! Bookmark not defined. |
| | Publications | 210 |
| | Contributions to conferences | 211 |

Summary

This dissertation focuses on the host innate immune response in the context of hepatitis A virus (HAV) and hepatitis C virus (HCV) infections in human hepatocytes.

Innate immunity is the body's first line of defense against invading pathogens, functioning via a network of cells and molecules that quickly respond to infections. Central to this response are pattern recognition receptors (PRRs), which recognize pathogen-associated molecular patterns (PAMPs) and trigger the production of Interferons (IFNs) and the expression of Interferon-Stimulated Genes (ISGs), critical to antiviral defenses. In the case of viral infections like HAV and HCV, the host's immune response plays a pivotal role in disease outcome, and these viruses, in turn, have developed strategies to evade and manipulate the immune system. Thus, the interplay between viruses and the host's immune response is a key aspect of viral pathogenesis.

HAV and HCV are both positive-strand RNA (+ssRNA) hepatotropic viruses with a strict human tropism. Despite sharing a number of similarities in terms of genome structure and replication, they have unique characteristics and induce different immune responses, with HAV being cleared and HCV establishing chronic infections in >70% of the cases, making them intriguing subjects for comparative studies.

Notably, the only comparative *in vivo* study conducted on HAV and HCV-infected chimpanzees revealed that HAV, albeit replicating to a higher degree than HCV, barely elicited an innate immune response, as opposed to that solidly mounted upon HCV infection. This was attributed to a potent counteractive activity by the HAV protease 3C, and their precursors 3CD and 3ABC, towards the PRRs pathways. Therefore, I aimed at elucidating how HAV and HCV triggered, and counteracted, the intrinsic immune response in the liver, potentially associating these mechanisms to their strikingly different infection outcomes.

To this aim, I employed relevant cell culture models to examine the efficiency with which HAV and HCV were sensed by endoplasmic Toll-Like-Receptor 3 (TLR3) and the cytoplasmic Rig-I-Like-Receptors (RLRs). I furthermore quantified the proteolytical cleavage of the TLR3 adaptor TIR-domain-containing adapter-inducing interferon- β (TRIF) and the RLR adaptor Mitochondrial Antiviral-Signaling protein (MAVS) via transient and stable expression of the

respective viral proteases. My results indicated that both HAV and HCV infections induced similar levels of ISGs and IFNs in human hepatocytes, signaling the activation of innate immunity. HAV sensing primarily involved Melanoma Differentiation-Associated protein 5 (MDA5) and Laboratory of Genetics and Physiology 2 (LGP2), with limited interference to MAVS and to TRIF by the HAV proteases 3ABC and 3CD. In contrast, HCV sensing by Retinoic acid-Inducible Gene I (RIG-I) and MDA5 was entirely blocked by the efficient cleavage of the RLRs adaptor protein MAVS, leading to the activation of TLR3 as the primary source of ISG response for HCV. TRIF, the adaptor protein for TLR3, was not cleaved by HCV NS3-4A, contrary to previous reports. In addition, my research found that Huh7 cells were found to be defective on the MDA5-LGP2 axis.

My approach then shifted to an *in vivo* examination of SCID Alb-uPA humanized mice infected with patient-derived as well as cell culture adapted HAV and HCV, where I observed that both HAV and HCV triggered ISGs to similar extents, confirming the results obtained *in vitro*.

Overall, my results suggest that while HCV primarily triggers a TLR3-mediated response, HAV relies on an MDA5-mediated sensing mechanism, which is not sufficiently blocked. This challenges the established understanding that HAV does not induce IFN, or fully inhibits them, in infected hepatocytes both *in vitro* and *in vivo*. However, caution must be applied when interpreting both the results *in vitro*, due to models with limited physiological relevance, and *in vivo*, due to a limited number of animals. These findings underscore the need for fully immunocompetent animal models to carry out comprehensive investigations of the determinants of viral persistence and clearance, which are currently lacking.

Zusammenfassung

Die im Rahmen dieser Dissertation durchgeführte Forschungsarbeit konzentriert sich auf die angeborene Immunität, insbesondere auf die Untersuchung der Immunantwort des Wirts im Zusammenhang mit Hepatitis-A- (HAV) und Hepatitis-C- (HCV) Infektionen in der menschlichen Leber. Die angeborene Immunität ist die erste Verteidigungslinie des Körpers gegen eindringende Krankheitserreger und funktioniert über ein Netzwerk von Zellen und Molekülen, die schnell auf Infektionen reagieren. Im Mittelpunkt dieser Reaktion stehen Pattern Recognition Receptors (PRRs), die Pathogen-Associated Molecular Patterns (PAMPs) erkennen und die Produktion von Interferonen (IFNs) sowie die Expression von durch Interferon Stimulated Genes (ISGs) auslösen, die für die antivirale Abwehr entscheidend sind. Bei Virusinfektionen wie HAV und HCV spielt die Immunantwort des Wirts eine entscheidende Rolle für den Krankheitsverlauf, und diese Viren haben ihrerseits Strategien entwickelt, um das Immunsystem zu umgehen und zu manipulieren. Daher ist das Zusammenspiel zwischen Viren und der Immunantwort des Wirts ein wichtiger Aspekt der viralen Pathogenese. HAV und HCV sind beide positive-strand (+ssRNA) Viren mit striktem Tropismus für den Menschen. Obwohl sie eine Reihe von Gemeinsamkeiten in Bezug auf Genomstruktur und Replikation aufweisen, haben sie einzigartige Merkmale und lösen unterschiedliche Immunreaktionen aus, wobei HAV in >70 % der Fälle beseitigt wird und HCV chronische Infektionen verursacht, was sie zu interessanten Themen für vergleichende Studien macht. Die einzige vergleichende In-vivo-Studie, die an HAV- und HCV-infizierten Schimpansen durchgeführt wurde, ergab, dass HAV, obwohl es sich in höherem Maße repliziert als HCV, kaum eine angeborene Immunreaktion hervorruft, während HCV-Infektionen eine solide Immunantwort auslösen. Dies wurde auf eine starke Gegenaktivität der HAV-Protease 3C und ihrer Vorläufer 3CD und 3ABC gegenüber den PRR-Signalwegen zurückgeführt. Daher wollte ich herausfinden, wie HAV und HCV die intrinsische Immunantwort in der Leber auslösen und ihr entgegenwirken, was möglicherweise mit den auffallend unterschiedlichen Infektionsergebnissen zusammenhängt. Zu diesem Zweck habe ich relevante Zellkulturmodelle verwendet, um die Effizienz zu untersuchen, mit der HAV und HCV durch den endoplasmatischen Toll-Like-Receptor 3 (TLR3) und die zytoplasmatischen Rig-I-Like-Receptors (RLRs) wahrgenommen wurden. Außerdem habe ich

die proteolytische Spaltung des TLR3-Adaptors TIR-domain-containing adapter-inducing interferon- β (TRIF) und des RLR adaptor Mitochondrial Antiviral-Signaling protein (MAVS) durch transiente und stabile Expression der jeweiligen viralen Proteasen quantifiziert. Meine Ergebnisse zeigten, dass sowohl HAV- als auch HCV-Infektionen ähnliche Mengen an ISGs und IFNs in menschlichen Hepatozyten induzieren, was die Aktivierung der angeborenen Immunität signalisiert. Am HAV-Sensing waren in erster Linie das Melanoma Differentiation-Associated protein 5 (MDA5) und das Laboratory for Genetic and Physiology 2 (LGP2) beteiligt, wobei die HAV-Proteasen 3ABC und 3CD nur begrenzt auf MAVS und TRIF einwirkten. Im Gegensatz dazu wurde die HCV-Erkennung durch das durch Retinoic acid-Inducible Gene I (RIG-I) und MDA5 durch die effiziente Spaltung des RLR-Adapterproteins MAVS vollständig blockiert, was zur Aktivierung von TLR3 als primäre Quelle der ISG-Antwort für HCV führte. TRIF, das Adaptorprotein für TLR3, wurde im Gegensatz zu früheren Berichten nicht von HCV NS3-4A gespalten. Darüber hinaus ergab meine Untersuchung, dass Huh7-Zellen auf der MDA5-LGP2-Achse defekt sind. Mein Ansatz verlagerte sich dann auf eine *in-vivo*-Untersuchung von humanisierten SCID-Alb-uPA-Mäusen, die mit von beiden Patienten und Zellkultur-stammenden HAV- und HCV-Viren infiziert waren, wobei ich ein ähnliches Ausmaß an angeborener Immunantwort bei HAV- und HCV-Infektionen sehen konnte, die die *in vitro* Ergebnisse bestätigt. Insgesamt deuten meine Ergebnisse darauf hin, dass HCV in erster Linie eine TLR3-vermittelte Reaktion auslöst, während HAV auf einen MDA5-vermittelten Erkennungsmechanismus angewiesen ist, der nicht ausreichend blockiert wird. Dies stellt die bisherige Erkenntnis in Frage, dass HAV in infizierten Hepatozyten sowohl *in vitro* als auch *in vivo* kein IFN induziert oder diese vollständig hemmt. Allerdings ist bei der Interpretation der Ergebnisse sowohl *in vitro* aufgrund von Modellen mit begrenzter physiologischer Relevanz als auch *in vivo* Vorsicht geboten, da sie von einer begrenzten Anzahl von Tieren stammen. Diese Ergebnisse unterstreichen den Bedarf an vollständig immunkompetenten Tiermodellen, um umfassende Untersuchungen zu den Determinanten der viralen Persistenz und Clearance durchführen zu können, an denen es derzeit mangelt.

List of figures

| | |
|---|-----|
| Figure 1. Anatomical arrangement of the liver as an immune organ..... | 26 |
| Figure 2. Structure of the liver lobule and liver sinusoids with patrolling immune cells..... | 27 |
| Figure 3. The three phases of an immune response..... | 29 |
| Figure 4. Simplified schematic of the RLRs-mediated signaling cascade..... | 35 |
| Figure 5. Simplified schematic of the Toll-Like-Receptor 3-mediated signaling cascade. | 37 |
| Figure 6. Viral infection can trigger induction of interferon and interferon stimulated genes. | 40 |
| Figure 7. Various interferon-stimulated genes (ISGs) target specific stages in the viral replication cycle. | 42 |
| Figure 8. Distribution of HCV-infected patients categorized by genotype and global burden of disease (GBD) region..... | 45 |
| Figure 9. HCV genome organization. | 46 |
| Figure 10. HCV replication cycle. | 48 |
| Figure 11. Distribution of human hepatitis A virus genotypes over the endemic Global Burden of Disease regions. | 49 |
| Figure 12. HAV genome organization. | 50 |
| Figure 13. HAV replication cycle. | 52 |
| Figure 14. Interplay of the intracellular innate immunity response with HCV. | 55 |
| Figure 15. Current knowledge of HAV-mediated interference to the host innate immune response. | 60 |
| Figure 16. Establishment of the first cell culture models for HCV replication. | 62 |
| Figure 17. Different approaches to study HCV in animal models. | 64 |
| Figure 18. The SCID alb/uPA chimeric mice with humanized livers as HAV / HCV infection model. | 65 |
| Table 3. Comparison between HAV- and HCV-induced immunity..... | 69 |
| Figure 19. ISG induction upon HAV or HCV subgenomic replication. | 108 |
| Figure 20. ISG induction upon HAV or HCV infection Huh7 Lunet TLR3 cells. | 109 |
| Figure 21. Responsiveness of Huh7 and Huh7.5 TLR3 cells and full length HAV or HCV replication in Huh7.5 TLR3 cells. | 110 |
| Figure 22. TLR3 subcellular localization in Huh7.5 TLR3 and PH5CH cells..... | 111 |
| Figure 23. Transfection of total RNA from HAV and HCV subgenomic replicon cell lines in Huh7 Lunet TLR3 IRF3-GFP cells..... | 114 |
| Figure 24. TRIF RNA and protein expression overview from The Human Protein Atlas database ³¹⁴ | 115 |

| | |
|---|-----|
| Figure 25. TRIF expression constructs and their limitations..... | 116 |
| Figure 26. Different approaches to investigate HAV and HCV viral protease counteraction. | 117 |
| Figure 27. Expression vectors encoding viral protease..... | 117 |
| Figure 28. Analysis of TRIF cleavage by HCV and HAV proteases. | 118 |
| Figure 29. Titration of viral proteases to test TRIF cleavage..... | 119 |
| Figure 30. TRIF cleavage detection in HAV and HCV stable subgenomic replicon cells..... | 120 |
| Figure 31. Analysis of TRIF cleavage by HCV Gt2a. | 121 |
| Figure 32. Biochemical detection of TRIF cleavage upon in HAV and HCV-infected Huh7 Lunet T7 cells. | 122 |
| Figure 33. Pivotal dependence of the TLR3 pathway on TRIF..... | 123 |
| Figure 34. Rescue of the TRIF KOs with ectopic TRIF mutants..... | 124 |
| Figure 35. HAV subgenomic replication in TRIF wild-type or TRIF cleavage resistant reconstituted cells. | 125 |
| Figure 36. HCV subgenomic replication in TRIF wild-type or TRIF cleavage resistant reconstituted cells..... | 126 |
| Figure 37. HAV replication and innate immune induction in presence or absence of a cleavage-resistant TRIF. | 128 |
| Figure 38. Cytotoxicity of HAV 3CD protease and necessity to switch to a transient expression system. | 129 |
| Figure 39. Impact of HAV and HCV protease mediated cleavage of TRIF on cell intrinsic innate immune response. | 130 |
| Figure 40. Modulation of HCV-NS3-4A protease expression levels in Huh7.5 TLR3 cells. | 131 |
| Figure 41. Functional counteraction to TLR3 in HAV and HCV subgenomic replicon cell lines. | 132 |
| Figure 42. Functional counteraction to the TLR3 pathway by HAV and HCV at single-cell level through immunofluorescence analysis. | 134 |
| Figure 44. Viral proteases transfection assay to evaluate cleavage of the RLR adaptor MAVS..... | 138 |
| Figure 45. Biochemical detection of MAVS cleavage in HAV or HCV subgenomic replicon and HAV or HCV infected cells..... | 139 |
| Figure 46. Assessment of MAVS-cleavage by HAV and HCV proteases based on nuclear translocation of GFP upon protease transfection. | 140 |
| Figure 47. Assessment of MAVS-cleavage by HAV and HCV proteases based on nuclear translocation of GFP upon infection. | 141 |
| Figure 48. Impact of HAV and HCV protease mediated cleavage of MVAS on cell intrinsic innate immune response. | 142 |
| Figure 49. Immunofluorescence analysis of viral proteases stable expression in reconstituted cell lines..... | 143 |
| Figure 50. Innate immune response upon RIG-I and MDA5 transient expression in HAV and HCV subgenomic replicon cells..... | 144 |

| | |
|--|-----|
| Figure 51. ISGs induction upon HAV or HCV infection in stable RIG-I and MDA5 cells..... | 145 |
| Figure 52. Functional counteraction to the RLR pathways in HAV and HCV subgenomic replicon cells. | 147 |
| Figure 53. Functional counteraction to the MDA5 pathway by HAV and HCV at single-cell level through immunofluorescence analysis. | 148 |
| Figure 54. Functional counteraction to the RIG-I pathway by HAV and HCV at single-cell level through immunofluorescence analysis. | 149 |
| Figure 55. FACS analysis of HAV-mediated interference to MDA5 signaling pathway. | 150 |
| Figure 56. Quantification of RLR functional counteraction through analysis of single Huh7.5 MDA5 and RIG-I infected cells. | 153 |
| Figure 57. Attempts of HAV and HCV replication in PH5CH immortalized hepatocytes. | 155 |
| Figure 58. Infection attempts of PHH with HAV. (A-D) Primary Human Hepatocytes (PHHs) were infected with HAV HM175/18f. | 156 |
| Figure 59. Innate immune response in PHH infected with HAV wild-type virus and HCV Jc1. | 157 |
| Figure 60. Innate immune response in PHH infected with HAV wild-type virus and HM175/18f “naked” and “enveloped” inoculums. | 159 |
| Figure 61. HAV HM175/18f infection of Upcyte© Hepatocytes and Hepatocyte-Like-Cells (HLCs)..... | 160 |
| Figure 62. HAV HM175/18f infection of Upcyte© Hepatocytes and Hepatocyte-Like-Cells (HLCs)..... | 161 |
| Figure 63. HAV and HCV infection of Hep3B cells..... | 163 |
| Figure 64. HAV infection of HepG2 and HepaRG cells. | 164 |
| Figure 65. Attempt of HCV infection in HepG2 miR122 CD81h cells (HepG2 HFL). | 165 |
| Figure 66. Attempt of HCV spinoculation infection in HepG2 miR122 CD81h cells (HepG2 HFL). | 166 |
| Figure 67. Reconstitution of LGP2 in Huh7.5 MDA5 in the attempt of restoring innate immunity to HAV. | 167 |
| Figure 68. Assessment of the sensing PRR for HAV in HepG2 cells. | 168 |
| Figure 69. Assessment of the sensing PRR for HAV in HepG2 cells. | 169 |
| Figure 70. Assessment of the sensing PRR for HAV in HepG2 cells. | 170 |
| Figure 71. Quantification of human engraftment in SCID alb/uPA chimeric mice with human livers..... | 171 |
| Figure 72. ISGs mRNA expression upon HAV and HCV infection in SCID alb/uPA chimeric mice with human livers. | 173 |
| Figure 73. Gene expression array of ISGs upon HAV and HCV infection in SCID alb/uPA chimeric mice with human livers. | 175 |
| Figure 74. Upregulation of ISGs and chemokines at protein level upon HAV and HCV wild-type infection of SCID alb/uPa mice with humanized livers..... | 177 |

Figure 75. Upregulation of ISGs and chemokines at protein level upon infection with HAV HM175/18f and HCV genotypes 2a and 1a of SCID Alb/uPA mice.179

Figure 76. TRIF structure predictions.....184

Figure 77. Model of intracellular innate immune induction and counteraction by HAV and HCV.196

List of tables

| | |
|--|----|
| Table 1. Transmission and Epidemiology of the Major Hepatitis Viruses..... | 32 |
| Table 2. Controversial role of TLR3 in viral infections. | 38 |
| Table 3. Comparison between HAV- and HCV-induced immunity..... | 69 |
| Table 4. Reagents used in this study..... | 73 |
| Table 5. Buffers used in this study. | 75 |
| Table 6. Kits used in this study..... | 75 |
| Table 7. Cell lines used in this study..... | 77 |
| Table 9. Antibodies used in this study. | 79 |
| Table 10. Antibodies used in this study. | 80 |
| Table 11. Infection of uPA-SCID mice with humanized liver | 81 |
| Table 12. Infection of uPA-SCID mice with humanized liver..... | 82 |

Abbreviations

| | |
|--------------|---|
| dsRNA | double-stranded RNA |
| CXCL10 | C-X-C motif chemokine ligand 10 |
| ER | Endoplasmic reticulum |
| EV68 | Enterovirus 68 |
| EV71 | Enterovirus 71 |
| FMDV | Foot and mouth disease virus |
| HAV | Hepatitis A Virus |
| HBV | Hepatitis B Virus |
| HCV | Hepatitis C Virus |
| HDV | Hepatitis Delta Virus |
| HEV | Hepatitis E Virus |
| HSV | Herpes Simplex Virus |
| IFIT1 | Interferon Induced Protein With Tetratricopeptide Repeats 1 |
| IFN | Interferon |
| IL | Interleukin |
| IRF | Interferon Regulatory Factor |
| ISG | Interferon Stimulated Gene |
| JAK | Janus kinase |
| LGP2 | Laboratory of genetics and physiology 2 |
| LSECS | Liver sinusoidal endothelial cells |
| MAVS | Mitochondrial antiviral-signaling protein |
| MDA5 | Melanoma differentiation-associated protein 5 |
| NEMO | NF-kappa-B essential modulator |
| NFkB | Nuclear factor 'kappa-light-chain-enhancer' of activated B-cells |
| NK | Natural Killer (cells) |
| NLR | NOD-Like-Receptor |
| pDCs | Plasmacytoid Dendritic Cell |
| PRR | Pattern Recognition Receptor |
| RIG-I | Retinoic acid inducible gene I |
| RuV | Rubella virus |
| RVFV | Rift Valley fever virus |
| SCID Alb/uPA | Severe combined immunodeficiency disorder – albumin urokinase plasminogen activator |

| | |
|----------|--|
| STAT1 | Signal transducer and activator of transcription 1 |
| TBK1 | TANK-binding kinase 1 |
| TLR3 | Toll-Like-receptor 3 |
| TNF | Tumor Necrosis Factor |
| TRAF6 | TNF Receptor Associated Factor 6 |
| TRIF | TIR domain containing adaptor molecule 1 |
| WNV | West Nile Virus |
| YFW | Yellow Fever Virus |
| CypA | Cyclophilin A |
| PI4KIIIa | Phosphatidylinositol 4-Kinase Alpha |
| LDs | Lipid Droplets |
| LDV | Low Density Lipoparticles |
| VLDL | Very Low Density Lipoparticles |
| DMVs | Double Membrane Vesicles |
| CD81 | Cluster of differentiation 81 |
| OCLN | Occludin |
| STING | stimulator of interferon genes |
| cGAS | Cyclic GMP- AMP synthase |
| SeP | Selenoprotein |
| IRES | Internal Ribosomal Entry Site |
| IV | Intravenous |
| IVT | In Vitro Transcript |
| RLU | Relative Light Units |
| RANTES | Regulated upon Activation, Normal T Cell Expressed and Presumably Secreted |
| AHA | Acute Hepatitis A |
| SNP | Single Nucleotide Polymorphism |
| ISGF3 | Interferon-stimulated gene factor 3 |
| T-regs | Regulatory T cells |
| FRHk4 | Fetal Rhesus Kidney 4 |
| MRC-5 | Medical Research Council cell strain 5 |
| RT-qPCR | Real Time-quantitative Polymerase Chain Reaction |
| PCR | Polymerase Chain Reaction |
| NHP | Non Human Primate |
| eHAV | Enveloped HAV |

| | |
|-------|--|
| cGAMP | cyclic guanosine monophosphate–adenosine monophosphate |
| TRAF | Tumor necrosis factor receptor (TNFR)-associated factors |
| IKKe | inhibitor of nuclear factor kappa-B kinase ϵ |
| PABP | Poly(A)-binding protein |
| PCBP2 | Poly(rC)-binding protein 2 |
| PTB | Polypyrimidine tract-binding protein |
| GAPDH | Glyceraldehyde 3-Phosphatase Dehydrogenase |
| HPRT | Hypoxanthine Phosphoribosyltransferase 1 |
| MX1 | Interferon-induced GTP-binding protein |
| ESCRT | endosomal sorting complex required for transport. |
| ALIX | apoptosis-linked-gene-2 interacting protein X. |
| VPS4B | vacuolar protein sorting 4 homolog B |
| Con1 | Consensus 1 |
| JFH1 | Japanese Fulminant Hepatitis 1 |
| GLT1 | German liver transplant 1 |

“Non ci si deve arrendere alla materia incomprensibile,
non ci si deve sedere. Siamo qui per questo, per sbagliare e correggerci,
per incassare colpi e renderli. Non ci si deve mai sentire disarmati:
la natura è immensa e complessa, ma non è impermeabile all'intelligenza;
devi girarle intorno, pungere, sondare, cercare il varco
o fartelo.”

(Primo Levi - Nichel, Il sistema periodico)

“Perché la ruota giri, perché la vita viva, ci vogliono le impurezze:
anche nel terreno, come è noto, se ha da essere fertile.”

(Primo Levi - Zinco, Il sistema periodico)

“Finite - to fail, but infinite - to Venture -”

Emily Dickinson

“One must not surrender to incomprehensible matter, one must not sit down.
We are here for this, to make mistakes and correct ourselves, to take blows and return
them. One must never feel disarmed: nature is immense and complex, but it is not
impervious to intelligence; you have to go around it, prick, probe, search for an opening,
or make one.”

(Primo Levi - Nickel, The periodic table)

"For the wheel to turn, for life to live, impurities are needed: even in the soil,
as is well known, if it is to be fertile."

(Primo Levi - Zinc, The periodic table)

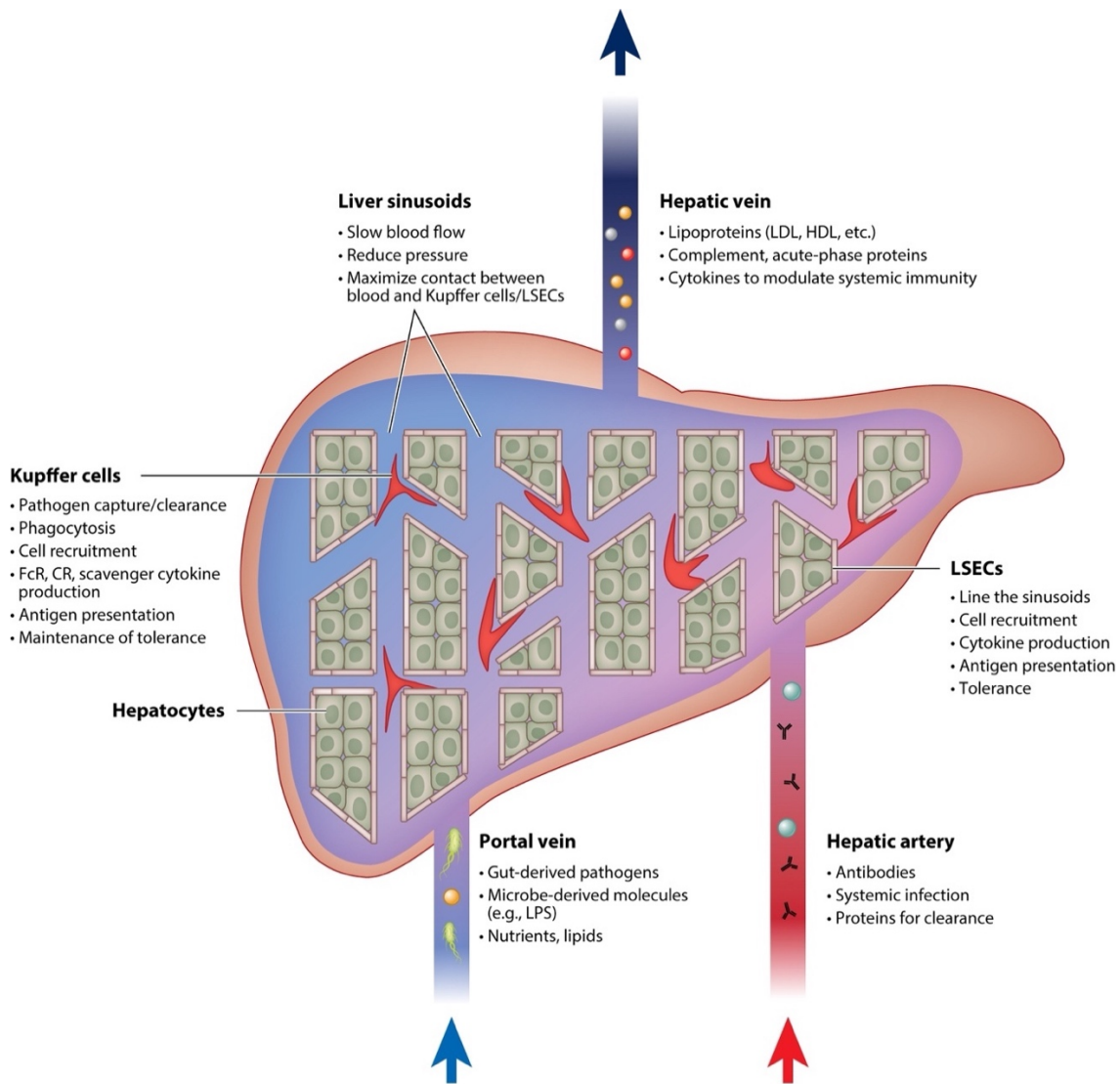
Introduction

1.1 The human liver

The liver performs a wide range of vital functions that contribute, among others, to metabolism, digestion, detoxification, synthesis and storage¹. Recognition of the liver's importance dates back to the ancient Babylonians² and the following Mesopotamic doctrine of *hepatocentrism*, that placed it at the center of the whole human being, and persisted until the seventeenth century in Western countries³. It is therefore not surprising that the etymology of the word "*liver*" shares its roots with German and English terms for "*life, living*" and the meaning of "*hèpar*" was in ancient Greek "*soul*"⁴.

The liver's involvement extends to nearly every organ system, but its most compelling role remains undoubtedly immunological: firstly, because of the liver's strategic location, which allows the collection, through the gut-enriched bloodstream, of potential harmless substances (such as food antigens) as well as of dangerous bacteria or viruses; and, secondly, for its unique anatomy (illustrated in Figure 1). On a microscopic level, the liver consists of cells, called *hepatocytes*, that are organized into lobules and serve as the liver's structural units. Each lobule has a hexagonal shape, is drained by a central vein and surrounded by a characteristic capillary structure, called sinusoid, which is enclosed by a discontinuous, fenestrated endothelium. Therefore, circulating immune cells, residing in this structure, are allowed direct contact with the hepatocytes⁵; the liver, in fact, houses the largest collection of immune cells⁶, serving as a crucial barrier between our body and the external environment and aiming at maintaining a delicate homeostasis between tolerance (acceptance) and immunity (reaction)⁷.

Rather than being randomly distributed, these immune cells are strategically located: a significant number of them, whose function will be examined later, can be observed actively patrolling the sinusoidal lumen (Figure 2), as professional innate immune cells or specialized white cells subpopulations: macrophages, neutrophils, lymphocytes known as B cells and T cells, among others⁸.



Kubes P, Jenne C. 2018. *Annu. Rev. Immunol.* 36:247–77

Figure 1. Anatomical arrangement of the liver as an immune organ.

The liver receives blood supply from both the hepatic artery and the portal vein (bottom). These sources can transport various substances, including potential pathogens, molecules derived from microbes (such as pathogen-associated molecular patterns, PAMPs), nutrients, as well as old or damaged molecules for clearance. Upon entering the liver, the blood is directed into a network of sinusoids which reduces the flow rate and pressure. This slowing of blood flow maximizes the exposure of the blood to the liver resident macrophages (Kupffer cells) and liver sinusoidal endothelial cells (LSECs), which act as filters, removing pathogens and molecules from the blood. Between the liver sinusoids there are columns of hepatocytes, the primary cell type responsible for producing clotting factors, complement proteins, and acute-phase proteins. After filtration, the blood leaves the liver through draining venules, eventually merging into the hepatic vein. LSECs, Kupffer cells and hepatocytes can all initiate an immune response by producing cytokines and recruiting additional immune cells. Other abbreviations: CR (complement receptor), FcR (Fc receptor), HDL (high-density lipoprotein), LDL (low-density lipoprotein), and LPS (lipopolysaccharide). Adapted from ⁶.

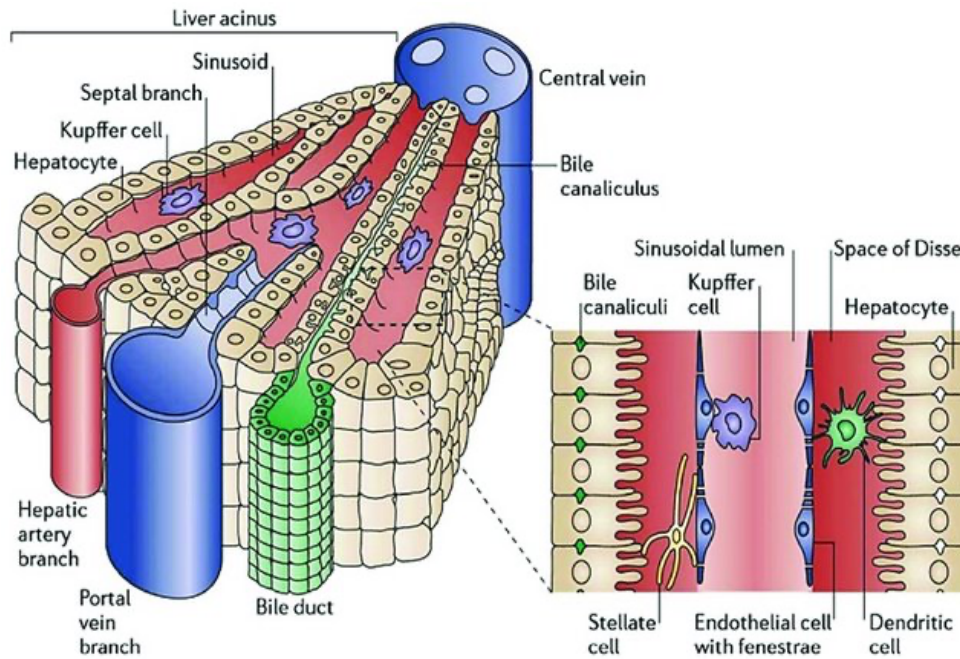


Figure 2. Structure of the liver lobule and liver sinusoids with patrolling immune cells.

The hepatocytes are arranged in lobules and surrounded by the sinusoids. The space situated between the liver plate and the sinusoids, termed space of Disse, contains extracellular matrix components and more specialized immune cells, as Kupffer, hepatic stellate and dendritic cells (adapted from ⁹).

Having established an understanding of the liver's anatomical structure, it's important to consider that this exchange can also introduce potentially harmful elements, including pathogens which are carried through the bloodstream and reach the fenestrated sinusoidal epithelium, getting then in touch with the hepatocytes. Because of this possibility, the liver is equipped with means to deal with potential intruders.

1.2 Immune responses in the liver

“Immunity” is a broad term which encompasses two distinct families of mechanisms targeting a potential threat: an early response, denominated *innate*, which takes place quickly and targets common structures shared by groups of microbes; and a systemic one, more delayed but highly specific and providing long term protection, called *adaptive*. These two distinct reactions take place in three consequent phases, summarized in Figure 3.

Innate immunity includes a range of components, including physical barriers such as the skin and mucous membranes, chemical barriers as fluids or secretions, as well as humoral factors such as complements and interferons (IFNs)¹⁰. Phagocytic cells, such as neutrophils and

macrophages, along with lymphocytic cells like natural killer (NK) and natural killer T (NKT) cells, are also integral parts of innate immunity¹⁰.

Adaptive immune responses take place upon activation of specialized cells, termed effector cells, and can be categorized into two classes: antibody responses and cell-mediated immune responses, executed by distinct types of B and T lymphocytes, respectively. In antibody responses, B cells are stimulated to secrete immunoglobulins (antibodies), which are specialized proteins. These circulate in the bloodstream and body fluids, binding specifically to foreign antigens and preventing their attachment to receptors on host cells. Additionally, antibody binding facilitates the recognition and destruction of invading pathogens by effector cells (phagocytes)¹¹.

In cell-mediated immune responses, instead, activated T cells directly engage with foreign antigens presented on the surface of host cells, to prevent pathogen spread, and release signaling molecules that activate macrophages to eliminate the invaded cells, or the invading microbes, through phagocytosis¹¹.

Compared to innate immunity, the adaptive immune response is less marked in the liver¹²: this organ has been shown to be provided with tolerance mechanisms, for instance in the event of a spontaneous acceptance of liver transplant¹³, or upon persistent infections, such as HBV, HCV, malaria¹⁴, as well as within tolerance mechanisms to food antigens¹⁵. Yet, under specific circumstances, the liver can also undergo uncontrolled responses, as with immunosuppression in the context of viral infections and cancer^{16,17} or, in contrast, within exacerbated immunity within autoimmune disorders¹⁸.

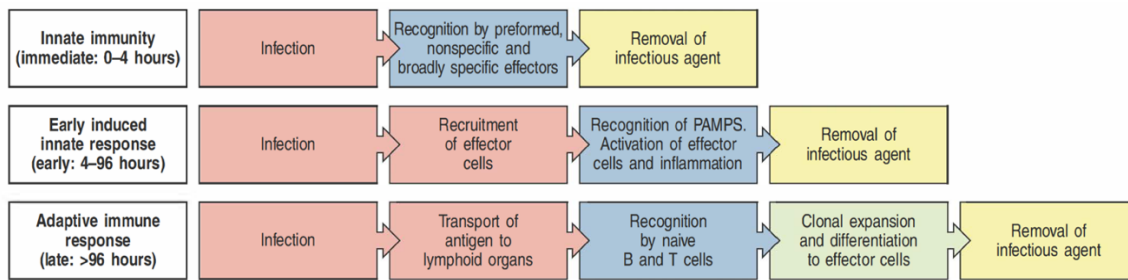


Figure 3. The three phases of an immune response.

The immediate response to a threat, as an infectious agent, occurs within 4 hours and relies on effector cells, subpopulations of white blood cells, as monocytes, granulocytes and dendritic cells which remove the pathogen. The early onset of innate immunity occurs within 4 to 96 hours following exposure to an infectious agent, triggering the mobilization of effector cells through the recognition of pathogen-associated molecular patterns (PAMPs) binding to pattern-recognition receptors (PRRs) and amplifying the cytokine – interferon release in a paracrine and autocrine manner. The “late”, adaptive response is established from 96 hours after infection, once naïve B and T cells are exposed to peptide fragments derived from the pathogen, which infected cells display on their surface. This brings to clonal expansion, differentiation to specialized effector cells, and establishment of memory. Adapted from¹⁹.

The liver is indeed considered an “innate immune organ”. This is due to the resident liver macrophages (defined as Kupffer cells), mainly involved in waste phagocytosis, which represent here the largest macrophage population of the entire body²⁰. Approximately half of the intrahepatic lymphocytes consists of NK cells, which possess a distinct liver-specific imprint²¹. In addition, both liver sinusoidal endothelial cells and hepatocytes are particularly rich of specialized receptors involved in innate immune sensing²², termed Pattern Recognition Receptors (PRRs). And exactly this intrinsic immediate cell response, based on local recognition of pathogens directly in the insulted cell, the hepatocyte, is of special importance for the liver, since hepatocytes have been shown to be responsible for production of around 90% of the circulating innate immune proteins – complement and cytokines²³.

The complement system is a complex network of proteins that plays a pivotal role in immune defense against pathogens by enhancing (“*complementing*”) the ability of antibodies and macrophages to clear microbes and damaged cells, promoting inflammation, and attacking the pathogen's cell membrane²⁴.

Cytokines are, instead, a group of signaling proteins which include Interleukin (ILs) - produced predominantly by leukocytes and fundamental in mediating communication between cells, orchestrating complex immune responses, and bridging the innate and

adaptive immune systems²⁵ - and Interferons (IFNs) - produced and secreted by host cells in response upon recognition of diverse pathogens, such as viruses, bacteria, parasites, or cancer cells²⁶. The latter are so called because they possess the ability to *interfere* with viral replication, stimulate immune cells, and upregulate the expression of genes that inhibit cell proliferation and promote apoptosis. They serve as a critical bridge between innate and adaptive immunity, making them an essential component in controlling various stages of immune responses, ultimately resulting in the activation of numerous interferon-stimulated genes (ISGs). Interestingly, IFNs also have the ability to regulate a substantial portion of the human genome, with approximately 10% of genes being potentially influenced by their activity²⁷. These molecules exert significant influences on various aspects of cellular physiology, including cell proliferation, survival, differentiation, protein translation, and metabolism; but, most importantly, they effectively hinder mainly viruses, targeting their replication at multiple stages^{28,29} and, according to research, play also a role in bacterial infections³⁰.

Having briefly explored the multifaceted immune landscape of the liver, it is essential to highlight the outcomes when this intricate system fails to coordinate effectively. Such failures between innate and adaptive immunity can lead to a spectrum of health challenges, from chronic conditions to acute infections.

1.3 Hepatitis and viral hepatitis

More in general, when an inflammatory process takes place in the liver, this is termed *hepatitis*. Acute hepatitis refers to an initial phase of liver inflammation, defined by a rapid onset of symptoms, elevated liver enzymes, and usually resolving within six months⁶. In contrast, chronic hepatitis is a persistent liver inflammatory condition lasting longer than six months and, if untreated, possibly leading to progressive liver damage, fibrosis, cirrhosis, and an increased risk of liver cancer³¹.

Hepatitis can result from a large variety of noninfectious causes that include, among others, usage of drugs and toxins (drug-induced hepatitis) or alcohol (alcoholic hepatitis)³²; furthermore, it can surge from inflammatory conditions (autoimmune hepatitis) or as a result of indirect damage of the tissue (cholestatic hepatitis, CH)³³; but, most commonly, hepatitis occurs in consequence of a viral infection³⁴.

Viral hepatitis is mostly due to infection by viruses described *hepatotropic*, having hepatocytes as their primary target. The hepatitis viruses, namely A, B, C, D, and E, belong to distinct viral families and exhibit various molecular properties. They also differ in their modes of transmission, despite causing similar clinical symptoms (summarized in Table 1). However, viral hepatitis can also be caused by numerous other viral agents: among them are Epstein-Barr virus (EBV), Cytomegalovirus (CMV), Herpes simplex virus (HSV), Varicella-Zoster virus (VZV), Coxsackieviruses and Yellow Fever virus (YFV)³⁵.

Hepatitis A (HAV) and hepatitis E (HEV) typically do not lead to chronic infections, and individuals who experience primary infection develop lifelong immunity against these viruses³⁶. On the other hand, hepatitis B (HBV) often leads to chronic infection in more than 90% of infants, 25% to 50% of kids between 1 to 5 years old, and 6% to 10% of older children and adults, with augmented risk in case of coinfection with hepatitis D (HDV), its satellite virus³⁷. In contrast, approximately 70% of those infected with hepatitis C (HCV) will develop a persistent infection³⁷. With more than 325 million individuals living with chronic hepatitis across the globe, and Hepatitis B and hepatitis C being causative of the 80% of liver

cancer cases worldwide, viral hepatitis ranks among the top 10 leading causes of death from infectious diseases³⁷, thereby still representing to this day a highly relevant research field.

| | HAV | HBV | HCV | HDV | HEV |
|---|----------------------|---|---|---|---------------------------------------|
| Mode of transmission | Fecal–oral | Blood, sexual contact, perinatal | Predominantly blood, also sexual contact, perinatal | Blood | Fecal–oral |
| Average incubation period (range) | 28 days (15–50 days) | 90 days (60–150 days) | 45 days (14–180 days) | Coinfection: 90 days (45–60 days) Superinfection: 14–56 days | 40 days (15–60 days) |
| Chronic infection? | No | Yes (occurs 5%–10% overall, very likely in infants) | Yes (occurs 70%) | Yes (<5% with coinfection, up to 90% with superinfection) | No (chronic only in immunosuppressed) |
| Worldwide incidence of acute infection (2019 WHO data) | 1.5 million/year | 15–30 million/year | 2.1 million/year | 200,000–400,000 | 20 million |
| Worldwide prevalence of chronic infection (2019 WHO data) | No chronic infection | 296 million | 58 million | 15 million | Very rare |
| Vaccine available? | Yes | Yes | No | Yes (HBV vaccine prevents) | Only in China |

Table 1. Transmission and Epidemiology of the Major Hepatitis Viruses.

Comparative overview of the various hepatitis viruses, taking into account key characteristics including their modes of transmission, epidemiology, incubation periods, availability of vaccines and potential for chronicity. Adapted from ³⁷.

While examining viral hepatitis, particularly noteworthy are instances where disease progression can swing between chronicity and resolution, dependent on the efficiency of the immune response. HAV and HCV infections provide a good example in this respect: they share a number of important structural and replicative similarities, yet their distinct courses of infection underscore the profound influence of liver immunity on disease outcome. Thus, before delving into the specificities of these viral infections, it is critical to look at how exactly hepatocytes mount their responses.

1.4 Innate immunity within the hepatocytes: from Pattern Recognition Receptors...

For the constant challenges and potential insults coming from the exchange with the blood stream, hepatocytes must be equipped with sophisticated mechanisms that enable them to detect and respond to diverse types of threats as, for instance, a set of specialized sensors.

Within this repertoire, Pattern Recognition Receptors (PRRs) emerge as particularly refined components. These are an especially evolutionally conserved line of receptors^{38,39} expressed on cell membranes and cytoplasm of prevalently, but not exclusively, immune cells. The main role of PRRs is detecting potentially noxious, specific *molecular patterns* of two types: PAMPs (pathogen-associated molecular patterns) or DAMPs (danger-associated molecular patterns), initiating then the recruitment of distinct sets of adaptor molecules and initiate a signaling cascade which leads to the involvement of adaptive immunity (^{11,40}).

PAMPs consist typically of “signature” molecule - like mannose-rich oligosaccharides, lipopolysaccharides from the bacterial cell wall, and unmethylated CpG DNA⁴¹ - that are commonly expressed by bacteria, viruses, fungi, and parasites, but not from the body (*non-self*). Such structures are evolutionary well conserved⁴² and, therefore, excellent targets for the innate immune system. DAMPs stem, instead, from different subcellular compartments upon tissue injury, or cellular stress⁴³.

PRRs can be classified into several types based on their cellular location and the specific threats they are designed to detect. Before we delve into these categories, it's worth mentioning that some of these sensors have particularly significant roles especially when it comes to infections: the nucleotide binding oligomerization domain (NOD)-like receptors, involved in recognition of bacterial fragments; a diverse array of cytoplasmic and nuclear sensors sensing DNA⁴⁴; RIG-I-like receptors (RLRs) and Toll-like receptors (TLRs) sensing double-stranded RNA (dsRNA). The latter two are extremely relevant when it comes to the forementioned HAV and HCV infections, as these viruses generate dsRNA as a replication intermediate, and therefore will be described in greater detail.

The cytoplasmic RLRs include retinoic acid inducible gene (RIG-I), melanoma differentiation-associated gene 5 (MDA5), and Laboratory of genetics and physiology 2 (LGP2)⁴⁵. RIG-I recognizes primarily short - < 500 base pairs (bp) dsRNA and displays a preference for RNA sequences containing 5' triphosphorylated (5'ppp) ends, which serve as a distinguishing feature of non-self RNA known as a PAMP⁴⁶; moreover, it can also bind to single-stranded RNA⁴⁷. MDA5, conversely, mainly recognizes longer dsRNA molecules.

LGP2 expression is low in uninfected cells, but it augments upon viral infection⁴⁸. It has the ability to recognize various RNA molecules, irrespective of their length or 5' phosphate ends⁴⁹⁻⁵¹. This sensor plays a supporting role in RNA recognition for MDA5, enhancing the capability of the latter to form a stable complex with dsRNA^{52,53} while inhibiting RIG-I⁵⁴. Furthermore, LGP2 can negatively regulate the Tumor necrosis factor receptor-associated factor (TRAF) family proteins, which are engaged on the TLR3-downstream signaling but also have a key role in regulating inflammation and apoptosis^{55,56}, making LGP2's influence going beyond the simple IFN antiviral response.

When dsRNA binds to either the MDA5 or RIG-I sensor, it induces a conformational change, exposing the N-terminal caspase activation and recruitment domains (CARD). However, this does not hold true for LGP2, which lacks the CARD domain and therefore does not take part to this process⁵². These CARD domains interact with an analogous CARD of a mitochondrially-localized adaptor molecule called MAVS (mitochondrial antiviral signaling). Recruitment of MAVS triggers TANK-binding kinase 1 (TBK1) and I κ B kinase- ϵ (IKK ϵ), which phosphorylate numerous transcription factors, as Interferon Regulatory Factor 3 (IRF3) and 7 (IRF7), and nuclear factor 'kappa-light-chain-enhancer' of activated B-cells (NF κ B). These activated proteins form homo- and heterodimers that migrate and accumulate in the nucleus, where they facilitate gene transcription of genes encoding interferons, ISGs⁵⁷ and immunoregulatory genes^{26,58}. The RLRs-mediated signaling cascade is depicted in Figure 4.

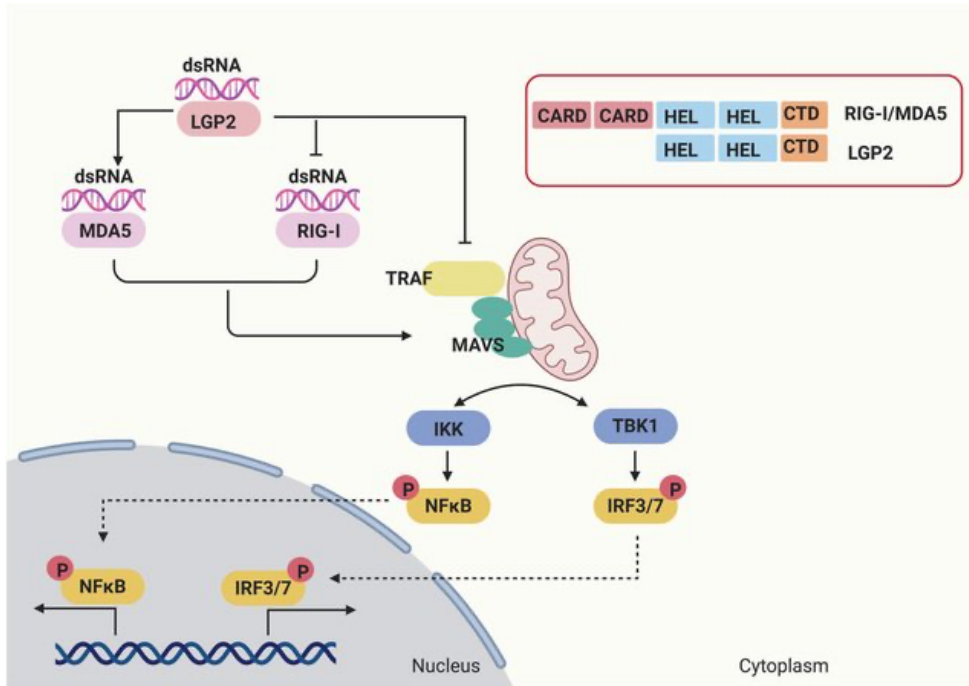


Figure 4. Simplified schematic of the RLRs-mediated signaling cascade.

RLRs, namely RIG-I, MDA5, and LGP2, share common features with one another, such as the DExD/H-box helicase domain and C-terminal domain (CTD). But RIG-I and MDA5 possess two N-terminal caspase activation and recruitment domains (CARD), whereas LGP2 lacks it. RIG-I specifically detects short cytoplasmic double-stranded RNA (dsRNA) molecules that bear a 5'-triphosphate or 5'-diphosphate moiety, while in principle MDA5 recognizes longer dsRNA structures. LGP2 can hinder the activation of RIG-I by binding to its RNA ligands, thus impeding IKK recruitment to mitochondrial antiviral-signaling protein (MAVS) through protein-protein interaction. LGP2 can also directly bind to RIG-I via a repressor domain. Moreover, LGP2 enhances the capability of MDA5 to form stable filaments on dsRNA, thus promoting the MDA5-mediated pathway. When activated, RIG-I and MDA5 trigger the recruitment and polymerization of the adapter molecule MAVS on the mitochondrial membrane. MAVS then activates TBK1 and the IKK complex, leading to the activation of IRF3, IRF7, and NF-κB. This cascade induces the expression of interferons (IFNs), pro-inflammatory cytokines, and chemokines, thereby defending against viral infections and modulating the immune response. Adapted from ⁵⁹.

Activation of RLR signaling by viral infections has been thoroughly examined in literature. RIG-I has been shown to be involved in recognition of a plethora of viruses belonging to different families: Paramyxoviruses, Newcastle disease virus (NDV), Sendai virus (SeV), Rhabdoviruses, Vesicular Stomatitis virus (VSV), Respiratory syncytial virus (RSV), Rabies, Hepatitis C virus (HCV), Japanese Encephalitis virus (JEV), Ebola virus, Rubella virus (RuV) and many others⁶⁰⁻⁶³. By contrast, to MDA5 was attributed recognition of mainly Picornaviruses, as encephalomyocarditis virus (EMCV), Theiler's murine encephalomyelitis virus (TMEV), Hepatitis A Virus (HAV), but also to Coronaviruses, as SARS-CoV2, Murine Hepatitis Virus (MHV), and Flaviviruses as HCV ⁶⁴⁻⁶⁸. Yet, both RIG-I and MDA5 were reported capable of detecting the Flaviviruses Dengue virus (DENV) and West Nile virus (WNV) as well as the

dsRNA viruses Reovirus and Rotavirus⁶⁹, highlighting a potential adaptability of these RLRs to their dsRNA structural recognition requirements.

Complementing the actions of RLRs in the cytoplasm, TLR3, offers a parallel and distinct pathway for sensing within a separate cellular compartment. Among the 13 members of the TLR family, all membrane-bound and with variable expression across cell types and tissues⁷⁰, TLR3 stands out as relevant sensor for dsRNA. In resting cells, TLR3 is situated within the endoplasmic reticulum and trafficked via the classical secretory pathway to endosomes⁷¹, a process dependent of the low pH⁷², which typifies the endosomal lumen, and there dimerizes⁷². Upon dsRNA recognition the activated TLR3 dimer gives rise to signaling by recruiting the adaptor molecule TRIF⁷³. This association can lead to three significant consequences, as illustrated in Figure 5: (i) the propagation of the antiviral response through IRF3 activation and subsequent type I and type III Interferon (IFN) production, (ii) the induction of cell death via caspase-8 activation, through MYD88 innate immune signal transduction adaptor(MyD88) and Receptor-interacting serine/threonine-protein kinase 1 (RIP1), and (iii) the creation of a pro-inflammatory environment through the stimulation of NF- κ B and Activator protein 1 (AP-1). For the first branch, TRIF undergoes a structural alteration that enables interaction with the kinase TRAF3. The interaction between TRAF3 and TRIF leads, in turn, to recruitment and activation of the kinases IRF3 / IRF7, TBK1, and IKK ϵ , promoting the formation of an active “kinase complex”⁷⁴⁻⁷⁶, culminating in nuclear translocations of the single transcription factors and production of type I and type III interferons (IFNs) through the involvement of IRF3 and/or IRF7⁷⁷.

The second pathway, based on MyD88 engagement, centers on RIP1 and TRAF6, which interact with TRIF to recruit Mitogen-activated protein kinase kinase kinase 7 (MAPK7 also termed TAK1) and TAK-binding proteins 2 and 3 (TAB2, TAB3). The process triggers the activation of the IKK complex, the MAPK pathway, and the further stimulation of NF- κ B and AP-1⁷⁸, respectively. These two pathways, RIP1 and TRAF3, coordinate to activate the antiviral and pro-inflammatory response via NF- κ B signaling.

Lastly, the RIP1-TRIF interaction also results in apoptosis via a RIP1/FAS-associated protein with death domain.⁷⁹ This intriguing facet underlines the cytopathic potential of the TLR3–TRIF axis^{80,81}.

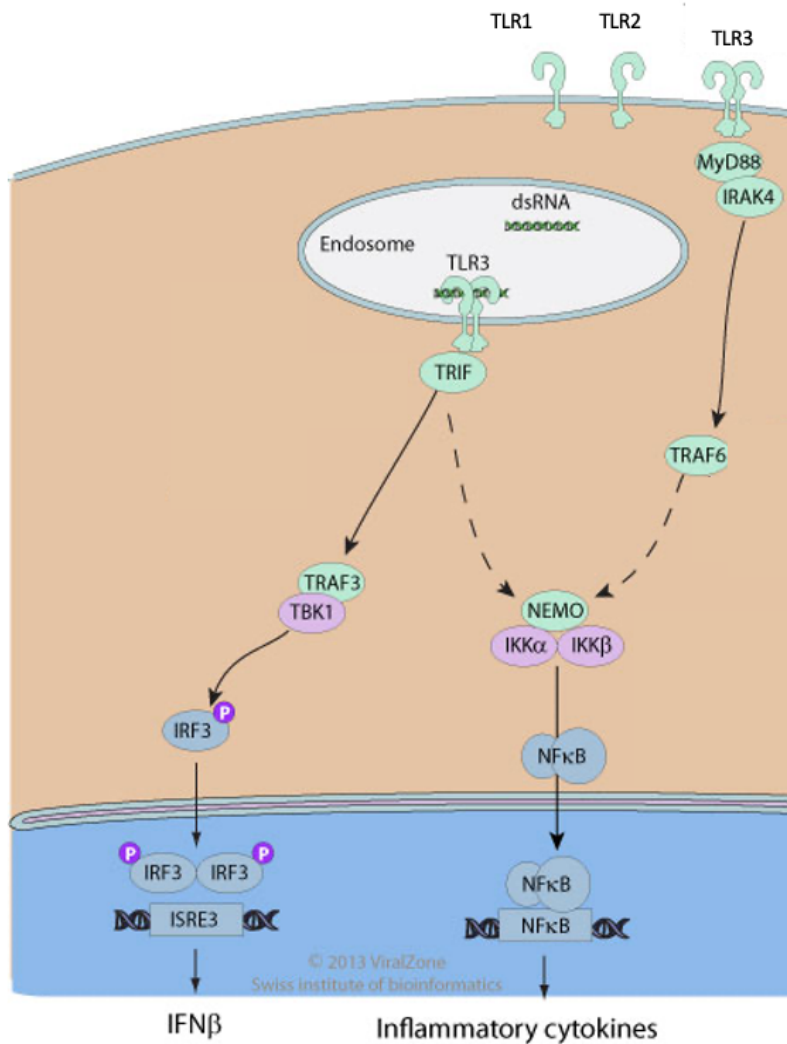


Figure 5. Simplified schematic of the Toll-Like-Receptor 3-mediated signaling cascade.

TLR3, situated within acidic endosomes that are formed during clathrin-dependent endocytosis, signals through recruitment of TRIF and leads to the activation of kinases, as TRAF3/TBK1, which phosphorylate transcription factors as IRF3 / IRF7, culminating in transcription of IFNs and ISGs. In addition, TLR3 can also directly engage also the modulatory protein NEMO, which complexes with IKKalpha, IKKbeta to promote activation of NFκB and transcription of pro-inflammatory cytokines. Adapted from⁸².

This discrepancy in RLRs and TLR3 localizations allows them to detect dsRNA from viruses following varied fates. Specifically, the N-terminus of TLR3 is oriented towards the endosomal lumen, thereby potentially limiting its direct interactions to viruses that replicate within membrane-associated vesicles tied to the endo-lysosomal pathway, such as HCV⁸³, West-Nile Virus (WNV)⁸⁴, and Rhinovirus (RV)⁸⁵.

However, it's crucial to consider that both TLR3 and RLRs are interferon-stimulated genes (ISGs) themselves⁸⁶⁻⁸⁸, with the potential of employing an indirect antiviral function also when triggered by IFN because of the action of other sensors, rather than by exclusive

detection of dsRNA. Therefore, in a system where all pattern recognition receptors (PRRs) are present, the antiviral contributions of TLR3 and RLRs could also result from their interplay with one another.

Yet, it's worth noting that, delving into the complexities of this immunological interplay, the function of TLR3 in viral infections has emerged as a point of contention. Unlike the generally agreed-upon roles for RLRs, some studies suggest that TLR3 activation can be exploited by certain viruses to their benefit, adding complexity to its precise function in such infections (summarized in Table 2).

| Virus^a | Target system, organ, tissue, and/or cells expressing TLR3 | Role of TLR3^b |
|--|---|---------------------------------|
| Influenza A virus | Respiratory tract | - |
| | CNS | + |
| Respiratory syncytial virus | Respiratory tract | + |
| Rabies virus | CNS (neuronal cells) | -? |
| Herpes simplex virus 1 | CNS (neuronal cells) | -? |
| West Nile virus | CNS | - |
| Theiler's murine encephalomyelitis virus | CNS (astrocytes) | +? |
| Encephalomyocarditis virus | Heart | + |
| Human immunodeficiency virus | Skeletal muscle | -? |
| Punta Toro virus | Liver | - |
| Hepatitis C virus | Liver | +/-? |
| | Kidney | -? |
| Herpes simplex virus 2 | Female genital tract | +? |

^aViruses are listed in the order of their appearance in the text.

^b+, protective; -, detrimental; +/-, protective or detrimental.

Table 2. Controversial role of TLR3 in viral infections.

Some studies show that TLR3 contributes to the elimination of specific viruses, but according to other reports, some benefit from TLR3 stimulation. Adapted from⁸⁹

Among other important dsRNA sensors, it is worth mentioning protein kinase R (PKR), located in the cytosol, which functions as a kinase sensing stress and modulating translation through interaction with eukaryotic initiation factor 2-alpha (eIF2 α), as other pathways⁹⁰. PKR can also trigger interferon signaling upon recognizing double-stranded RNA (dsRNA), independently from the other PRRs, or work synergistically with RIG-I and MDA-5⁹¹. Numerous more RNA-binding proteins have been implicated in recognition of cytosolic RNA^{92,93} but, as the focus in this dissertation revolves around hepatitis viruses and their

interaction with the innate immune system, we will now narrow our attention solely to the PRRs here involved – TLR3, MDA5, RIG-I - and their associated downstream effects.

1.5 ...to IFN signaling and induction of ISGs

Once the signaling cascades downstream of PRRs such as TLR3 and RLRs are activated, IFNs and ISGs transcription follows.

The expression of IFN genes is usually maintained at very low levels in absence of an external stimulus⁹⁴. This is achieved through a combination of the absence of activated transcription factors and the constant presence of a repressive machinery, which binds to the positive regulatory elements in their promoters, suppressing transcription. This repressor (typically IRF2⁹³) is then, upon stimulation, replaced by an activating IRF protein, typically IRF3 or IRF7⁹⁵.

Interferons are categorized in type I (to which belong IFN- α and IFN- β , among others), type II (IFN- γ), and type III (IFN λ 1-4), based on the receptor they bind to and their specific cellular sources, distribution, and roles in the immune response^{96,97}. Type II IFNs are the only type of IFN family not to be induced downstream of PRR recognition, but rather by immune cells in response to other cytokines⁹⁸. Once – upon infection, or other stimuli - type I and type III interferons are induced, they are released by infected cells and can bind to specific receptors (Figure 6), in an autocrine and / or paracrine manner - involving a cell responding to it through its own interferon receptors or effective on neighboring cells, respectively. Professional immune cells, as pDCs, secrete up to 95% total IFNs produced during an infection; particularly, their production of IFN- α has been shown to have a dramatic outcome on B cell function⁹⁹. Although the downstream signaling pathways triggered by the engagement of type I and type III receptors lead to similar transcriptional responses, the receptors themselves are different. IFN- α and - β bind to a receptor called IFNAR¹⁰⁰; IFN- λ , on the other hand, binds to a distinct receptor composed of IFN- λ receptor 1 (IFNLR1) and a shared subunit with the IL-10 receptor, known as IL10R2¹⁰⁰. Binding of any of these IFNs to their respective receptors leads to the activation of a transcription factor called ISGF3, which encompasses STAT1, STAT2, and IRF9¹⁰¹. This activation results in the transcriptional upregulation of a common set of ISGs^{102,103}. The proteins encoded by the ISGs are

responsible for a myriad of effects²⁸: antiviral, immunostimulatory, and antiproliferative, so pivotal for our survival, that it has been reported that the only three known patients who lacked IFN- α/β responsiveness ever identified did not survive beyond infancy^{104,105}. The fact that IFN- α and - β also have a prominent impact on the activation, proliferation, and migration of professional immune cells involved in long term protection from infections¹⁰⁶ underscores their importance further.

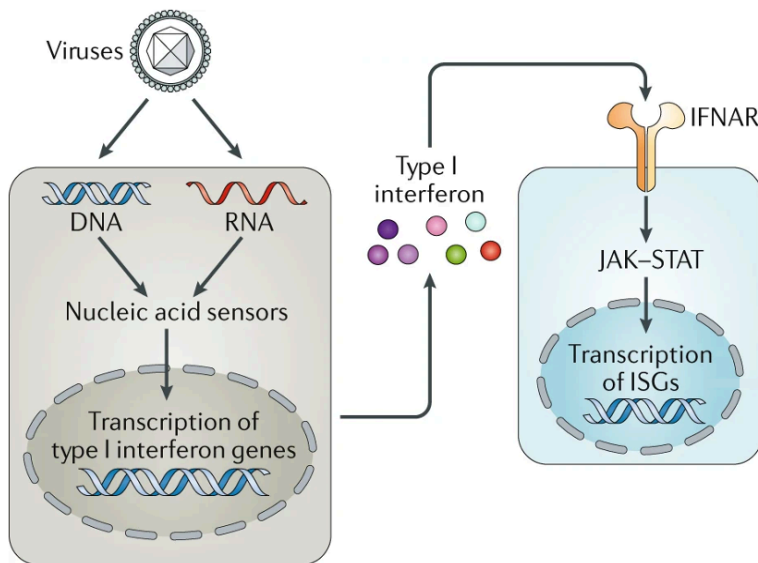


Figure 6. Viral infection can trigger induction of interferon and interferon stimulated genes.

The presence of viral nucleic acids can activate pattern recognition receptors (PRRs) within the cell resulting in the expression of interferons (IFNs). This process involves paracrine signaling, where IFNs released by infected cells can bind to neighboring cells, leading to the activation of the JAK-STAT pathway, which further enhances IFN and ISG expression. Adapted from²⁸.

ISGs, besides exhibiting a diverse array of functions, can also be activated through various distinct mechanisms, showcasing their versatile nature. For instance, they are known to be triggered by IFNs, but not exclusively¹⁰⁷. Within the Interferon-induced proteins with tetratricopeptide repeats (IFIT) family - which includes IFIT1, IFIT2, IFIT3, and IFIT5 in humans – IFIT1, one of the most relevant ISGs downstream of RLRs / TLR3 and IRFs^{58,60}, displays an interferon-stimulated response elements (ISREs) present within the first 200 bp upstream of its transcriptional start site, providing prompt and direct activation upon IFN⁶⁰. But in the case of the cytokine CXCL10, also downstream of of RLRs / TLR3, IRFs and NF κ B⁶⁰, previous studies highlighted that, besides encompassing a similar upstream regulatory sequence containing critical regulatory elements for nuclear factor- κ B (NF- κ B) and an

ISRE¹⁰⁸, it can also be potentially triggered independently from IFN and directly by RIG-I¹⁰⁹ and by dsRNA¹¹⁰.

For what concerns their antiviral functions, IFIT1 can, among the most striking ones, employ direct sequestering mechanisms against viral nucleic acids through binding of a larger protein complex encompassing other IFIT family members^{111,112}, which leads to recognition and specific bond of viral RNA bearing a 5'-triphosphate group, thereby directly inhibiting viral protein synthesis^{112,113}.

CXCL10 antiviral activities have been described to be broad and diverse as well. CXCL10 exerts a “standard” ISG role in its enhancing innate and adaptive immune responses, by promoting NK cells recruitment¹¹³ or regulating CD8+T cells³³, but holding at the same time the ability to competitively inhibit viral binding to cell surface¹¹³ or directly exerting antimicrobial effects in vitro¹¹⁴.

Countless more astonishing interferences of ISGs, towards different angles of the viral life cycles, have been reported²⁸ and are exemplified in Figure 7.

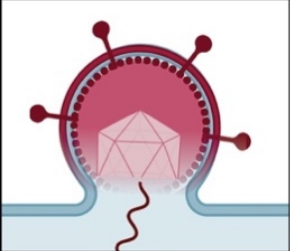
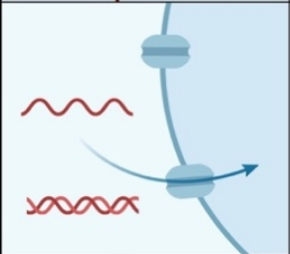
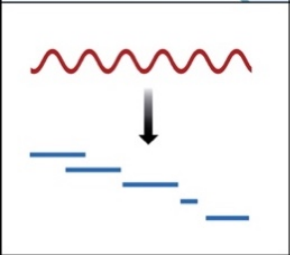
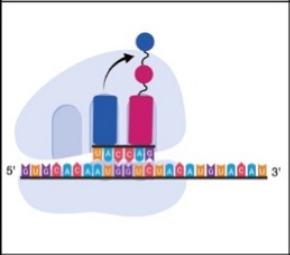
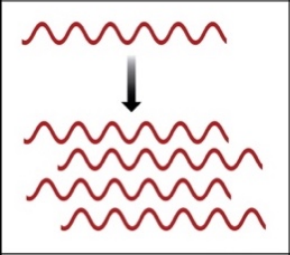
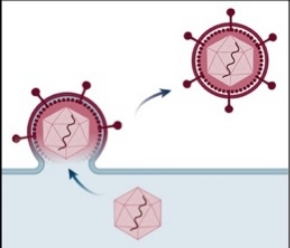
| | |
|---|---|
|  | <p>Entry CH25H IFITM1, -2, -3 NCOA7</p> <p>Post entry TRIM5α</p> |
|  | <p>Nuclear import MX1 MX2</p> |
|  | <p>mRNA synthesis APOBECs IFI16 MX1</p> |
|  | <p>Protein synthesis PKR IFIT1, -2, -3, -5 ZAP PARP12 SFLN11 SAT1</p> |
|  | <p>Replication IFI6 Viperin APOBECs</p> <p>Degradation ZAP ISG20 OAS1, -2, -3</p> |
|  | <p>Assembly/egress Tetherin CNP GBP5</p> |

Figure 7. Various interferon-stimulated genes (ISGs) target specific stages in the viral replication cycle.

The different steps of viral replication are depicted in boxes, with examples of ISG effectors that act on viral entry, nuclear import of viral genome, synthesis of viral genes or proteins, replication of viral genome, or assembly/egress of virions. Abbreviations= APOBEC (apolipoprotein B mRNA-editing enzyme catalytic polypeptide-like), ISG (interferon-stimulated gene), mRNA (messenger RNA), PKR (protein kinase R), and ZAP (zinc antiviral protein). Adapted from²⁸.

Having established a general understanding of innate immunity, in particular upon viral infections, it becomes crucial to delve into specific viruses that exemplify acute and chronic cases, as before mentioned: HAV and HCV.

These viruses not only differ in their infection outcomes, but also in their interaction with the host immune system, thus serving as ideal paradigm for further understanding the innate immune responses within hepatocytes. We will explore the unique attributes of these viruses, their replication cycles, and the specific pathologies they induce.

1.6 Hepatitis C Virus (HCV)

Hepatitis C Virus (HCV) genome was identified in 1989¹¹⁵, almost two decades after evidence of its infection in transfusions-associated hepatitis patients¹¹⁶. Despite still being a significant global health concern with an estimated prevalence of 71 million people infected worldwide, remarkable progress has been made in understanding and treating the infection¹¹⁷. The World Health Organization (WHO) has set the ambitious goal of reducing new HCV infections by 90% by 2030, aiming for complete HCV elimination¹¹⁸. However, to current day, no vaccine has been developed to protect against HCV, questioning the feasibility of this ambitious goal, and the morbidity and mortality associated with HCV-related hepatocellular carcinoma remain high, as HCV cirrhosis rates continue to rise¹¹⁹. Therefore, it is crucial to keep unraveling HCV persistence mechanisms for effective management of the disease.

HCV virus is classified into seven different genotypes. Globally, genotypes 1 and 3 are prevalent, accounting to approximately 46% and 30% of cases, respectively. Genotype 4 is prevalent in Egypt, the Middle East, and Central Africa, while genotypes 5 and 6 are commonly found in South Africa and Asia (Figure 8)¹²⁰. In patients, HCV exists as a population of heterogeneous viral mutant variants termed *quasispecies*¹²¹.

The advent of direct antiviral agents has revolutionized antiviral therapy, achieving viral eradication in over 98% of HCV-infected individuals¹²². Treatment options used to be limited to a combination of the antiviral Ribavirin and interferon (IFN)- α , an innate immune protein modified with polyethylene glycol (PEG) for stability. Yet, this treatment's efficacy varied based on virus

genotype and was coupled with severe side effects¹²³. Over the past 15 years, a significant advancement in HCV therapy has been the approval of direct-acting antivirals (DAAs) which target specific non-structural (NS) proteins of HCV, such as NS3 and NS5A/B. Examples of these DAAs include Boceprevir, VX950, Daclatasvir, and Sofosbuvir¹²⁴. The combined therapy of Sofosbuvir/IFN- α , approved by the FDA, varied in efficacy depending on the genotype. Clinical trials reported cure rates of over 90% for patients infected with genotype 2 or 4, approximately 80% for genotype 3, and only around 60% for genotype 1¹²⁴.

Recent developments include combinations of two or more DAAs, such as Sofosbuvir/Daclatasvir, used since 2015 to avoid resistance mutations. These combinations have shown a 90% clearance rate in patients, regardless of genotype¹²⁴.

A breakthrough came in 2016 when the FDA approved the combination therapy of Sofosbuvir and a new NS5A inhibitor, Velpatasvir, for patients infected with genotypes 1 to 7, paving the way for pangenotypic treatment¹²⁴.

Direct-acting antivirals (DAAs) have diversified treatment, with varied effectiveness across genotypes, and some resistance has emerged, particularly with genotype 1a. Response rates and treatment durations are generally lower and longer respectively for genotypes 2 and 3, and genotypes 5, 6, and 7 are less studied due to their localized prevalence.

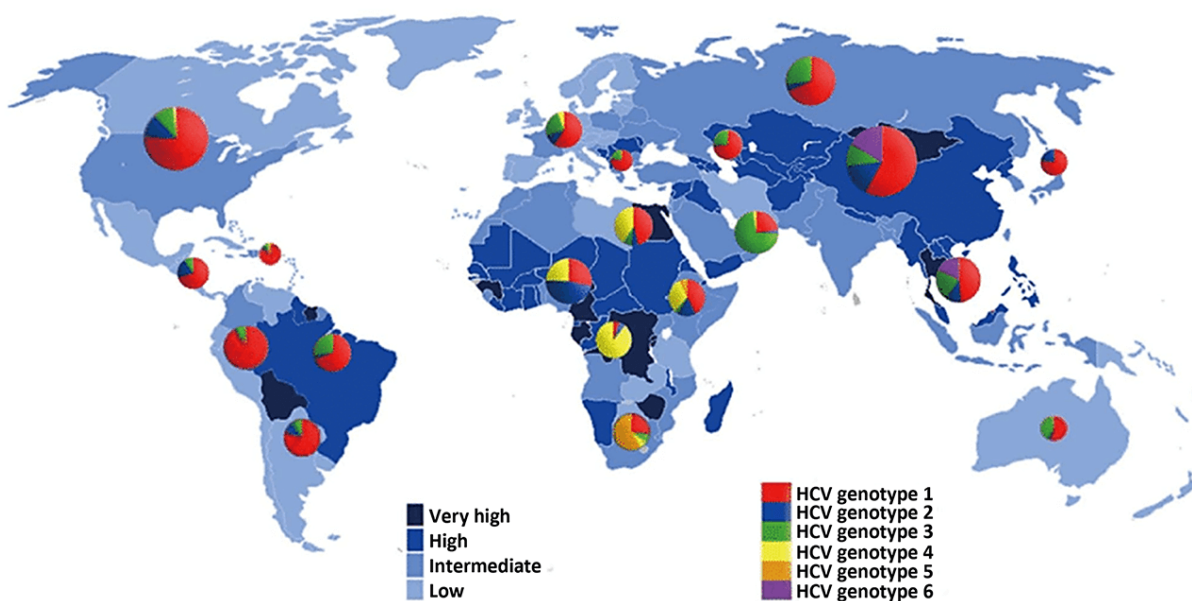


Figure 8. Distribution of HCV-infected patients categorized by genotype and global burden of disease (GBD) region. The HCV dominant genotypes differ regionally; genotypes 1a and 1b are most prevalent in Western Europe and the United States, followed by genotypes 2 and 3. In contrast, other genotypes have limited geographical distribution; genotype 4 is chiefly observed in Egypt, genotype 5 in South Africa, and genotype 6 is primarily found in Southeast Asia. Adapted from¹²⁵.

HCV is a member of the *Flaviviridae* family. The virion has a diameter of 55-65 nm and features a lipid-rich envelope, surrounding a putatively icosahedral capsid containing a single-strand (ss) + RNA genome. The genome is approximately 9600 nucleotides long, includes two non-translated regions (NTRs) at the 5' and 3' ends, and encodes a single polyprotein, as illustrated in Figure 9. Since the genome is not capped, an internal ribosomal entry site (IRES) resides in the 5'NTR, facilitates translation. Viral and cellular proteases process the polyprotein, resulting in the production of various components which can be divided in two groups: the structural proteins, being physical components of the virion, and the nonstructural (NS) proteins. The structural proteins encompass the core protein, which constitutes the nucleocapsid, and the envelope glycoproteins (E1 and E2) which exhibit high variability, contributing to the virus' antigenic diversity¹²⁶. Assembly and egress of infectious virus particles require almost all structural and nonstructural proteins^{127,128}. However, p7, acting as an ion channel in lipid membranes¹²⁹ and NS2, a cysteine proteinase participating in cleavage of the NS2-3 junction^{130,131}, are of particular importance for viral assembly and egress and do not contribute to genome replication¹³².

The nonstructural proteins from NS3 to NS5B assemble into a membranous replicase complex that forges the amplification of the viral RNA genome^{133,134}. NS3 has several crucial roles, displaying serine protease activity at the N-terminal domain, that needs NS4A for activation and membrane association, and a C-terminal domain characterized by NTPase/helicase activities essential for RNA replication, besides a clear role in counteraction of innate immune responses which will be examined later in detail¹³⁵⁻¹³⁸; NS4B triggers membrane remodeling and modulates the organization of the membrane-associated viral replication complex^{136,139,140}. NS5A, a highly phosphorylated protein, is necessary for both RNA replication and virus assembly. Lastly, NS5B is the viral RdRp (RNA-dependent RNA polymerase)^{136,140}.

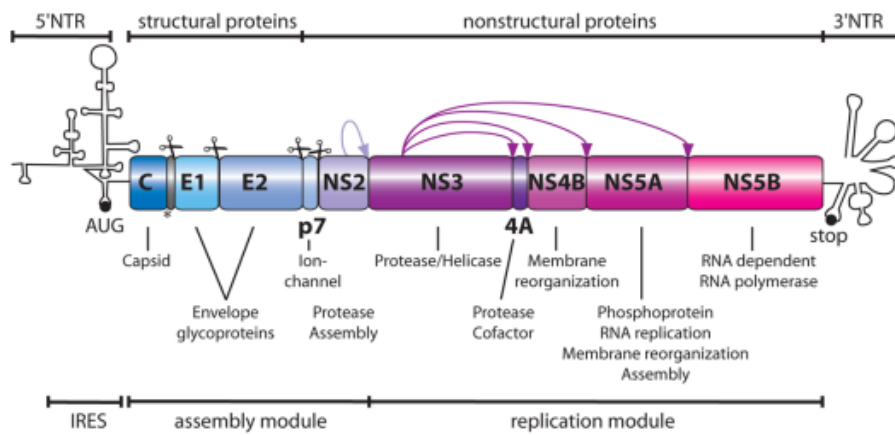


Figure 9. HCV genome organization.

The 5' and 3' non-translated regions (NTRs) are represented by their hypothesized secondary structures, while the coding regions with structural and non-structural proteins are indicated by boxes. The viral polyprotein is processed by viral (represented by arrows) and cellular (denoted by scissors) proteases, and roles are indicated for the single deriving proteins. Adapted from ¹⁴¹.

Primarily, HCV is transmitted through blood-mediated routes, which means it infiltrates the body's circulatory system. Once HCV reaches the liver sinusoidal endothelium, it binds to entry receptors expressed by hepatocytes and B lymphocytes, as well as to low-density lipoprotein (LDL) receptors, since the virion is LDL-associated¹⁴². The bond of Hepatitis C Virus (HCV) particles with host lipoproteins benefits the virus in two main ways: firstly, these lipoproteins potentially conceal the viral epitopes of E1 and E2 proteins, enabling the virus to evade detection by the humoral immune system. Secondly, they promote the liver-specific targeting (*hepatotropism*) of HCV¹⁴³. This process involves the attachment of HCV to the hepatocytes via Apolipoprotein-E (Apo-E) and/or Apolipoprotein-B (Apo-B), which interact with cellular components like the low-density lipoprotein receptor (LDLR) to facilitate viral entry¹⁴⁴. This happens thanks to a complex multistep process involving several host cell proteins, including Cluster of Differentiation 81 (CD81) and Scavenger receptor (SR)-BI, both directly interacting with E2, as well as the tight-junction proteins Claudin 1 (CLDN1), and Occludin (OCLN), all of which are required for successful HCV uptake¹⁴⁵⁻¹⁴⁸. After fusion with the endosomal membrane, the HCV capsid disassembles, releasing its positive-sense RNA from endosomes (Figure 10, a). This functions as mRNA, engaging ribosomes for direct translation initiated by the IRES, leading to the production of a polypeptide of about 3,000 amino acids (Figure 10, b) that undergoes proteolytic cleavage by the cellular and the forementioned viral proteases¹⁴⁹ (Figure 10, c). A concerted action of NS proteins NS3-5B with several host factors, including lipids^{133,150,151}, induce the formation of viral replication organelles, mainly consisting of Double Membrane Vesicles (DMVs), at the endoplasmic reticulum (ER)

(Figure 10, d). Viral genome replication is associated with these replication organelles, after which the viral RNA-dependent RNA polymerase NS5B amplifies the viral genome, first by synthesizing a negative stranded complementary genomes, which results in a dsRNA replication intermediate. Importantly, the dsRNA acts as template for synthesis of new positive stranded (+)RNA viral genomes and, at the same time, can be sensed by innate immunity. The membrane association of the viral replication complex is regarded in part as a way to disclose sensing of dsRNA from PRRs. The replication process of hepatitis C virus (HCV) is intricately intertwined with host lipid metabolism at various stages¹⁵², but also other cellular host factors have been shown to be involved in HCV replication, such as cyclophilin A (CypA), SEC14 Like Lipid Binding 2 (SEC14L2)¹⁵³, phosphatidylinositol 4-kinase III alpha (PI4Ka)¹⁵⁴ and microRNA-122 (miR-122)¹⁵⁵.

In the final stages of the HCV lifecycle, the newly synthesized HCV (+)RNA genomes and structural proteins assemble into nascent virions. Viral assembly is thought to be regulated by phosphorylation of NS5A¹⁵⁶, culminating in the delivery of (+)ssRNA genomes to core protein on cellular lipid droplets (LDs)¹⁵² (Figure 10, e), where the process of viral assembly occurs, forming the nucleocapsid. The HCV capsids bud into the ER and acquire a host cell-derived envelope¹³². Eventually, the viruses leaves the cell, exploiting the secretory pathway and associating closely with the Very Low Density Lipoprotein (VLDL) synthesis pathway¹⁵⁷ (Figure 10, f). Autophagy was also shown to be involved in facilitating the release of the virus from infected hepatocytes through an exosome-mediated mechanism¹⁵⁸, aided by the ESCRT system¹⁵⁹.

As a result, HCV virions circulate in the bloodstream, complexed with host lipoproteins.

HCV can also spread directly from cell to cell *in vitro*, requiring fewer of the above mentioned host factors¹⁶⁰.

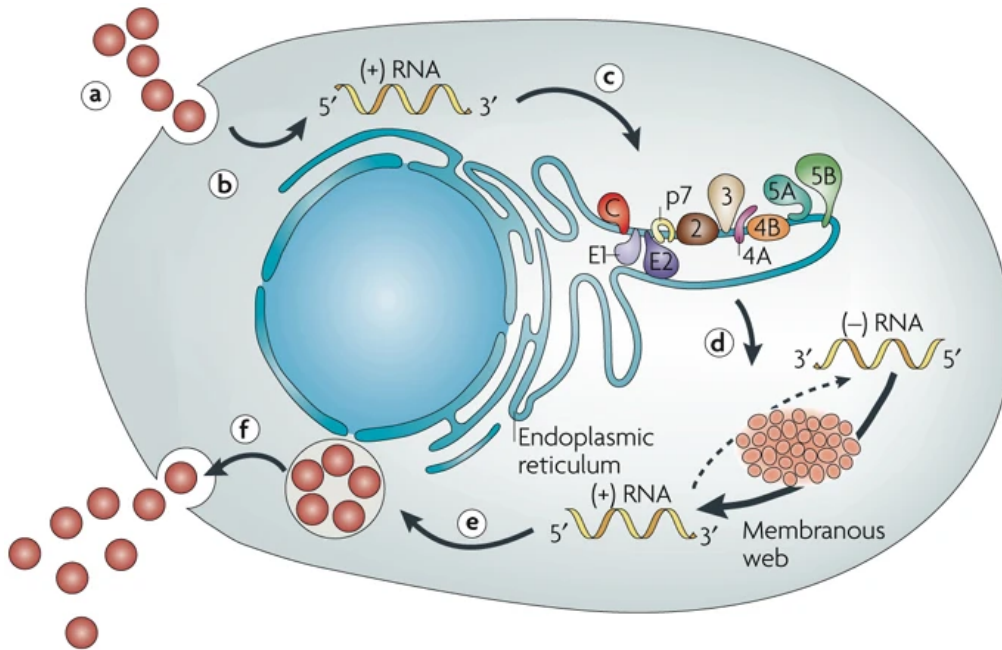


Figure 10. HCV replication cycle.

Hepatitis C virus (HCV) enters host cells via clathrin-mediated endocytosis, where the virus envelope fuses with the endosomal membrane in a low pH environment, releasing the HCV RNA genome into the cytosol. The RNA genome then undergoes translation at the endoplasmic reticulum by host ribosomes to generate a membrane-bound polyprotein, which is subsequently processed into structural and non-structural proteins. These proteins, along with host factors, assemble the HCV replication complex within a virus-induced specialized cytosolic compartment, the membranous web, where viral genome amplification occurs. Adapted from¹⁴⁰.

1.7 Hepatitis A Virus (HAV)

Hepatitis A virus (HAV) is a non-enveloped (+) ssRNA virus as well, 27 to 32 nm diameter in size, classified within the Hepatovirus genus of the *Picornaviridae* family, causative agent of Hepatitis A. This is an acute, self-resolving liver disease ranging from asymptomatic cases or mild liver inflammation and jaundice in absence of complications, to severe liver damage, in the rare scenarios of fulminant hepatitis which happens in 0,02% of the infections in adults¹⁶¹.

HAV is endemic in many developing countries, while developed countries experience occasional outbreaks^{162,163}. HAV genotypes I, II, and III infect humans, with genotype I subtype IA being most common worldwide. Subtype IB is prevalent in the Middle East and South Africa, while genotype III, subtype IIIA, is found in Asia and Europe (Figure 11).

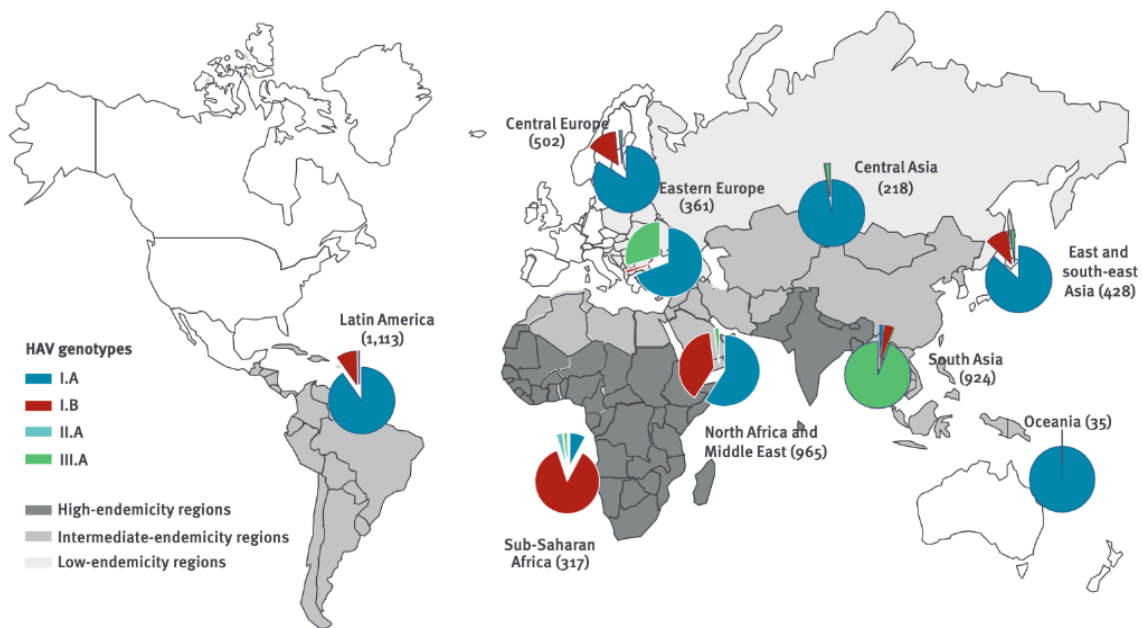


Figure 11. Distribution of human hepatitis A virus genotypes over the endemic Global Burden of Disease regions. Data relative to 2010–2017 (n = 4,863) HAV genotypes I, II, and III are further subcategorized into A and B subtypes. HAV genotype I is the most widespread, with subtype IA predominant in South America, Europe and Asia, and subtype IB mainly found in the Middle East and Sub-Saharan Africa. While genotype II is less common, genotype III is circulating in Asia and Europe. Adapted from ¹⁶⁴.

Parenteral and sexual transmission of HAV is infrequent¹⁶⁵, while HAV has been also found transmitted among drug users¹⁶⁶. Remarkably, the HAV capsid demonstrates exceptional resistance compared to other picornaviruses. In terms of environmental persistence, HAV's genetic material has been shown to survive up to 232 days in water or saltwater, especially if at low temperatures (<4°C), resist detergents, endure temperatures up to 60 °C, and tolerate highly acidic (pH 1) conditions¹⁶⁷.

Even if HAV is not considered a threat to current days, because of the high rate of resolved infections, its spreading potential requires attention in underdeveloped countries as well as in context with immunocompromised patients. Therefore, efforts have been conducted in antiviral drug research for HAV, but for its peculiarities, which set HAV apart it from the other members of *Picornaviridae*¹⁶⁸, to this day no specific antiviral therapy is approved.

Looking at its structure, HAV's single-stranded, positive-sense RNA genome, approximately 7,500 nucleotides in length (2000 less than HCV) is contained in an icosahedral capsid organized in distinct polypeptides: VP1, VP2, VP3 and VP4 (Figure 12).

Upon binding to the host cells and receptor mediated endocytosis, the virus undergoes a conformational change which permits the viral RNA to penetrate the endosomal membrane via a channel that forms upon displacement of VP1 and release of VP4. The RNA is infectious, acting as mRNA and allowing direct translation of the single polyprotein. The long NTR at the 5' end contains a type III IRES¹⁶⁹, and has a viral protein (VPg) instead of a methylated nucleotide cap structure, while the shorter 3' NTR is polyadenylated and is important in (-)strand synthesis. The viral polyprotein is initially processed by the viral proteinase 3C into three precursor proteins, P1, P2, and P3. The primary cleavage products are then subjected to further processing by the 3C protein, a cysteine proteinase. In contrast to other Picornaviruses, who exhibit proteolytic activity through 3C and 2A, HAV's sole protease is the 3C¹⁷⁰. HAV 3C processes the precursor P1 to yield the structural proteins, and precursors P2 and P3 into the VPg and the non-structural proteins¹⁷¹. The same 3C protein also reaches maturation through autoprocessing, giving rise to several precursors in a hierarchical process: 3ABCD, which in turn liberates 3ABC and 3CD and, through a further cleavage, 3C¹⁷². These 3C intermediate species have been shown to have a certain stability, not only exhibiting an exclusive proteolytic activity, with different substrate cleavage site preference compared to the final product 3C¹⁷²⁻¹⁷⁵ but also binding to viral RNA, thereby influencing viral genome replication¹⁷⁶.

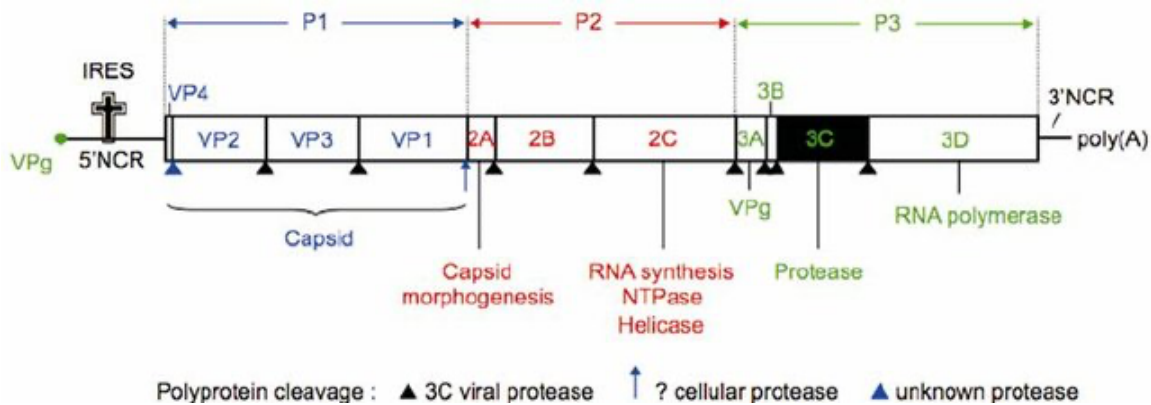


Figure 12. HAV genome organization.

The capsid polypeptide is composed of three structural protein components in the precursor (P) 1 section, including VP2, VP3, VP1, contributing to capsid formation (in blue) and nonstructural ones, between P2 and P3, namely 2A, 2B, 2C, 3A, 3B, 3C, 3D, essential for viral replication (in red and green) with the exception of 2A, participating to capsid morphogenesis. 3A serves as an anchor for the replication component to the cell membranes; 3B (VPg) acts as a primer during RNA synthesis. 3C acts as a cysteine protease that breaks down polypeptides into proteins (black triangles), while 3D functions as an RNA-dependent RNA polymerase. Adapted from¹⁷⁷.

The different protease specificities in terms of substrate binding are related to the activity of the single proteins constituting the intermediate complexes. 3ABC shows membrane anchoring

activity driven by the 3A domain¹⁷⁸, while 3D was discussed being able to redirect the 3C catalytic triad for the precursor 3CD¹⁷³.

HAV entry is not as well characterized as HCV's. Initially, TIM1 (T cell immunoglobulin mucin receptor 1) - which was known to be an entry factor for Tick-Born-Encephalitis-Virus (TEBV)¹⁷⁹ as well as for Ebola Virus (EbV)¹⁸⁰ - was considered to be the receptor for HAV, and thus also re-termed as HAV cellular receptor 1 (HAVCR1)¹⁸¹. However, a new study neglected its essential role and reframed the protein as only "supportive"¹⁸². On the other hand, recently gangliosides have been proposed as critical molecules that promote HAV entry by enabling the lysosomal escape of HAV particles¹⁸³.

The HAV replication cycle is summarized in Figure 13. Upon binding, entry and uncoating, the virus releases its genome and undergoes direct translation of its RNA, which acts as mRNA as for HCV. The translation initiation is cap-independent and relies on an IRES unique to HAV, requiring initiation proteins like eIF4E and intact eIF4G; therefore, unlike other picornaviruses, HAV infection does not block cap-dependent host protein synthesis by cleaving eIF4G (cleavage which by other members of *Picornaviridae* is processed by the 3C protease)¹⁷⁰. However, HAV displays highly deoptimized codon usage, probably causing the resulting slow translation rate observed, which might contribute to the high stability of viral capsid¹⁸⁴.

The initiation of translation from the HAV IRES is further enhanced by sequences in the 5' terminal coding region and cellular poly(A) binding protein (PABP). The process involves interactions with host cellular proteins, like poly(C) binding protein 2 (PCBP2), polypyrimidine tract binding protein (PTB), and glyceraldehyde 3-phosphate dehydrogenase (GAPDH), but their exact role remains uncertain¹⁸⁵.

During translation, the polyprotein is proteolytically processed by the viral 3C protease, which differs from other picornaviruses as it lacks additional cellular substrates, as for instance the forementioned eIF4G, the La autoantigen, PTB, TBP and TFIIC¹⁸⁶. Following translation, the nonstructural proteins spanning 2B to 3D induce the assembly of a replication complex on membranes derived from the endoplasmic reticulum. Proteins 2B, 2C, and 3A are reported to contribute to structural rearrangements of intracellular membranes¹⁸⁷.

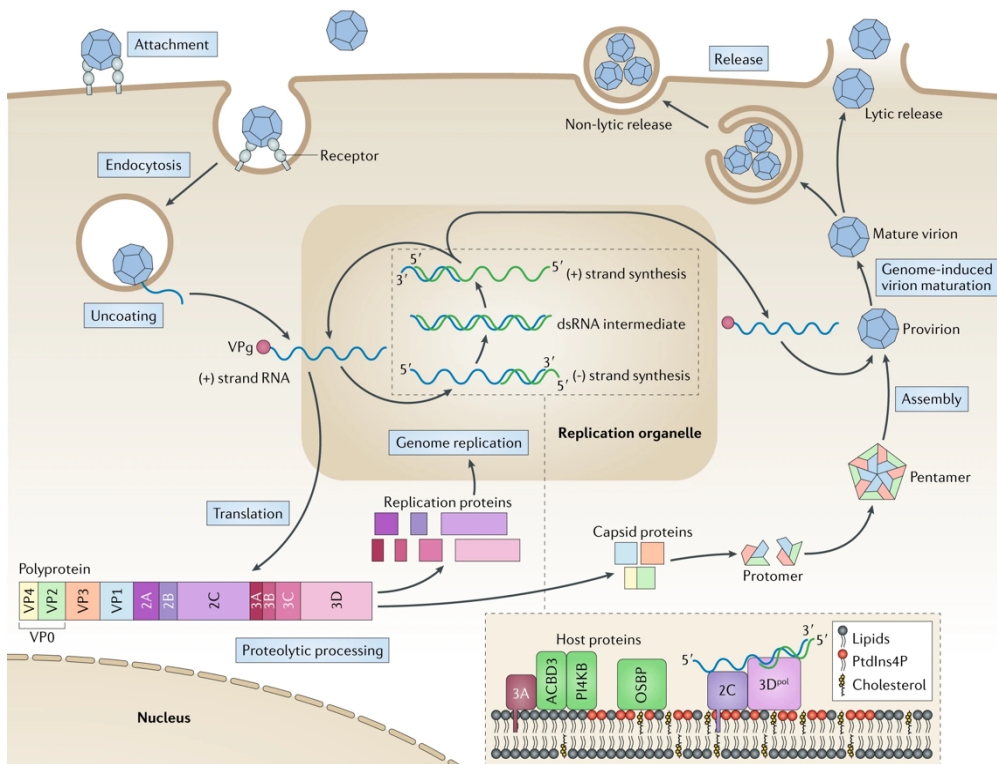


Figure 13. HAV replication cycle.

Once the virion attaches to its receptor or receptors and is taken up by the cell via endocytosis, it translocates its positive-strand (+) RNA genome across the endosomal membrane and into the cytoplasm. This viral genome is chemically attached to the viral protein VPg (3B), a necessary primer for replication. Translation of the viral genome produces a single polyprotein, which is then proteolytically split into proteins for replication (2A–2C and 3A–3D) and capsid proteins (VP0, VP1, and VP3). Replication of the genome, facilitated by the virus's RNA-dependent RNA polymerase (3Dpol), begins with the creation of a negative-strand (–) RNA, serving as a template for new (+) RNA molecule synthesis. This replication occurs on membranous replication structures, where a suitable lipid environment is created by viral proteins 2BC and 3A, with support from host proteins ACBD3, PI4KB (which synthesizes PtdIns4P), and OSBP (which brings in cholesterol). Newly synthesized (+) RNA molecules can either engage in a new round of replication or be incorporated into offspring virions. Capsid proteins arrange themselves into protomers and pentamers. Alongside the replication machinery and genomic RNA, these assemble into virions that transform into infectious, mature virions following the genome-triggered cleavage of VP0 into VP4 and VP2. These mature virions then exit the host cell either through non-lytic extrusion of extracellular vesicles or through cell lysis in the later stages of infection. Adapted from¹⁸⁸.

The replication process of the viral RNA is facilitated by a viral RdRP (the 3D protein)¹⁶⁹. Viral RNA synthesis is protein-primed, with the uridylylated VPg protein 3B acting as the primer for production of the negative-sense RNA replication intermediate, leading to formation of dsRNA, which is, as for HCV, pivotal in innate immune sensing and subsequent positive-sense genomic RNA synthesis¹⁶⁹. The 5' terminal NTR structures are suggested to be involved in switching from translation to replication on the same viral RNA¹⁸⁸.

HAV replication has been shown to depend on fewer host factors compared to HCV; a recent study highlighted the role of ZCCHC14, which binds a small stem-loop in the HAV 5' untranslated

region, while the protein TENT4 polymerases lengthen and stabilize the 3' poly(A) tail of HAV viral RNA¹⁸⁹; previously, a possible dependence on Cyclophilin A was also suggested¹⁹⁰.

HAV replication cycle ends with non-lytic release; until recently, given that the HAV virions shed in stool were found to exclusively naked, non-enveloped virions, the capacity of the virus to acquire a so-called *quasi-envelope* was not demonstrated. In a recent study the enveloped HAV form (eHAV) was found to circulate predominantly in the blood of infected humans and chimpanzees and to be nearly absent in fecal samples¹⁹¹. The eHAV has a unique, lighter buoyant density and appears to be shielded from adaptive immune detection, unless treated with detergent. But on the other hand, innate immune cells as pDCs have been shown to sense exclusively eHAV¹⁹². Importantly, disruption of its envelope significantly reduces eHAV infectivity, suggesting its vital role in a distinct viral entry pathway¹⁹¹. The cellular endosomal sorting complex required for transport (ESCRT) proteins ALIX and VPS4B play a role in the budding of quasi-enveloped eHAV particles, allowing their nonlytic release similar to exosome biogenesis. The process involves the interaction of ALIX with specific VP2 domains in the capsid, leading to eHAV envelopment and release¹⁹³.

The viral particles that are then released from the liver are excreted into the bile duct and transported into the gastrointestinal tract, ultimately being shed in the feces, with the highest viral shedding occurring during the final stages of the incubation period¹⁶⁹. HAV's resistance to inactivation by bile and intestinal proteolytic enzymes facilitates its survival in feces, thereby enabling fecal-oral transmission commonly through ingestion of contaminated water or food, particularly bivalve mollusks such as oysters, clams, or mussels that filter water containing fecal matter harboring the virus^{194,195}. HAV primarily replicates in the liver; however, evidences of extrahepatic sites of replication have been brought on by previous studies, as salivary glands and lymphnodes¹⁹⁶ as well as the gut¹⁹⁷.

Even if HAV is not considered a threat to current days, because of the high rate of resolved infections, its spreading potential requires attention in underdeveloped countries as well as in context with immunocompromised patients. Therefore, big efforts have been conducted in antiviral drug research for HAV, but for its peculiarities, which set HAV apart it from the other members of *Picornaviridae*, to this day there is very limited choice of options.

Despite HAV encoding an evolutionary well conserved 3C proteinase (3C^{pro}) shared by a high number of other viral families (*Enteroviridae*, *Caliciviridae*, *Picornaviridae*, *Coronaviridae*)^{170,198,199}, broad antiviral peptidomimetic drugs targeting the 3C to this day have not been effective against HAV. A study originating from our lab has been shown effectiveness in inhibiting HAV subgenomic replication by using the milk thistle-derived Sillibinin, whose mode of action is still unrevealed, and the immunophilin Cyclosporin A, even though with low efficiency¹⁹⁰; only recently, upon discovery of the host factor required for replication ZCCHC14/TENT4, the dihydroquinolinone compound RG7834 has been shown the potential to ablate viral replication and reverse liver inflammation in a mouse model of hepatitis A²⁰⁰.

On the other hand, various hepatitis A vaccines are commercially available already from the early 90s, with different manufacturing specifications, mostly based on either an inactivated hepatitis A virus produced in human fetal lung fibroblast cells MRC-5 cells (available also in combination with hepatitis B vaccine), or on the hepatitis A antigen into virosomes, combined with synthetic lipids and influenza proteins²⁰¹⁻²⁰⁴.

To summarize, HCV and HCV possess distinct similarities in the ways their genomes are organized and replicate: however, to understand how two relatively comparable hepatotropic viruses can give rise to strikingly opposed infection scenarios, it is now noteworthy to have closer look at their complex interplay with the host immune system.

1.8 HCV and immunity

As mentioned beforehand, HCV infection is primarily detected by cytosolic PRRs, namely the RIG-I-like receptors – the role of RIG-I is universally recognized, but for MDA5 there are controversial reports^{68,205,206} - and by TLR3^{68,207-209}. This activation, which leads to IFNs and ISGs expression, has been observed in cell culture as well as in vivo in chimpanzees and human patients²¹⁰⁻²¹².

Antiviral defenses against HCV infection are rapidly initiated, yet approximately 70% of HCV-infected patients fail to effectively control the virus and develop chronic infection, highlighting the virus's ability to impair host innate immunity^{208,213}. HCV's proteins, including core, E2, NS3-4A, and NS5A, play multifunctional, essential roles during infection, including essential roles in immune evasion, summarized in Figure 14.

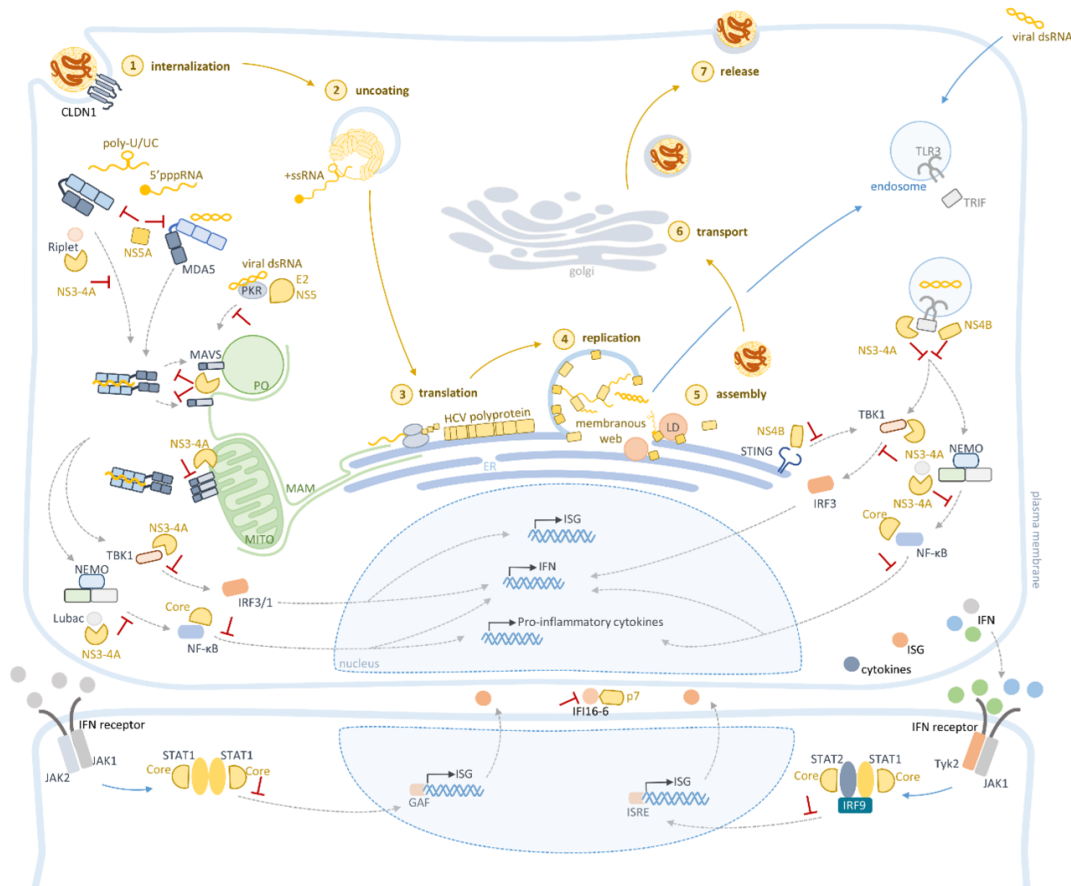


Figure 14. Interplay of the intracellular innate immunity response with HCV.

Viral RNA is recognized by the cytosolic sensors retinoic acid-inducible gene-I (RIG-I), melanoma differentiation-associated protein 5 (MDA5), and protein kinase R (PKR), as well as the pattern recognition receptor on the membrane, toll-like receptor 3 (TLR3). This recognition triggers the downstream activation of interferons (IFNs) and leads to the production of proinflammatory cytokines, thus activating the internal innate immune system in response to HCV. Several HCV proteins are described to be involved in interfering to innate immunity: NS3-4A, E2, NS5A, NS4B, p7, and core target several steps of the PRRs signaling. Adapted from²¹⁴.

The contribution of NS3 to innate immune escape is of great relevance and deserves special attention. NS3 is a non-covalent heterodimer consisting of a catalytic subunit (the N-terminus of NS3 protein) and an activating cofactor (NS4A), cleaving at four sites of the HCV polyprotein¹³². The initial 21 amino acids of NS4A create a transmembrane alpha-helix, while the amphipathic helix alpha in NS3's residues 12-23 ensures the serine protease's correct membrane positioning. From this cooperation results the capacity of NS3-4A to associate to membranes²¹⁵ including the mitochondrion-associated endoplasmic reticulum (ER) membrane (MAM), where RIG-I is recruited to bind MAVS²¹⁶. MAVS is cleaved at Cys508 in a NS3-4A canonical cleavage site, defined by the analysis of sequence requirement for the HCV polyprotein cleavage²¹⁷. Here, HCV disrupts downstream signaling thereby impairing the expression of IFNs and ISGs^{135,137,213,218-220}. Interestingly, NS3-4A has been described to cleave the adaptor protein TRIF as well, associated

with TLR3, thereby suppressing IFN and ISG expression¹³⁸. However, the TRIF molecule displays only a limited homology to a NS3-4A canonical cleavage site²²¹ and the cleavage of TRIF by HCV was promptly disputed by another study²²². MAVS cleavage is instead well understood and described to be critical for inhibiting the host's initial antiviral response, possibly preventing excessive inflammation or delaying immune cell-mediated defense^{137,219}; besides its relevance in innate immunity, the MAVS cleavage site by HCV was also manipulated to be used as a tool to monitor HCV infection, already for more than a decade²²³.

Beyond its impact on these primary adaptor proteins, NS3-4A inhibits other components of the cellular innate immune response. For instance, the NS3 helicase domain binds to TBK1, a kinase activated by the activation of RLRs or TLR3, inhibiting its interaction with IRF3, which consequently impairs the induction of IFN expression²²⁴. NS3-4A also targets Riplet, an E3 ubiquitin ligase, essential for RIG-I activation. This targeting leads to the reduction of endogenous Riplet levels and inhibition of RIG-I polyubiquitination²²⁵. Furthermore, NS3-4A is linked to the inhibition of NF- κ B activation, although the exact mechanism remains unclear, and has also been reported to promote the degradation of STAT1. These multifaceted interactions aid in HCV persistence, as they potentially contribute to subdued inflammatory and immune responses^{137,214}.

Moreover, HCV has been suggested to manipulate PKR through its NS5A and E2 proteins^{226,227}, affecting the production of IFN- β and ISGs. NS5A can also interact with nucleosome assembly protein 1-like 1 (NAP1L1)²²⁸, which influences various host pathways, including transcription or cell cycle progression. Sequestering NAP1L1 results in reduced transcription of key genes essential for innate immunity, such as RIG-I- and TLR3-mediated responses^{137,227}. The role of the HCV core protein in immune evasion remains contentious, especially regarding its function on the NF- κ B pathway. While some studies suggest core protein overexpression blocks this pathway to suppress inflammatory responses²²⁹, others report that the core protein actually activates the NF- κ B pathway to induce inflammation²³⁰. The core protein also interferes with the JAK/STAT pathway required for cellular responses to IFN-mediated stimulation, but the exact mechanism is disputed²³¹. The p7 protein, a viral membrane-spanning protein necessary for virion production, was found to interact with IFI16-16, an ISG highly inducible upon type I IFN treatment of viral infections, inducing depolarization of mitochondrial membrane potential to inhibit its function²³². Finally, HCV is known to alter host microRNA (miRNA) expression to impact various host functions. It induces miR-208b and miR-499a-5p expression, which hinders the expression of IFNL3,

supposed in aiding HCV to evade innate immunity²³³. Additionally, HCV induces selenoprotein P (SeP), an hepatokine (protein secreted by the liver, which acts as an hormone) linked with insulin resistance and type 2 diabetes, which binds and inhibits RIG-I activity²³⁴. However, the process behind SeP upregulation remains uncertain²³⁴.

Importantly, an alternative escape mechanisms from innate immune recognition has been recently reported and it bases on HCV's ability to keep the intracellular replicative intermediates at a low level through extracellular secretion of dsRNA and consequent lowered TLR3 activation⁸³.

Taking into account the numerous actions here described, targeting the early events after infection, it does not come as a surprise that HCV manages to partially escape the innate immune response and establishes a persistent infection in $\frac{3}{4}$ of the cases. However, the phenotype is not black and white and many aspects of the way the host deals with acute and chronic HCV are not well understood: for example, despite the protein-mediated abrogation, during acute HCV infection there is a notable delay in the appearance of HCV-specific T cells, with the reason for this delay remaining unknown²³⁵. The presence of these T cells, especially CD8+ T cells, and IFN γ expression in the liver are pivotal for the outcome of acute HCV infection, with a strong CD8+ T cell response associated with the spontaneous resolution of the disease^{161,208}. However, the effectiveness of these cells can be negated by virus escape mutations, indicating that the breadth of the HCV-specific CD8+ T cell response, targeting multiple epitopes, is crucial to overcome the emergence of these mutants^{236,237}. CD4+ T cells also play a vital role in spontaneous HCV resolution, with their loss leading to diminished HCV-specific CD8+ T cell responses, and recent studies show that an increased frequency of T regulatory cells (Treg cells) and a decrease in IL-21-producing CD4+ T cells correlate with CD8+ T cell dysfunction in patients who develop a chronic HCV infection¹⁶¹.

During an HCV chronic infection, instead, IFNs and ISGs are expressed, despite viral interference mechanism, as shown in HCV-infected patients²¹⁰; further in vivo studies on chimpanzees confirm robust upregulation of ISGs upon HCV infection, although not in the context of a HCV persistent infection^{211,212}. Several mechanisms have been proposed to explain the sustained expression of ISGs upon HCV. A transcription factor complex called unphosphorylated ISGF3 (U-ISGF3), formed by high protein levels of STAT1, STAT2, and IRF9 without tyrosine phosphorylation of the STATs, plays a crucial role in the augmented innate immune response¹⁰⁵. However, this persistent ISG

expression negatively impacts spontaneous virus clearance and interferon-alpha (IFN α)-based treatment response, particularly in patients with high liver ISG levels²³⁸. Ubiquitin-specific peptidase 18 (USP18), an ISG that interacts with IFNAR2 and blocks downstream signals initiated by IFN α , has been highlighted as a significant factor in the unresponsiveness to IFN α ²³⁹. Additionally, ISG15, one of the most abundantly expressed ISGs in HCV-infected livers, stabilizes the USP18 protein and causes resistance to external IFN α treatment. This response to IFN α -based therapy is also profoundly affected by the recently identified IFNL4 genotype, which correlates HCV resolution to the specific expression of a Single Nucleotide Polymorphism (SNP) in the IFNL-dG allele^{240,241}.

Even though the current drug therapies for HCV are very effective, the disease's propensity for chronicity and its potential to cause liver cancer underscore the urgent necessity for further research. A look at HAV which, instead, gets cleared by the host and does not lead to persistence, might elucidate pivotal factors in the interplay between HCV and the immune response.

1.9 HAV and immunity

Since the Hepatitis A Virus (HAV) genome has a covalently linked 5' VPg, recognition by RIG-I is unlikely, as this PRR typically identifies RNAs with free 5' triphosphate²⁴². Instead, MDA5 sensing, typical for Picornaviruses, has been already confirmed for HAV⁶⁵, while the function of LGP2 during HAV infection hasn't been thoroughly studied²⁴².

HAV-infected chimpanzees display a poor innate immune response, based on transient pDCs appearance and lack of ISGs²¹²; this has been quickly associated with HAV's ability to interfere with the innate immune response, which is attributed to different HAV proteins and was discussed in numerous studies (Figure 15).

HAV protease precursors 3ABCpro and protein 2B have been found able to disrupt the MAVS-mediated pathway, thus hampering IFN β ^{243,244} induction. The 3ABC cleavage of MAVS was described to require both the protease activity of 3Cpro and a transmembrane domain in 3A that directs the 3C precursor 3ABC to the mitochondria. The non-structural HAV 2B protein was hypothesized to interact with MAVS thereby disrupting the activity of the TBK1/IKK ϵ kinases^{245,246}. However, further investigation is required to comprehend the exact mechanism of this protein. The TLR3 signaling pathway, instead, solely mediated by the TRIF adapter, seems to be another target for the 3C precursor; TRIF was shown to be proteolytically cleaved by 3CD, but not by the mature 3Cpro protease or the 3ABC precursor that were reported to degrade MAVS^{173,208}. 3CD-mediated degradation of TRIF was thought dependent on both the cysteine protease activity of 3Cpro and the downstream 3Dpol sequence, but not on 3Dpol polymerase activity^{173,208}. Furthermore, proteolytic cleavage of NEMO by 3Cpro has been evidenced as well, directly contributing to the inhibition of IFN- β transcription, as NEMO has been shown to bridge the TLR3-IRF3 pathway¹⁷⁴. Last but not least, recently it has been reported that infection with HAV triggers an increase in the expression of the microRNA hsa-miR-146a-5p, which would target and degrades TRAF6 mRNA; this was subsequently associated to a reduction of IFN- β synthesis and boosting of virus replication²⁴⁷.

HAV's host range, limited to humans and non-human primates, is thought to depend on its ability to evade MAVS-mediated type I IFN responses^{248,249}. MAVS-dependent, RLR-induced²⁴⁷ IFN

responses are more effective in restricting HAV replication than TLR3, despite HAV targeting both signaling pathways²⁴⁹. HAV's inability to infect small mammals could be due to its inability to disrupt IFN responses. Notably, while type I IFNs play a key role in restricting HAV infection in mice, type III IFNs are predominant in human hepatocytes²⁵⁰.

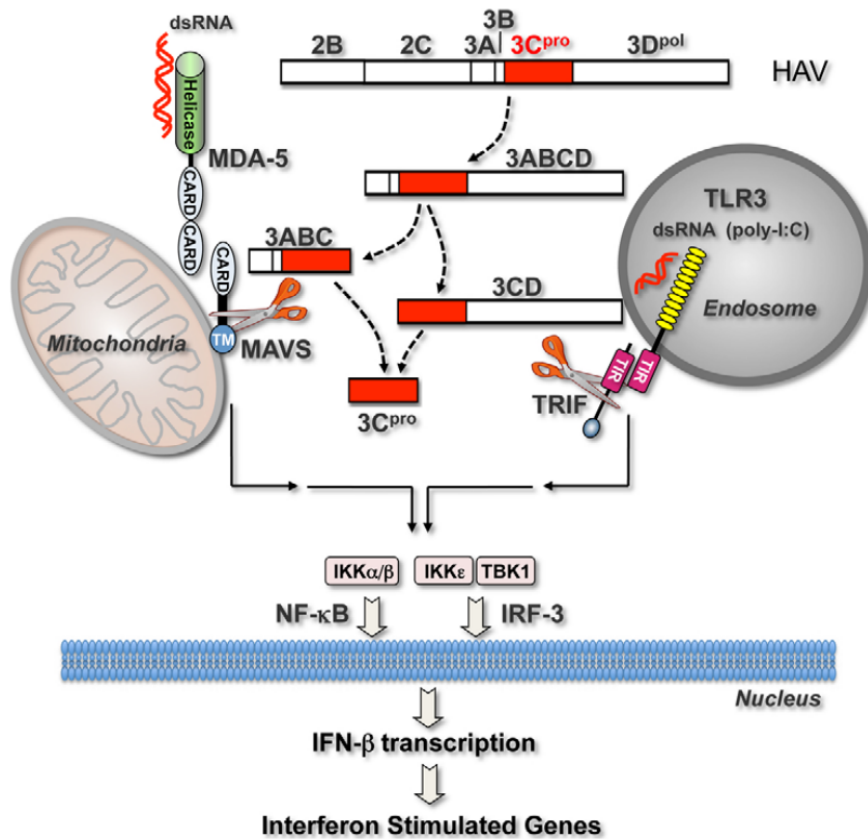


Figure 15. Current knowledge of HAV-mediated interference to the host innate immune response.

This figure presents our current understanding of how Hepatitis A virus (HAV) counteracts the host's immune response. The protease precursors in HAV have been found capable to ablate the RLRs and TLR3 pathways through the proteolytic cleavage of MAVS and TRIF, respectively, resulting in diminished IFN and ISGs. While the formation of the HAV polyprotein is also mediated by the cleavage action of the 3C protease, the different products of this process are capable of interfering with the immune response at various stages. Adapted from²⁰⁸.

Despite the various described mechanisms of interference by HAV, adaptive immune responses are alerted and solidly take over in nearly 100% of the cases of HAV infection, in some cases accounting for liver damage: during acute Hepatitis A (AHA), it has been reported from patients studies that non-HAV-specific memory CD8+ T cells are activated by the IL-15 produced by HAV-infected cells, exerting innate-like cytotoxicity via activating receptors NKG2D and Nkp30 without TCR engagement. This innate-like cytotoxicity of CD8+ T cells is related to liver injury in AHA^{251,252}.

In acute Hepatitis A Virus (HAV) infection, CD8⁺ T cells have been long believed to play a crucial role, as HAV-specific CD8⁺ T cells have been observed with an activated phenotype in patients. However, a study in chimpanzees found that these cells were either undetectable or nonfunctional during acute HAV infection²¹². Instead, polyfunctional HAV-specific CD4⁺ T cells were detected when virus titers started to decline, suggesting that acute HAV infection might be primarily controlled by CD4⁺ T cells rather than CD8⁺ T cells. Moreover, virus-specific T cells appeared earlier during acute HAV infection compared to Hepatitis C Virus (HCV) infection¹⁶¹, and the frequency of regulatory T cells (Tregs) in the blood decreased due to FAS-mediated apoptosis, with the suppressive function of these Tregs being inhibited directly by the binding of HAV particles to the Tregs through the TIM1 receptor²⁵¹.

In summary, despite their similarities as hepatotropic pathogens, HAV and HCV differ significantly in their life cycle, pathogenesis, and immune responses they elicit. These differences not only pose unique challenges for research but also emphasize the necessity of diverse investigative methods and tools. Each virus has specific requirements for efficient replication, necessitating carefully tailored approaches especially when willing to effectively study their interactions with the immune system.

1.10 Models to study HCV and HAV replication

Since its discovery in 1989, research on HCV replication has been hindered by the lack of an efficient cell culture system. Attempts to infect primary human hepatocytes and hepatoma cells with patient-isolated virus have been largely unsuccessful, likely due to a potent early innate immune response¹⁴¹. The development of subgenomic replicons, inspired by naturally occurring pestivirus subgenomes, revolutionized HCV research, allowing detailed studies of viral replication in cell culture²⁵³⁻²⁵⁵ and is illustrated in Figure 16. However, this model, initially based on gt1b isolates (e.g. Con1) and later extended to g2a, requires adaptive mutations to allow efficient replication in permissive cells, interfering with virion production¹⁴¹. Subsequent engineering of different subgenomic replicons has allowed to address various scientific questions, with visualization through mCherry or quantification through Firefly luciferase¹⁴¹.

In the quest of a permissive cell line, Huh7 was established in 1982, stemming from a highly differentiated cancer cell line derived from hepatocellular carcinoma²⁵⁶. Two of its subclone

derivates, Huh7 Lunet²⁵⁷ and Huh-7.5 cells²⁵⁸, were former HCV replicon cell clones in which the HCV adapted subgenomic replicon was removed through interferon treatment, and are up to current days the gold standard of HCV cell culture applications^{257,259}. Both Huh7 and Huh7.5 express the entry receptors required for HCV infection, to similar degrees for what concerns SR-BI, while CD81 surface expression is higher on Huh7.5 cells than on Huh7-Lunet cells²⁶⁰. However, reconstitution of CD81 in Huh7Lunet cells confers support of for HCV infection to a level comparable to that for Huh7.5 cells²⁶⁰. It is noteworthy to know that Huh7 cells have a lowered expression of PRRs compared to primary human hepatocytes²⁶¹. In addition, the clone Huh7.5 contains a dominant missense mutation in the RIG-I gene that was also considered contributing to higher replication of HCV in these cells relative to Huh7 Lunet²⁶², although this was questioned by a later study²⁶³. Importantly, PI4KA expression is particularly high in Huh7 and Huh7-derived cells compared to PHH, which is deleterious for replication of HCV wildtype isolates, thereby necessitating cell culture adaptive mutations²⁶⁴.

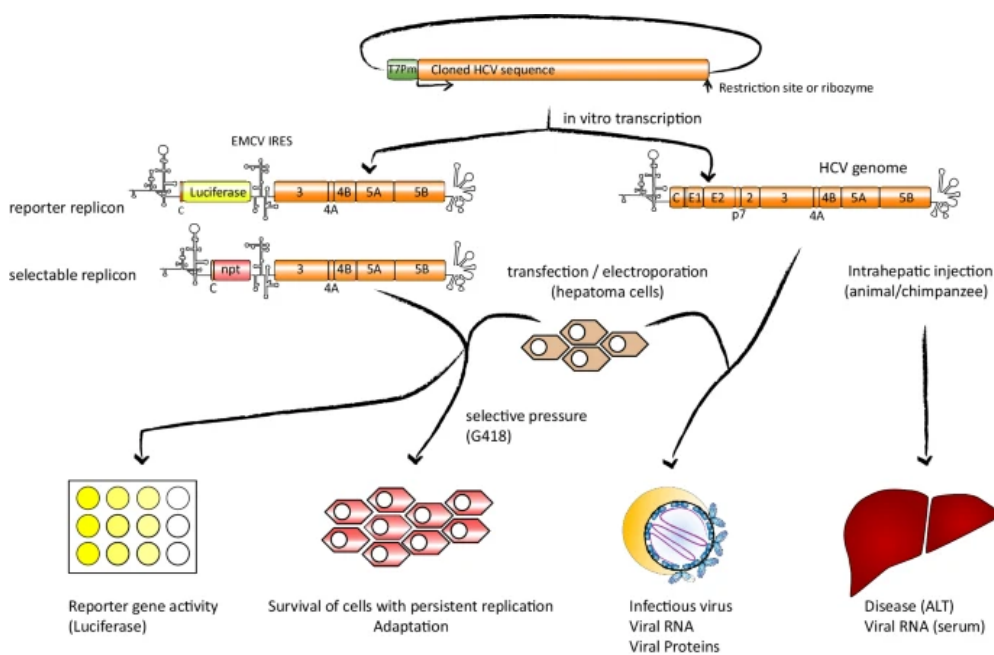


Figure 16. Establishment of the first cell culture models for HCV replication.

Viral consensus genomes for HCV were cloned into a plasmid under the control of the T7-RNA polymerase promoter and then amplified in bacteria. After in vitro transcription, the RNA constructs were transfected into permissive cells or intrahepatically, leading to trackable replication (including reporter genes (as Firefly luciferase), selectable persistent cells (through the use of selection markers, as neomycin), or the production of infectious virus, or disease, depending on the approach used. Adapted from¹⁴¹.

An important contribution to HCV culturing came from the Japanese Fulminant Hepatitis 1 (JFH1) genotype 2a isolate, becoming the first to exhibit high replication levels in vitro without the need of adaptation due to its efficient replicase complex^{265,266}, thereby allowing the generation of infectious virus in cell culture. To current days, a chimeric virus encompassing elements of two different Gt2a strains, termed Jc1, is used as gold standard in cell culture approaches²⁶⁷. However, according to previous reports, it might remain challenging to address questions on innate immune response upon HCV infections, since full immune competence might hinder HCV replication in cell culture, and its absence promote it, like in the case of forementioned clone Huh7.5²⁶². Few are the cell lines with robust endogenous PRRs expression which support HCV replication: for Primary Human Hepatocytes (PHH) several reports of permissiveness for HCV are available^{268,269}, but the high variability, along with the limited purity of most PHH preparations, given by the donor-to-donor differences makes it a difficult model^{270,271}.

HepG2, a commonly used human hepatoma cell line in virology studies, can be made more susceptible to HCV infection by expressing CD81 and miR-122 according to previous research^{272,273}. The hepatoma cell line Hep3B was also reported to be permissive for HCV upon reconstitution of miR122^{274,275}; however, immortalized hepatocytes line, as HepaRG (defined as potentially the best PHH surrogate model) or PH5CH were seemingly not supportive of HCV replication, potentially for abrogative immune responses and a lack of host factors necessary for replication²⁷⁶. Few subclones of PH5CH were instead used for establishment of HCV persistent infection by a Japanese group²⁷⁷.

The development of animal models for studying HCV is hindered by the virus' limited range of host species, which is a unique challenge. Approaches have varied, from modifying mice to accommodate HCV infection, to identifying and adapting HCV-like viruses for studying liver infection and diseases.

Martin and colleagues have demonstrated that inoculations of in vitro transcribed George Baker Virus (GBV)-B RNA can generate high-titer viremia, akin to chronic hepatitis C in humans, suggesting that GBV-B could induce a chronic hepatitis C-like disease in marmosets and tamarins²⁷⁸. Additionally, non-primate hepaciviruses (NPHVs) such as equine hepacivirus (EqHV) and Norway rat hepacivirus (RHV), discovered in horses and rats, respectively, present closely related new hepaciviruses to explore. Experiments using immunocompetent rats susceptible to

RHV-rn1 demonstrated the crucial role of T-cell immunity in preventing viral persistence, with a T-cell vaccination successfully protecting 40%–60% of rats against RHV persistence. The rat model could provide unprecedented insights into HCV persistence and help optimize more efficacious HCV vaccination approaches, although more thorough investigations on the roles of innate and humoral immunity would be needed.²⁷⁹ (Figure 17).

Finally, advancements have been made in HCV genetic adaptation. Identification of CD81 and occludin as key human-specific factors enables facilitated entry of the engineered Murine-Tropic Hepatitis C Virus (mtHCV) into mouse hepatocytes, both *in vivo* and *in vitro*, without the necessity for transgenic expression of human factors²⁸⁰.

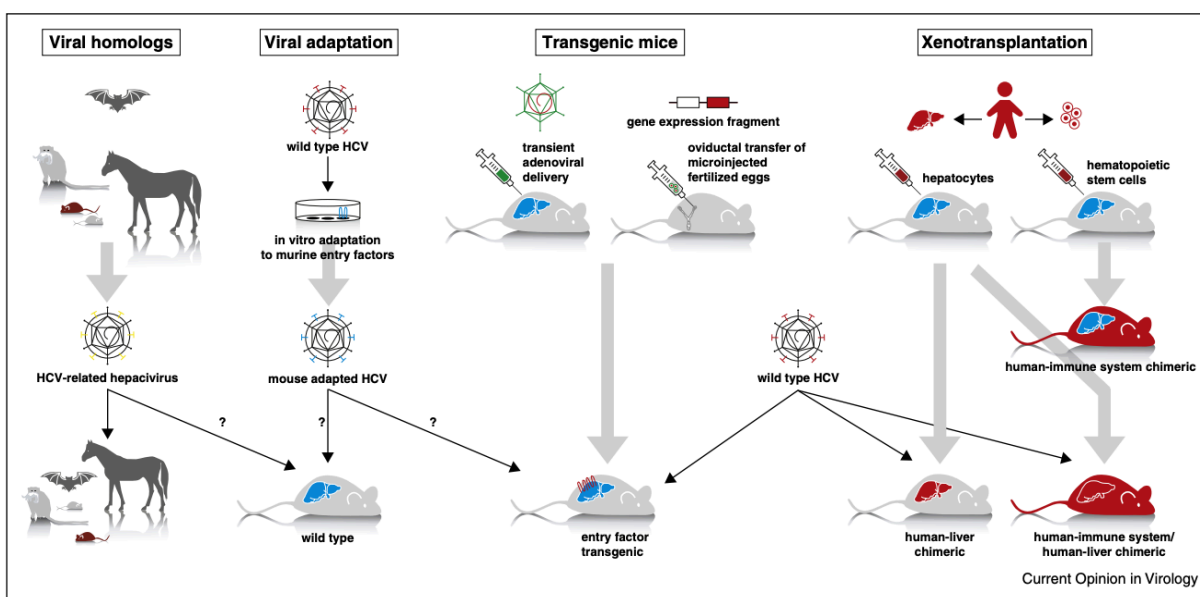


Figure 17. Different approaches to study HCV in animal models.

From the left: 1) Various HCV-related viruses that affect a variety of animal species including wild mice, rats, tamarins, bats, and horses. These infections can be examined either in their natural hosts or potentially in immunocompetent inbred laboratory mouse strains. 2) The potential of *in vitro* adaptation of HCV to mouse hepatoma cells, which may facilitate the isolation of viral variants capable of initiating an infection in wild type mice. 3) Temporary or permanent expression of human factors crucial for supporting infection by wild type HCV. 4) Xenotransplantation models, where the host's genetic background enables liver repopulation following the transplantation of human hepatocytes. Subsequent transplantation of HLA-compatible hematopoietic stem cells results in mice reconstituted on dual fronts. Adapted from²⁸¹.

This model served as an excellent platform to analyze the humoral-mediated response in HCV vaccine research²⁸². But for the purposes of understanding innate immunity upon HCV *in vivo*, a revolutionary animal for hepatotropic virus with a strictly human tropism, as HAV, HBV, HCV and HDV was represented by the SCID alb/uPA chimeric mice with humanized livers^{267,283-286} (Figure 18). These mice, lacking B and T cells, express a combination of noxious genes, under control of an

albumin promoter, promoting the action of plasminogen activators which lead to degradation and necrosis of the murine hepatocytes. Upon loss of the endogenous tissue, the mice can then be repopulated with human biopsies-derived PHHs; the engraftment success is followed through measuring of albumin levels in serum. The mice are then supportive of human hepatotropic infections and have been consistently used, to this day, for addressing questions on innate immune response, being this a valuable model in which the main professional adaptive immune cells are missing. ²⁸⁷.

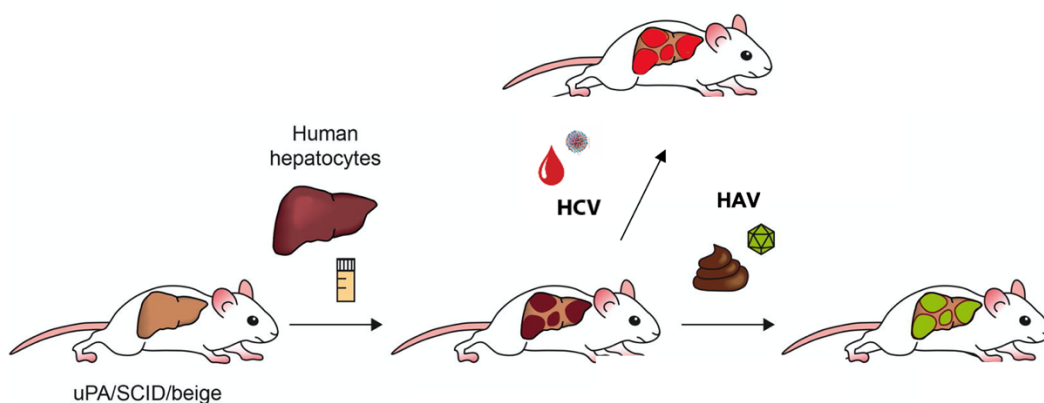


Figure 18. The SCID alb/uPA chimeric mice with humanized livers as HAV / HCV infection model.

The mice undergo loss of their own hepatocytes upon expression of the noxious urokinase plasminogen activator (uPA= and can be reingrafted with Primary Human Hepatocytes from liver biopsies. Therey, hepatotropic viruses like HAV and HCV can successfully infect their liver. Adapted from²⁸⁴.

SCID alb/uPA chimeric mice have been infected with HCV before: here, ISGs induction was correlating negatively to high replication, recapitulating *in vivo* data from patients²⁸⁷. However, a large mouse-to-mouse phenotype difference underpinned the complexity of this model.

Similar to HCV, wild-type HAV exhibits limited propagation in cell culture, necessitating a process of adaptation for efficient replication to occur^{288,289,290}. Once adapted, HAV can replicate in various cultured mammalian cells, including human and simian fibroblasts, as well as human hepatoma cells (Huh7, Huh7.5)²⁹¹. These adaptations are attributed to mutations within the internal ribosome entry site (IRES), promoting cap-independent viral translation, or mutations in 2B, which enhance viral RNA replication^{291,292}.

Unlike other members of the family, HAV requires a long adaptation period to grow in cell culture, replicates slowly, and rarely produces a cytopathic effect²⁹³, leading to a slow and persistent infection in cell culture with low virus yields. To implement physiological relevance, wild-type viral

strains have also been isolated directly from human feces and stool specimens²⁹⁴. *In vitro* infection is self-limiting, and the virus down-regulates its replication in common cell lines (FRhK-4 and MRC-5 cells) typically used for propagation. This effect, combined with the absence of an adaptive immune response *in vitro*, contributes to the establishment of a persistent infection *in vitro*²⁹¹. However, this pattern contrasts with *in vivo* conditions where infection and illness are typically acute and the virus induces an immune-mediated cytopathic response^{196,197,252,295}. Studies have suggested that the attenuation of virulence compared to the wild-type strains may require multiple mutations, as in HAV 3A regions, which have been linked to two cytopathic HAV strains²⁹⁶. Upon passaging, these strains – termed as *rr/cpe+*, were used to create chimeras that would gain full adaptability. The P2 region from one of these specific *rr/cpe+* viruses, named HM175/18f, was inserted into a less cytopathic strain, HAV/7, resulting in an increased replication linked to proteins 2B and 2C. Additionally, mutations were found in parts of the 5'NTR and P3, contributing to the boost^{293,297}. This adapted virus is currently the most widely used model to study HAV replication in cell culture²⁹⁸. From here, research has also led to the cloning of a cell culture-adapted HAV genome and the generation replicons, to allow genetic manipulation of the virus sequence, similar to HCV (Figure 16)²⁹².

Culture attempts with wild-type as well as cell culture adapted virus have been made in primary marmoset hepatocytes, the normal fetal rhesus kidney cell line (FRhK6), the human hepatoma cell line Alexander (PLC/PRF/5), human embryo fibroblasts, and others^{201,244,291}; cell lines from different animals, including pigs, mice, and monkeys, have been shown to support HAV replication. The same applies to Fetal Rhesus Kidney cell 4 (FRhk4)²⁸⁹ and primary human hepatocyte PXB (PhoenixBio) from chimeric mice with hepatocyte-humanized liver (PXB-mice)²⁹⁹. Interestingly, innate immune studies have been conducted on FRhk4 cells upon HAV infection, but only in presence of an IFN β enhancer construct, ectopically expressed, and not basing on measurement of endogenous IFNs or ISGs, hinting at FRhk4 being immune defective²⁴⁵. However, other reports exist on innate immune responses in FRhk4 cells upon viral infection³⁰⁰ or interferon treatment³⁰¹. PXB cells, despite having exhibited support of HAV replication, have not been sought in regards of their innate immune response upon HAV²⁹⁹, but their immune competence was evidenced upon interferon treatment in other studies³⁰².

Various animal models have been explored for studying HAV infection. Nonhuman primates (NHPs), such as chimpanzees, marmosets, and owl monkeys, offer valuable insights due to their

resemblance to humans, but their use is limited by scarcity and ethical concerns^{196,197,303}. Pigs, which share similarities with humans in their immune system, have been successfully infected with human HAV strains, providing a promising alternative model³⁰⁴. Tree shrews, with a close evolutionary relationship to humans, have shown potential as candidate models for HAV infection³⁰⁵; and additionally, recent discoveries of HAV strains in various animals like seals, bats, rodents, hedgehogs, ducks, and woodchucks may expand the range of animal models used in HAV research³⁰³.

Wild-type mice have been shown to not be permissive for HAV, but in recent literature it was shown that among the restrictive factors limiting its replication there might be innate immune competence, as MAVS KO and IFNAR KO mice could instead support HAV infection²⁴⁹. The aforementioned alb/uPa SCID mice with humanized liver, mentioned earlier, would offer for HAV as well the possibility to investigate the sole innate immune response *in vivo*: in this regard only unpublished data are available, where HAV seemed to recapitulate the features of the infection in chimpanzees³⁰⁶.

Conclusively, after surveying the myriad of animal and cell culture models for HAV and HCV research, it becomes clear that, wanting to keep the investigation in liver-based models and to allow for simultaneous cultivation of both viruses, only limited options seem to be available. Interesting side-by-side comparative studies on HAV and HCV replication were conducted in Huh7 Lunet¹⁹⁰, but in absence of functional PRRs. In contrast, the only available model investigating immunity is the complex *in vivo* infection in chimpanzees, which implies an even too high level of intricacies because of the involvement of adaptive immune responses.

1.11 Comparison of immune responses by HAV and HCV

To summarize, we saw that acute HCV infection often leads to chronicity, while acute HAV typically resolves spontaneously, and that the foundation for these disparate outcomes can be attributed to their immune responses. Resolution of HCV infections is primarily steered by robust CD8+ T cell responses, reinforced by CD4+ T cells, even as the contribution of HCV-specific antibodies remains a topic of contention^{235-237,307}. On the contrary, acute HAV infection is primarily neutralized by antibodies and polyfunctional CD4+ T cells, with the role of CD8+ T cells still being debated^{14,252,308,309}. The dynamic of regulatory T cells, or Tregs, further complicates the

scenario: their population surges in acute HCV infection, potentially suppressing HCV-specific T cells, while they decline in acute HAV infections¹⁶¹.

When analyzing the intrahepatic interferon response, stark contrasts emerge. Acute HCV infections are characterized by a potent, enduring IFN response, whereas HAV showcases a comparatively feeble ISG response (but mainly examined in chimpanzee models)²¹². While these models for HCV recapitulate the strong IFN responses observed in chronic human cases, it's evident that in humans this doesn't invariably lead to resolution. Instead, it might hinder virus-specific T cell responses, granting the virus a temporal advantage to mutate and evade the neutralizing mechanisms of antibodies and T cells^{119,23}. Such a delay starkly contrasts with HAV infections where the immune system's counter-response is swift¹⁶¹ (summarised in Table 3).

However, for both HAV and HCV mechanisms of clearance correlate strongly with a correctly mounted adaptive immune response. Instead, analyzing what precedes adaptive immunity and the different induction and counteraction mechanisms of innate immune response, we learn from the existing literature that there are still major gaps in our understanding on how HAV and HCV lead in one case to limited ISGs *in vivo* and clearance, while the other in robust ISGs and potential chronicity, if both viruses are equipped with counteractive mechanisms towards the same pathways (Table 3).

| Immune response | HAV | HCV |
|-----------------------------------|---|---|
| Type I and type III IFN responses | • Type III IFN reported | • Type I and III IFN reported |
| Virus-sensing receptors | MDA5 reported | RIG-I, MDA5, PKR and TLR3 reported |
| Interference mechanisms | • 3ABC is reported to cleave MAVS | • NS3–NS4A is reported to cleave MAVS |
| | • 3CD is reported to cleave TRIF | • NS3–NS4A is reported to cleave TRIF |
| | | • NS4B is reported to induce TRIF degradation |
| | • 3C is reported to cleave NEMO | |
| | • 2B is reported to interfere with IRF3 | |

| | | |
|--|---|---|
| | <ul style="list-style-type: none"> • hsa-miR-146a-5p is reported to interfere with TRAF6 | |
| | | <ul style="list-style-type: none"> • NS3 has been shown binding to TBK1 |
| | | <ul style="list-style-type: none"> • p7 is reported to interfere with IFI6-16 |
| | | <ul style="list-style-type: none"> • NS3 is reported to inhibit RIG-I polyubiquitination |
| | | <ul style="list-style-type: none"> • p7 is reported to interfere with IFI6-16 |
| | | <ul style="list-style-type: none"> • NS5A and E2 are reported to manipulate PKR |
| ISG induction | | |
| ISG induction in the infected liver of chimpanzees | Minimal induction of ISG expression reported | Increased expression of many ISGs reported |
| ISG induction in the infected liver of humans | no data available | Increased expression of many ISGs reported, depending on patient |
| Antibodies | | |
| Neutralizing antibodies | Protective immunity by HAV-specific antibodies | HCV escapes from the neutralizing activity of E1- and E2-specific antibodies |
| Vaccines inducing neutralizing antibodies | Inactivated virus, viral antigen | No available vaccine |
| T cells | | |
| Timing | From 4 to ~6 weeks after infection | 8–12 weeks after infection |
| Relation to the outcome of infection | Not determined | Vigorous and broad (multiple epitope-specific) T cell response in case of clearance of infection |

Table 3. Comparison between HAV- and HCV-induced immunity.

Comparison of the immunological responses initiated by HAV and HCV. The table highlights the involvement of Type I and III IFN responses in both viruses, with HAV majorly engaging Type III IFN. The putative key virus-sensing receptors, such as MDA5 for HAV and a broader spectrum including RIG-I, MDA5, PKR, and TLR3 for HCV, are outlined. Additionally, the specific viral interference mechanisms are summarized: for HAV, these include the cleavage of MAVS by 3ABC, TRIF by 3CD, NEMO by 3C, and the interference with IRF3 by 2B. For HCV, the NS3–NS4A complex is reported to cleave both MAVS and TRIF, with NS4B inducing TRIF degradation. ISG induction in infected chimpanzee livers is detailed, pointing to minimal induction in HAV but extensive induction in HCV. The role of neutralizing antibodies, with HAV-specific antibodies providing protective immunity and HCV managing to escape the activity of E1- and E2-specific antibodies, is also discussed. Finally, the table showcases the timing and potential outcome-related aspects of T cell responses for both viruses. Adapted from¹⁶¹.

Altogether, there are still open questions on for the reported mechanisms of protein adaptors cleavage, in some cases controversial and needing to be revisited^{138,173,175}; at the same time, the lack of studies focusing on pathway induction for HAV might leave unsolved the contribution of innate immunity to persistence or clearance, for instance hinted for HCV and TLR3⁸³.

The question of how these interactions dictate the clinical courses of HAV and HCV infections remains unsolved. With adaptive immunity, particularly T-cell responses, being pivotal in clearing both viruses, this leads to the pressing question: could instead the innate immune system be the key differential in dictating the progression of these infections, and how to address this question in physiological contexts?

Aims of the thesis

In light of the previous observations on the distinct ways HAV and HCV interact with the innate immune system in the human liver, and the gaps in our understanding of their mechanisms of clearance and persistence, respectively, the aims of this thesis are:

Investigating patterns of PRRs induction upon HAV and HCV: I will aim to elucidate how HAV and HCV are sensed by innate immune receptors in the liver, focusing on TLR3 and RLRs. This will involve examining the activation profiles of these receptors upon viral infection in relevant cell culture models.

Quantifying proteolytic cleavage: The counteractive activities towards the PRRs pathways by the HCV protease NS3-4A and the HAV proteases 3C, with their precursors 3CD and 3ABC, will be assessed biochemically, solving previous contradicting questions from literature. I aim to quantify the efficiency of proteolytical cleavage of innate immune adaptors by viral proteases, such as the cleavage of TLR3 adaptor TRIF and RLR adaptor MAVS.

Evaluating the functional meaning of the proteolytic cleavage: The intention here is to determine how these viruses modulate the innate immune pathways, correlating the efficiency of adaptor proteins cleavage to the functional abrogation of TLR3 / RLRs in presence of an external immunostimulant. This will further establish the extent to which these viruses can modulate innate immune responses.

Verifying the findings In vivo in humanized mice: I intend to examine the immune responses in SCID Alb-uPA mice with humanized livers infected with HAV and HCV. The goal will be to determine if in vitro observations about viral sensing and ISG responses hold true in a more physiological context.

By pursuing these aims, I anticipate shedding light on the intricate mechanisms through which HAV and HCV interact with, and subvert, the host's immune system. The overarching goal is to expand our understanding of the determinants of viral clearance and persistence in the liver.

2. Materials

2.1 Reagents and other products

| Reagent | Source |
|--|--------------------------|
| 30% Acrylamide/Bis Solution 37.5:1 | BioRad |
| 4',6-Diamidine-2'-phenylindole dihydrochloride (DAPI) | Sigma-Aldrich |
| agarose | Invitrogen |
| Albumin Fraction V (BSA) | Sigma-Aldrich |
| ammonium persulfate (APS) | Sigma-Aldrich |
| ampicillin | Roche |
| Bacto agar | BD Biosciences |
| Bacto tryptone | BD Biosciences |
| Bacto yeast extract | BD Biosciences |
| blasticidin | Invitrogen |
| Borosilicate Glass Capillaries (1.2 mm O.D. x 0.94 mm I.D.) | Harvard Apparatus |
| bromophenol blue | Waldeck GmbH&Co. KG |
| Complete Mini EDTA-free | Roche |
| carbenicillin | Applichem |
| Centricon Plus-70 Centrifugal Filters | Merck Millipore |
| chloroform | Sigma-Aldrich |
| Dextran, tetramethylrhodamine (TMR) 70.000 MW | Thermo Fisher Scientific |
| digitonin | Sigma-Aldrich |
| dimethylsulfoxide (DMSO) | Merck Millipore |
| dithiothreitol (DTT) | Roche |
| D-Luciferin | PJK |
| dNTPs | Roche |
| Dulbecco's modified Eagle medium (DMEM) | Gibco |
| ECL Plus Western Blot Detection System | Perkin-Elmer |
| ethanol (100%) | VWR Chemicals |
| ethylene glycol-bis (β-aminoethyl ether)-N,N,N',N'-tetraacetic acid (EGTA) | Applichem |
| Fluoromount G | Southern Biotech |
| Formaldehyde (37%) | Thermo Fisher Scientific |
| G418 sulfate | Invitrogen |
| GelRed® Nucleic Acid Gel Stain | Biotium |
| GeneRuler 100bp marker | Thermo Fisher Scientific |
| glucose | Applichem |

| | |
|---|---------------|
| glycerol | Carl Roth |
| glycyl-glycin | Sigma-Aldrich |
| isopropanol | Sigma-Aldrich |
| kanamycin | Applichem |
| Lipofectamine2000 | Invitrogen |
| magnesium sulfate (MgSO ₄) | Merck |
| methanol | Honeywell |
| nonessential amino acids | Gibco |
| nucleoside triphosphates | Roche |
| OptiMEM | Gibco |
| paraformaldehyde (PFA) | Carl Roth |
| polyethyleneimine (PEI) | Sigma-Aldrich |
| polyinosinic:polycytidylic acid (poly(I:C)) | Invivogen |
| potassium chloride (KCl) | Sigma-Aldrich |
| potassium dihydrogen phosphate (KH ₂ PO ₄) | Applichem |
| potassium phosphate (K ₂ PO ₄) | Sigma-Aldrich |
| ProLong Gold Antifade Mountant | Thermo Fisher |
| Protein Assay Dye Reagent | BioRad |
| puromycin | Sigma-Aldrich |
| RNase-free water | Qiagen |
| Rotiphorese Gel 30 (BAA) | Carl Roth |
| skim milk powder | Carl Roth |
| sodium acetate | Grüssing GmbH |
| sodium arsenite | Sigma-Aldrich |
| sodium chloride (NaCl) | Bernd Kraft |
| sodium dodecyl sulfate (SDS) | Carl Roth |
| sodium fluoride (NaF) | Sigma-Aldrich |
| sodium hydrogen phosphate (Na ₂ HPO ₄) | Honeywell |
| sodium orthovanadate | Sigma-Aldrich |
| Simeprevir | Olysio® |
| tetramethylethylenediamine (TEMED) | BioRad |
| tris(hydroxymethyl)aminomethane (Tris) | Carl Roth |
| Triton X-100 | Merck |
| Tween-20 | Carl Roth |
| Ultra Pure ATP | Promega |
| β-glycerophosphate | Sigma-Aldrich |
| β-mercaptoethanol | Sigma-Aldrich |

Table 4. Reagents used in this study.

2.2 Buffers and solutions

| Name | Composition |
|-------------------------------------|--|
| acetate buffer | 35 mM sodium acetate, 14 mM acetic acid |
| annealing buffer | 25 mM HEPES, 50 mM NaCl |
| cryo solution | 90% FCS, 10% DMSO |
| Cytomix | 120 mM KCl, 0.15 mM CaCl ₂ , 10 mM KPO ₄ pH 7.6, 25 mM HEPES, 2 mM EGTA, 5 mM MgCl ₂ , pH 7.6; supplement with 2 mM ATP and 5 mM glutathione freshly before use |
| Firefly Luciferase assay buffer | 25 mM glycyl-glycine, 15 mM K ₃ PO ₄ pH 7.8, 15 mM MgSO ₄ , 4 mM EGTA; supplement with 1 mM DTT and 2 mM ATP before use |
| Firefly Luciferase injection buffer | 200 μM D-Luciferin, 25 mM glycyl-glycine pH 7.8 |
| Firefly Luciferase lysis buffer | 1 % Triton X-100, 25 mM glycyl-glycine, 15 mM MgSO ₄ , 4 mM EGTA, 50 ml Glycerol; supplement with 1 mM DTT before use. |
| IF blocking buffer | 5% BSA |
| Laemmli protein sample buffer (6x) | 375 mM Tris-HCl pH 6.8, 50% glycerol, 9% SDS, 9% β-mercaptoethanol, 0.03% bromophenol blue |
| luciferin injection solution | 200 μM D-luciferin, 25 mM glycyl-glycine pH7.8 |
| orange DNA loading dye (10x) | 16.5 ml 0.15 M Tris-HCl pH 7.5, 30 ml glycerol, 3.5 ml H ₂ O |
| phosphate-buffered saline | 8 mM Na ₂ HPO ₄ , 2 mM NaH ₂ PO ₄ , 1.4 M NaCl |

| | |
|---|---|
| protein lysis buffer | 50 mM Tris-HCl pH7.4, 150 mM NaCl, 1% Triton X-100, 60 mM β-glycerophosphate, 15 mM 4- nitrophenylphosphate, 1 mM sodium orthovanadate, 1 mM sodium fluoride; supplement with cOmplete EDTA-free protease inhibitor before freezing |
| RRL buffer (5x) | 400 mM HEPES pH 7.5, 60 mM MgCl ₂ , 10 mM spermidine, 200 mM DTT |
| separating gel buffer (SDS-PAGE) | 1.5 M Tris-HCl pH 8.8, 0.4% (w/v) SDS |
| stacking gel buffer (SDS-PAGE) | 1 M Tris-HCl pH 6.8, 0.8% (w/v) SDS |
| T4 DNA ligase buffer (10x) | 400 mM Tris-HCl, 100 mM MgCl ₂ , 100 mM DTT, 5 mM ATP |
| TAE (50x) | 242 g Tris, 100 ml 0.5 M EDTA (pH 8.0), 57.1 ml glacial acetic acid, total volume 1 liter H ₂ O |
| TBS (10x) | 88 g NaCl, 2 g KCl, 30 g Tris in 1 liter H ₂ O, adjust pH 7.5 |
| TCID ₅₀ development solution | 77% acetate buffer, 0.00074% 3-amino-9-ethyl-carbazole, 0.0009% H ₂ O ₂ |
| TGS (10x) | 250 mM Tris, 1.92 M glycine, 1% (w/v) SDS |

| | |
|---------------------------------------|--|
| Western blot blocking buffer | 1x TBS, 0.1% (w/v) Tween 20, 5% skim milk powder or 5% BSA |
| Western Blot semi-dry transfer buffer | 48 mM Tris, 39 mM glycine pH 8.3, 0.00375 % (v/w) SDS; supplemented with 20 % (v/v) methanol before use. |
| Western blot wet transfer buffer | 25 mM Tris pH 8.3, 150 mM glycine; supplemented with 20 % (v/v) methanol before use. |
| Western Blot washing buffer (TBS-T) | 0.1 % (w/v) Tween 20 in 1x TBS |

Table 5. Buffers used in this study.

2.3 Kits

| Name | Manufacturer |
|--|--------------------------|
| High-Capacity cDNA Reverse Transcription Kit | Thermo Fisher Scientific |
| NucleoBond® PC500 (maxiprep) | Macherey-Nagel |
| NucleoSpin® PCR clean-up/gel extraction kit | Macherey-Nagel |
| NucleoSpin® Plasmid (miniprep) | Macherey-Nagel |
| NucleoSpin® RNAPlus (RNA extraction) | Macherey-Nagel |
| ORFeome cDNA library | Invitrogen |
| Phusion Flash High-Fidelity PCR kit | Thermo Fisher Scientific |
| qScript XLT One-Step RT-qPCR kit | Quanta |
| RNA Mini Kit | Bio&Sell |

Table 6. Kits used in this study.

2.4 Cell lines used in this study

| | |
|---------------|---|
| Huh7 | Human hepatocarcinoma cell line (Nakabayashi et al., 1982) |
| Huh7.5 | Sub-clone of Huh7 generated by curing a stable HCV replicon cell line (Blight K.J., McKeating J.A., Rice C.M.J. <i>Virology</i> 76:13001-13014(2002)) |
| HEK 293T | Human embryonic kidney cells, transformed by SV40 large T- antigen (Graham et al., 1977) |
| FRhK4 | Fetal Rhesus monkey kidney cell line used for propagation of HAV 18f and HAV/7 (Wallace et al., 1973) |
| Huh7 Lunet T7 | Hepatoma cell line with reconstituted expression of T7 polymerase (Backes P, et al. <i>Journal of Virology</i> 2010;84:5775-5789) |

| | |
|-------------------------------------|---|
| Huh7.5 empty Blr | Sub-clone of Huh7, generated in this study |
| Huh7.5 MDA5 Blr | Sub-clone of Huh7, with reconstituted expression of MDA5, generated in Grünvogel Gastroenterology. 2018 Jun;154(8):2237-2251 |
| Huh7.5 MDA5 Blr LGP2 Puro | Sub-clone of Huh7, with reconstituted expression of MDA5 + LGP2, generated in this study |
| Huh7.5 RIG-I Blr | Sub-clone of Huh7, with reconstituted expression of RIG-I, generated in Grünvogel Gastroenterology. 2018 Jun;154(8):2237-2251 |
| Huh7.5 TLR3 Blr | Sub-clone of Huh7, with reconstituted expression of TLR3, generated in this study |
| Huh7.5 TLR3 Puro | Sub-clone of Huh7, with reconstituted expression of TLR3, Grünvogel Gastroenterology. 2018 Jun;154(8):2237-2251 |
| Huh7.5 TLR3 Blr NS3-4A wt high Puro | Sub-clone of Huh7, with reconstituted expression of TLR3 and NS3-4A at high levels, generated in this study |
| Huh7.5 TLR3 Blr NS3-4A wt low Puro | Sub-clone of Huh7, with reconstituted expression of TLR3 and NS3-4A at low levels, generated in this study |
| HepG2 naïve | Human hepatoma cells, Treichel, U., zum Büschenfelde, K.H.M., Dienes, H.P. . Arch. Virol. 142, 493–498 (1997). |
| HepG2 TLR3 Hygro | Human hepatoma cells with reconstituted expression of TLR3, generated by Dr. Oliver Grünvogel |
| HepG2 TLR3 Hygro MDA5 KO Puro | Human hepatoma cell pool, with reconstituted expression TLR3 and KO of MDA5, generated in this study |
| HepG2 TLR3 Hygro RIG-I KO Puro | Human hepatoma cell pool, with reconstituted expression TLR3 and KO of RIG-I, generated in this study |
| HepaRGNTCP | Immortalized hepatic cell line, Gillich N, Zhang Z, J Hepatol. 2023 PMID: 36152765. |
| HepaRGNTCP-LGP2KO | Immortalized hepatic cell line, Gillich N, Zhang Z, J Hepatol. 2023 PMID: 36152765. |
| Con1 HCV SGR clone 9-13 | HCV subgenomic replicon Gt1b, clone 9-13, Lohmann V, et al. J Virol 2001;75:1437-1449. |
| ET Neo HCV SGR | HCV subgenomic replicon Gt1b Lohmann, clone ET Neo V, et al. J Virol 2001;75:1437-1449. |
| Lucubineo JFH1 | HCV subgenomic replicon JFH1, Jo J, et al. Gastroenterology 2009;136:1391-1401. |
| HAV SGR | HAV subgenomic replicon based on HM175/18f, Esser-Nobis, K., Hepatology, 62: 397-408. |
| Hep3B | Hepatoma cells, Windisch MP, J Virol. 2005 Nov;79(21):13778-93 |

Table 7. Cell lines used in this study.

2.5 Bacteria

E. coli DH5 α were used for cloning experiments and plasmid amplification:

***E. coli* DH5 α** F'/endA1 hsdR17A (rk-mk+) supE44 thi-1 recA1 gyrA (Nalr) relA1 Δ (lacZYAargF) U169 deoR (Φ 80dlac Δ (lacZ)M15) (Grant et al., 1990)

2.6 Culture media

Bacterial culture media

Luria-Bertani Broth (LB): 10 g Bacto-tryptone, 5 g yeast extract, 10 g NaCl in 1 liter dd Terrific

Broth (TB): 12 g Bacto-tryptone, 24 g yeast extract, 4 ml glycerol in 900 ml ddH₂O supplemented with 100 ml "10x salt solution for Terrific Broth" before use.

salt solution (10x) for Terrific Broth: 23.1 g of KH₂PO₄, 125.4 g of K₂HPO₄ in 1 liter ddH₂O

For selection of resistant clones, media was supplemented with ampicillin or carbenicillin (100 μ g/ml) or kanamycin (30 μ g/ml).

2.7 Cell line culture media

DMEM complete (Gibco) was used for routine culturing of all cell lines, except in the case of Lentiviral particles production and HAV / HCV infection experiments, which required **DMEM "starvation medium"**, and HAV / HCV infection passaging experiments for microscopy, which required **DMEM 1.5% DMSO**.

DMEM "starvation medium": Dulbecco's modified Eagle medium, unsupplemented.

DMEM complete: Dulbecco's modified Eagle medium supplemented with 10 % FCS, 2 mM L- glutamine, 1x non-essential amino acids, 100 U/ml penicillin and 100 μ g/ml streptomycin

DMEM 1.5% DMSO: Dulbecco's modified Eagle medium supplemented with 1.5% DMSO, 10 % FCS, 2 mM L- glutamine, 1x non-essential amino acids, 100 U/ml penicillin and 100 μ g/ml streptomycin

Isolated PHHs were cultured in Williams E medium (Life Technologies), supplemented with 10% fetal calf serum (heat inactivated; Capricorn, Ebsdorfergrund, Germany), 50 U/mL penicillin/50 μ g/mL streptomycin, 50 μ M hydrocortisone, and 5 μ g/mL insulin (SAFC; Sigma-Aldrich), and incubated at 37°C and 5% CO₂.

2.8 Viruses

| Virus | Strain | Source |
|---------------|------------------------|----------------------------|
| HCV Jc1 | J6/JFH1 chimera (gt2a) | (Pietschmann et al., 2006) |
| HAV HM175/18f | cell culture-adapted | (Lemon et al., 1991) |

| | | |
|--|--|--|
| | | |
|--|--|--|

Table 8. Viruses used in this study.

2.9 Primary antibodies

| Name | Citation | Supplier | Cat no. | Clone no. |
|-----------------|--|---------------------------|-------------------------|-----------|
| Anti-HA | - | Sigma Aldrich | H3663 | HA-7 |
| Anti-FLAG | - | Sigma Aldrich | F1804 | 2MG |
| Anti-Actin beta | - | Sigma Aldrich | A5441 | 2ML |
| Anti-TLR3 | - | Abcam | [40C1285] | 13915 |
| Anti-RIG-I | - | Adipogen | Alme-1 | |
| Anti-MDA5 | - | Cell Signaling Technology | D74E4 | #5321 |
| Anti-HCV NS5A | Lindenbach et al., Science, Vol. 309, July 2005, pp. 623-626 | - | - | - |
| Anti-MAVS | - | Enzo life sciences | AT107 | |
| Anti-HAV Vp3 | - | Thermo Fisher Scientific | C22H | |
| Anti-HAV 3C | Kusov et al., AntivRes, Vol 73, Issue 2, 2007,Pages 101-111 | - | - | - |
| Anti-IFIT1 | - | ABCAM | H00003434 | D01 |
| Anti-CXCL10 | - | Thermo Fisher Scientific | JA10-82 | - |
| Anti-GAPDH | - | Cell Signaling | 5174S | - |
| HCV NS3 | | (#49, made in house) | | |
| Mx1 | | Abcam | EPR19967] (ab237299) | |

Table 9. Antibodies used in this study.

2.10 Secondary antibodies

| Name | Supplier | Clone no. |
|------------------------------------|--------------------------|-------------|
| Goat anti-mouse IgG - Peroxidase | Sigma Aldrich | A4416-5X1ML |
| Goat anti-rabbit IgG - Peroxidase | Sigma Aldrich | A6154-5X1ML |
| Donkey anti-rabbit Alexa Fluor 488 | Invitrogen | |
| Donkey anti-mouse Alexa Fluor 488 | Invitrogen | |
| Donkey anti-rabbit Alexa Fluor 568 | Invitrogen | |
| Donkey anti-mouse Alexa Fluor 568 | Invitrogen | |
| Phalloidin AlexaFluor 568 | Thermo Fisher Scientific | |
| MitoTracker™ Red CMXRos | Thermo Fisher Scientific | M7512 |

Table 10. Antibodies used in this study.

2.11 Chimeric mice

| Name | Citation | Supplier | Strain | Sex | Age | Overall n number |
|------------------------------------|----------------------------------|--------------|--------------|-------|---|------------------|
| uPA/SCID mice with humanized liver | Meuleman et al., Hepatology 2005 | Own breeding | Alb-uPA/SCID | mixed | 2 weeks (transplantation) 1,5-2 months (infection) | 2 - 3 |

Table 11. Infection of uPA-SCID mice with humanized liver

2.12 Infection of chimeric mice

| Mouse ID | Inoculum | Sacrification date | HAV in feces (copies/ml) | HAV in plasma (copies/ml) | HCV in plasma (IU/ml) | Viral load detection |
|---------------|--|--------------------|--------------------------|---------------------------|-----------------------|----------------------|
| M162L 071119 | HCV GLT1; 50 μ L IS | 4/06/2020 12 wpi | | | 1,37E+07 | 10 wpi |
| M166R 090720 | HCV GLT1; 50 μ L; IS | 26.11.2020 8 wpi | | | 5,02E+06 | 8 wpi |
| M174LR 100720 | HCV GLT1; 50 μ L; IS | 26.11.2020 8 wpi | | | 1,28E+06 | 8 wpi |
| M143L 201119 | HAV patient 2; 25 μ L IS | 4/06/2020 12 wpi | 1,96E+10 | 1,74E+08 | | 8 wpi |
| M131RL 241119 | HAV patient 2; 25 μ L IS | 4/06/2020 12 wpi | 1,13E+10 | 5,82E+08 | | 8 wpi |
| M150 160120 | HAV patient 3; 25 μ L IP | 4/06/2020 8 wpi | 4,41E+09 | 3,24E+08 | | 6 wpi |
| M69L 160419 | HAV (HM175/18f); 100 μ L IP | 27/11/2019 20 wpi | 5,50E+06 | 1,25E+07 | | 19 wpi |
| M69RL 160419 | HAV (HM175/18f); 100 μ L IP | 27/11/2019 20 wpi | 6,61E+06 | 5,83E+06 | | 19 wpi |
| M216L 100720 | HAV patient 3 (dilution 1/10); IP 100 μ L | 26.11.2020 8 wpi | 9,81E+09 | 1,83E+08 | | 8 wpi |
| M216R 100720 | HAV patient 3 (dilution 1/10); 100 μ L IP | 26.11.2020 8 wpi | 8,46E+09 | 8,48E+07 | | 8 wpi |
| M222 100720 | HAV patient 3 (dilution 1/100); 100 μ L IP | 26.11.2020 8 wpi | 2,65E+09 | 1,41E+08 | | 8 wpi |
| M222L 100720 | HAV patient 3 (dilution 1/100); 100 | 26.11.2020 8 wpi | 2,58E+09 | 2,85E+08 | | 8 wpi |

| | | | | | | |
|------------------|--|---------------------|----------|----------|--------------|--------|
| | μL IP | | | | | |
| M230LL 050720 | HAV patient 3 (dilution 1/1000); 100 μL IP | 26.11.2020 8 wpi | 4,88E+09 | 5,01E+08 | | 8 wpi |
| M226L 280520 | HCV mH77c, 10 ⁶ IU/ml (stock), 150 μL IS | 03/03/21, 14 wpi | | | 2,19E+0 6 | 13 wpi |
| M226LL 280520 | HCV mH77c, 10 ⁶ IU/ml (stock), 150 μL IS | 03/03/21, 14 wpi | | | 3,71E+0 5 | 13 wpi |
| M124 030120 | control (no infection) | 26/03/20 | | | | |
| M124L 030120 | control (no infection) | 26/03/20 | | | | |
| M166L 090720 | control (uninfected feces) | 30/07/20 | | | | |
| M174LL 100720 | control (uninfected feces) | 30/07/20 | | | | |

* IS = intrasplenically

* IP = intraperitoneally

* IV = intravenously

Table 12. Infection of uPA-SCID mice with humanized live

2.13 Vectors

The following list provides an overview of standard plasmids used in this study.

| Vector | Description | Source |
|------------|---|------------------------|
| pWPI | vector for EMCV IRES-driven expression; can be used for lentiviral packaging; confers blasticidin, puromycin or neomycin resistance (Amp ^R) | (Klages et al., 2000) |
| pCMV Δ8.91 | packaging plasmid for pWPI vectors (Amp ^R) | (Klages et al., 2000) |
| pMD2.G | vector encoding VSV envelope glycoprotein for pseudotyping of pWPI-based lentiviruses (Amp ^R) | (Klages et al., 2000) |
| pFK | pBR322-derived vector with a T7 promoter for <i>in vitro</i> transcription of viral genomes (Amp ^R) | (Lohmann et al., 1999) |
| pTM | Recombinant vector with a T7 promoter and a MCS under translational control of the encephalomyocarditis virus (EMCV) IRES | (Fuerst et al. 1986) |

Table 13. Standard vectors used in this study.

2.14 Plasmid constructs

The following list provides all plasmids used for cloning and experimental procedures in this study.

| Nr. | Vector | Description | Source |
|-----|--|--|-----------------------------------|
| 1 | pWPI blr / puro / hygro / neo | vector for EMCV IRES-driven expression; can be used for lentiviral packaging; confers blasticidin resistance (Amp ^R) | (Klages et al., 2000) |
| 2 | pTM eGFP | expressing enhanced GFP (eGFP) for transfection purposes | In house |
| 3 | pTM HA_TRIF_HA | expressing TRIF wild-type (HAV and HCV cleavage susceptible) for transfection purposes, with N term HA tag | This study |
| 4 | pTM HA_TRIF_Q554A | expressing TRIF HCV NS3-4A cleavage resistant for transfection purposes, with N term HA tag | This study |
| 5 | pTM HA_TRIF_C372A | expressing TRIF HAV Q554A cleavage resistant for transfection purposes , with N term HA tag | This study |
| 6 | pTM HA_TRIF_Q554 + C372A_HA | expressing TRIF HCV NS3-4A + HAV Q554A cleavage resistant for transfection purposes , with double HA tag | This study |
| 7 | pTM HA_TRIF_delRHIM_HA | expressing TRIF wild-type (HAV and HCV cleavage susceptible) but lacking the C-term domain RHIM which is responsible for apoptosis, and with double HA tag | This study |
| 8 | pTM HA_TRIF_Q554 + C372A_delRHIM_HA | expressing TRIF HCV NS3-4A + HAV Q554A cleavage resistant but lacking the C-term domain RHIM which is responsible for apoptosis, with double HA tag | This study |
| 9 | pTM HA_MAVS | expressing MAVS wild-type (HAV and HCV cleavage susceptible) with N term HA tag | Generated by Dr. Oliver Grünvogel |
| 10 | pTM HA_MAVS_CR | expressing MAVS HAV and HCV cleavage resistant (Q428 - C508), with N term HA tag | Generated by Dr. Oliver Grünvogel |
| 11 | pWPI MAVS-GFP-NLS Q428 + C508 | pTM plasmid with a GFP-nuclear translocation signal fused to the C-term. membrane anchor of MAVS including HAV and HCV cleavage sites | Generated by Rahel Klein |
| 12 | pTM Flag 3CD | pTM plasmid encoding HAV 3CD | Generated by Jannik Traut |
| 13 | pTM Flag 3CD C172A | pTM plasmid encoding HAV 3CD mutant (abrogated cleavage) | Generated by Jannik Traut |

| | | | |
|----|-----------------------------------|--|-----------------------------------|
| 14 | pTM Flag NS3-4A | pTM plasmid encoding HCV NS34A; confers puromycin resistance | Generated by Dr. Oliver Grünvogel |
| 15 | pTM Flag NS3-4A S193A | pTM plasmid encoding HCV NS34A mutant (abrogated cleavage); confers puromycin resistance | Generated by Dr. Oliver Grünvogel |
| 16 | pWPI Flag 3CD Blr | pWPI plasmid encoding HAV 3CD mutant (abrogated cleavage); confers blasticidin resistance | Generated by Jannik Traut |
| 17 | pWPI Flag 3CD C172A Blr | pWPI plasmid encoding HAV 3CD mutant (abrogated cleavage); confers blasticidin resistance | Generated by Jannik Traut |
| 18 | pWPI Flag NS3-4A Puro | pWPI plasmid encoding HCV NS3-4A; confers puromycin resistance | Generated by Jannik Traut |
| 19 | pWPI Flag NS3-4A S193A Blr | pTM plasmid encoding HCV NS34A mutant (abrogated cleavage); confers puromycin resistance | Generated by Jannik Traut |
| 16 | pWPI Flag 3ABC Blr | pWPI plasmid encoding HAV 3ABC; confers blasticidin resistance | This study |
| 17 | pWPI Flag 3ABC C172A Blr | pWPI plasmid encoding HAV 3ABC mutant (abrogated cleavage); confers blasticidin resistance | This study |
| 20 | pWPI_ROSA_T7_ Blr | vector for ROSA26-driven T7 expression;; confers blasticidin resistance | |

Table 14. Plasmid constructs used in this study.

Amp^R, ampicillin resistant; Kan^R, kanamycin resistant.

2.15 Oligonucleotides used for plasmid cloning

Shown is a list of primers and probes used in this study. All DNA oligonucleotides were synthesized by Sigma-Aldrich. The lyophilized nucleotides were resuspended in ddH₂O to a final concentration of 100 μM. Branching-DNA probes were ordered from Affymetrix, Thermo Fisher Scientific.

| # | Primer | Sequence 5' → 3' |
|---|------------------|---|
| 0 | XmaI-Flag-3C_for | gatccccgggatcatggactacaaagacgatgacgacaagtcaacttgg aaatagcaggactg |
| 2 | SpeI-stop-3D rev | ggatccactagttcatgaaaggta |
| 3 | 3C C172A for | gccaaggtcttctggaatggccggtgggccttggttc |

| | | |
|----|----------------------------|--|
| 4 | 3C C172A rev | gaaaccaaggccccaccggccattccaggaagaccttcgc |
| 5 | SpeI-stop-3D rev | ggatccactagttcatgaaaggtca |
| 6 | NcoI-NS34A for | gatcccatggactacaaagacgatgacgacaagatggcgcctattaccgc |
| 7 | SpeI-stop-NS34A rev | gactactagttcagcactcttccatctc |
| 8 | SmaI_HA_TRIF for | gatccccgggcaccatgtatccctatgacgtccccgactacgcgccatggc ctgcacaggc |
| 9 | SpeI TRIF rev | gactactagtcgcggtcattctgctcctcgcg |
| 10 | TRIF C372R for | cctcctcctcctcctcctcatctactcctcgttcagctcacctgacccc |
| 11 | TRIF C372R rev | ggggtcaggtgagctgaacgaggagtagatgaaggaggaggaggaggag g |
| 12 | TRIF Q554A for | cctgcgggaacagagcgcacacctggacggtgagc |
| 13 | TRIF Q554A rev | gctcacctccagggtgctgctctgttcccgcagg |
| 14 | 3C shuttle pTM for | gatcccatggactacaaagacgat |
| 15 | TRIF dRHIM_Spe C-HA rev | gactactagttcaggccgtagtcggggacgtcatagggataggactgcg ggaaggg |
| 16 | SmaI HA MAVS forward | gatccccgggcaccatgtatccctatgatgacgtccccgactacgcgccat gccgtttgctgaagacaag |
| 17 | MAVS wt 3' reverse | gcccgtagtttactagttcatttcattc |
| 18 | MAVS C508R 3' SpeI reverse | gcccgtagtttactag actagt catctactc |
| 19 | XmaI-Flag-3A_for | cccggggatcatggactacaaagacgatgacgacaag ggaatttcagatgataatgatagtcag |
| 20 | Rosa T7_fwd | tcttttctgtggacccttaccttg |
| 21 | Rosa T7_rev | gccacgttgtagttggatagtt |

Table 15. Cloning oligonucleotides used in this study.

2.16 Oligonucleotides and probes used for qPCR

Shown is a list of primers and probes used in this study. All DNA oligonucleotides were synthesized by Sigma-Aldrich. The lyophilized nucleotides were resuspended in ddH₂O to a final concentration of 100 µM. Branching-DNA probes were ordered from Affymetrix, Thermo Fisher Scientific.

| # | Primers (Human targets) | Sequence 5' → 3' |
|---|-------------------------|-------------------------|
| 1 | GAPDH_for | GAAGGTGAAGGTCGGAGTC |
| 2 | GAPDH_rev | GAAGATGGTGTATGGGATTTC |
| 3 | S_IFIT1 | GAAGCAGGCAATCACAGAAA |
| 4 | A_IFIT1 | TGAAACCGACCATAGTGGAA |
| 5 | S_CXCL10 | GGCATTCAAGGAGTACCTCTCTC |

| | | |
|----------|---------------------------------|---------------------------------|
| 6 | A_CXCL10 | TGGACAAAATTGGCTTGCAGGA |
| 7 | ISG20 F | TAGCCGCTCATGTCCTCTT |
| 8 | ISG20 R | TGAGGGAGAGATCACCGAT |
| 9 | A_219_JFH | GGG CAT AGA GTG GGT TTA TCC A |
| 10 | S_146_JFH | TCT GCG GAA CCG GTG AGT A |
| 11 | S59_Con | TGT CTT CAC GCA GAA AGC GTC TAG |
| 12 | A165 | TAC TCA CCG GTT CCG CAG A |
| 13 | HAV IRES fwd | GGTAACAGCGGCGGATATTGG |
| 14 | HAV IRES rev | AGTCAATCCACTCAATGCATCCA |
| 15 | RANTES fwd | TCATTGCTACTGCCCTCTGC |
| 16 | RANTES rew | TACTCCTTGATGTGGGCACG |
| 17 | S_ISG15 | TGTCGGTGTCAGAGCTGAAG |
| 18 | A_ISG15 | AGAGGTTTCGTCGCATTTGTC |
| 19 | HPRT Fwd | GCGTCGTGATTAGCGATGATG |
| 20 | HPRT Rev | CTCGAGCAAGTCTTTCAGTCC |
| # | Primers (Murine targets) | Sequence 5' → 3' |
| 19 | Mouse GAPDH | GTTGTCTCCTGCGACTTCA |
| 20 | Mouse GAPDH | GGTGGTCCAGGGTTTCTTA |
| 21 | S_ISG15 | CATCCTGGTGAGGAACGAAAGG |
| 22 | A_ISG15 | CTCAGCCAGAACTGGTCTTCGT |
| 23 | S_CXCL10 | ATCATCCCTGCGAGCCTATCCT |
| 24 | A_CXCL10 | GACCTTTTTTGGCTAAACGCTTTC |
| 25 | S_IFIT1 | TACAGGCTGGAGTGTGCTGAGA |
| 26 | A_IFIT1 | CTCCACTTTCAGAGCCTTCGCA |

Table 16. qPCR oligos used in this study.

| Probe | Fluorophore | Sequence 5' → 3' | Quencher |
|---------------------|--------------------|---|-----------------|
| HAV_IRES (probe) | FAM | 5'-6-FAM- TGTTAAGACAAAAACCAATTCAACGCCGGA TAMRA-3' | TAMRA |
| P_GAPDH (probe) | VIC | 5'-6-VIC-CAAGCTTCCCGTTCTCAGCCT-TAMRA- 3' | TAMRA |
| Mouse GAPDH | VIC | cctgctgcttatcgtggctg | MGBNFQ |
| Con1 5' UTR | FAM | 6-FAM - TCC TGG AGG CTG CAC GAC ACT CAT | TAMRA |
| JFH1 5' UTR | FAM | 6-FAM - AAA GGA CCC AGT CTT CCC GGC AAT T | TAMRA |

| | | | |
|----------------|-----|----------------------|--------|
| Mouse GAPDH | VIC | cctgctgcttatcgtggctg | MGBNFQ |
|----------------|-----|----------------------|--------|

Table 17. qPCR probes used in this study.

2.17 Instruments

| Instrument | Manufacturer |
|--|-----------------------------------|
| Biosafe liquid nitrogen tanks | Cryotherm |
| Branson sonifier 450 | G. Heinemann |
| C1000 Touch™ Thermal Cycler with a CFX96™ Real-Time System | BioRad |
| Centrifuge 5417C | Eppendorf |
| Centrifuge RC-5C plus | Sorvall |
| DNA gel electrophoresis chamber | BioRad |
| ECL Chemocam Imager | Intas Science Imaging Instruments |
| FlexCycler 2 | Analytik Jena |
| Gene Pulser II | BioRad |
| HeraSafe Laminar Flow cabinet | Thermo Fisher Scientific |
| Luminometer Lumat LB 9507 | Thermo Fisher Scientific |
| Luminometer Mithras LB 940 | Thermo Fisher Scientific |
| Nanodrop | Thermo Fisher Scientific |
| pH meter 7110 | inoLab |
| Pipetboy | Integra |
| Stericult 200 Incubator | Thermo Fisher Scientific |
| Thermomixer C | Eppendorf |
| Ti Eclipse fluorescence microscope | Nikon |
| Ultra-centrifuge 90 SE | Sorvall |
| Wet-blot transfer system | BioRad |

Table 17. Instruments used in this study.

2.18 Enzymes

| Enzyme | Manufacturer |
|-----------------------------------|---------------------|
| Calf intestinal Phosphatase (CIP) | New England Biolabs |
| DNA restriction enzymes (various) | New England Biolabs |
| RNase-free DNase RQ1 | Promega |
| RNAasin | Promega |
| T4 DNA ligase | Fermentas |
| T7 RNA polymerase | in house |
| Trypsin/EDTA | Sigma-Aldrich |

Table 18. Enzymes used in this study.

2.19 Software

| Software name | Manufacturer | Version |
|--------------------|--|---------|
| GraphPad Prism | GraphPad Software | 9 |
| Fiji | Schindelin, J., Arganda-Carreras, I., Frise, E., Kaynig, V., Longair, M., Pietzsch, T. Cardona, A. (2012). Fiji: an open-source platform for biological-image analysis. <i>Nature Methods</i> , 9(7), 676–682. | 1.53o |
| BioRad CFX Maestro | BioRad Laboratories | 2.0 |
| QuPath | Bankhead, P. et al. QuPath: Open source software for digital pathology image analysis. <i>Scientific Reports</i> (2017). | 0.4.3 |
| Excel | Microsoft Corporation | 16.68 |
| Word | Microsoft Corporation | 16.65 |
| Illustrator | Adobe | 27.1.1 |

Table 19. Softwares used in this study.

2.20 Other (e.g. drugs, proteins, etc.)

| Name | | Manufacturer | Product no. |
|-------------------------|--|-----------------------------|-------------|
| Simeprevir | | Hölzel Diagnostika | HY-10241 |
| MitoTracker Deep Red | | ThermoFischer Scientific | M22426 |
| DAPI | | Invitrogen | |
| Digitonin | | Sigma-Aldrich | |
| Poly (I:C) HMW | | Invivogen | |

Table 20. Others molecules used in this study.

3. Methods

3.1 Handling, culturing and storing cells

Cells were cultured in DMEM complete medium (see *Materials*) and kept at 37°C, 5% CO₂, and 90% relative humidity. When cells reached 90-100% confluency, they were rinsed with PBS and incubated with a thin layer trypsin/EDTA for 5 minutes at 37°C. Upon shaking and assessment through microscopy of cell detachment, the solution containing the detached cells was then collected with pre-warmed DMEM at 37°C and cells were split with different ratio according to the cell lines: 1:6 for Huh7-Lunet, 1:8 for Huh7.5, 1:5 for HepG2 or 1:15 for 293T cells. Cells that were stably transduced received half the antibiotic dose used during the first passaging: 2.5 µg/ml blasticidin, 1 µg/ml puromycin, 80 µg hygromycin or 500 µg/ml G418.

For long term storage, cells were kept in a Biosafe liquid nitrogen tank at -190°C. For preparing cells for this freezing process, they were cultivated until they reached about 90% confluence. Cells were then trypsinised and then centrifuged with DMEM complete for 5 minutes at 700 x g. Cells from a 15 cm culture dish were typically reconstituted in 6 ml of an ice-cold cryo solution and then distributed evenly across four cryo vials.

For thawing cells from frozen storage, they were let thaw on the air flow of the laminar hood and mixed with 6 ml DMEM pre-warmed at 37°C. Cells were then centrifuged with DMEM complete for 5 minutes at 700 x g and washed once with PBS with subsequent centrifugation at 700 x g; the pellet was then solved in pre-warmed DMEM and distributed to a 15cm² dish. The cells were checked after 16 to 24 hours after thawing.

3.2 Electroporation of cells

For cell transfection through electroporation, following trypsinization the cells were washed twice and re-suspended in a freshly prepared Cytomix solution³¹⁰ that was enriched with 5 mM of glutathione and 2 mM ATP, ensuring a concentration of 1×10^7 Huh7 Lunet or 1.5×10^7

Huh7.5 cells per milliliter. 400µl of this cell suspension were then combined with 10 µg of the RNA in vitro transcript. The mixture underwent electroporation in a 0.4 cm cuvette utilizing a Gene Pulser device with settings of 975 µF and 270 V. After the electroporation, cells were seeded according to the experimental requirements.

3.3 Production of Lentiviral Vectors and Selection of Stable Cell Lines

Selectable lentiviral vectors were generated and used for transient transduction or for generation of stable cell lines, as described before³¹¹. Briefly, HEK293T cells were seeded in 10 cm cell culture dishes (5×10^6 cells /10 ml DMEM) 16 hours prior transfection and fed from around one hour before transfection with FCS-depleted DMEM (“starvation DMEM”). A DNA mixture was prepared with the plasmids pSPAX2-Gag-Pol (5.14 µg), pMD2-VSVG (1.71 µg) and a pWPI vector encoding the gene of interest (5.14 µg) in 400 µL of Opti-MEM. The polyethylenimine (PEI) mixture was purchased by Polysciences Inc (23966-2, PA, USA) and diluted to a concentration of 1mg/ml. A transfection mixture was prepared with 36 µL of PEI in 400 µL of Opti-MEM. The plasmid mixture was then thoroughly mixed with the PEI mixture in a total of 800 µL Opti-MEM and incubated at room temperature (RT) for 20 minutes, then added to HEK293T cells drop-wise. Media was changed to complete DMEM after 6 hours. 48 hours and 72 hours after transfection, the supernatant was collected and filtered through a 0.45 µm filter to remove cells and cell debris and then was either aliquoted and stored at -80°C or directly added to target cells. Newly generated vectors were HAV 3ABC wild-type and mutant C172A (Puro), HAV 3CD wild type and mutant C172A (Puro) and HCV NS3-4A wild type and mutant S193A (Puro) (see “Plasmid constructs”).

3.4 DNA transfection

For all overexpression experiments through pTM plasmid transfections, TransIT-LT1 Reagent (Mirus Bio LLC, Madison, Wisconsin) was used according to the manufacturer’s protocol (Mirus Bio LLC). Briefly, 1.5×10^5 Huh7-T7 cells were seeded in a 6-well plate in a 2 ml/well volume. One hour prior to transfection, cells were fed with FCS-depleted medium and a mix was prepared with 2.5 µg of DNA combined with 7.5 µl of TransIT-LT1 Reagent in a total of 250 µl Opti-MEM. After mixing completely by pipetting gently, the mixture was incubated at

RT for 20 minutes and was added dropwise to the cells, which were harvested 16 hours after transfection.

3.5 Infection of cells

For infection experiments with Huh7 cells, a density of 1×10^5 cells/ well 16 hours before infection in 12 well plates for microscopy and at 1.2×10^5 / well for RNA extraction. For Huh7.5 cells, I seeded a density of 0.8×10^5 / well 16 hours before infection in 12 well plates for microscopy and at 1.2×10^5 / well for RNA extraction. Seeding of HepG2 cell lines was done 16 hours before infection in 12 well plates at a density of 3.5×10^5 / well. One hour before infection, complete medium was replaced with FCS-depleted medium (“starvation medium”, *Materials*) to improve viral delivery³¹². I then inoculated the cells with HAV and HCV, diluting them in FCS-depleted medium at a multiplicity of infection (MOI) of 4 for HAV and 1 for HCV unless stated differently. I chose different MOIs for both viruses to achieve similar replication levels, which I assessed based on positive strand RNA detection in the total RNA of the infected cells. Three hours post-infection, I washed the cells with phosphate-buffered saline (PBS) and added the complete medium back.

Huh7-Lunet cells and Huh7-Lunet T7 cells have been described before³¹¹, as well as the Con1 subgenomic replicon clone 9-13³¹³ (gt1b, GenBank accession number AJ238799) and LucubineoJFH1²³⁷ (gt2a, GenBank accession number AB047639), along with the HAV replicon cell lines¹⁹⁰. Huh7-Lunet “ROSA T7” cells were generated through lentiviral transduction of a pWPI ROSA26-T7 Blr construct (described in “Plasmid constructs”).

Huh7.5 cell lines stably expressing HCV viral proteases were obtained through lentiviral transduction of the pWPI respective constructs (described In “Plasmid constructs”). To obtain Huh7.5 HCV NS3-4A and Huh7.5 HCV NS3-4A S139A at low expression, the respective lentivirus inoculums were 5-fold diluted.

Huh7 and HepG2 cell lines were cultured in Dulbecco’s Modified Eagle Medium (DMEM; Life Technologies, Darmstadt, Germany), supplemented with 10% fetal calf serum (FCS, Capricorn Scientific, Germany), non-essential amino acids (Life Technologies, Darmstadt, Germany), 100 U/ml penicillin and 100 ng/ml streptomycin (Life Technologies) and

cultivated at 37°C and 5% CO₂. HepaRG-derived cells were cultured in William's E Medium (Life Technologies, Germany), supplemented with 10% fetal calf serum (GE Healthcare, Germany), 100 U/ml penicillin, 100 µg/ml streptomycin (Sigma Aldrich, USA), 2 mM L-glutamine (Life Technologies, Germany), 5 µg/ml insulin (Sigma Aldrich) and 50 µM hydrocortisone (Sigma Aldrich). For culture experiments longer than 3 days, DMSO was always added to the final concentration of 1.5 %. All stably transduced cells were kept under selection pressure by addition of 1mg/ml G418 (Geneticin, Life Technologies), 1µg/ml puromycin (Sigma-Aldrich, Steinheim, Germany) or 5µg/ml blasticidin (Sigma-Aldrich).

3.6 Immunostimulation

For TLR3-specific activation, cells were treated with poly (I:C) High Molecular Weight (HMW; purchased from Invivogen, San Diego, California) in the supernatant at concentrations of 10 or 50 µg/ml. Cells were collected six hours post-treatment to extract RNA and conduct RT-qPCR. To stimulate both cytosolic PRRs (including RIG-I and MDA5) and TLR3, poly (I:C) was transfected using Lipofectamine2000, provided by Life Technologies, Karlsruhe, Germany. For transfecting a single well in a 24-well setup, varying concentrations of poly (I:C) ranging from 0.001 to 1 µg were combined with 0.1 to 0.5 µl of Lipofectamine2000 reagent in 100 µl OptiMEM. This mixture was left to incubate at room temperature for 5 minutes before being administered to the cells. Six hours subsequent to this transfection, RNA was extracted from the cells.

3.7 Immunostimulation of infected cells

To check for viral functional counteraction, cells were infected with HAV or HCV for 4 or 3 days, respectively, in 10cm² dishes at a multiplicity of infection of 4 and 1, respectively. At the indicated time, cells were trypsinized and re-seeded onto coverslips at the indicated densities for microscopy experiments, ensuring the sufficient spread of the monolayer (chapter "Handling of cells"). One day later, the cells were stimulated with poly(I:C) delivered either with supernatant feeding or through lipofectant. 6 hours later, cells were fixed and analyzed further (see "immunofluorescence").

3.8 Cell viability assay

Cell proliferation/viability was assessed by WST-1 assay (Cell-proliferation reagent WST-1; Roche, Basel, Switzerland) as described by the manufacturers' protocols in 96-well plates. Background was determined by measuring absorbance of medium in empty wells incubated with the reagent, and was subtracted from absorbance in experimental wells. Values were normalized to control samples.

3.9 Protease inhibitor treatment

Huh7 Lunet T7 cells and JFH-1 cells, seeded in 6 well plates, were incubated with 1 μ M Simeprevir (Hözel Diagnostika) starting 16 hours before the treatment, or control treated with DMSO, for 24 hours. Furthermore, Simeprevir was implemented every 24 hours freshly onto the cells.

Manipulation of DNA and RNA

3.10 Plasmid constructs

Plasmids encoding HCV or HAV replicons were described before¹⁹⁰, as well as the HCV Jc1 plasmid used for HCV virus production²⁶⁷. The HAV 18f plasmid used for HAV virus production was a kind gift from Stanley Lemon.

Plasmids used in the overexpression experiments were designed based on pTM vectors,³¹⁴ described in³¹⁵ with the cloned genes under translational control of an EMCV IRES. For HAV 3CD, the 3CD wt CDS was amplified from the HAV genome (HM-175/18f) and N-terminal FLAG-tagged using forward primer #1 (see Supplementary Table 2) and reverse primer #2. The C172A mutant was produced from the same template by overlap extension PCR using primers #1 + #4 and primers #2 + #3. PCR fragments were first cloned into vectors pWPI-Neo/Bla using XmaI and SpeI restriction sites. For cloning into pTM-1-2 we used NcoI and SpeI restriction sites, after amplification of the FLAG-tagged 3CD wt and mutant with primers #14 and #5. For HCV NS3/4A, pWPI-GUN encoding untagged NS3/4A (Con1) wt and catalytically inactive mutant S139A (described before in²¹³) were used for cloning into pTM-1-2, amplifying the NS3/4A CDS with an N-terminal FLAG-tag using primers #6 and #7 and NcoI and SpeI restriction sites. A pTM vector encoding Flag-tagged NS3/4A gt2a was based on JFH1, GenBank accession number AB047639²³⁷. For TRIF-encoding plasmids, we amplified the human TRIF wt CDS from a cloned TRIF cDNA. An N-terminal HA-tag was added using forward primer #8 and reverse primer #9. The C372R and the Q554A mutants were produced by overlap extension PCR from the same template using either primers #8 + #10 and #11 + #9 or primers #8 + #13 and #12 + #9. The C372R Q554A double mutant was produced by overlap extension PCR from HA-TRIF Q554A cloned into pTM-1-2 using primers #8 + #10 and #11 + #9. For cloning into pTM-1-2 and pWPI-Neo, PCR products and vectors were digested with XmaI and SpeI. For deletion of the RHIM domain and addition of an extra C-HA tag, pTM HA-TRIF TRIF Δ RHIM was produced using primers #8 and #15. N-terminally HA tagged MAVS and MAVS mutant C508A were generated based on pTM-MAVS²¹³ using primers #16 + #17 and #16 + #18, respectively, and restriction enzymes SmaI and SpeI. To generate MAVS-GFP-NLS, a pTM plasmid was cloned with a nuclear translocation signal with

GFP fused to the C-terminal membrane anchor of MAVS (MAVS-GFP-NLS), where the MAVS coding region was extended to encode the canonical protease cleavage sites of both viruses (Q428 - C508).

Plasmids generated on a pWPI backbone with genes were used for generation of lentiviral vector particles. pWPI specifically encoding TLR3 Puro, RIG-I Blr and MDA5-Gun have been described before⁸³. pWPI 3ABC and 3CD were cloned with forward primers #19 and #1, respectively, and reverse primer #2. To obtain 3ABC mutants, overlap PCR was performed using primers #19 and #4 and #3 and #2. For the same mutant in 3CD, primers #1 and #4 and #3 and #2 were used. All PCR products were digested with SmaI and SpeI. pWPI NS3-4A Neo and pWPI NS3-4A S193A Neo were already described before²¹³. Cloning of pWPI ROSA26-T7 Blr was obtained with an amplification via PCR on the plasmid pWPI eF1 α -T7-GUN³¹¹ using the primers #20 and #21 indicated in Supplemental Table 2. A partial digestion of the insert was then obtained with PaeI and MluI. A 2900 bp obtained product was then ligated in the vector pWPI-ROSA26-empty-Blr (kind gift from Marco Binder).

All cloning PCR reactions employed the Phusion Flash High-Fidelity PCR Master Mix from ThermoFisher Scientific. Restriction enzyme digestions followed the manufacturer's protocols provided by NEB. For gel purification, PCR cleanup, and both Mini and Maxi plasmid preparations, Macherey Nagel kits were used (NucleoSpin Gel, PCR Clean-up, NucleoSpin Plasmid and NucleoBond PC500). DNA ligation was conducted using the T4 DNA Ligase from ThermoFisher Scientific, letting the reactions proceed for a minimum of 30 minutes at room temperature and preferentially at 16°C overnight. Bacteria transformation was carried out using chemically competent DH5 α E. coli bacteria (see Bacteria transformation). To verify the accuracy of all newly created plasmids, their sequences were examined through Sanger sequencing at Eurofins Genomics in Germany.

3.11 Bacterial transformation

Plasmid DNA was amplified mixing 30-50 μ l of E. coli DH5 α with the ligation mixture or with 500 ng of isolated plasmid DNA. This combination was then kept on ice for a duration of 20 minutes. After this, the bacteria underwent a heat shock at 42°C for 1 minute and were

subsequently placed on ice for another 2 minutes. Following this, 700 μ l of LB medium, devoid of any antibiotics, were added, and the resulting culture was placed in a bacterial shaker set at 37°C for a period of 30 to 90 minutes. To isolate individual bacterial colonies, the transformed bacteria were then spread onto LB agar plates prepared with the appropriate selection antibiotics, and then incubated overnight at 37°C or for 2 days at room temperature.

3.12 DNA extraction from bacteria

Post-transformation, bacterial colonies were selected using a sterile pipette tip and inoculated into 3 ml of LB medium enriched with the corresponding selection antibiotic. The inoculated medium was subsequently placed in a shaker at 37°C for overnight growth. Following this, a 1.5 ml aliquot of the overnight culture was subjected to centrifugation for 2 minutes at 1000 x g, after which the supernatant was removed. Using the NucleoSpin® plasmid kit, the plasmid DNA was then extracted from the remaining bacterial pellet, following the guidelines provided by the manufacturer (“Mini Prep” procedure). Typically, the elution of plasmid DNA was achieved in 40 μ l of ddH₂O per column.

For large-scale plasmid stock production (“Maxi Prep”), the 3 ml bacterial cultures were subjected to an extended incubation period of 10 hours at 37°C in a shaker. Thereafter, these cultures were used to inoculate larger volumes (ranging from 50 to 400 ml) of TB medium, implemented with the corresponding selection antibiotic. The larger culture was then incubated at 37°C overnight with continuous shaking, post which it was centrifuged at 5000 x g for a duration of 5 minutes. The supernatant was carefully removed, and the plasmid DNA was purified using the NucleoBond® PC500 kit as per the instructions provided by the manufacturer. The isolated plasmid was typically reconstituted in 100 μ l of ddH₂O.

3.13 Polymerase Chain Reaction (PCR)

To obtain specific amplification of DNA of interest, reactions were conducted as follows:

In 25 μ l were mixed:

- 1x HF buffer (provided with the Phusion kit)
- 200 μ M dNTPs

- 500 nM each of forward and reverse primers
- 100 ng of template DNA
- 0.5 units of Phusion DNA polymerase.

The PCR cycle was initiated with a denaturation step at 98°C for 30 seconds. This was followed by 40 cycles of:

- 98°C for 10 seconds (denaturation)
- 50-72°C for 30 seconds (annealing, the exact temperature depends on the primers used)
- 72°C for 20 seconds/kbp (elongation)

The final extension was carried out at 72°C for 2 minutes.

The amplified DNA fragments were then purified using the NucleoSpin® Extraction II kit and visualized on an agarose gel to check for purity and correct size.

3.14 Agarose gel separation

To separate digested DNA fragments, agarose was mixed with 1x TAE buffer to achieve concentrations ranging from 0.8 to 2% (w/v). The concentration was selected based on the size of the DNA fragments being analyzed. The mixture was gently heated in a microwave, with intermittent stirring, to completely dissolve the agarose. After the solution cooled to around 50°C, GelRed, a nucleic acid stain, was added at a dilution of 1:20,000. The solution was stirred for uniform distribution and poured into a mold to set. The gel was run in 1x TAE buffer at a voltage of 120 V.

Following electrophoresis, DNA bands were visualized under UV light. Desired bands or fragments were carefully excised with a scalpel for further procedures

3.15 DNA endonuclease digestion

Restriction endonucleases, or restriction enzymes, were used to cut DNA at specific sites. Restriction enzymes from New England Biolabs were used for all digest reactions, along with the corresponding buffer (either 1.1, 1.2, 1.3, or CutSmart®).

For further purification, after performing agarose gel electrophoresis the entire volume of the restriction digest was loaded onto the gel. Upon completion of the run, the desired band was visualized under UV light. Using a sterile surgical knife, the band corresponding to the correct size was carefully excised from the gel.

The NucleoSpin® Extraction II kit was employed to purify the DNA from the gel piece. Following the manufacturer's instructions, the isolated DNA fragment was typically eluted in 40 µl of double distilled water (ddH₂O).

3.16 *In vitro* transcription and virus stock production

Plasmids (10 µg) were linearized using restriction enzymes: MluI for HCV-based, SphI for HAV-based. Following linearization, the DNA was purified.

For the transcription reaction, a mix was created in RRL buffer consisting of each nucleoside triphosphate (3.125 mM), RNasin (100 U), and T7 RNA polymerase (4 µl) in a 100 µl total volume. The mixture underwent a 2-hour incubation at 37°C, post which an additional 2 µl of T7 RNA polymerase was added and incubated for another 2 hours. The transcription process was halted with 7.5 µl of RNase-free RQ1 DNase, followed by a 30-minute incubation at 37°C.

To purify the RNA, a combination of RNase-free water (500 µl), sodium acetate (60 µl, 2 M, pH 4.5), and phenol (400 µl) was added and thoroughly mixed. The mixture was kept on ice for 10 minutes and centrifuged at 20,000 x g for 10 minutes at 4°C. From the resultant solution, the upper aqueous phase was moved to a fresh tube and combined with 600 µl of chloroform, mixed, and centrifuged at 20,000 x g for 3 minutes at 22°C. The RNA was precipitated using 0.7 volumes of isopropanol, inverted, and settled for 15 minutes at room temperature. RNA was then centrifuged at max speed at room temperature for 10 minutes, washed with 70% ethanol twice, and air-dried in a fume hood. The dry RNA was redissolved in 100 µl RNase-free water at 65°C degrees with shaking. Purity was confirmed if both the OD₂₆₀/OD₂₃₀ and OD₂₆₀/OD₂₈₀ ratios were above 2.0 and the sample was producing a clean band upon a 5 minutes run onto a pure agarose gel.

For HCV virus generation, Huh7.5 cells were transfected with the in vitro transcribed RNA of the Jc1 variant. At 72 hours post-transfection, the supernatant was collected and filtered using a 0.45- μ m filter from Whatman plc (Maidstone, UK). Viral stocks were then concentrated via ultrafiltration with a Centricon Plus-70 device (Millipore, Bedford, MA) and aliquoted for storage at -80°C , and subjected to TCID_{50} for evaluation of infectivity.

For the production of the HAV virus, in vitro transcripts of the full-length genome RNA of the HAV strain HM-175/18f (gratefully received from Stanley Lemon) were generated like follows. 14 μ g of HM-175/18f DNA were subjected to a 2-hour SmaI digestion in a 100 μ l mixture at 37°C , followed by purification with the NucleoSpin[®] Extraction II kit (Macherey-Nagel). This DNA was eluted in 63 μ l of water. Subsequently, in vitro transcription was conducted on 5 μ g of this DNA in a 100 μ l solution, incorporating 12.5 μ l of 25 mM rNTP, 80 U T7 polymerase, and 100 U RNasin[®] Ribonuclease Inhibitor (both from Promega). This also included 20 μ l of 5X RRL buffer. The reaction proceeded for 2 hours at 37°C , after which an additional 2 μ l of T7 polymerase was added and the mixture was incubated overnight at the same temperature. To get rid of the DNA template, 20 μ l of RNase-free DNase (Promega, 1 U/ μ l) was included, followed by a 30-minute incubation at 37°C and RNA extraction using a chloroform-phenol method like shown before³¹¹.

To electroporate the HAV (HM-175/18f) IVT into the cells, 1.5×10^7 Huh7.5 cells were mixed in 1 ml of Cytomix, and 10 μ g of the transcribed RNA was utilized to transfect 400 μ l of this cell mixture. The cells were then plated onto 175 cm^2 with ventilated and filtered cap. Both cell lysates and the supernatant were collected on the 11th day post-transfection. They underwent three freeze/thaw cycles (to obtain „naked“ virions) or the supernatant were stored („enveloped“ virions) and were then passed through a 0.45- μ m filter. The viral titer was determined using the TCID_{50} method.

Analytical procedures

3.17 HAV purification from stool samples

Stool specimens were procured from two patients, denoted as “2” and “3”, both of whom were infected with the HAV genotype IA. These samples were collected 12 to 13 days post the initial clinical symptom presentation and underwent Sanger sequencing, specifically targeting the VP1-P2A junction. The samples, then, when compared alongside a non-infected control, were diluted to a 10% v/v solution using PBS. The specimen underwent preliminary homogenization through sequential pipetting and vortexing. To further refine the homogenate, it was subjected to sonication using a Branson sonicator, consisting of three cycles each with 1 minute of 160 W pulsing, followed by a 1-minute resting phase on ice. The sample was then centrifuged at 1,500 x g for a duration of 10 minutes.

Subsequently, the supernatant underwent filtration through a 5µm CHROMAFIL Xtra PES filter (25 mm, luer lock #ref 729242, Macherey-Nagel, Germany). Further centrifugation steps involved spins at 15,000 g for 15 minutes, and again at the same speed for an extended 30 minutes. A filtering sequence was employed, encompassing 0.8µm, 0.45µm, and 0.22µm filter units (sourced from Whatman® Puradisc 13 syringe filter) to ensure the isolation of viral particles from the sample.

3.18 RNA Extraction from livers of uPA-SCID mice with humanized liver

To extract RNA from liver tissues, 100 mg of samples were preserved by freezing in 1.5 ml RNAlater solution from ThermoFisher Scientific. A 20 mg portion of this tissue was then ground to a powder using a Dounce tissue grinder set from Merck, Germany, on dry ice. For the subsequent RNA extraction, samples were processed with the Bio&SELL RNA-Mini Kit, based in Nuremberg, Germany, following the manufacturer’s protocol.

3.19 Immunofluorescence analysis and microscopy

For the purpose of immunofluorescence (IF) analysis, typically 2×10^4 cells were seeded onto coverslips situated in 24-well plates. After a 48-hour seeding period, the cells underwent fixation using 4% paraformaldehyde in PBS for 15 minutes at room temperature. This was

followed by permeabilization with 50 µg/mL digitonin (Sigma-Aldrich, Steinheim, Germany) in PBS for 15 minutes on ice. Subsequent to three PBS washes, the primary antibodies, diluted in 3% bovine serum albumin/PBS, were introduced for an hour at room temperature. The employed primary antibodies included anti-Flag (1:400, Sigma Aldrich - F1804-2MG), anti-3C (1:1500, a provision from Verena Gauss-Müller), anti-HAV Vp3 (C22H, 1:250, Thermo Fisher Scientific, MA USA), and anti-NS5A (9E10, a gift from Charles Rice, at 1:150 dilution).

Following another round of washing, the cells were exposed to secondary antibodies for 45 minutes, in the dark and at room temperature. The secondary antibodies used were anti-mouse IgG2a-AlexaFluor488 and anti-rabbit Ig-AlexaFluor568, both diluted at 1:1000 and sourced from Invitrogen, Carlsbad, CA. Post-wash, the nuclei were marked using 250 ng/mL 4',6-diamidino-2-phenylindole (DAPI) from Invitrogen in PBS for a duration of 1 minute. After a final wash, they were mounted on microscopy slides. Mitochondrial structures were highlighted using MitoTracker Deep Red (M22426) and beta actin filaments using Phalloidin AlexaFluor 568, both from ThermoFisher Scientific. Microscopy was performed on a Nikon Ti-Eclipse epifluorescence microscope, with a ×40 oil immersion objective, examining a minimum of 30 cells for each set condition. For removal of the background interference from all channels, signal intensity analyses was performed using the Measure plug-in macro in the Fiji software.

3.20 FACS analysis

To study counteraction to the PRR pathways at a single cell level in alternative to IF staining, FACS was attempted. Cells were seeded as usual in 10cm² dish and infected with HAV for 4 days. After re-seeding onto 6 wells and poly(I:C) stimulation, cells were harvested 6 hours later and firstly washed with 1x PBS, trypsinized and promptly collected into 1.5 ml tubes. To fix the cells, they were treated with 100µl of a 3% PFA solution at room temperature for about 10-15 minutes. Cells were washed twice with abundant PBS, each time filling the eppendorf tube up to 1 ml at least. After each wash, cells were centrifuged at a speed of 1000 RPM for 5 minutes to ensure optimal sedimentation.

For permeabilization, a solution of 0.1% Triton X-100 in PBS, amounting to 100µl, was applied to the cells and let incubate 2 minutes. Another round of washing with 1x PBS was conducted, followed by a 5-minute centrifugation at 1000 RPM.

The primary antibody staining took place on ice for 45 minutes (Rabbit Mx1 at a 1:50 dilution, and Mouse HAV Vp3 at a 1:50 dilution).

Cells were washed twice using 1x PBS and subsequently centrifuged for 5 minutes at 1000 RPM. For the secondary antibody staining, cells were treated with Anti-rabbit 568 TexasRed and Anti-mouse 388 FITC, both at a 1:200 dilution. This staining process took place on ice and was allowed to continue for a period of 20-30 minutes. Following this, a concluding double wash with 1x PBS was performed. Cells were then resuspended in 300 µl of PBS and stored at 4°C for up to 12 hours, for subsequent measurement or analysis through a BD FACS Celesta flow cytometry reader.

3.21 Quantitative Real-Time PCR (RT-qPCR)

Total RNA was isolated from cultured cells or supernatant using the NucleoSpin RNA Plus kit (Macherey-Nagel, Düren, Germany). RT-qPCR was performed as described before⁸³. For gene expression analysis, complementary DNA (cDNA) was generated from RNA samples using High-Capacity cDNA Reverse Transcription Kit (ThermoFisher Scientific, Waltham, MA), and was used for qPCR analysis with the 2x iTaq Universal SYBR Green supermix (Bio-Rad, Munich, Germany). Reactions were performed on a CFX96 Touch Real-Time PCR Detection System (Bio-Rad) as follows: 95°C for 3 minutes, 95°C for 10 and 60°C for 30 seconds. Primers used are indicated under „Oligonucleotides for qPCR“, *Materials*. Glyceraldehyde-3-phosphate dehydrogenase (GAPDH) or Hypoxanthine-guanine phosphoribosyltransferase (HPRT) were used as internal reference genes, and relative gene expression was determined using the 2- $\Delta\Delta$ CT method by normalizing to untreated samples. In the case of time course experiments, all samples were normalized to the untreated sample at the relative timepoint.

For analysis of HCV and HAV genomic RNA, 1-step RT-qPCR was performed using qScript XLT One-Step RT-qPCR ToughMix (Quanta Biosciences, Gaithersburg, MD), according to the

manufacturer's instructions. In brief, 15 μ L of reaction mixture contained 7.5 μ L 2x enzyme/buffer mix, 1 μ M of each HCV-specific primer (TCTGCGGAACCGGTGAGT and GGGCATAGAGTGGGTTTATCCA), 0.27 μ M HCV-specific probe (AAAGGACCCAGTCTTCCCGCAATT), or HAV-IRES-specific primers (GGTAACAGCGGCGGATATTGG and AGTCAATCCACTCAATGCATCCA) with a HAV specific probe (TGTTAAGACAAAAACCAATTCAACGCCGGA); 3 μ L template RNA and RNase-free water. To determine absolute RNA amounts, a serial dilution of an RNA standard (10^1 to 10^8 HAV or HCV RNA copies per reaction) was processed in parallel. Reactions were performed using the following program: 50°C for 10 minutes, 95°C for 1 minute, and 40 cycles as follows: 95°C for 10 seconds, 60°C for 1 minute.

3.22 Immunoblotting

20 to 50 μ g cell extracts were separated on 10 or 12% SDS-PAGE and subjected to immunoblotting. SDS-PAGE gels were prepared with a 4% acrylamide stacking gel and a separating gel with an acrylamide concentration between 8-10%, tailored to the needs of the experiment. For the analysis of proteins across a broad molecular weight spectrum, gradient gels containing 6-12% acrylamide were utilized.

The polymerization of acrylamide was initiated using ammonium persulfate and TEMED. To ensure a flat surface during the polymerization of the separating gel, isopropanol was layered on top. Proteins in the samples were then loaded onto the gels and separated at an electric field of initial 90V and up to 120 V. A bi-colored protein ladder was loaded in an adjacent well to track the protein separation process.

After completing the SDS-PAGE, the proteins were transferred onto PVDF membranes. The PVDF membrane was first activated by a 2-minute immersion in methanol and subsequently rinsed in blotting buffer for another 2 minutes before assembling the Western blot setup. Onto the device, a blotting buffer-soaked sponge was placed on the bottom and following it two sheets of wet Whatman paper; then, the SDS-page gel, transferred carefully with a comb, and on top of it the activated PVDF membrane, layered flat to avoid bubbles, followed by another two wet sheets of Whatman paper. This assembly was then positioned inside the gel cassette holder of the Mini Trans-blot Cell device; the chamber was filled with

wet blot buffer. Protein transfer was carried out over 1-2 hours using an electric current set to 400 mA.

After transfer to polyvinylidene difluoride membranes and blocking at room temperature in PBS containing 0.1% Tween 20 (PBS/Tween) and 5% skim milk for 1 hour, the polyvinylidene difluoride blots were incubated with antibodies specific for MDA5 (1:1000; Cell Signaling, Danvers, MA), RIG-I (1:1000; Adipogen, San Diego, CA), TLR3 (1:1000; Abcam), actin (1:4000; Sigma-Aldrich), HA tag (1:1000; Abcam), Flag tag (1:2000; Sigma Aldrich - F1804-2MG); 3C (1:200, kindly received from Verena Gauss Müller), NS5A (9E10, 1:5000; generous gift from Charles Rice), NS3 (#49, made in house, 1:1000) at 4°C overnight. After washing in PBS/Tween, the membranes were incubated with anti-mouse (1:10,000) and anti-rabbit (1:5000) horseradish peroxidase antibodies (Sigma-Aldrich) at room temperature for 1 hour. Proteins were detected by using the ECL Plus Western Blotting Detection System (Pierce, GE Healthcare, Little Chalfont, UK) according to the instructions of the manufacturer. Signal was recorded using the Advance ECL Chemocam Imager (Intas Science Imaging, Goettingen, Germany).

3.23 Statistics

For significance testing, either the 2-tailed paired or unpaired t-test, or Welch's test, was employed utilizing the GraphPad Prism 5 software (GraphPad Software, La Jolla, CA, USA). Significance levels are denoted as *P < .05; **P < .01; ***P < .001. The number of independent biological replicates is represented with the n-value.

3.24 TRIF protein structures predictions

An existing AlphaFold prediction of protein structures for full-length TRIF was taken from alphafold.ebi.ac.uk ^{316,317}, last updated using AlphaFold v2.0 2021-07-01. Per residue and global predicted local distance difference test score (pLDDT) was taken from the mmCIF file. ColabFold predictions including delRHIM TRIF and superimpositions with full-length TRIF were made using an unmodified version of ColabFold ³¹⁸, with the default MSA pipeline, a MMseqs2 and HHsearch.

4. Results

4.1 Potential role of TLR3 in HAV and HCV infections

HAV infections are almost always acute and self-resolving, whereas HCV becomes persistent in above 70% of the cases³¹⁹. In addition, HAV is described to be associated to a lack of innate immune activation *in vivo*²¹², in striking contrast to HCV which, instead, is pictured as an ISGs inducer, in chimps as well as in patients^{210,211}. This raised the question whether these two divergent features – infection outcome and innate immune response - could be linked with one another by specific HAV- or HCV mechanisms of activation and/or evasion of innate immunity. From this outset, my initial aim was to develop a direct comparison between HAV and HCV using a homogeneous cell culture approach that would allow both viruses to robustly replicate while maintaining immune competence and physiological relevance. To achieve this, since both HAV and HCV are known to be hepatotropic²⁰⁸, liver-based cell lines - not always used in previous studies^{138,173,174} – were an obvious choice. In order to disentangle the intricacies of the innate immune response, former members of the Lohmann group already established, in the years preceding my work, stable or transient expression models of PRRs in immune-deficient cell lines, such as Huh7²⁵⁶ or the subclones Huh7.5³²⁰ or Huh7-Lunet. In parallel to this, to overcome the challenges of BSL-3 working conditions for HCV, a reverse approach to study innate immunity was already attempted, based on transient PRRs expression onto stably selected subgenomic replicon cell lines, already available for HCV²⁵³ as well as for HAV¹⁹⁰ (Figure 19C). Persistent replicons provide the advantage of ensuring an even expression of viral proteins - and thereby viral replicating genomes - potentially in the entire cell population. Since the specific contribution of TLR3 was also relevant for parallel projects in our lab^{83,190}, and because of evidences of HCV triggering TLR3^{68,83,321}, whereas TLR3 sensing of HAV was not yet assessed, this PRR was investigated first. Lentiviral particles encoding TLR3 were transduced onto HAV and HCV stable replicon cell lines and mRNA expression of canonical ISGs relevant for +RNA viruses sensing⁶⁸ was measured via qPCR. Here, moderate upregulation of IFIT1 upon TLR3 expression was detected exclusively in HCV replicon cells (Figure 19B). To exclude a dose-dependent effect due to discrepancies in viral copy number between HAV and HCV, viral

RNA was measured as well (Figure 19A). In average, for both, HCV - genotypes 1b and 2a – and HAV, a robust amount of RNA was quantified, potentially sufficient to trigger a similar response, and therefore rather hinting at either a lack of TLR3 sensing by HAV, or at a HAV-specific TLR3-evasion mechanism, such as the reported cleavage of TRIF¹⁷³.

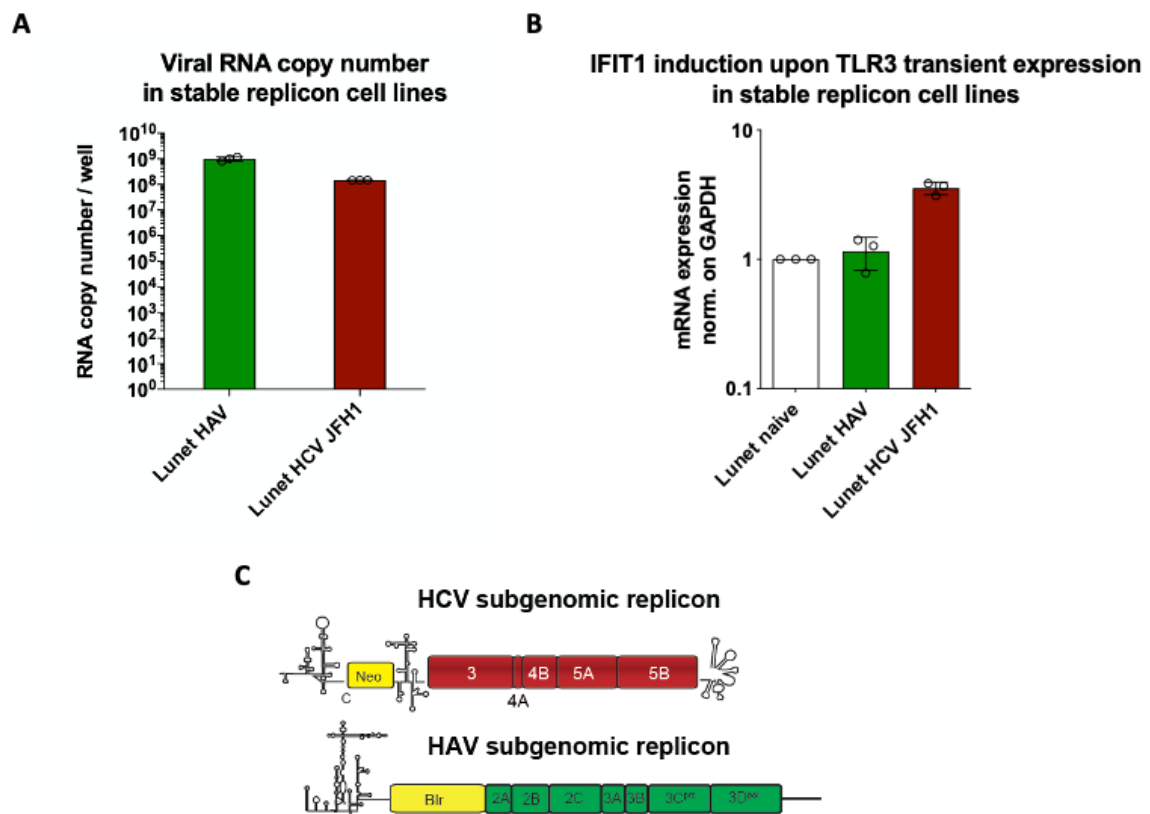


Figure 19. ISG induction upon HAV or HCV subgenomic replication.

Lentiviral particles encoding TLR3 were transiently transduced onto the hepatoma cell clone Huh7 Lunet (“Lunet naïve”) and HAV- or HCV-based subgenomic replicons, based for HAV on HM175/18f gt1b and for HCV on JFH1 gt2a (JFH1). (A) Total RNA was isolated from cell lysate and TaqMan RT qPCR was performed aiming at viral RNA copy number expression detection. (B) IFIT1 mRNA was measured on total RNA through RT qPCR. mRNA levels were normalized to GAPDH expression and shown as fold expression relative to unstimulated cells. Shown values are mean values with SD from one biological replicate with technical triplicates. (C) Schematic of the persistent, selectable subgenomic replicons used to select HCV / HAV stable cell lines. Neo/Blr: genes conferring resistance to G418 or blasticidine, respectively.

To better mimic the complex physiological conditions and interactions found *in vivo* in HAV and HCV infections, I generated - through lentiviral transduction and following selection - stable Huh7 Lunet TLR3 overexpressing cell lines and infected them with either HAV or HCV. Here, again, in spite of similar and robust replication for both viruses, - which was obtained by modulating the MOI (see *Methods*), I observed moderate induction of ISGs upon HAV,

whereas HCV virus replication seemed to trigger a more robust TLR3-specific response (Figure 20A,B).

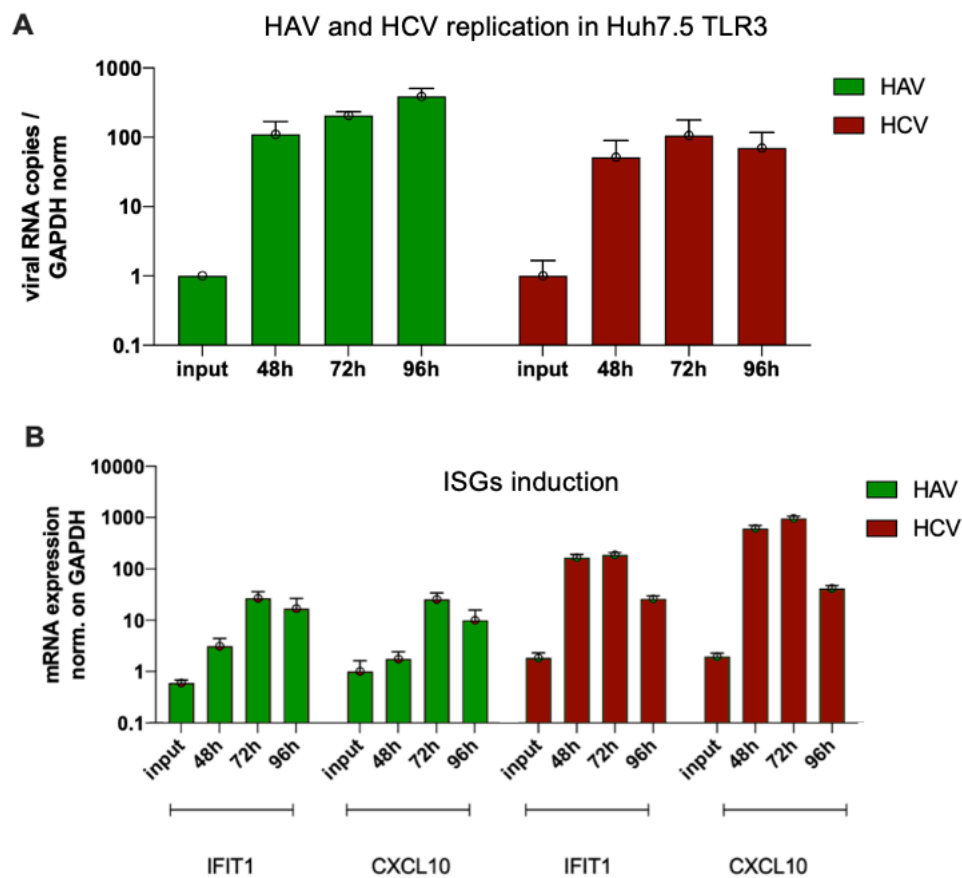


Figure 20. ISG induction upon HAV or HCV infection Huh7 Lunet TLR3 cells.

Huh7 cells stably expressing TLR3 and CD81 were infected with HAV (HM175/18f, green) or HCV (Jc1, red), respectively. At the indicated time points total RNA was isolated and IFIT1 mRNA (B), and viral RNA (A), were quantified as indicated. IFIT1 mRNA levels are normalized to GAPDH expression and shown as fold expression relative to uninfected cells. Shown values are mean values with SD from two biological replicates.

Because both approaches, HAV/HCV- stable replicons and infection, were based on Huh7 Lunet cells – which, despite the several mutations acquired that render them suitable as a cell culture model, conserve traces of RLR expression²⁵⁶ - I decided to infect with HAV and HCV full length (schematized in Figure 21F) the Huh7 subclone Huh7.5, which results “cleaner” due to of the expression of a RIG-I dominant negative variant²⁶² (Figure 21). Reconstitution of TLR3 in both Huh7 Lunet and Huh7.5 cells rendered the cells capable of mounting an ISG response upon poly(I:C) transfection, a synthetic mimic of dsRNA, (Figure 21A,B) but, as seen for Huh7 Lunet, the Huh7.5 subclone as well did not show a significant TLR3-mediated innate immune upregulation, as opposed to HCV (Figure 21C,D) despite robust HAV replication (Figure 21E).

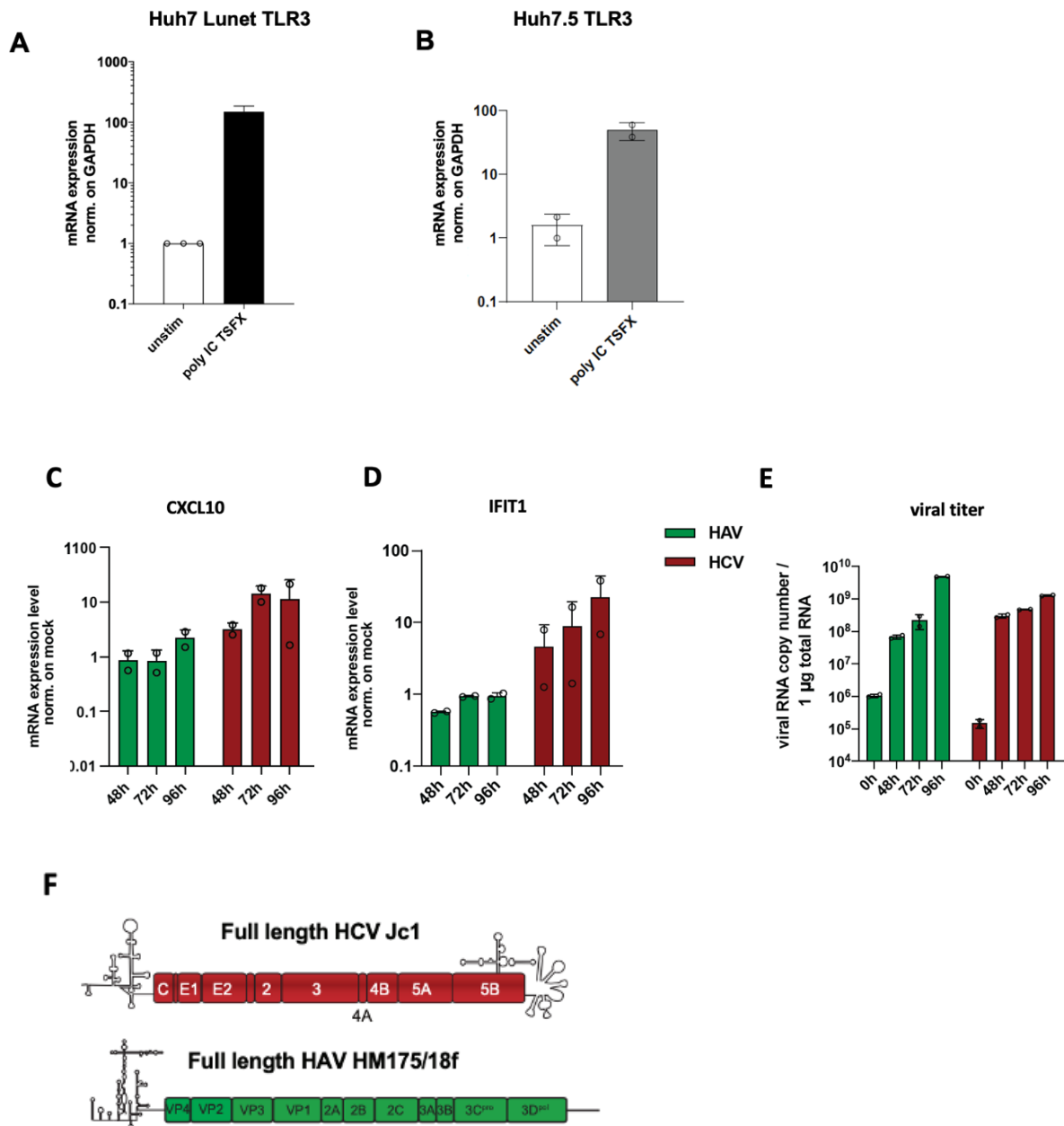


Figure 21. Responsiveness of Huh7 and Huh7.5 TLR3 cells and full length HAV or HCV replication in Huh7.5 TLR3 cells.

(A,B) Lentiviral particles encoding TLR3 were stably transduced onto the hepatoma cell clone Huh7 Lunet or the subclone Huh7.5. Immunostimulation was performed through lipofectant-mediated transfection of 0.5µg poly(I:C) incubating for 6 hours. Shown are mean values with SD from one biological replicate with technical triplicates (A) and biological duplicates (B). (C-E) Lentiviral particles encoding TLR3 were transduced onto the subclone Huh.7.5 and, upon antibiotic selection, stable TLR3-expressing cells were selected. Cells were infected with HAV HM175/18f (green) or HCV Jc1 (red). Total RNA was isolated from cell lysate and Sybr RT qPCR was performed aiming at CXCL10 (C) or IFIT1 (D) mRNA expression detection. (E) Viral copy number was measured on total RNA through TaqMan RT qPCR. mRNA expression levels for ISGs target genes were normalized to GAPDH expression and shown as fold expression relative to unstimulated cells. Shown are mean values with SD from two biological duplicates. (B) Schematic of the HCV / HAV genomes used for infection.

To further check for differences upon ectopic reconstitution of TLR3, I assessed subcellular TLR3 expression in Huh7.5 TLR3 and compared it with that of a cell line with endogenous and functional TLR3, PH5CH, which will be examined later (Figure 22A-H).

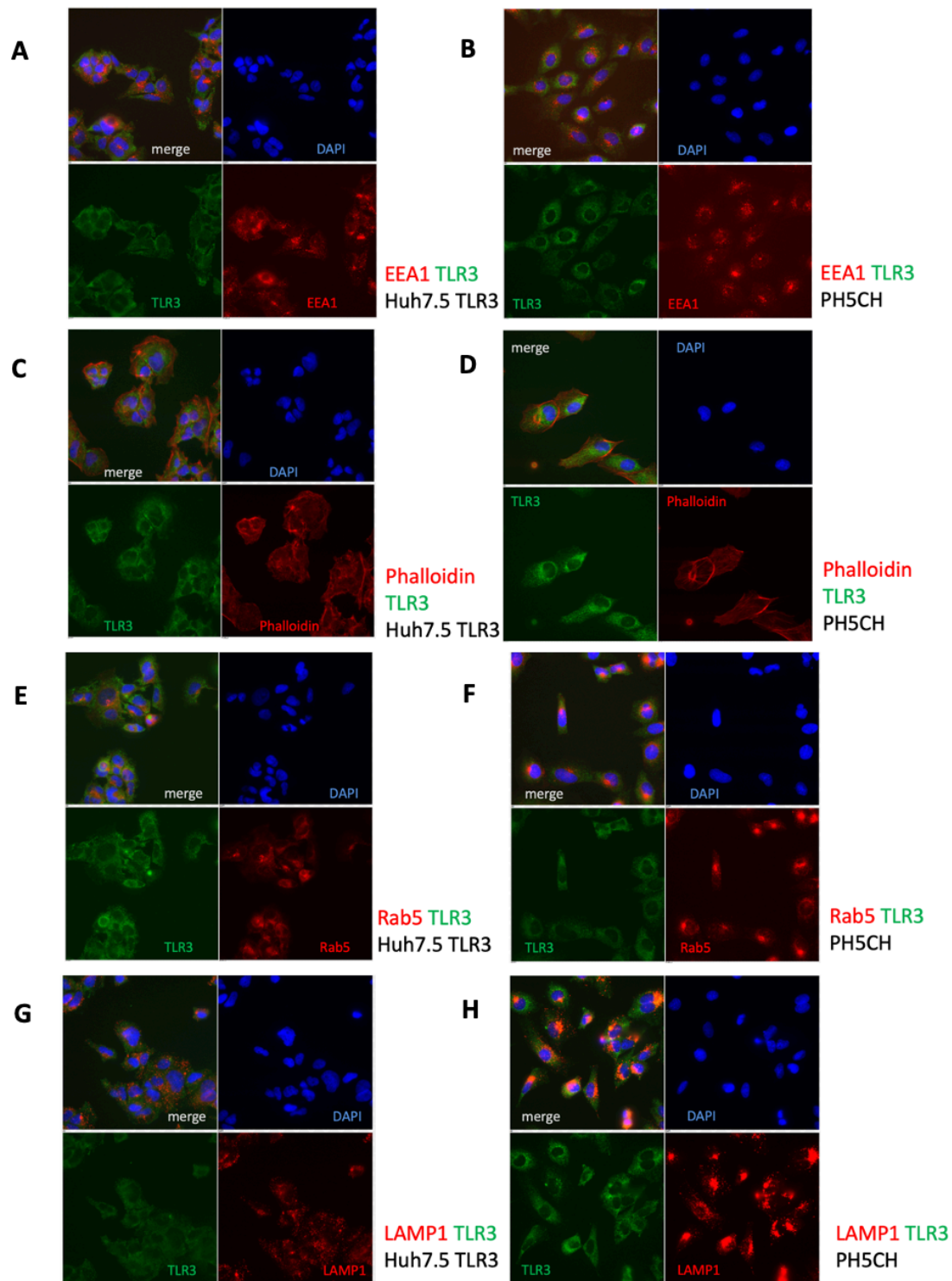


Figure 22. TLR3 subcellular localization in Huh7.5 TLR3 and PH5CH cells.

(A-H) TLR3 protein expression was assessed in Huh7.5 TLR3 stable cells and PH5CH cells through Immunofluorescence (IF) staining using cellular markers: the endosomal markers EEA1 (A, B), Rab5 (E, F) and LAMP1 (G, H) and the actin filament dye Phalloidin (B) aiming at plasma membrane staining.

Using a set of endosomal marker and staining of actin filaments, aiming at localizing not only the endosomal TLR3 (Figure 22A,B,E,F,G,H) but also the one described at the plasma membrane⁷⁸ (Figure 22C,D) I could not find disparities between Huh7.5 TLR3 and PH5CH and therefore I went further with my characterization.

In these first approaches, I detected clearly less TLR3 mediated ISGs upon HAV compared to HCV. Taking into account potential differences between the replicative intermediate dsRNA molecules of HAV and HCV and their exposure to TLR3, based on literature describing Flavi- and Picornavirus replication^{187,322}, I tried to stimulate Huh7 Lunet TLR3 cells directly with total RNA extracted from HAV or HCV subgenomic replicon cells, which supposedly included dsRNA. In order to have an additional readout, illustrative of an innate immune activation, I stably transduced Huh7 Lunet TLR3 cells with a previously generated IRF3-GFP construct (Grünvogel, unpublished data). Huh7 Lunet IRF3-GFP cells harbor a cytoplasmic fluorescence which turns nuclear upon activation of a PRRs-mediated signaling cascade²⁴². I firstly titrated poly(I:C), supernatant- or transfection-based, to assess functionality of this system (Figure 23A), and then, upon realization that a potent stimulation was necessary to provoke <90% of IRF3 nuclear translocations in the cell population, I transfected high amounts of total RNA from subgenomic replicons (Figure 23B).

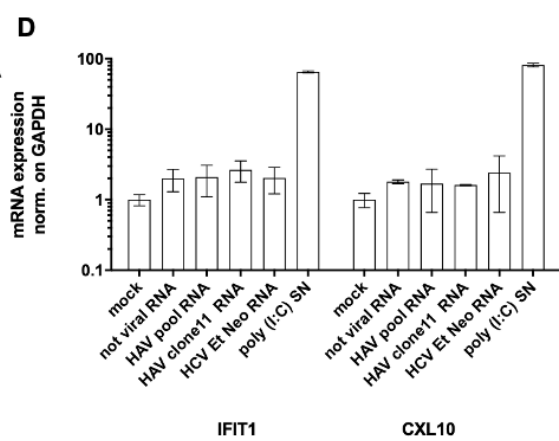
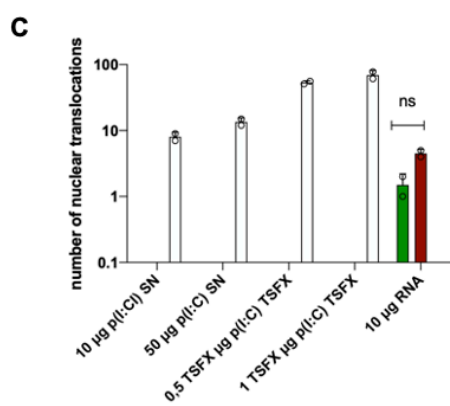
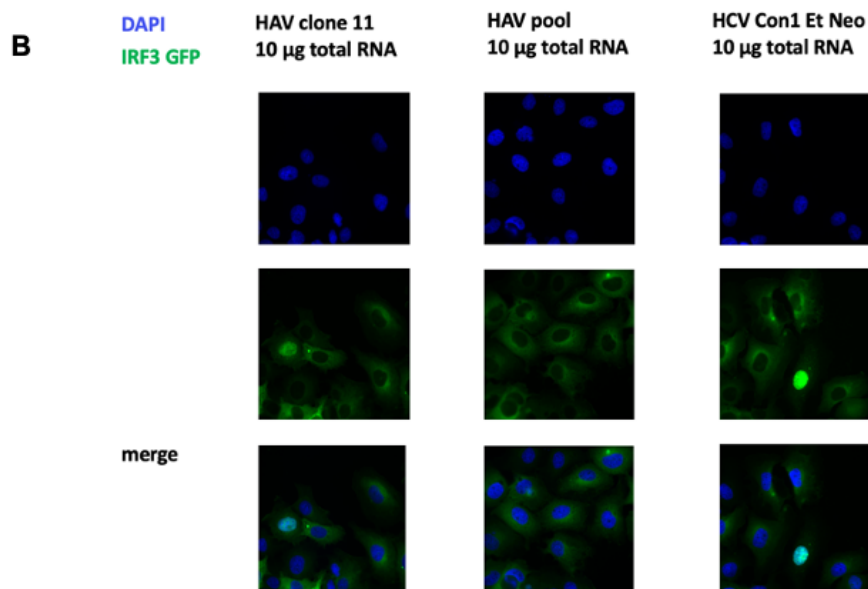
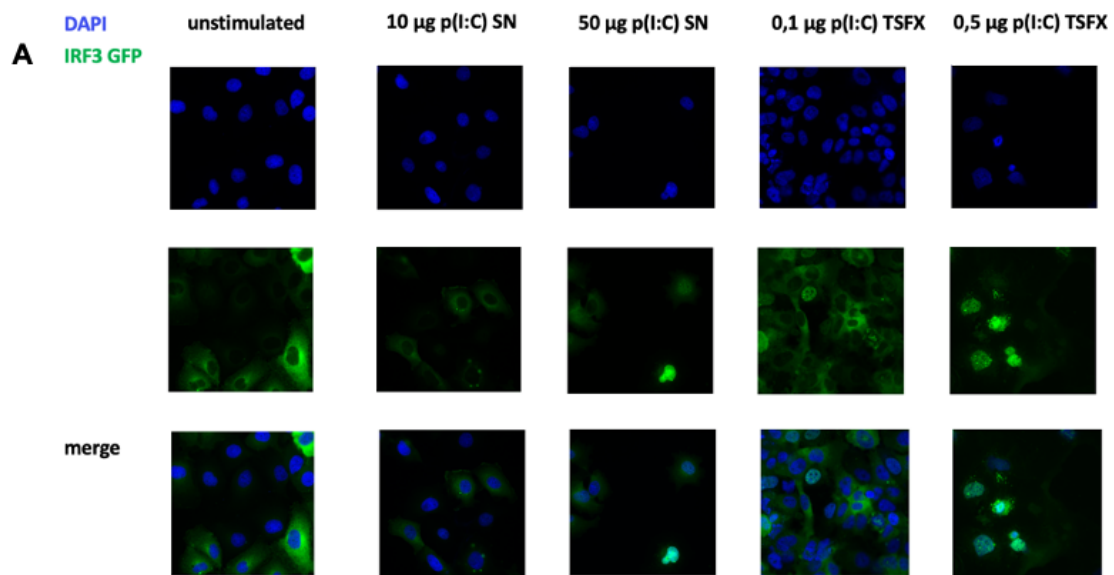


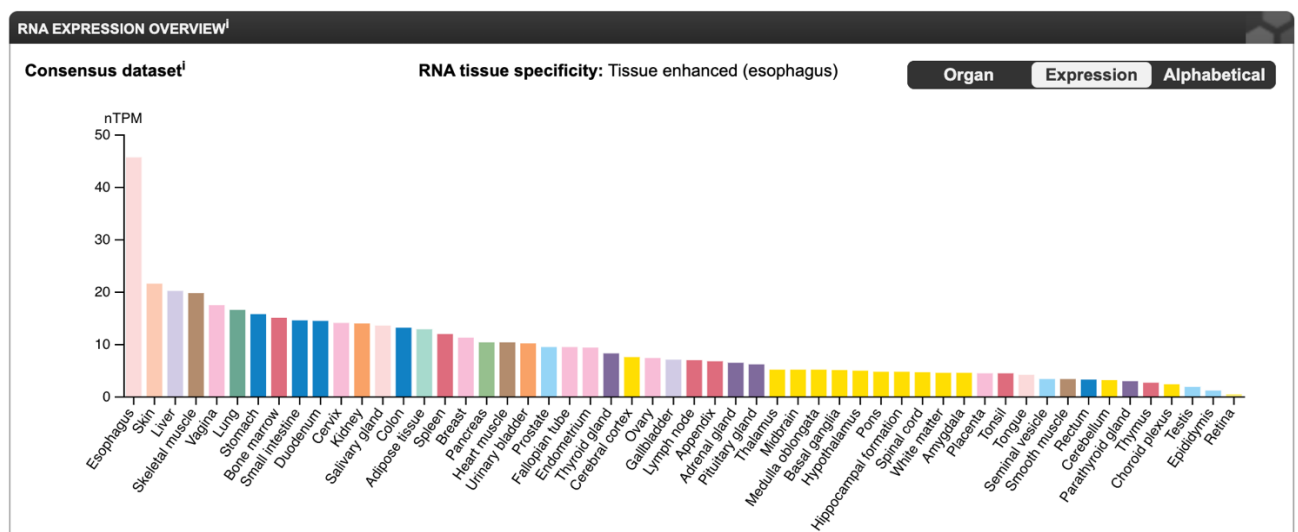
Figure 23. Transfection of total RNA from HAV and HCV subgenomic replicon cell lines in Huh7 Lunet TLR3 IRF3-GFP cells.

(A-B) Lunet TLR3 cells were stably transduced with lentiviral particles containing an IRF3-GFP construct and selected. To test their function, cells were seeded onto coverslips and either supernatant-fed or transfected with the indicated amounts of poly(I:C) (A); transfection of HAV- or HCV total RNA extracted from replicon cells was then performed (B) and nuclear translocation was quantified by eye in a total range of around 100 cells (C). HAV-, including “HAV pool” and “HAV clone 11” which harbor a mutation in the protein 3A increasing replication (Essex-Nobis, unpublished data), or HCV total RNA extracted from replicon cells, was transfected onto Huh7 Lunet TLR3 IRF3 GFP cells. Total RNA was isolated from cell lysate and Sybr RT qPCR was performed aiming at IFIT1 or CXCL10 (D) mRNA expression detection. IFIT1 and CXCL10 mRNA levels were normalized to GAPDH expression and shown as fold expression relative to unstimulated cells. Shown are mean values with SD from two biological replicates.

However, upon quantification, the difference between HAV- or HCV- activated cells turned out to be not significant (Figure 23C). I then transfected different amount of total HAV or HCV RNA and tried to increase the sensitivity in order using qPCR as a readout, but the results were inconsistent, not allowing discrimination between non-viral RNA, HAV or HCV (Figure 23D).

At this point, given the difficulties to functionally exclude TLR3 sensing from an active viral abrogation of the pathway, it seemed important to explore the possibility - described in previous studies¹⁷³ - of an active interference by the HAV protease precursor 3CD through cleavage of the TLR3 key adaptor protein TRIF. As a similar activity was shown for HCV NS3-4A as well ¹³⁸ – but also, interestingly, questioned by a later study ²²² – I decided to assess quantitatively and qualitatively cleavage of TRIF through a direct comparison of HAV and HCV protease efficiencies.

To lay the foundation of protein quantitative detection, robust expression of the protein of interest is key; however, after numerous failed attempts to detect endogenous TRIF in numerous liver-derived cell lines (data not shown), upon interrogation of the human proteome database tissue-based map I realized that TRIF protein expression is kept at low levels in the liver, in spite of a solid mRNA expression in hepatocytes (Figure 24).



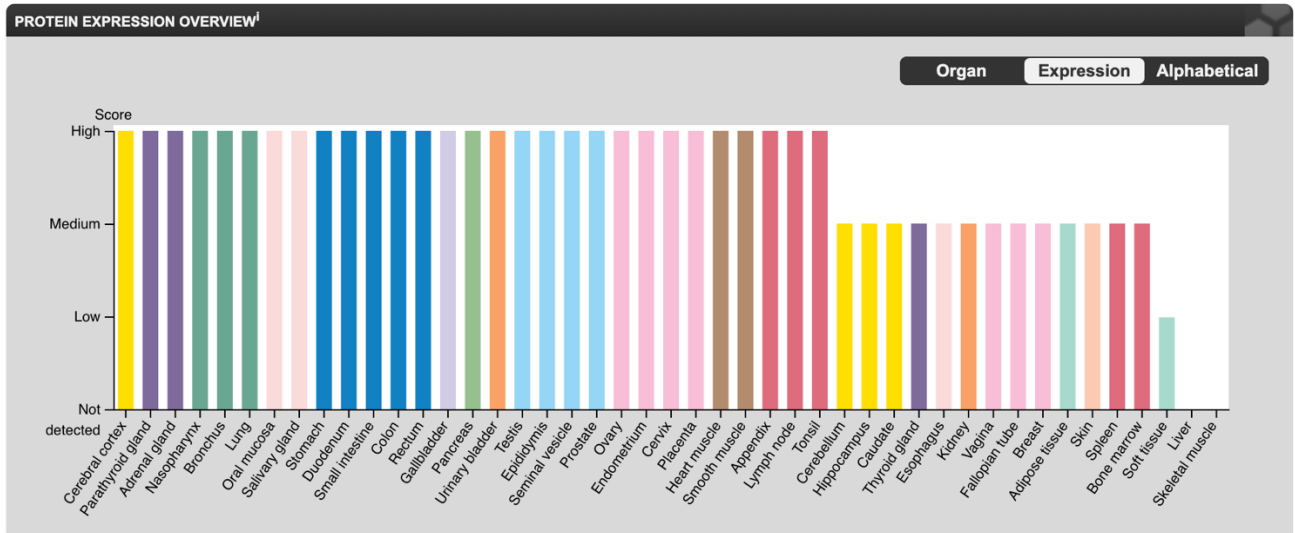


Figure 24. TRIF RNA and protein expression overview from The Human Protein Atlas database³²³. Despite robust TRIF mRNA expression in the liver, its protein levels are under detectable threshold.

Thus, I tried to increase TRIF expression ectopically, using TRIF-harboring expression constructs, fused with C- or N-terminal Hemagglutinin (HA)-tag, under transcriptional control of a T7 promoter and under translational control of the encephalomyocarditis virus (EMCV) IRES (vector pTM, Figure 25A)³¹⁵. But when I transiently overexpressed these TRIF-based constructs in Huh7 Lunet cells stably expressing the T7 polymerase, I observed rapid cell death, distinctly due to cytotoxicity (Figure 25B).

Previous research examined the association between TRIF expression and apoptosis, showing how the latter depended on the expression of a specific TRIF domain, designated RHIM⁸⁰. With respect to this evidence, I generated a new pTM TRIF construct devoid of the RHIM domain, named pTM TRIF delRHIM (Figure 25A,D); cell viability was indeed restored upon transfection of pTM TRIF delRHIM in Huh7 Lunet T7 cells (Figure 25B).

Since it would have certainly been more favorable to work with the full-length TRIF – albeit Kaiser et al. showing that the pRM TRIF delRHIM did not present defects in signaling function⁸⁰ – I tried to establish a cell line in which ectopic expression could be lower. I generated a T7 polymerase construct under control of the ROSA26 promoter³²⁴, which, if compared with the EF1 α promoter, canonically found in pWPI vectors used for lentiviral vector generation, was shown to drive a weaker gene transcription³²⁵. I stably transduced Huh7 Lunet cells, obtaining a cell line potentially capable of mild ectopic expression due to lower levels of T7 RNA polymerase. Transfection of pTM-GFP I confirmed much lower GFP expression in ROSA-T7 compared to the regular Huh7 Lunet T7 (Figure 25C, right panel); nonetheless, TRIF WT caused apoptosis in all cells which expressed it (Figure 25C, left panel), corroborating the need of RHIM domain deletion. At this point, I generated a pTM TRIF delRHIM construct, C- and N- HA-tagged, to allow robust detection and quantification, upon viral protease activity, of the full length molecule as well as the cleaved products (Figure 25A, right panel). In addition, I generated individual mutants and a double mutant of the HA-TRIF delRHIM-HA construct, rendering TRIF HAV- or HCV protease cleavage resistant (Q554A or C372R for the single mutants and Q554A + C372R for the double mutant, respectively), according to literature^{138,173} (Figure 25D).

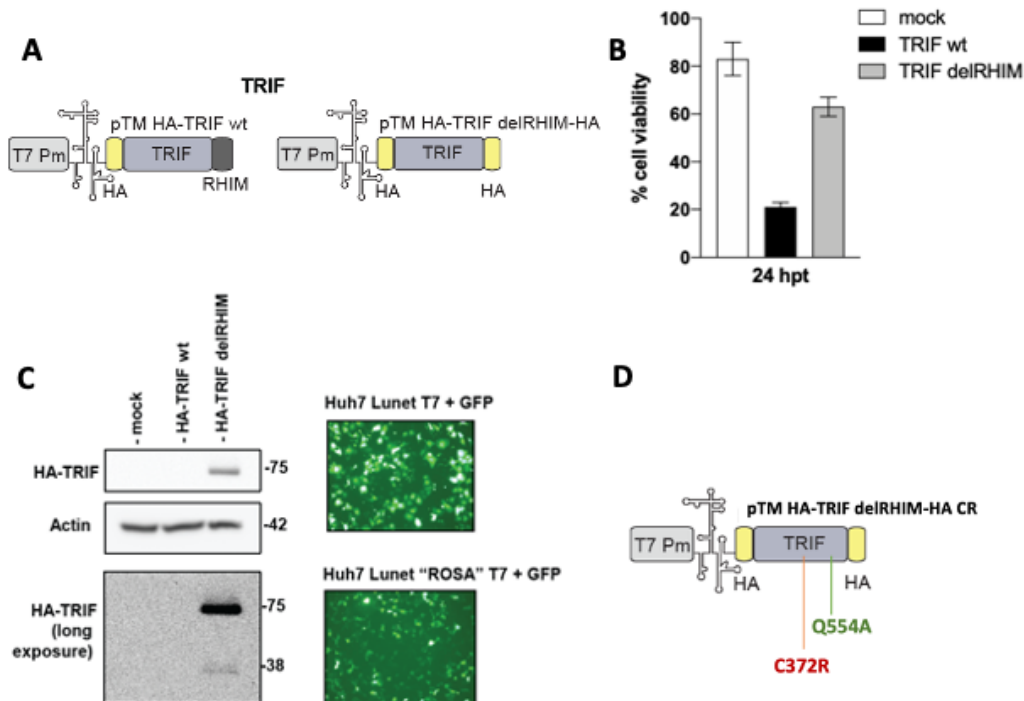


Figure 25. TRIF expression constructs and their limitations.

(A). Schematic of the expression vectors used for transfection experiments, with or without the RHIM domain. (B) Huh7-Lunet T7 cells were transfected with a pTM vector encoding TRIF WT or TRIF delRHIM. WST-1 assay was performed to determine cell viability after 24 hours. (C) Huh7-Lunet "ROSA" T7 were transfected with a mock plasmid, a pTM plasmid encoding TRIF full length (HA-TRIF WT) or a pTM plasmid encoding a truncated TRIF (HA-TRIF-delRHIM) (left panel). Huh7 Lunet T7 cells were compared to Huh7-Lunet "ROSA" T7 cells upon a test transfection of a pTM plasmid encoding GFP (right panel). (D). Schematic of the TRIF expression vectors carrying the putative TRIF cleavage resistance mutations C372R (HCV) and Q554A (HA)

To precisely quantify TRIF cleavage, I chose three different approaches which would allow me to modulate the protease expression in different settings: 1) co-transfection of both pTM-TRIF-delRHIM and viral proteases, to obtain a transient, but strong protease expression (Figure 26, top panel); 2) pTM-TRIF-delRHIM transfection in the previously mentioned HAV and HCV replicon cell lines additionally expressing T7 polymerase. Replicon cell lines express viral proteins to moderate levels in all cells, thereby avoiding detection of uncleaved TRIF molecules in cells which do not express the viral protease (Figure 26, middle panel); 3) pTM TRIF delRHIM transfection in Huh7 Lunet T7 cells, infected with either HAV or HCV full length genomes, to investigate the cleavage in a more physiological context. (Figure 26, lower panel).

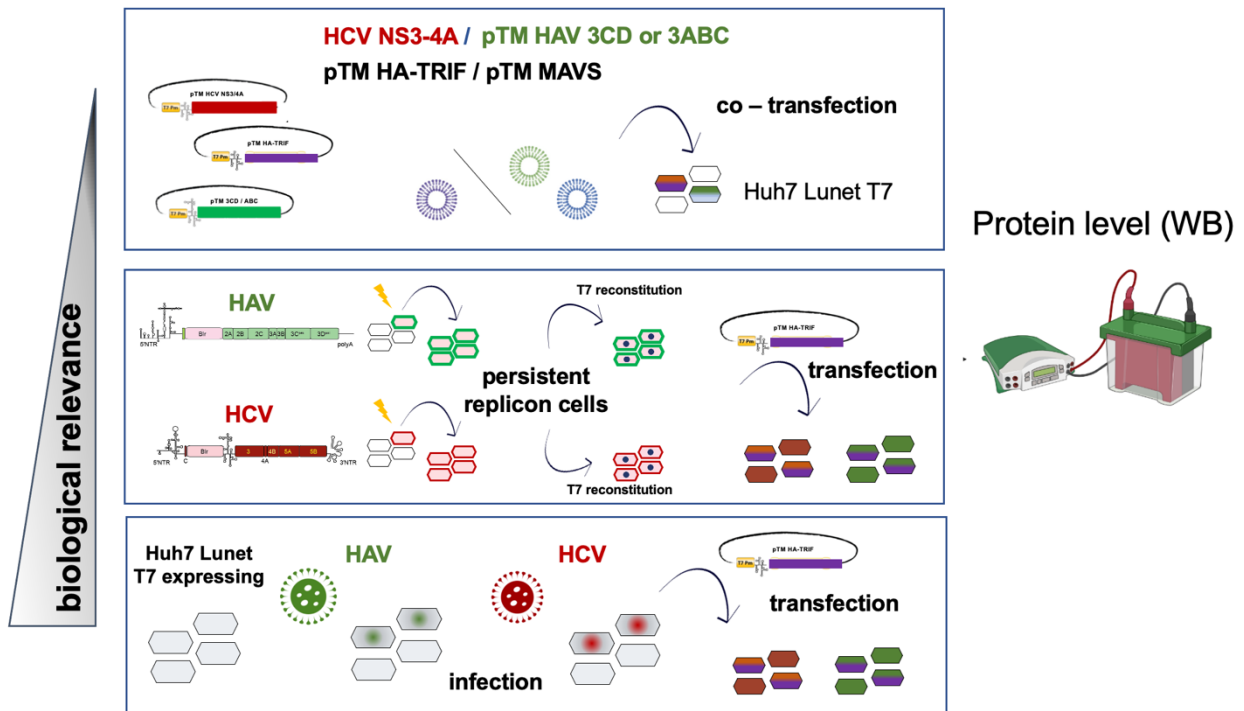


Figure 26. Different approaches to investigate HAV and HCV viral protease counteraction.

From the top panel, co-transfection of the viral protease of interest along TRIF ensures high expression levels, which probably exceed the ones findable in infected cells, thereby being the least biologically relevant approach. Middle panel, transfection of TRIF in the selected HAV or HCV subgenomic replicon populations provides moderate, homogeneous levels in all cells which express TRIF. In the lower panel, transfection of TRIF in HAV- or HCV-infected cells allows to assess the cleavage in a physiological system.

To establish the first approach, I took advantage of previously generated pTM plasmids, encoding HAV 3CD and HCV NS3-4A proteases along with a N-terminal Flag tag (Figure 27A), with the latter not only allowing easier detection³²⁶ but also ensuring comparable quantification analysis between HAV and HCV proteases, avoiding differences due to antibody-specific sensitivities (Figure 27B,C). In both cases, active site mutants were generated, resulting in abrogation of HAV or HCV protease activity, indicated by the lack of NS3-4A or 3CD precursor cleavage (Figure 27B, C).

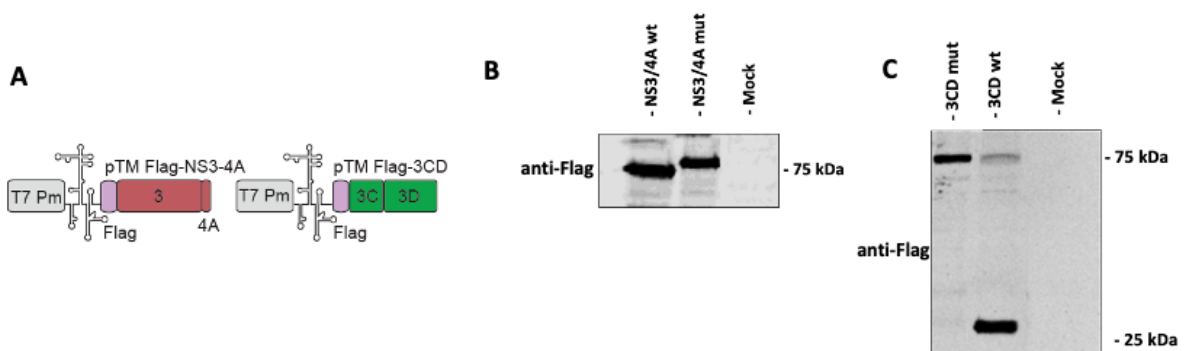


Figure 27. Expression vectors encoding viral protease.

(A) HCV NS3-4A and HAV 3CD are expressed under control of the T7 promoter in pTM vectors. (B, C) The protease genes are associated with a Flag-tag which allows homogeneous detection for both HCV and HAV

proteins, respectively, when transfected in Huh7 Lunet T7. Cells were harvested 16 hours after transfection and the cell lysate were subjected to immunoblotting.

With these premises, I co-transfected HA- TRIF delRHIM -HA (from now on named “TRIF WT”) or HA- TRIF delRHIM C372R + Q554A -HA (from now on named “TRIF CR”) along with either HAV 3CD or HCV NS3-4A, wild-type or inactive mutants^{171,218}. I observed a reduction of full-length TRIF upon HAV 3CD, and could detect the two previously described cleavage products¹⁷³ along with an HAV-unrelated band, potentially corresponding to host caspase cleavage activity⁸⁰ (Figure 28A,B).

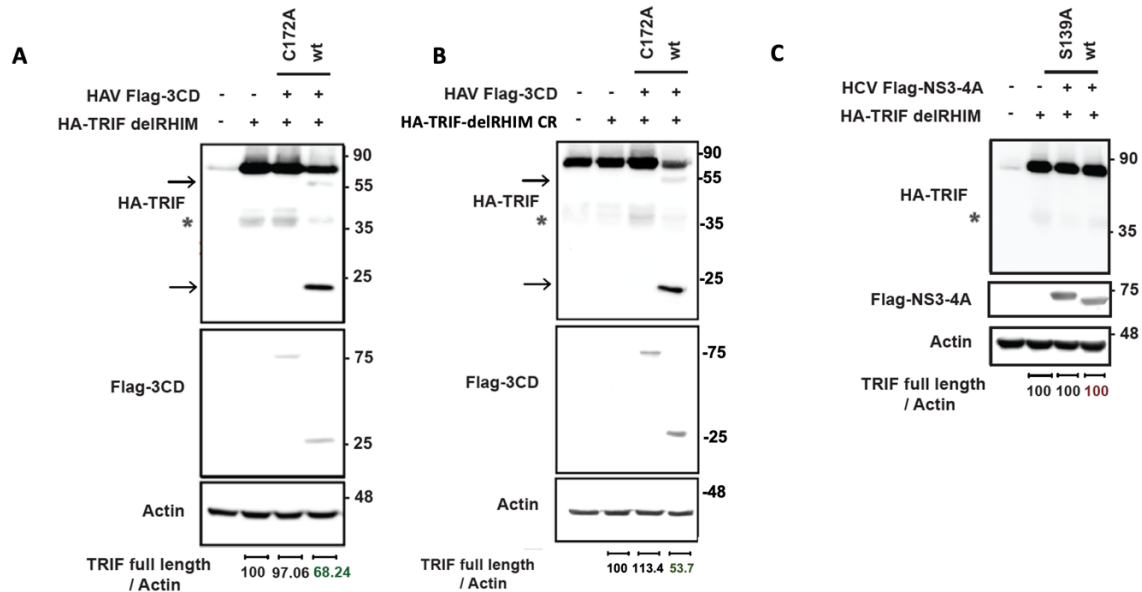


Figure 28. Analysis of TRIF cleavage by HCV and HAV proteases.

(A-C) Huh7-Lunet T7 cells were co-transfected with plasmids encoding the indicated wild-type or mutant proteases and TRIF and harvested sixteen hours after transfection. Arrows indicate specific cleavage products. Caspase-mediated TRIF cleavage products are indicated by an asterisk. Quantification of the cleavage was based on TRIF full length signal intensity measurement in absence of protease as a reference for the signals upon protease expression. Each signal was normalized on the actin band signal belonging to the same sample. (A) TRIF cleavage susceptible (wt) assessment upon transfection of HAV 3CD wild-type and mutant. (B) TRIF HAV cleavage resistant (Q554A) assessment upon transfection of HAV 3CD wild-type and mutant. (C) TRIF cleavage susceptible (wt) assessment upon transfection of HCV NS3-4A wild-type and mutant.

Interestingly, however, I found no indication of lack of cleavage upon usage of the described HAV cleavage resistant mutant (named “TRIF CR”)¹⁷³ (Figure 28B). For HCV, I did not detect cleavage of TRIF upon NS3-4A transfection(Figure 28C). Trying to elucidate the minimal amount of protease necessary for TRIF cleavage activity, I tested incremental amounts of HCV NS3-4A, quantifying the co-transfected full-length TRIF, and this confirmed the complete lack of cleavage reported before²²² (Figure 29B). The same titration approach was applied to confront the maximal TRIF cleavage reached by saturating amount of HAV 3CD protease (Figure 29A), comparable to the one shown in Figure 28A.

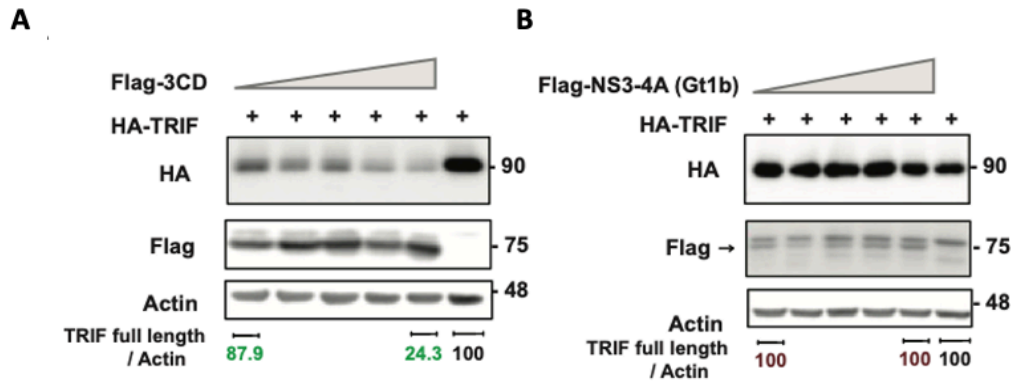


Figure 29. Titration of viral proteases to test TRIF cleavage.

Huh7-Lunet T7 cells were co-transfected with 1 μg of a plasmid encoding HA-TRIF and increasing amounts of plasmids encoding either FLAG-HAV 3CD (A) or FLAG HCV NS3-4A (B), as indicated by the grey triangle (0.05 μg; 0.1 μg; 0.25 μg; 0.5 μg; 1.25 μg), and harvested sixteen hours after transfection. Arrow indicates specific NS3-4A Flag-tag signal to distinguish it from the upper staining unspecific band. Quantification of the cleavage was based on TRIF full length signal intensity measurement in absence of protease as a reference for the signals upon protease expression. Each signal was normalized on the actin band signal belonging to the same sample.

Detection of the full-length TRIF species, despite usage of high amounts of proteases for both HAV and HCV could be an indication of successful TRIF transfection in cells which do not express the viral proteases. To exclude this artefact, I moved to test TRIF cleavage in the previously used HAV and HCV stable subgenomic cell lines, which I reconstituted with the T7 polymerase and selected. Upon transfection of pTM-TRIF delRHIM, I then measured and quantified the full-length band intensity comparing it with the one expressed in Huh7 T7 Lunet cells, transfected as a control. Interestingly, TRIF cleavage efficiency was higher for HAV compared to the first approach of co-transfection of viral proteases and TRIF (Figure 30), confirming that in our first approach I could have possibly included uncleaved TRIF molecules because of lack of concomitant viral protease expression in the same cell. However, the cleavage efficiently did not overcome 60%, with full-length TRIF still being clearly present (Figure 30A), with lack of clear cleavage products. For HCV, TRIF seemed mildly reduced upon transfection in the subgenomic cell line Con1 ET (Figure 30B). However, I could not detect any cleavage product when I examined the full immunoblot membrane and used a longer exposure, except for the usual caspase-specific bands at around 38kDa (Figure 30C).

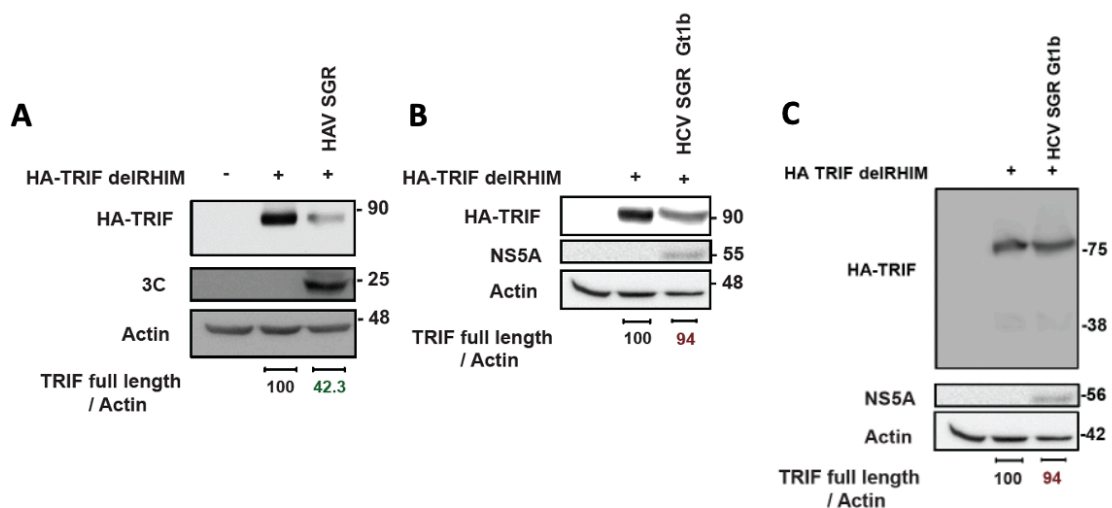


Figure 30. TRIF cleavage detection in HAV and HCV stable subgenomic replicon cells.

(A, B) HAV or (C) HCV persistent subgenomic replicon cells expressing T7 RNA polymerase were transfected with a plasmid encoding HA-TRIF under transcriptional control of a T7 promoter and harvested sixteen hours after transfection. Cell lysate were then subjected to immunoblotting as indicated in *Methods*. Quantification of the cleavage was based on TRIF full length signal intensity measurement in absence of protease as a reference for the signals upon protease expression. Each signal was normalized on the actin band signal belonging to the same sample.

Given the complete lack of TRIF cleavage upon HCV NS3-4A so far, and taking into account the limitation of the sole use of Gt1b as a source of NS3-4A in my expression constructs, I proceeded with two further assays to exclude any genotype-specific phenotype, transfecting NS3-4A protease of HCV Gt2a (JFH1), where lack of TRIF cleavage was confirmed here as well (Figure 31A). Moreover, I transfected TRIF onto a T7-reconstituted JFH1 stable replicon cell line (Figure 31B). Here, I included a specific drug, Simeprevir³²⁷, inhibiting the NS3-4A protease activity. Furthermore, I implemented the stringency of cleavage quantification by transfecting a plasmid encoding GFP and normalizing the expression of TRIF onto the GFP signal, to allow consideration of the different T7 levels of the newly generated cell line against the “canonical” Huh7 Lunet T7. Again, no indication for TRIF-cleavage by NS3-4A was found, comparing cells in presence and absence of replicon or upon inhibitor treatment. Only a slightly decreased expression of NS5A was found upon Simeprevir treatment, likely due to inhibition of RNA replication (Figure 31B).

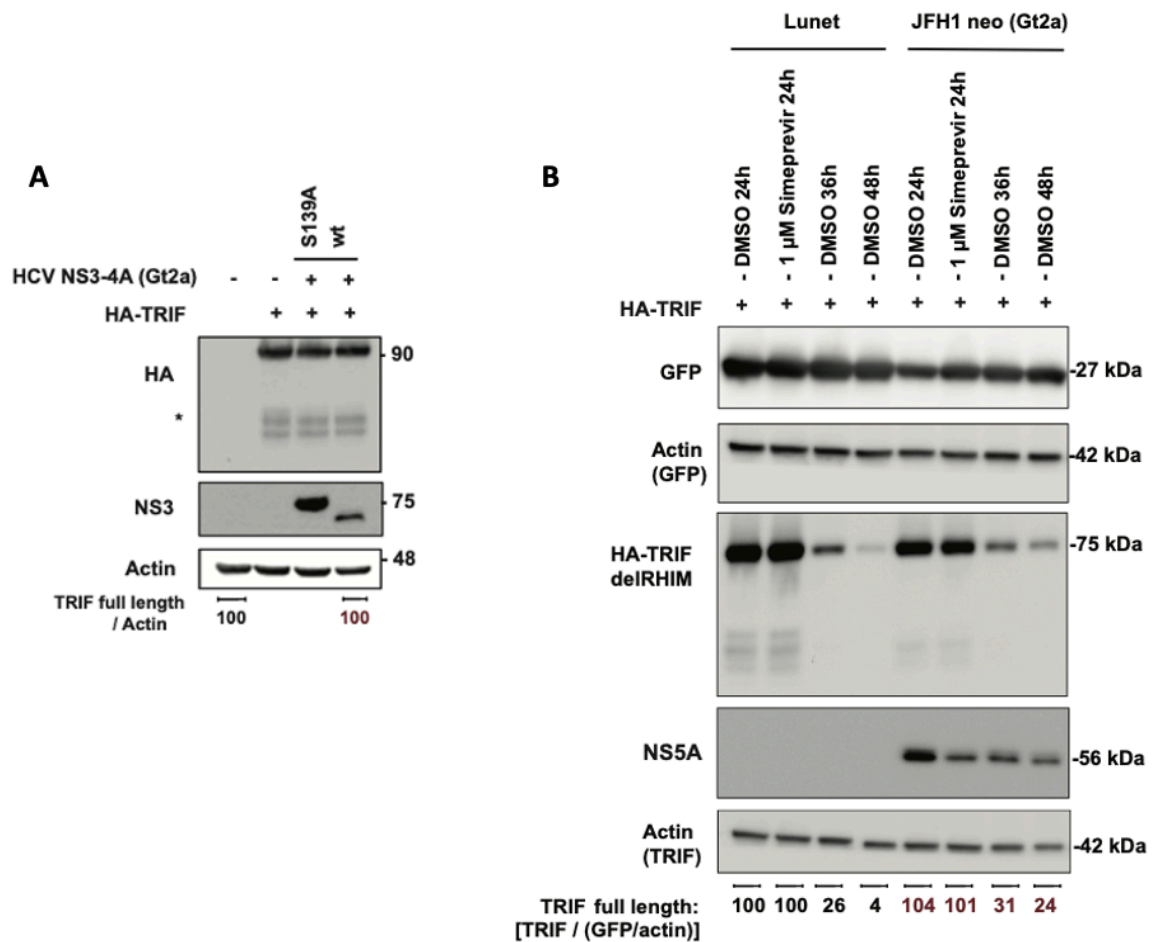


Figure 31. Analysis of TRIF cleavage by HCV Gt2a.

(A) TRIF cleavage detection upon co-transfection of pTM TRIFdelRHIM and pTM-NS3-4A from Gt2a (JFH1) for 16 hours. Caspase-mediated TRIF cleavage products are indicated by an asterisk. (B) Huh7 Lunet (left) or JFH1-subgenomic replicon cells, stably reconstituted with the T7 polymerase, were transfected with plasmids encoding either GFP (first membrane from the top) or HA-TRIF-delRHIM (third membrane from the top). Cells were treated with either DMSO or Simeprevir for 24h, as indicated, and with DMSO for 36h and 48h. 16 hours after transfection, cells were harvested. Blotting was performed by Helen Huang. To obtain a measure of transfection efficiency, GFP signal intensities were normalized to the respective b-actin levels, obtaining a “transfection score”. Signal intensities of TRIF were then normalized on the respective b-actin levels and then multiplied by the transfection score for each sample. Immunoblot courtesy of Helen Huang.

After having modulated the viral protease amount in the first two used methods, I moved on to attempt TRIF cleavage detection in infected cells. I infected Huh7 Lunet T7 with HAV HM175/18f and HCV Jc1, for 4 and 3 days, respectively, in order to obtain robust expression of the viral proteases, and transfected pTM TRIF-delRHIM (Figure 32). Here, cleavage quantification recapitulated the HAV- and HCV-specific phenotype observed before: mild for HAV 3CD (Figure 32A), lacking for NS3-4A (Figure 32B).

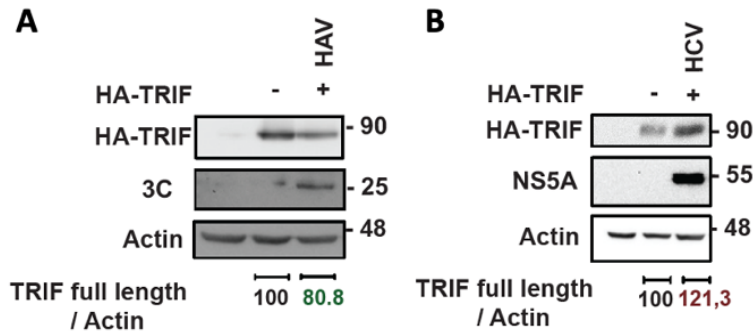


Figure 32. Biochemical detection of TRIF cleavage upon in HAV and HCV-infected Huh7 Lunet T7 cells. Huh7-Lunet T7 cells were infected with HAV (A) or HCV (B) and upon establishment of robust replication and expression of viral protease (3 to 4 days for HCV and HAV, respectively) they were transfected with TRIF. Sixteen hours later cells were harvested and subjected to immunoblotting. Quantification of the cleavage was based on TRIF full length signal intensity measurement in absence of protease as a reference for the signals upon protease expression.

4.2 Impact of TRIF cleavage on innate immune induction

Having assessed the limited, or absent, degree of TRIF proteolytical cleavage by HAV and HCV, respectively, I questioned the importance of TRIF for the TLR3 pathway function in our cell culture models. In the context of a parallel project which I supervised (see *Appendix*), I performed with my student Santa Olivera a siRNA-mediated gene-targeted knock-down (KD) pilot experiment, specifically inhibiting the TLR3 response in Huh7 Lunet TLR3 cells, through transfection of siTRIF and siTLR3 pools and subsequent exclusive stimulation of TLR3. The latter is obtained through supernatant feeding (SN) of poly(I:C), resulting in a specific activation of the endosomal receptor but not of cytoplasmic RLRs, in contrast to transfection (TSFX) of poly(I:C), stimulating both pathways. Curiously, upon siTLR3 the response to the supernatant-delivered poly(I:C) was minimally impacted, due to low knockdown efficiency or limited amounts required to mount a response, but siTRIF abrogated it completely (Figure33A). In addition, I selected and tested TRIF knock-out pools previously generated (Traut, unpublished) and, starting from the one showing a more prominent hindering of ISGs upregulation upon TLR3 stimulation, #sgRNA2 (Figure 33B), started selection of single cell clones. The KO single cell clones could not be validated through canonical immunoblotting aiming at TRIF detection, because of the difficulties in staining endogenous TRIF; but a functional test with poly(I:C) stimulation confirmed that the TLR3 pathway was nonresponsive in all the three populations, when compared to the #sgNT (Figure33C), corroborating the crucial reliance of TLR3 on the adaptor protein TRIF.

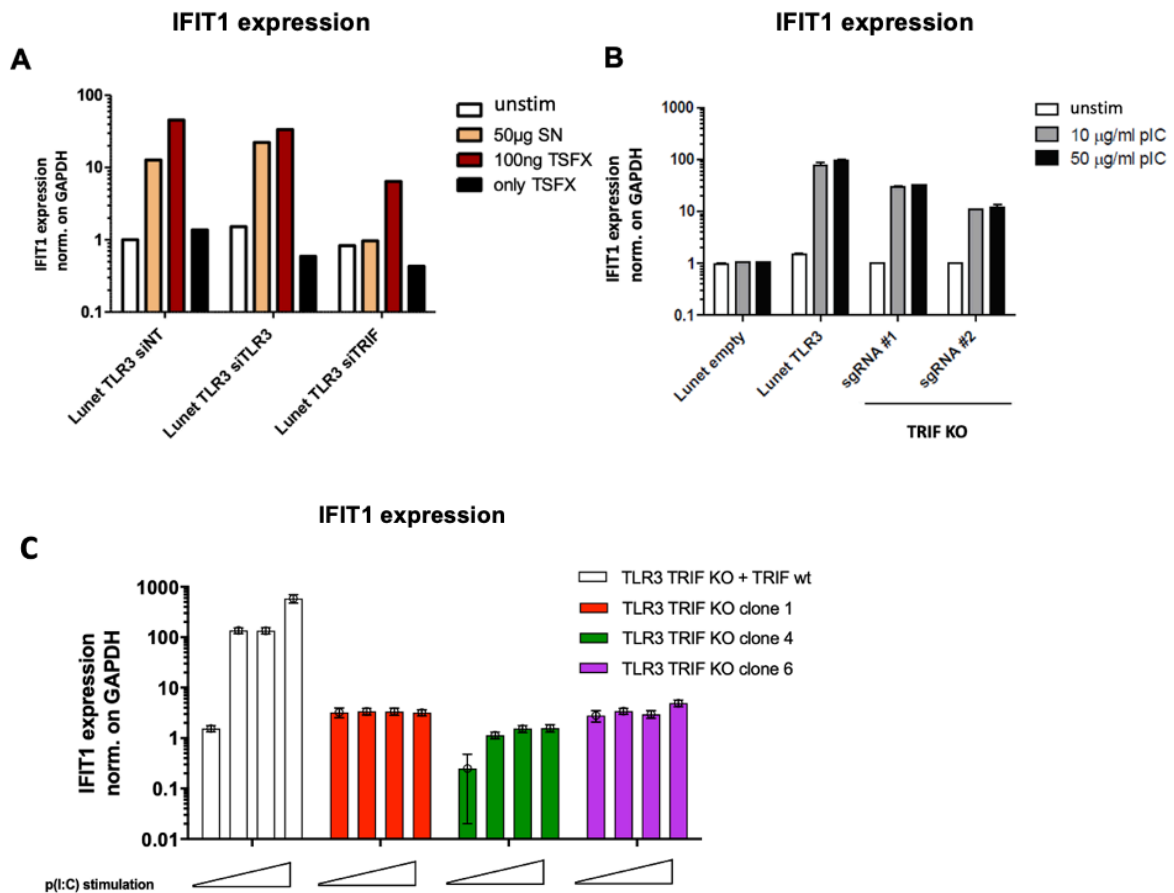


Figure 33. Pivotal dependence of the TLR3 pathway on TRIF.

(A) Huh7-Lunet cells stably expressing TLR3 were transfected with non-targeting siRNA as well as siRNA targeting TLR3 or TRIF, and 48 hours later, stimulated with 50µg poly(I:C) delivered in the supernatant for exclusive TLR3 stimulation, or 100ng transfected for a broader activation of cytoplasmic and endoplasmic PRRs. (B) Huh7-Lunet, Huh7 Lunet TLR3 and Huh7 Lunet TLR3 stably transduced with Lenti-CRISPR KO constructs targeting TRIF were seeded and stimulated with 10µg or 50µg poly(I:C) delivered in the supernatant for exclusive TLR3 stimulation. (C) Three Huh7 Lunet TLR3 TRIF KO clones were selected, expanded and seeded for a functional test against Huh7 Lunet TLR3 (“no KO”). Cells were stimulated with 5µg, 10µg or 50µg poly(I:C) delivered in the supernatant for exclusive TLR3 stimulation. (A-C) eight hours later, cells were harvested and total RNA was extracted. IFIT1 mRNA levels were normalized to GAPDH expression and shown as fold expression relative to unstimulated cells. Shown are mean values with SD from two biological replicates.

Albeit all the clone populations displaying a striking absence of ISGs upregulation upon immune stimulus, clone #1 showed a severe growth defect, whereas IFIT1 mRNA in clone #4 was strongly reduced at basal level (in absence of stimulus), which I feared could have led to artefacts. Therefore, I chose clone #6 for the following experiments.

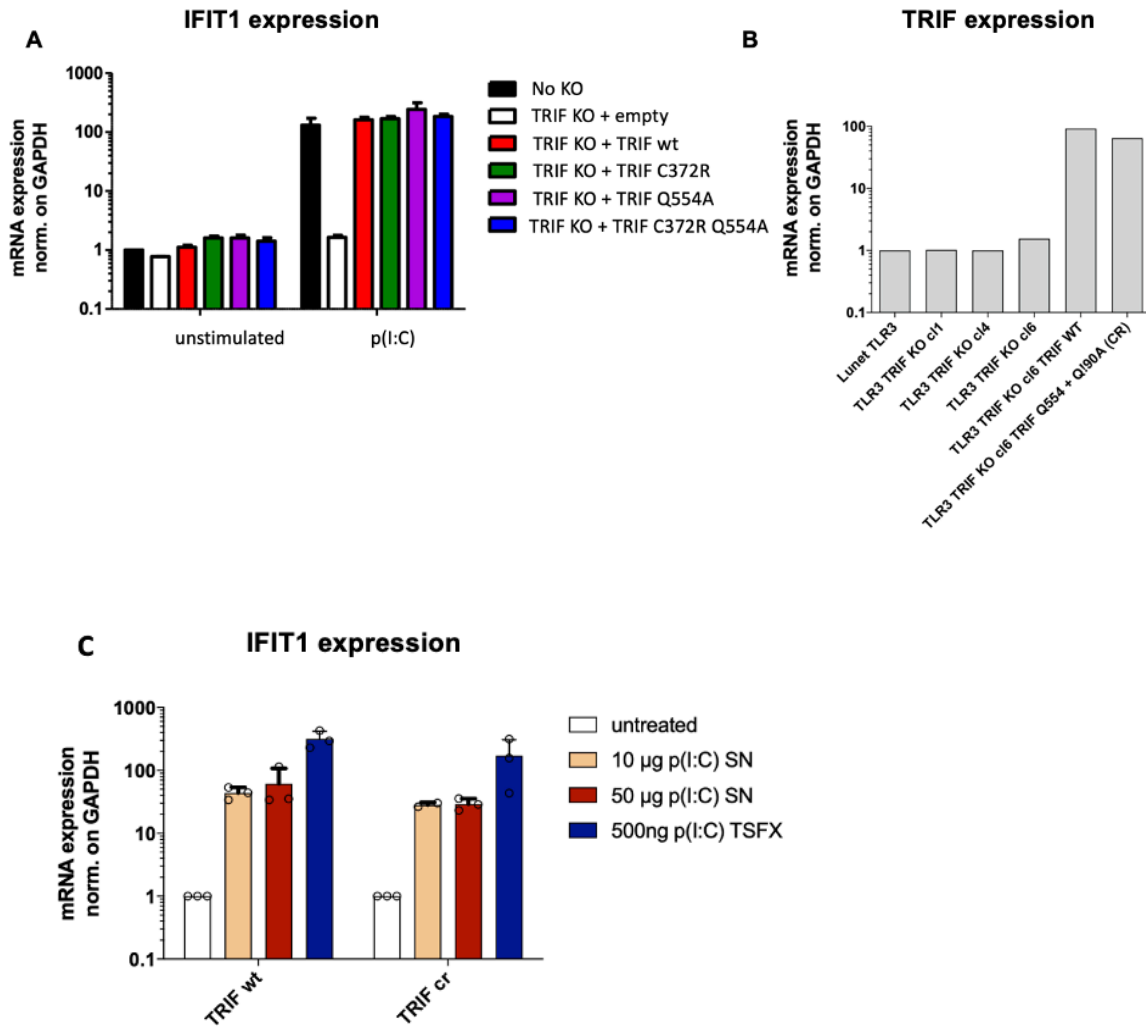


Figure 34. Rescue of the TRIF KO with ectopic TRIF mutants.

(A) Huh7 Lunet TLR3 TRIF KO clone #6 was reconstituted with different TRIF variants, wt or mutants, through lentiviral transduction. After selection and expansion, cells were seeded and functionally tested for TLR3 functionality through poly(I:C) stimulation. Eight hours after the treatment, cells were harvested, total RNA was extracted and IFIT1 mRNA levels were quantified via RT qPCR. All the reconstituted clone TRIF mutants showed full rescue of the pathway upon 50µg supernatant delivery of poly(I:C). TRIF WT = no mutation; TRIF C372R = resistant to HCV NS3-4A cleavage; TRIF Q554A = resistant to HAV 3CD cleavage; TRIF C372R + Q554A = resistant to both HCV and HCV cleavage. IFIT1 mRNA levels were normalized to GAPDH expression and shown as fold expression relative to unstimulated cells. Shown are mean values with SD from one biological replicate with technical triplicates. (B) TRIF mRNA expression levels were measured via RT qPCR in Huh7 Lunet TLR3 cells, the three single cell clones "TRIF KO" and the two reconstituted variants TRIF WT (cleavage susceptible) and TRIF CR (cleavage resistant for both HAV and HCV) cell lines. Despite showing an apparent similar response to poly(I:C) compared to the non-KO cell line, TRIF mRNA levels were highly elevated in the reconstituted TRIF WT and TRIF CR. TRIF mRNA levels were normalized to GAPDH expression and shown as fold expression relative to TLR3 cells. Shown are mean values with SD from two biological replicates. (C) For further experiments, only TRIF WT and TRIF CR were used in place of the single HAV- or HCV-cleavage resistant mutants. A functional test through poly(I:C) supernatant or transfection stimulation was performed on the two reconstituted cell lines. IFIT1 mRNA levels were normalized to GAPDH expression and shown as fold expression relative to unstimulated cells. Shown are mean values with SD from biological triplicates.

To tightly control the functional impact of HAV moderate 3CD-mediated cleavage of TRIF, I aimed at generating new cell lines devoid of endogenous TRIF expression and reconstituted with either “TRIF WT” (cleavage susceptible), TRIF C372R (resistant to HCV NS3-4A cleavage)¹³⁸, TRIF Q554A (resistant to 3CD cleavage)¹⁷³ or “TRIF CR” (cleavage resistant to both HAV and HCV, harboring the combination C372R + Q554A). Upon lentiviral mediated transduction and selection, I tested the cells for responsiveness to p(I:C), confirming the functional rescue (Figure 34A) and the enhanced TRIF mRNA expression levels (Figure 34B). Still expression levels seemed to be low enough to work with full-length TRIF, since no obvious cytotoxicity was observed. I focused exclusively on the “WT” and “CR” species, instead of working with the single resistant mutants, to have a more homogeneous system and found them equally responsive to poly(I:C) (Figure 34C).

I proceeded then by testing subgenomic replicons for both viruses, using Gt2a, JFH1, for HCV. Besides confirming HAV subgenomic replication being more limited than in the case of HCV (Figure 35A, 36A, respectively), I did not detect, in any case, induction of IFIT1 expression upon neither HAV nor HCV replication (Figure 35B, 36B, respectively).

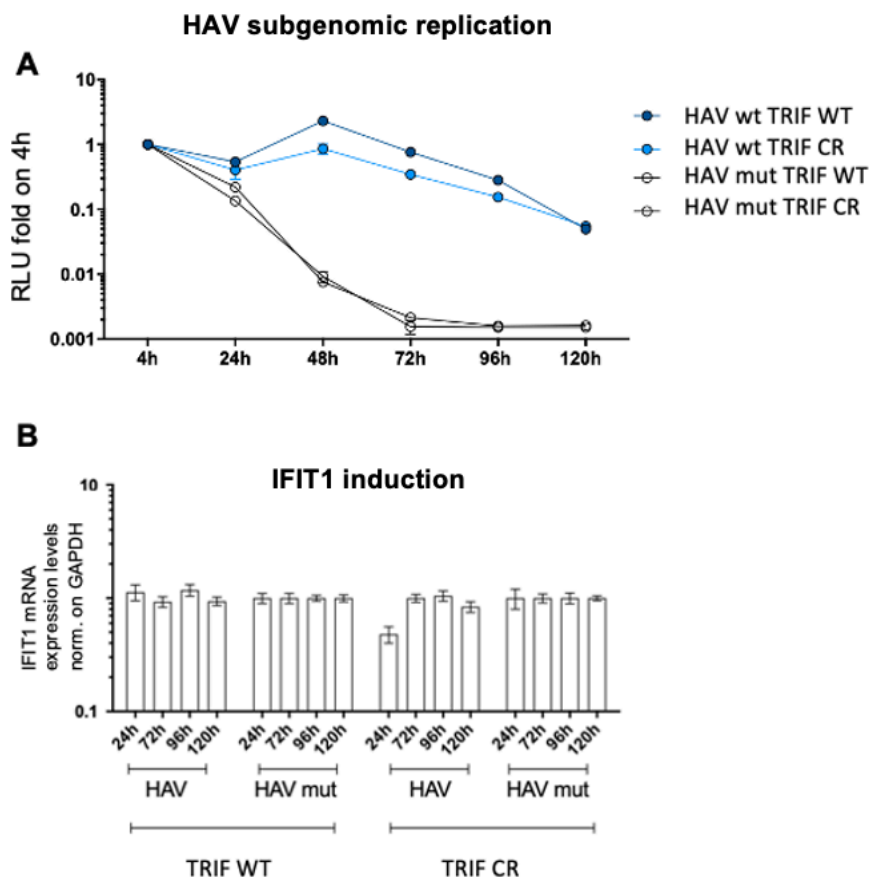


Figure 35. HAV subgenomic replication in TRIF wild-type or TRIF cleavage resistant reconstituted cells.

(A) Huh7 Lunet TLR3 TRIF KO clone #6 was reconstituted with different TRIF, wild-type or cleavage resistant mutant, through lentiviral transduction. After selection and expansion, the cells were electroporated with HAV in vitro transcripts (IVT) based on HM175/18f, wild-type or replication dead mutant (HAV mut) harboring a Firefly luciferase reporter. At the indicated time points, cells were harvested and subjected to measurement of Relative Light Units (RLU) indicative of viral replication. RLU counts were normalized on the initial timepoint as

illustrated in *Methods*. (B) Electroporated cell lysates were harvested at the indicated time points, total RNA was extracted and mRNA expression levels for IFIT1 were measured via RT qPCR. Expression levels were normalized to GAPDH expression and shown as fold expression relative to cells electroporated with replication dead mutant respective for each timepoint. Shown are mean values with SD from two biological replicates.

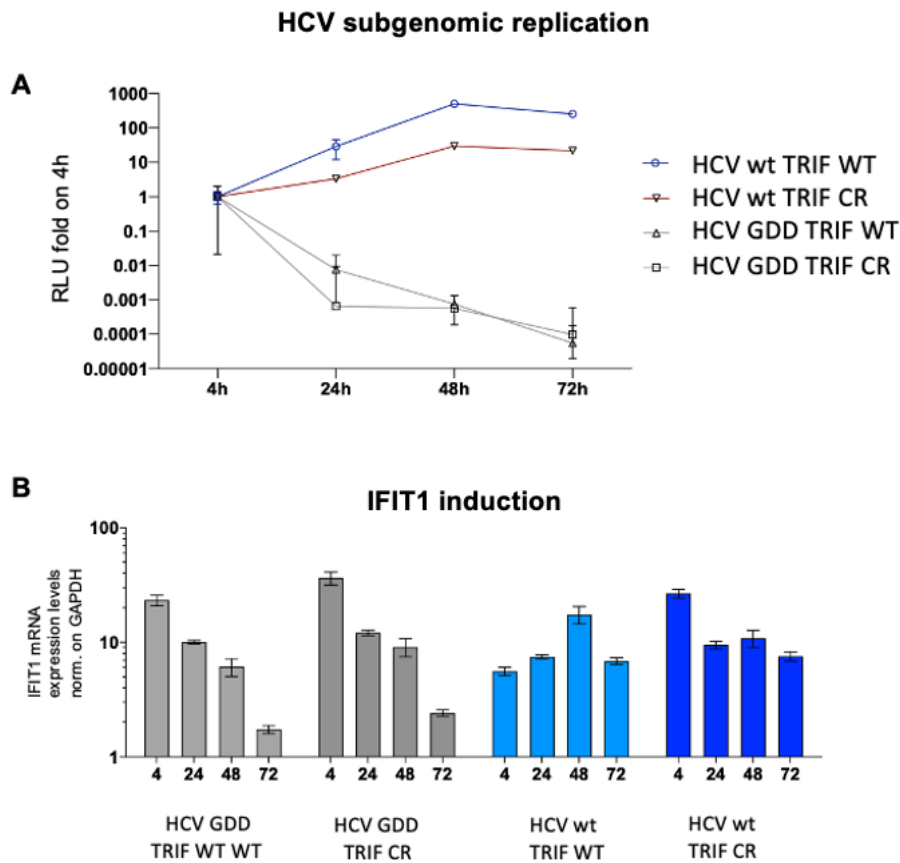


Figure 36. HCV subgenomic replication in TRIF wild-type or TRIF cleavage resistant reconstituted cells.

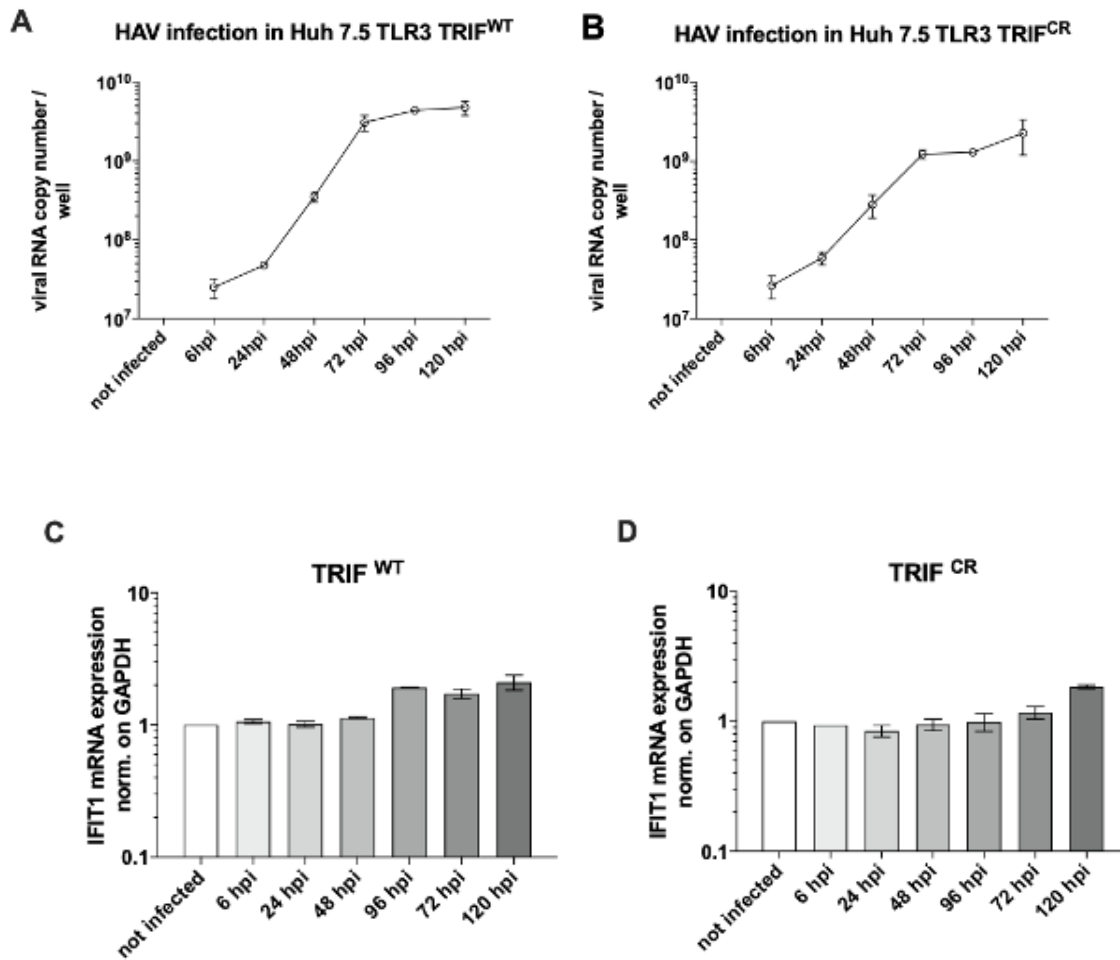
(A) Huh7 Lunet TLR3 TRIF KO clone #6 was reconstituted with different TRIF, wt or cleavage resistant mutant, through lentiviral transduction. After selection and expansion, the cells were electroporated with HCV in vitro transcripts (IVT) based on JFH1 wild-type or replication dead mutant (GDD) harboring a Firefly luciferase reporter. At the indicated time points, cells were harvested and subjected to measurement of Relative Light Units (RLU) indicative of viral replication. RLU counts were normalized on the initial timepoint as illustrated in *Methods*. (B) Electroporated cell lysates were harvested at the indicated time points, total RNA was extracted and mRNA expression levels for IFIT1 were measured via RT qPCR. Expression levels were normalized to GAPDH expression and shown as fold expression relative to cells electroporated with replication dead mutant respective for each timepoint. Shown are mean values with SD from two biological replicates.

This was likely due to high ISGs Ct baseline value in the TRIF overexpressing (OE) cell lines, which resulted pre-induced; since generally HCV replication did clearly activate TLR3, this model appeared not to be suitable for further studies.

At this point, fearing that the minimal HAV replication reached in the context of subgenomic replicon, not reaching the HCV replication levels as previously showed¹⁹⁰, I decided to move on to working with full-length HM175/18f, giving rise to more robust replication. Basing on the conditions I established for Huh7 of Huh7.5, I infected with HAV the two mentioned TRIF cell lines with HAV HM175/18f for five days.

IFIT1 and CXCL10 were in general not upregulated upon HAV replication, reminding previous results obtained in Huh7 TLR3 and Huh7.5 TLR3 cells, with the lack of induction even in presence of an uncleavable TRIF (Figure 37D,F). In addition, HAV replication was robust and homogeneous for both TRIF species equally (Figure 37A,B).

Thus far, I was not able to associate, in none of the systems used, HAV-mediated cleavage of TRIF with any reduction of the TLR3 function, thus not clarifying whether the degree of counteraction did not suffice to abrogate the pathway, or rather my approaches were not sensitive enough.



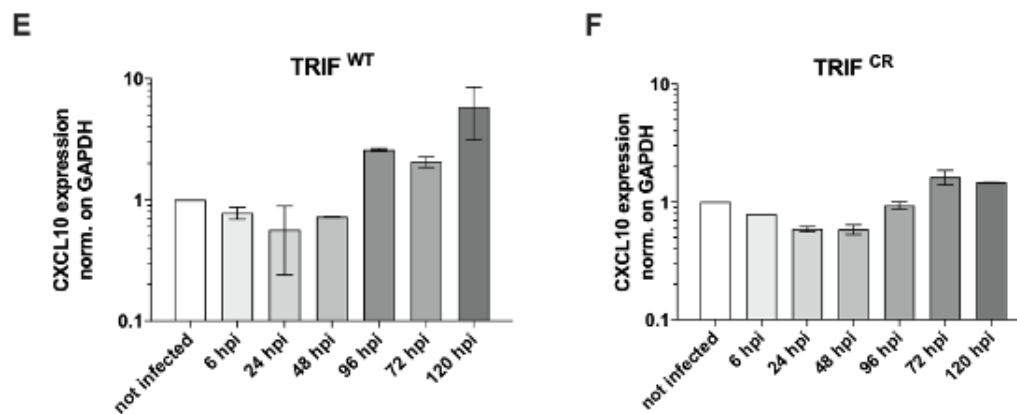


Figure 37. HAV replication and innate immune induction in presence or absence of a cleavage-resistant TRIF.

Huh7-Lunet TLR3 - TRIF KO - TRIF WT or CR cells were infected with HAV HM175/18f. Cells were harvested at the indicated timepoints. Total RNA was extracted and viral replication, as well as IFIT1 and CXCL10, were quantified via TaqMan (A, B) or Sybr (C, D, E, F) RT qPCR. IFIT1 and CXCL10 mRNA levels were normalized to GAPDH expression and shown as fold expression relative to unstimulated cells. Shown are mean values with SD from two biological replicates.

I therefore decided to generate, based on the TRIF KO + TRIF WT reconstituted clone (termed from now on “TRIF WT” for simplicity), stable cell lines, where both HAV and HCV viral proteases, wild-type or mutant, could be transduced on top, in order to force the cell lines, upon selection, to maintain their expression, possibly showing a different phenotype for wild-type versus mutant protease, at least in the case of HAV.

At the same time, I transduced the viral proteases onto Huh7 Lunet TLR3 cells as well, to compare the outcome with expression of endogenous TRIF.

However, I encountered two problems:

I noticed intense cell death upon expression of 3CD wild-type protease, and when I tried to detect HA-TRIF and 3CD / NS3-4A in the newly generated cell lines through IF, I discovered that the cells surviving the selection lost, or highly downregulated, 3CD expression (Figure38B) because of a high cytotoxicity, later confirmed with a WST assay (Figure38C); however, HCV NS3-4A was instead expressed to moderate levels and detectable (Figure 38A).

I detected excessive variations in the Ct values for what concerned the newly generated TRIF reconstituted cells lines which might have had impacted on evaluating correctly the ISGs upregulation.

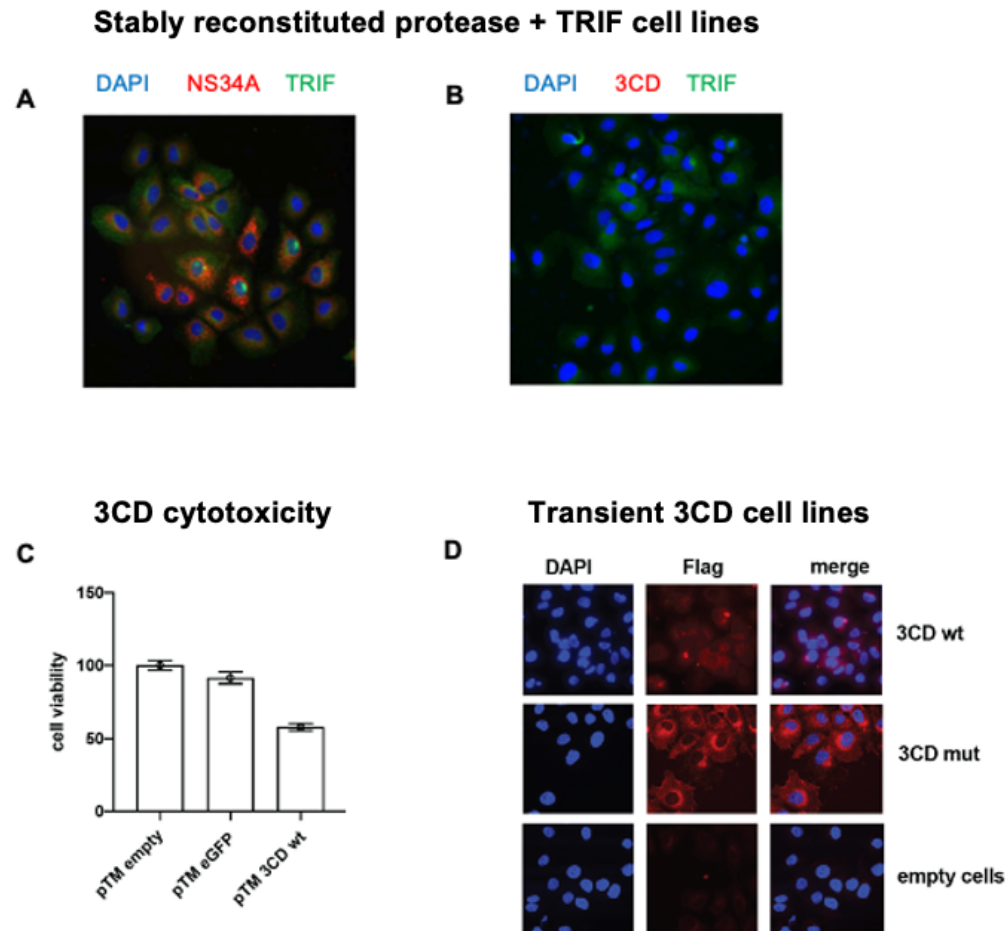


Figure 38. Cytotoxicity of HAV 3CD protease and necessity to switch to a transient expression system.

(A, B) Huh7-Lunet TLR3 TRIF cells were stably transduced with HAV Flag-3CD and HCV Flag-NS3-4A. After selection and expansion, cells were seeded onto coverslips and fixed sixteen hours later. Immunofluorescent staining was performed as described in *Methods*, targeting Flag (viral protease) in red (AlexaFluor 567), HA (TRIF) in green (AlexaFluor 488) and nuclei in blue (DAPI). (C) Huh Lunet T7 cells were transfected with pTM plasmids encoding GFP or the HAV protease precursor 3CD wild-type. 24 hours after transfection cell viability was determined through WST-1 assay. Cell viability was normalized on cells transfected with an empty vector. Shown are mean values and SD of triplicates from 1 experiment. (D) Huh7-Lunet TLR3 TRIF cells were transiently transduced with HAV Flag-3CD wild-type or mutant and subjected to IF staining, targeting Flag (viral protease) in red (AlexaFluor 567) and DAPI (nuclei) in blue.

For these two reasons, I decided that moving the assay towards the use of Huh7 Lunet TLR3 cells with endogenous TRIF expression, in which expression was lower compared to the TRIF KO + TRIF WT cells (to avoid ISGs pre-activation), and using only transient expression of HAV 3CD upon lentiviral transduction (to avoid cell death) could have been at the same time more physiological for our biological questions and less detrimental to the cells. I therefore generated new cell lines based on TLR3 stable and on proteases transient expression, and subjected them to poly(I:C) stimulation with titrating volumes of poly(I:C) to evaluate the potential impact of HAV 3CD and HCV NS3-4A on the pathway. As expected, the TLR3 pathway resulted functional upon expression of the proteases, wild-type or mutant, if compared to a cell line in which a mock transduction was performed (Figure39).

Transient proteases expression onto Huh7.5 TLR3

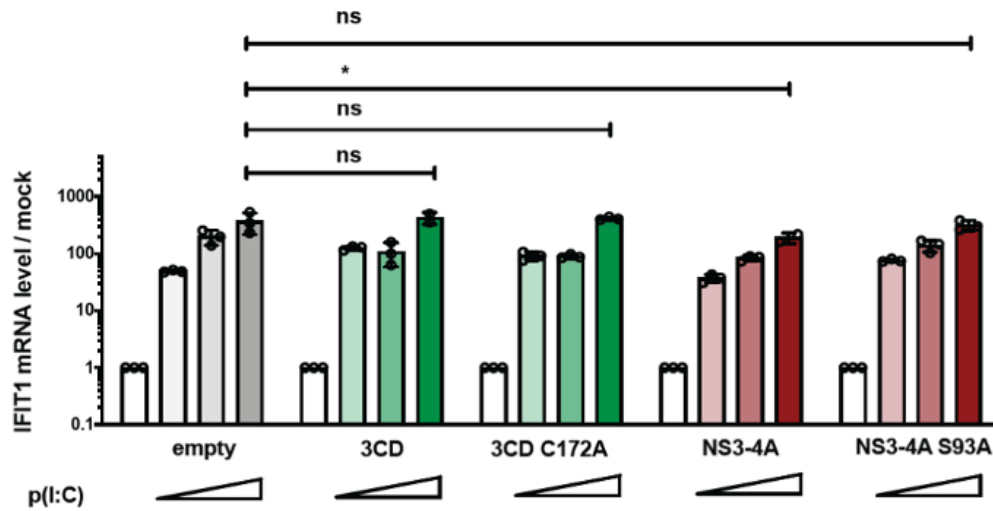


Figure 39. Impact of HAV and HCV protease mediated cleavage of TRIF on cell intrinsic innate immune response.

Huh7.5 cells stably expressing either TLR3 (A) were transduced with lentiviral vectors lacking inserts (empty) or encoding wt or mutant HAV proteases 3CD (A) or HCV protease NS3-4A (A, B, C), as indicated. After selection and passaging, cells were transfected with increasing amounts of poly(I:C) (0, 0.01 $\mu\text{g/ml}$; 0.1 $\mu\text{g/ml}$; 1 $\mu\text{g/ml}$) and harvested six hours after stimulation to isolate total RNA and quantify IFIT1 mRNA by RT-qPCR. Data are normalized to GAPDH and shown as fold expression relative to uninfected cells. Mean values with SD from biological replicates (n = 3). Statistical significance was assessed by Welsch's t-test.

Still, as upon the highest dose of poly(I:C) in the cell line expressing HCV NS3-4A, statistics highlighted a significant difference with the empty cell line, despite the lack of detectable TRIF cleavage observed previously (Figure 39, in red), I tried to modulate expression of HCV NS3-4A further to elucidate its impact. I generated two new cell lines in which NS3-4A, wild-type and mutant, could be expressed at either low or high amounts through different doses of lentiviral particles and, once selected, I stimulated them with the lowest of the poly(I:C) concentrations used in Figure 39, to try emphasizing the effect of the wild-type protease over the mutant (Figure 40). Again, I saw a full response to the poly(I:C) stimulation, which made me exclude any functional interfering activity by HCV NS3-4A towards TLR3. For HAV, the limited 3CD mediated TRIF cleavage we observed in our previous assays appeared to have no impact on the poly(I:C) response of TLR3 (Figure 39, in green).

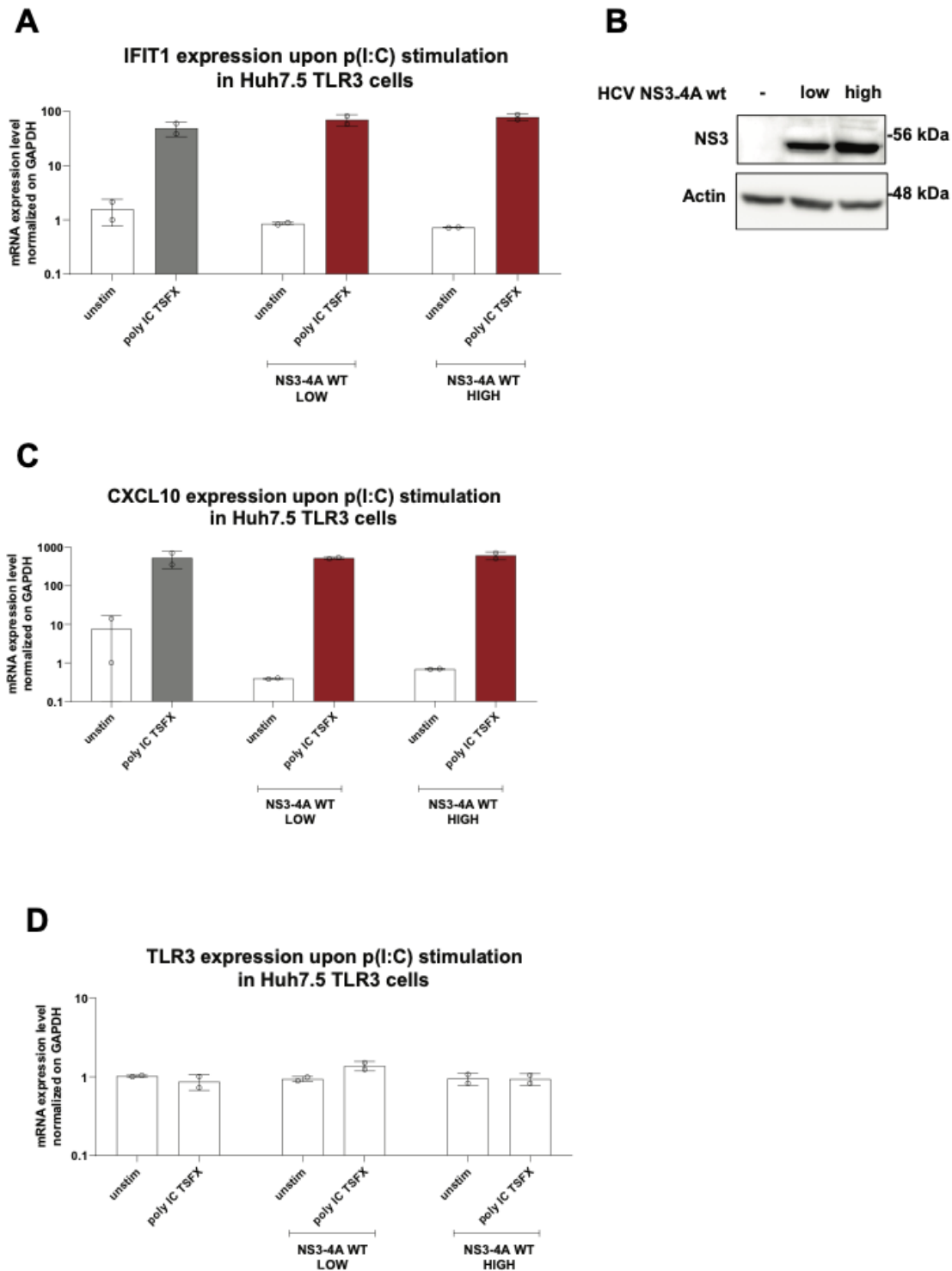


Figure 40. Modulation of HCV-NS3-4A protease expression levels in Huh7.5 TLR3 cells.

(A, C, D,) Huh7.5 TLR3 cells were stably reconstituted with HCV NS3-4A wt in either low or high amounts via lentiviral transduction, and immune stimulated with poly (I:C). IFIT1 (A) CXCL10 (C) and TLR3 (D) mRNA levels were detected in Huh7.5 cells. IFIT1, CXCL10 and TLR3 mRNA levels were normalized to GAPDH expression and shown as fold expression relative to unstimulated cells not expressing the viral protease. All values shown are mean values with SD from biological replicates (n = 2). (B) Cells were analyzed through immunoblotting, using specific antibodies against NS3 and beta-actin.

Expressing the sole protease over the full-length genome can be advantageous, because it allows to silence the “background noise” given by the other proteins which might act as confounder factor with their own activities. But, at the same time, old literature pointed at several different mechanisms exerted by HCV which could lead to downregulation of TLR3 responsiveness, indirectly targeting as well TRIF³²⁸. To gain a broader perspective, I revisited previous data from the lab (Esser-Nobis, unpublished), in which TLR3 was expressed transiently in HCV Gt1b and HAV replicon cell lines, and included a poly(I:C) titration to check if the pathway was intact here as well (Figure 41). Here, I did not find evidence of TLR3 abrogation, yet HCV replicon cells seemed to react to poly(I:C) significantly less compared to Huh7 Lunet control cells, but still 80 fold more if compared to unstimulated cells (Figure 41A). In contrast, the limited TRIF cleavage observed in HAV replicon cells (Figure 30) again had no impact on TLR3 activation.

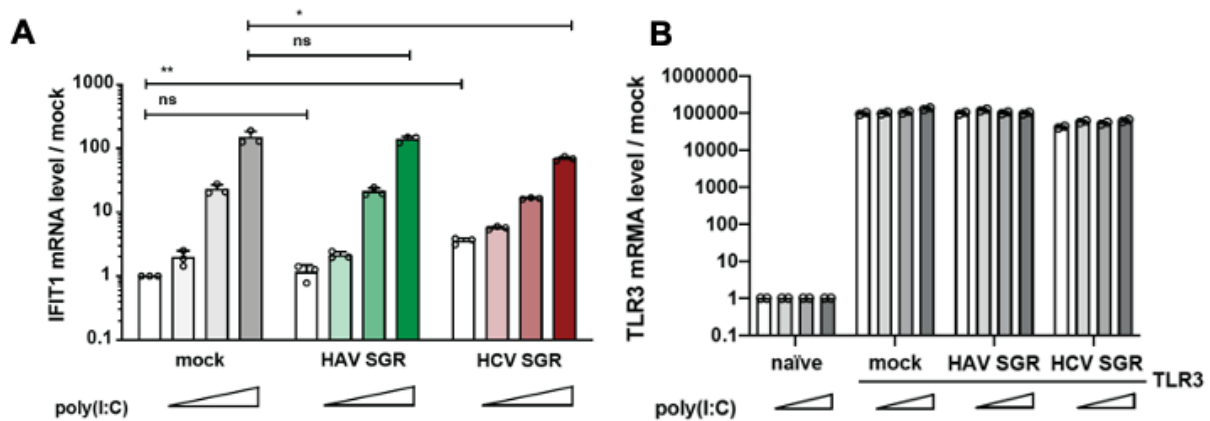


Figure 41. Functional counteraction to TLR3 in HAV and HCV subgenomic replicon cell lines.

(A) IFIT1 mRNA expression was detected in either Huh7 Lunet TLR3 cells (“mock”) or HAV / HCV stable replicon cell lines (HAV SGR and HCV SGR, respectively) transiently reconstituted with TLR3 and stimulated with poly (I:C) in increasing amounts as indicated by the white triangles. (B) TLR3 mRNA expression levels were measured through RT qPCR. IFIT1 and TLR3 levels were normalized to GAPDH expression and shown as fold expression relative to unstimulated cells (“mock”, Huh7 Lunet) not expressing the viral protease. All values shown are mean values with SD from biological replicates (n = 3).

Lastly, to take into account HAV and HCV full replicative cycles, I aimed at gaining insight at the potential abrogation of TLR3 activation in the context of infected cells. To ensure that the analysis would only take into account cells expressing viral proteins and thereby, being capable of potential interference, I established a single-cell approach based on seeding infecting cells onto coverslips prior to stimulating them with poly(I:C), to then detect via immunofluorescence at the same time the viral antigen and the breadth of the innate immune response. After collecting around 30 to 50 cells for each condition, (unstimulated or stimulated; uninfected or infected; infected and stimulated or only infected / only stimulated) and for each pathogen, I relied on a partially automated evaluation of the signal intensity performed through the software Fiji using a macro plugin (provided by Dr. Ji-Young Lee). In such a way, I could first set baseline threshold for uninfected and unstimulated cells and then monitor the breadth of the innate immune response upon poly(I:C) in presence of viral antigen (Figure 42). What stroked the eye immediately was that, for both HAV and HCV

infected cells, reactivity to poly (I:C) was still possible (Figure 42D,H). Interestingly, analyzing cells which are infected but not stimulated on top with poly(I:C), I could see that IFIT1 seemed not to be upregulated in HAV-infected cells (Figure 42B), while HCV infected cells seemed to activate TLR3, albeit preferentially the ones with a lower signal HCV viral antigen signal intensity (Figure 42F). As in the population there might be different expression levels among the cells, this might indicate that higher HCV replication is possible in cells with lower TLR3 baseline expression and consequent reduced ISGs activation.

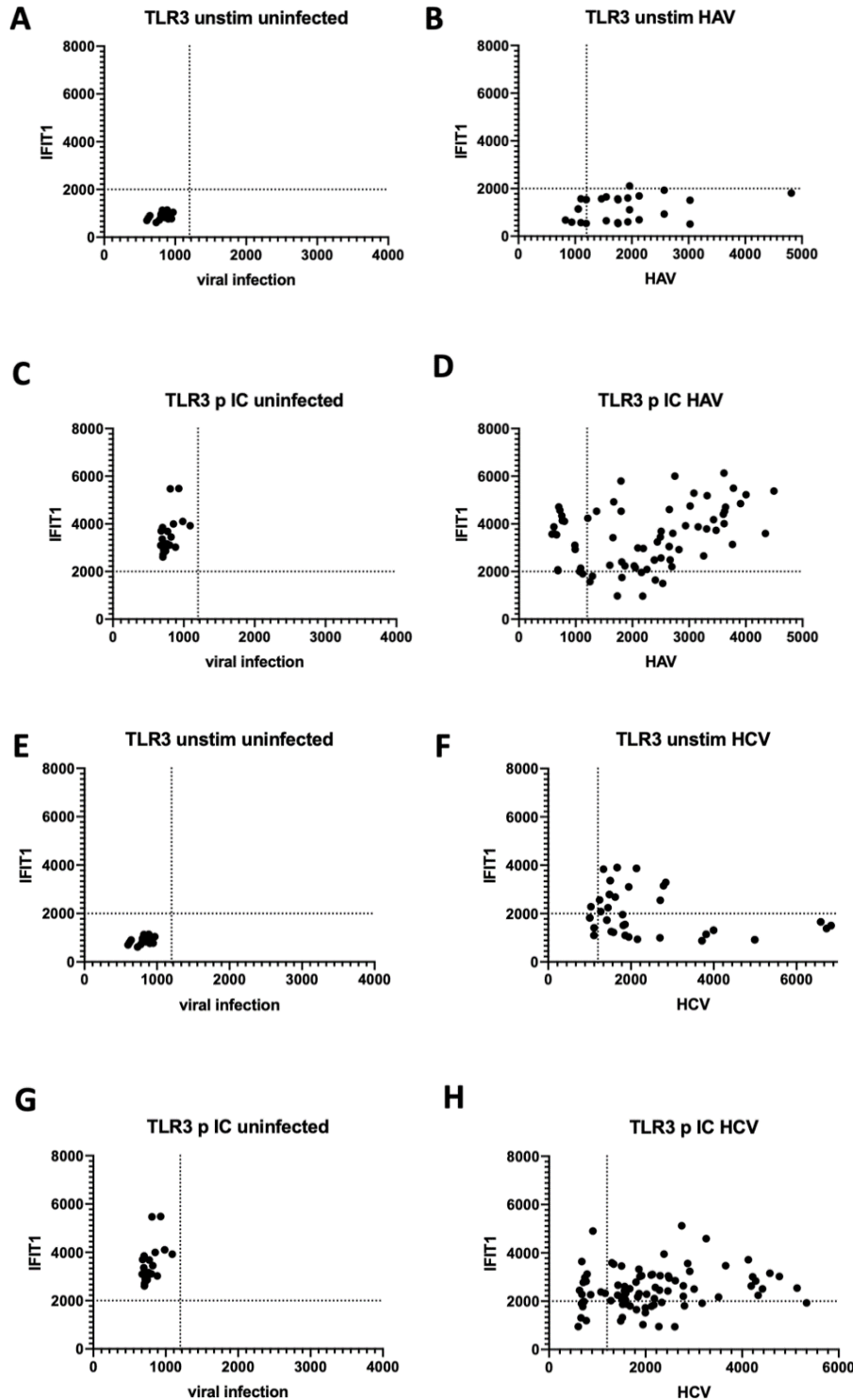


Figure 42. Functional counteraction to the TLR3 pathway by HAV and HCV at single-cell level through immunofluorescence analysis.

(A-H) Immunofluorescence-based approach to assess counteraction of innate immune response in infected cells. Huh7.5 cells expressing TLR3 were infected with HCV or HAV. On day 3 and 4, respectively, post infection, cells were re-seeded onto coverslips and transfected with poly(I:C); 6 hours later cells were fixed and stained for viral antigen and IFIT1 (ISG) expression. (A) unstimulated cells (B) HAV infected cells, unstimulated (C) uninfected cells and poly(I:C) -stimulated (D) HAV infected cells stimulated with poly(I:C) (E) unstimulated cells (F) poly(I:C) HCV infected cells, unstimulated (G) uninfected cells and poly(I:C) -stimulated (H) HCV infected cells stimulated with poly(I:C). Viral antigen and ISGs signals were measured using Fiji in $n \geq 30$ cells basing on IF acquisitions.

To avoid inclusion of neighboring cells, potentially reacting to secreted IFNs and cytokines, I then moved on and included in the dotplot analysis solely HAV and HCV infected cells stimulated with poly (I:C), to statistically test against mock cells in order to elucidate potential hinderances of TLR3 (Figure 43A,B).

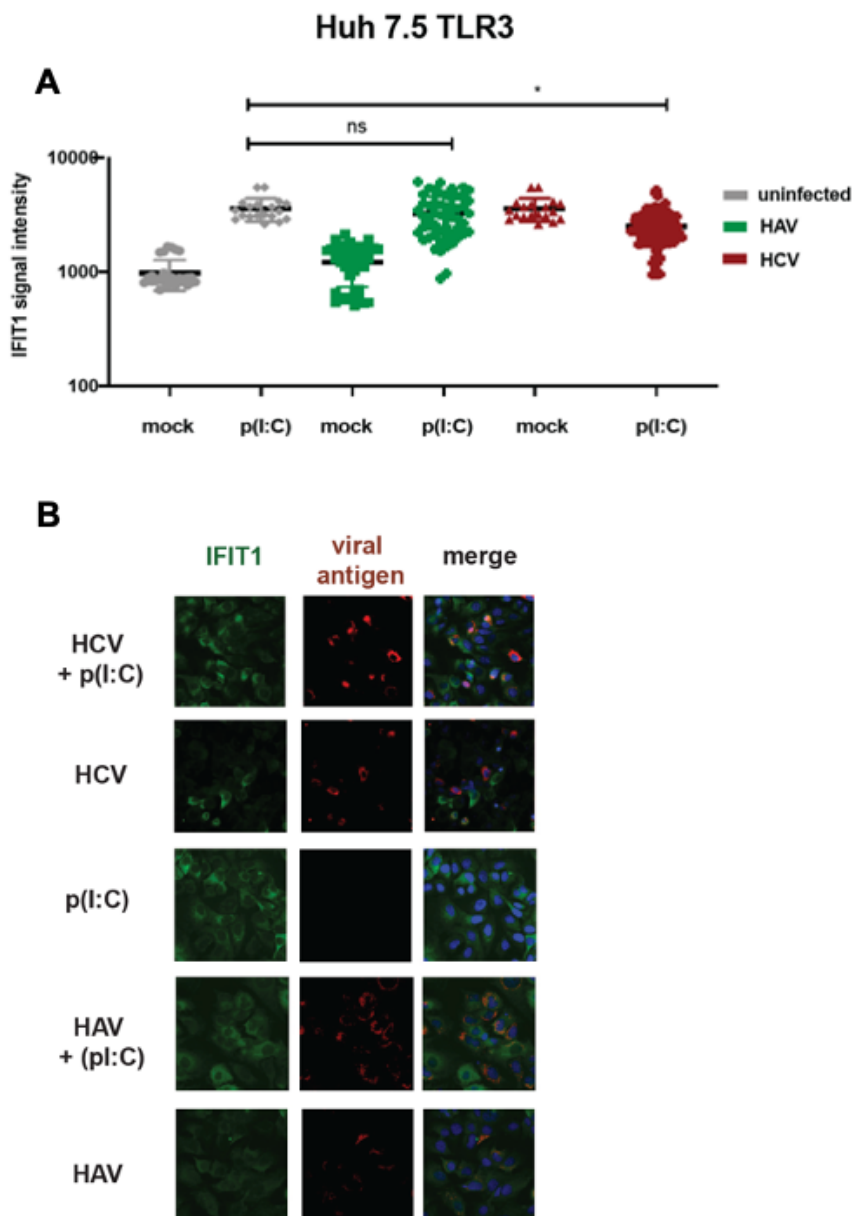


Figure 43. Quantification of TLR3 functional counteraction through analysis of single Huh7.5 TLR3 infected cells. Huh7.5 cells stably expressing TLR3 (D) were infected with HAV HM175/18f, green or HCV (Jc1, red), respectively. Three days after infection, cells were seeded onto coverslips and transfected with 0.5 μ g poly(I:C) or mock treated (mock). Six hours after stimulation, cells were fixed and IF staining was performed using viral antigen- (HAV Vp3 or HCV NS5A) and IFIT1- specific antibodies. Signal intensity for virus and innate immune response was quantified using Fiji and displayed in dot plots, where each dot represents a single cell. Statistical analysis was performed using Welch's *t*-test to compare the innate immune response to poly(I:C) in HAV or HCV infected cells compared to uninfected cells (grey).

Both HCV and HAV infected cells were in principle mounting an innate immune response upon external stimulus, for HAV comparable to the uninfected cells, while for HCV, some

infected cells were less reactive to poly (I:C) (Figure 43A) contributing to the observable statistically significant difference. However, the unstimulated HCV infected cells showed also upregulation of IFIT1. Therefore, the p(I:C) stimulation might have simply been covered by an already pre-activated state of TLR3, which also confirmed sensing of HCV by TLR3 like previously reported by others^{321,329} and seen by me in bulk (Figure 39-41). In the same way, the data further hinted on HAV not inducing any activation through TLR3 on a single cell level (Figure 42B).

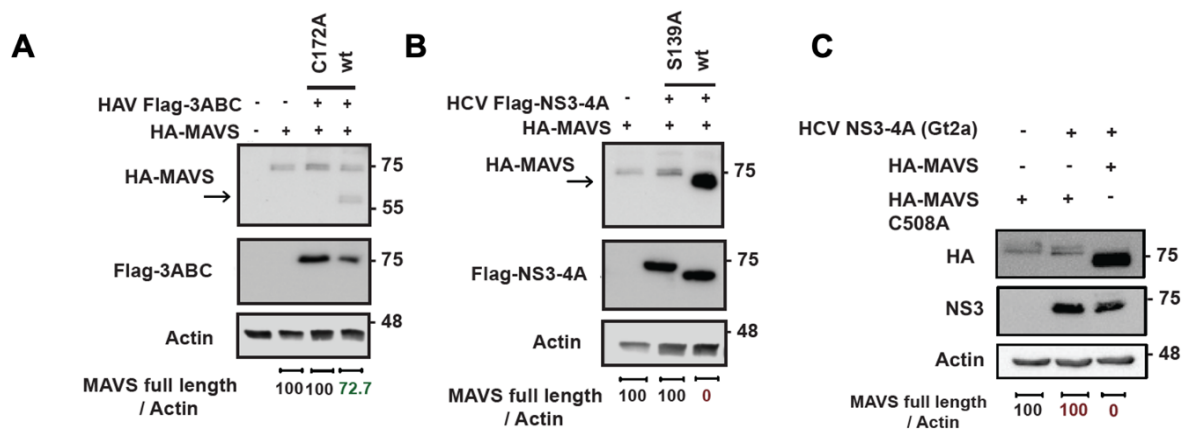
In conclusion, what I assessed so far was that HAV was potentially not sensed by TLR3, or disrupting the pathway through TRIF cleavage, although partial, and that my approaches were not sensitive enough to detect it. However, the lack of counteraction to poly(I:C) induction rather argued for the first option. In contrast, HCV was activating TLR3 without any NS3-4A-mediated abrogation.

4.3 Enhancing the robustness: investigating the interplay of HAV and HCV infections

Not having, so far, detected full cleavage of TRIF by HAV 3CD, and more importantly, not having assessed any functional counteraction by HAV to the TLR3 pathway, I started questioning the validity of the approaches used so far. I had to deal with potential artefacts, as a possible insufficient viral protease expression; the need of expressing TRIF ectopically and, in addition, truncated; the fact that HCV, despite seemingly not cleaving TRIF, showed the same lack of functional counteraction seen for HAV, despite the latter being able to degrade TRIF, at least partially. Thus, I decided to take advantage from previous and more established research on HCV NS3-4A counteraction to RLRs, namely through MAVS cleavage^{135,137,213}, to apply the same approaches that I used for TRIF and legitimate the chosen approaches. Incidentally, literature on HAV counteraction to the RLR pathways was scarce and in need of being revisited¹⁷⁵, similarly as it was for TLR3 and TRIF¹⁷³.

I started by biochemically detecting MAVS cleavage in an overexpression model, with HAV 3ABC / HCV NS3-4A, wild-type or mutant, co-transfected with HA-MAVS, under control of a T7 promoter Huh7 T7 expressing cells. Especially for what concerned HCV, I immediately noticed that the outcome was strikingly different, with full degradation of full-length MAVS (Figure 44B). This was corroborated by extending the immunoblot analysis on samples tested upon HCV NS3-4A from Gt2a, and including a MAVS cleavage resistant species (Figure 44C).

In the case of HAV, a MAVS cleavage product of the predicted size was detected, but signal intensity of the latter was similar as the one of full-length MAVS, hinting at a partial cleavage here as in the case of TRIF (Figure 44A).



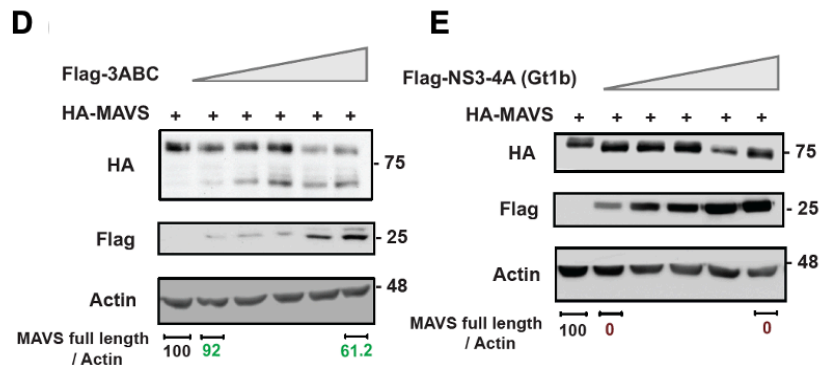


Figure 44. Viral proteases transfection assay to evaluate cleavage of the RLR adaptor MAVS.

(A-E) Huh7-Lunet T7 cells were co-transfected with pTM vectors encoding HA-tagged innate immune adapter protein MAVS and Flag-tagged viral proteases. Sixteen hours after transfection, cell lysates were harvested and 10 μ g of protein lysate was separated by SDS-PAGE and subjected to immunoblotting, using specific antibodies against HA-tag, Flag-tag or b-actin (Actin), as indicated. (A, B, C) Cells were co-transfected with plasmids encoding the indicated wild-type or mutant viral proteases and MAVS, and harvested sixteen hours after transfection. Quantification of the cleavage was based on MAVS full length signal intensity measurement in absence of protease as a reference for the signals upon protease expression. Each signal was normalized on the actin band signal belonging to the same sample. (D, E) 1 μ g of a plasmid encoding HA-MAVS was co-transfected increasing amounts of plasmids encoding either FLAG-HAV 3ABC (D) or FLAG HCV NS3-4A (E), as indicated by the grey triangle (0.05 μ g; 0.1 μ g; 0.25 μ g; 0.5 μ g; 1.25 μ g).

I then proceeded to test incremental doses of viral proteases to assess robustness of the HAV 3ABC-mediated cleavage, and could observe a dose-response in MAVS scission upon HAV protease expression (Figure 44D). Nonetheless, at the highest 3ABC expression dosage, still full-length MAVS was well detectable (Figure 44D) differently than for full-length MAVS in case of HCV, which got fully degraded upon transfection of the smallest amount of NS3-4A encoding plasmid (Figure 44E).

Lastly, I aimed at detecting endogenous MAVS in subgenomic replicon cell lines and upon infection, to increase the physiological relevance of the system. For TRIF, I had to stick to the use of a RHIM deletion mutant and therefore to ectopic expression also because of a lack of available antibodies against endogenous TRIF and the low expression level, while for MAVS this approach was applicable. In the HAV persistent subgenomic replicon cells, MAVS was cleaved to a low degree by HAV (Figure 45A) while completely by HCV (Figure 45B). In infected cells, MAVS cleavage was even lower in the case of HAV, likely reflecting a percentage of uninfected cells with intact MAVS, also considering the presence of uncleaved MAVS in lysates of HCV infected cells (Figure 45C,D).

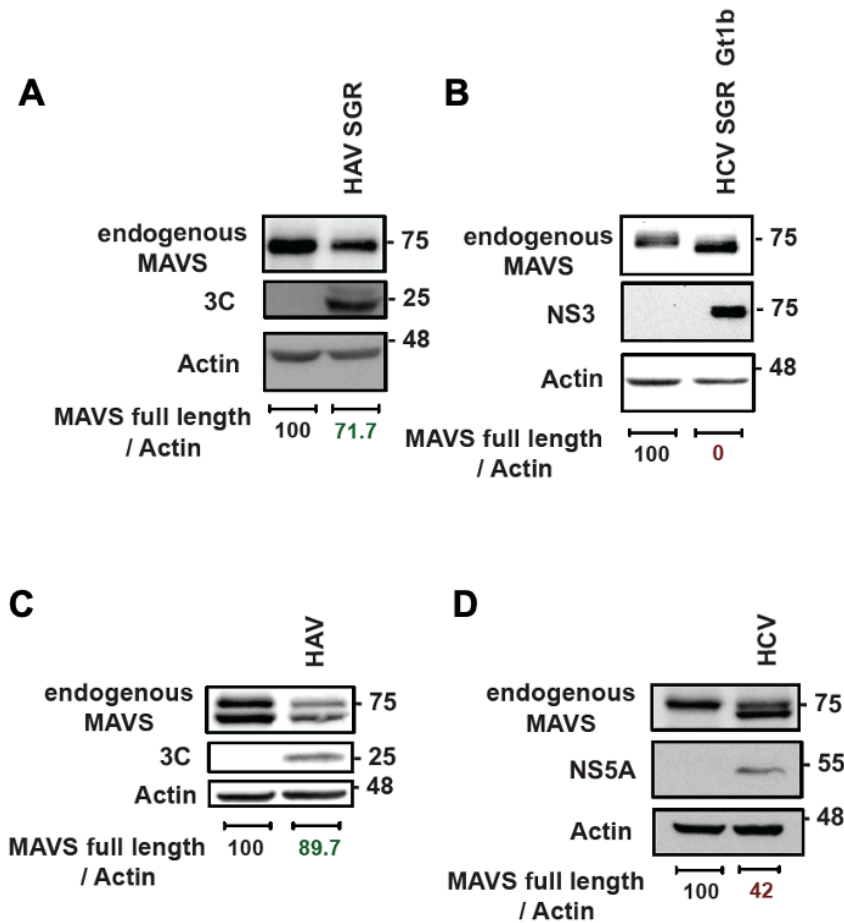


Figure 45. Biochemical detection of MAVS cleavage in HAV or HCV subgenomic replicon and HAV or HCV infected cells.

(A, B) Stable HAV (A) or HCV (B) replicon cell lines were lysed and subjected to immunoblotting to detect endogenous MAVS cleavage products and viral antigens. (C) (D), Huh7-Lunet T7 cells were infected with HAV or HCV and three days later subjected to immunoblotting with the aim of detecting endogenous MAVS cleavage products. Quantification of the cleavage was based on MAVS full length signal intensity measurement in absence of protease as a reference for the signals upon protease expression. Each signal was normalized on the actin band signal belonging to the same sample.

For this reason, my objective was again to look closer at MAVS cleavage in infected cells using a microscopy-based approach. I utilized here a fusion of GFP with a nuclear translocation signal, attached to the C-terminal membrane anchor of MAVS (MAVS-GFP-NLS)²²³. In contrast to previous studies, the MAVS coding region was expanded to include the canonical protease cleavage sites of both HAV and HCV, enabling the measurement of nuclear GFP as an indicator of protease cleavage. Upon infection, both proteases were capable of inducing nuclear GFP translocation, although HCV exhibited a higher degree of translocation (Figure 47A, B). However, when the proteases were transfected, despite similar expression levels and localization of HAV 3ABC and HCV NS3-4A (Figure 46C, D), MAVS translocation upon 3ABC cleavage appeared to be impaired (Figure 46A), suggesting that cleavage upon infection was the most efficient and physiologically relevant among the three approaches employed.

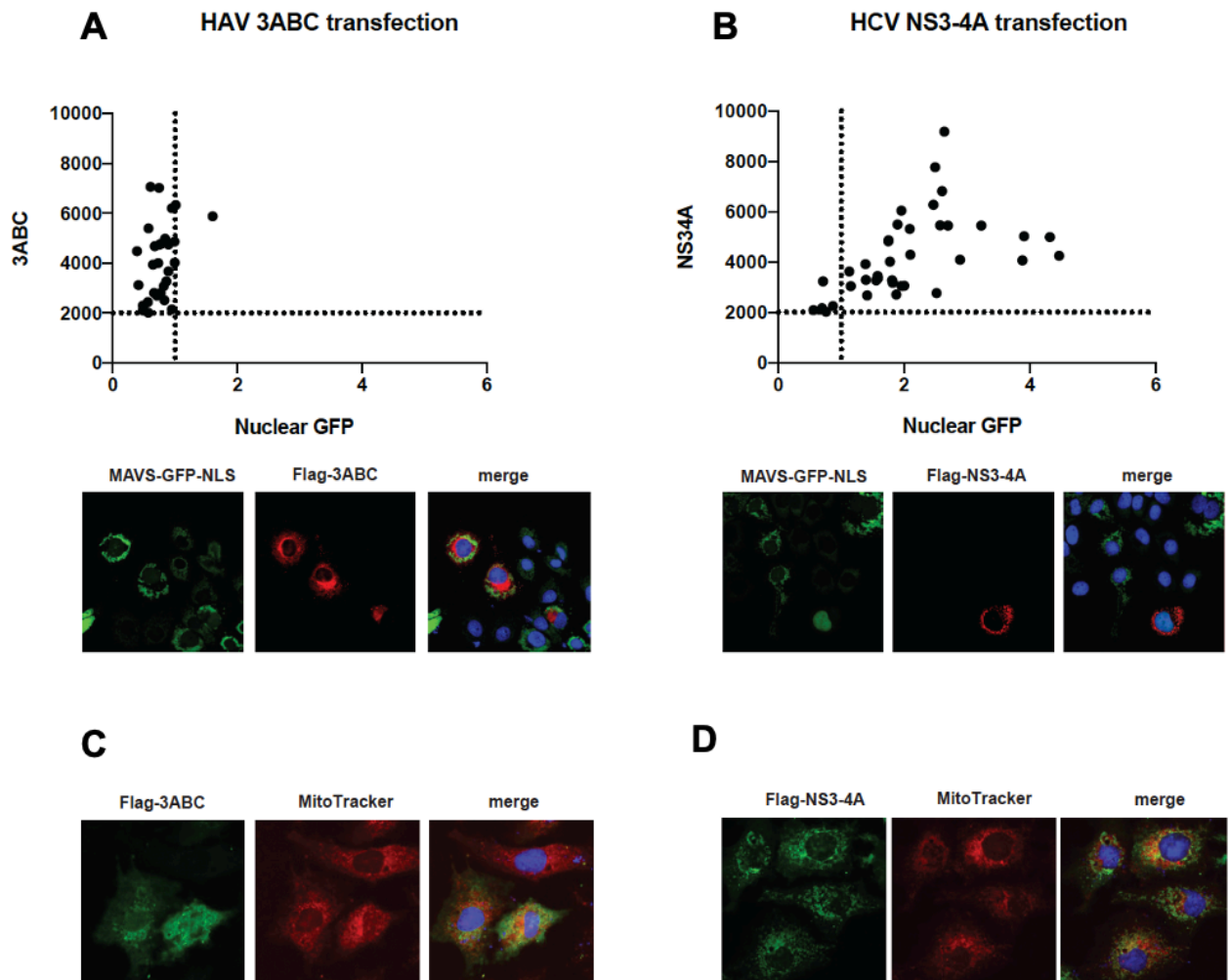


Figure 46. Assessment of MAVS-cleavage by HAV and HCV proteases based on nuclear translocation of GFP upon protease transfection.

(A - D) Huh Lunet cells were transduced with lentiviral vectors encoding GFP tagged with a nuclear translocation signal (NLS) fused to the C-terminal membrane anchor of MAVS (MAVS-GFP-NLS), where the MAVS coding region was extended to encode the canonical protease cleavage sites of both viruses, allowing the quantifying of nuclear GFP as a measure of protease cleavage. Nuclear GFP signals were measured using Fiji in $n \geq 30$ cells basing on IF acquisitions (A, B, lower panels). The ratio nuclear / cytoplasmic signal is expressed, along with the intensity of the signal from the viral antigen, as dot plot with each dot representing a single cell. (A, B) Cells were transfected with $1\mu\text{g}$ of either FLAG-HAV 3ABC (C, E) or FLAG HCV NS3-4A. Eight hours after transfection, cells were fixed and stained for Flag-tag to assess viral antigen and DAPI. (C, D) Huh Lunet T7 cells were transfected with $1\mu\text{g}$ of either FLAG-HAV 3ABC (E) or FLAG HCV NS3-4A (F). Eight hours after transfection, cells were fixed and stained for Flag-tag and mitochondria with MitoTracker Deep Red (M22426).

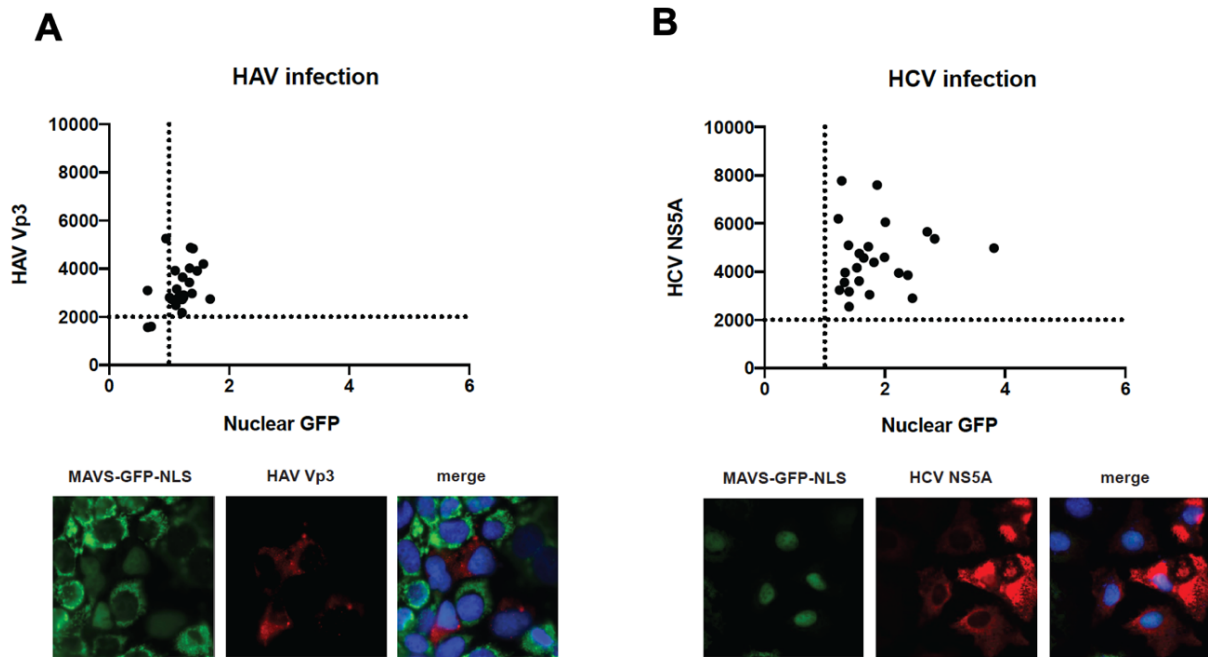


Figure 47. Assessment of MAVS-cleavage by HAV and HCV proteases based on nuclear translocation of GFP upon infection.

(A, B) Cells stably expressing MAVS-GFP-NLS were seeded onto coverslips and infected with either HAV (A) (MOI 4) or HCV (MOI 1). The ratio nuclear / cytoplasmic signal is expressed, along with the intensity of the signal from the Flag-tagged protease, as dot plot with each dot representing a single cell (upper panels A and B). Signal intensity was calculated through a macro in Fiji basing on IF acquisitions of >30 cells (A, B lower panels).

Overall, validation of my biochemical detection approach including HCV NS3-4A in the context of MAVS was an excellent way to confirm that, in presence of successful proteolytical cleavage, it is possible to detect 100% abrogation of the molecule in the immunoblot and in the microscopy-based approach.

4.4 Impact of MAVS cleavage on innate immune induction

At this point, I needed to link MAVS scission to the functional abrogation of RIG-I and MDA5 pathways, in order to prove its relevance in the context of innate immunity upon HAV / HCV. Cell lines expressing HAV 3ABC and HCV NS3-4A were generated in the context of RIG-I and MDA5 and then we stimulated with increasing concentrations of p(I:C) (Figure 48A,B).

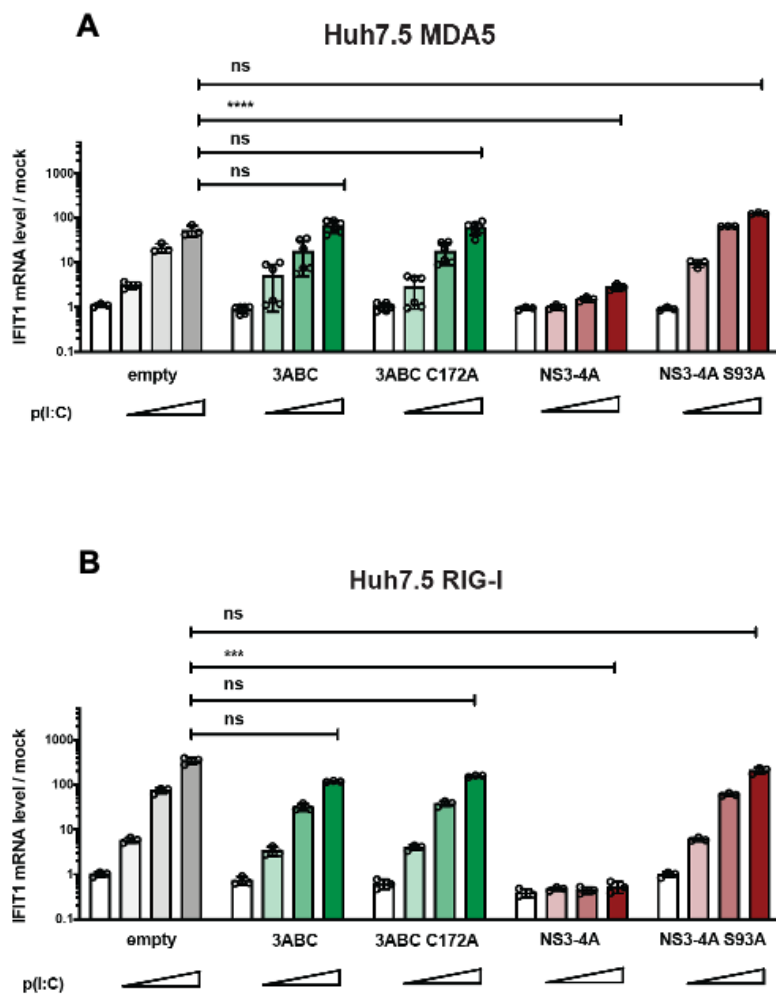


Figure 48. Impact of HAV and HCV protease mediated cleavage of MVAS on cell intrinsic innate immune response.

Huh7.5 cells stably expressing either MDA5 (A) or RIG-I (B) were transduced with lentiviral vectors lacking inserts (empty) or encoding wt or mutant HAV proteases 3ABC or HCV protease NS3-4A as indicated. After selection and passaging, cells were transfected with increasing amounts of poly(I:C) (0, 0.01 $\mu\text{g/ml}$; 0.1 $\mu\text{g/ml}$; 1 $\mu\text{g/ml}$) and harvested six hours after stimulation to isolate total RNA and quantify IFIT1 mRNA by RT-qPCR. Data are normalized to GAPDH and shown as fold expression relative to uninfected cells. Mean values with SD from biological replicates (n = 3).

This assay strikingly proved that, in presence of a cleaving protease, the innate immune response in MDA5 and RIG-I cells with enzymatically active HCV NS3-4A was abolished (Figure 48A, B in red). HAV 3ABC expression, instead, seemed to not hinder the pathways (Figure 48A, B in green), but given the challenges faced for cytotoxicity of 3CD, we decided to check its expression through IF (Figure 49). Here, we confirmed that 3ABC and NS3-4A, wild-type or mutant, were evenly expressed in the cells, and that therefore the innate immune response to poly(I:C) was simply not abrogated by HAV.

stable expression of HAV 3ABC and HCV NS3-4A

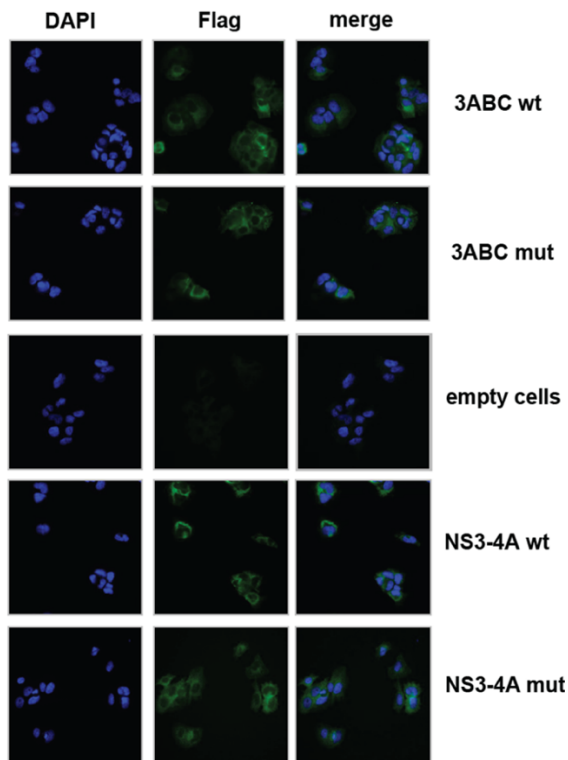


Figure 49. Immunofluorescence analysis of viral proteases stable expression in reconstituted cell lines.

Stable expression of HAV 3ABC and HCV NS3-4A, both wild-type and inactive mutant, was achieved in Huh7.5 cells through transduction with lentiviral vectors. After selection and passaging, the cells were fixed and stained for Flag-tag and for nuclear staining using DAPI

Once assessed the contribution of the single proteases, I investigated deeper on systems which would express a subgenomic / full-length HAV or HCV genomes.

Taking advantage of the previously established methods, I expressed, again with my student Helen Huang, RIG-I and MDA5 transiently onto the HAV and HCV stable replicon cell lines previously used (Figure 19) and measured IFIT1 via RT qPCR. Here, I did not detect an innate immune induction for any of the replicon cell lines, neither for RIG-I, nor for MDA5 (Figure 50).

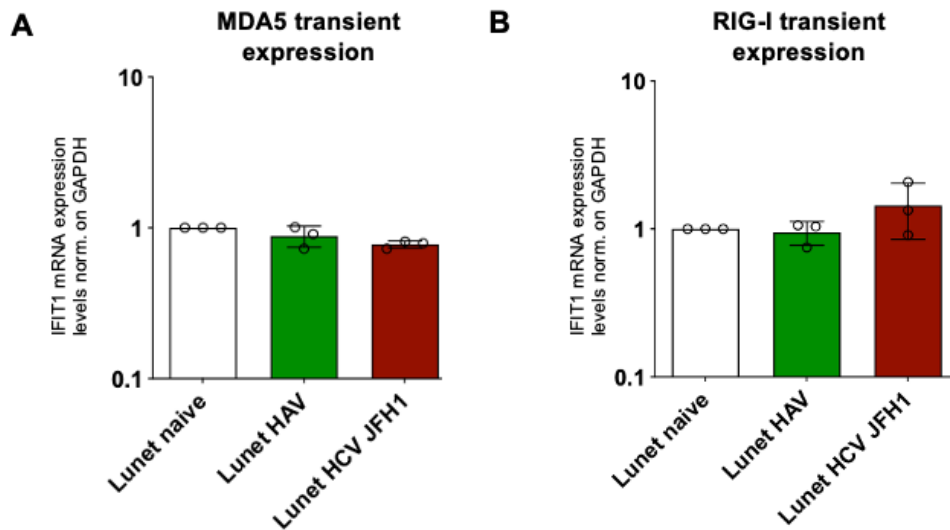


Figure 50. Innate immune response upon RIG-I and MDA5 transient expression in HAV and HCV subgenomic replicon cells.

(A, B) The hepatoma cell clone Huh7 Lunet (“Lunet naïve”) and HAV- or HCV-based subgenomic replicons, based for HAV on HM175/18f gt1b and for HCV on JFH1 gt2a (JFH1), were transiently transduced with lentiviral particles encoding RIG-I and MDA5. Total RNA was isolated from cell lysate and Sybr RT qPCR was performed aiming at IFIT1 mRNA expression detection. IFIT1 mRNA levels were normalized to GAPDH expression and shown as fold expression relative to Lunet naïve cells. Shown values are mean values with SD from one biological replicate with technical triplicates.

I then infected newly generated Huh7.5 MDA5 or Huh 7.5 RIG-I stable cell lines with HAV or HCV, with the aim of detecting ISGs mRNA expression upon full length genome replication. In RIG-I cells, HCV moderately induced IFIT1 and CXCL10 expression early after infection and decreasing over time, likely due to MAVS cleavage (Figure 51), whereas MDA5 expression resulted in a mild induction of ISGs at later timepoints, in line with previous reports^{68,83}.

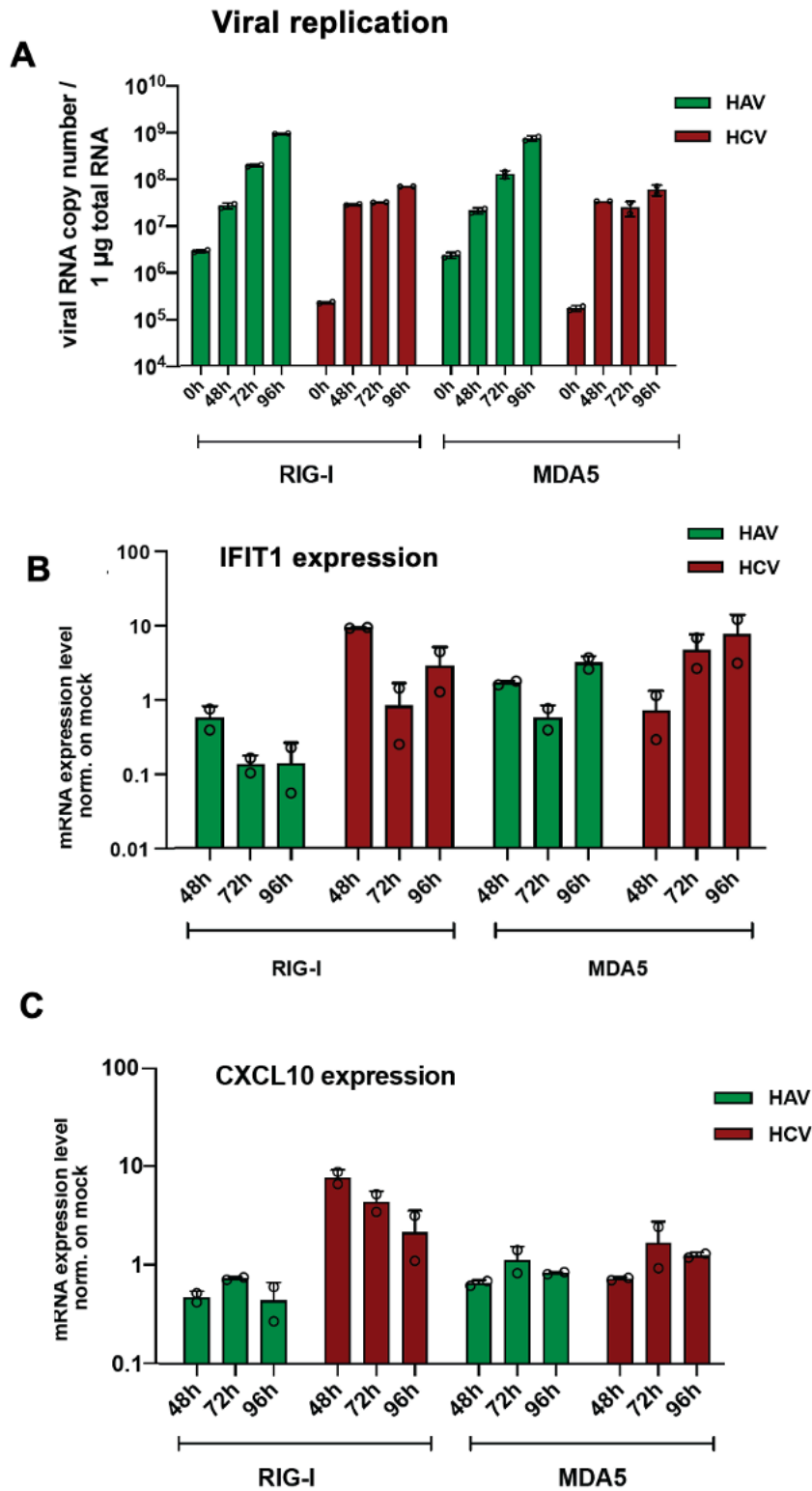


Figure 51. ISGs induction upon HAV or HCV infection in stable RIG-I and MDA5 cells.

Huh7.5 cells stably expressing RIG-I or MDA5 were infected with HAV (HM175/18f, green) or HCV (Jc1, red), respectively. At the indicated time points total RNA was isolated and viral RNA (A), IFIT1 mRNA (B), and CXCL10 mRNA (C), were quantified as indicated. IFIT and CXCL10 mRNA levels are normalized to GAPDH expression and shown as fold expression relative to uninfected cells. Shown values are mean values with SD from two biological duplicates.

For HAV, there was lack of induction in RIG-I cells and a moderate upregulation of IFIT1 in MDA5 overexpressing cells (Figure 51 A,B), while CXCL10 did not augment under any of the time points, despite robust replication (Figure 51C). The discrepancies between IFIT1 and CXCL10 upon HAV in MDA5 expressing cells hit my attention, and when I examined the raw Ct values in the RT qPCR analysis I realized that they could have originated from normalization artefacts. Nevertheless, given the difference in the window of induction when compared to HCV induction in TLR3 cells (Figures 20-21), my conclusion from the experiment was that either both HAV and HCV did not trigger RIG-I nor MDA5 in bulk or that, again, there could be counteraction of the pathways.

As in the case of TLR3, to investigate the functional relevance of MAVS cleavage my next step was examining the responsiveness to poly(I:C) while a replicating genome, with subsequently expression of viral proteases, was present in the cells. With Helen Huang in the context of her internship, I checked for the capacity of the HAV- or HCV subgenomic cell lines to react to titrating the amount of poly(I:C). Here, after having assessed even expression of the ectopically expressed PRRs (Figure 52B,D), I noted the striking phenotype of the MDA5 (Figure 52C) and RIG-I pathways, (Figure 52A) being fully abrogated in the HCV subgenomic replicon cell lines, which was well in line with the previously shown efficient MAVS degradation. For HAV, instead, responsiveness of the pathway was not impacted significantly if compared to mock cells (Figure 52A,C).

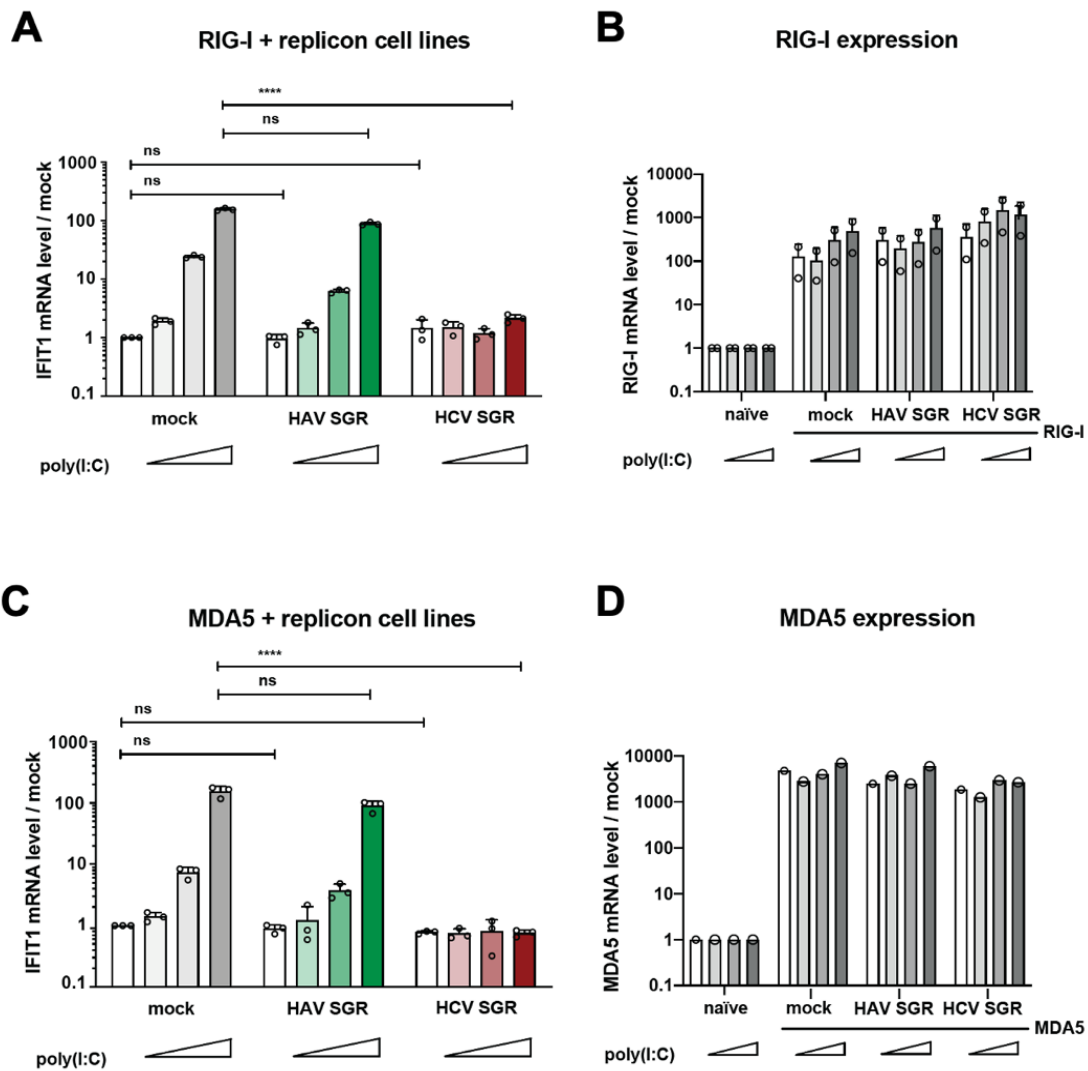


Figure 52. Functional counteraction to the RLR pathways in HAV and HCV subgenomic replicon cells.

Lentiviral vectors were used to stably express RIG-I (A) or MDA5 (C) in Huh7 cells harbouring subgenomic replicons (SGR) of HAV or HCV, or in naïve Huh7 cells (mock). After transduction, cells were selected and subsequently stimulated by transfection of increasing amounts of poly(I:C) (0.001 $\mu\text{g} / \text{ml}$; 0.01 $\mu\text{g} / \text{ml}$; 0.1 $\mu\text{g} / \text{ml}$). Six hours after transfection, total RNA was isolated, then IFIT1 mRNA was quantified by RT-qPCR and normalised to GAPDH expression (A, C). Data are shown as fold expression relative to untreated cells. All values shown are mean values with SD from independent experiments (n = 3). Successful reconstitution of PRRs expression was confirmed in one representative experiment with technical triplicates by RT-qPCR, and shown in B, D.

To gain more insight on the counteraction mechanisms at a single cell level, I infected RIG-I and MDA5 stable cell lines with HAV or HCV and detected IFIT1 upon poly(I:C) stimulation (Figure53,54).

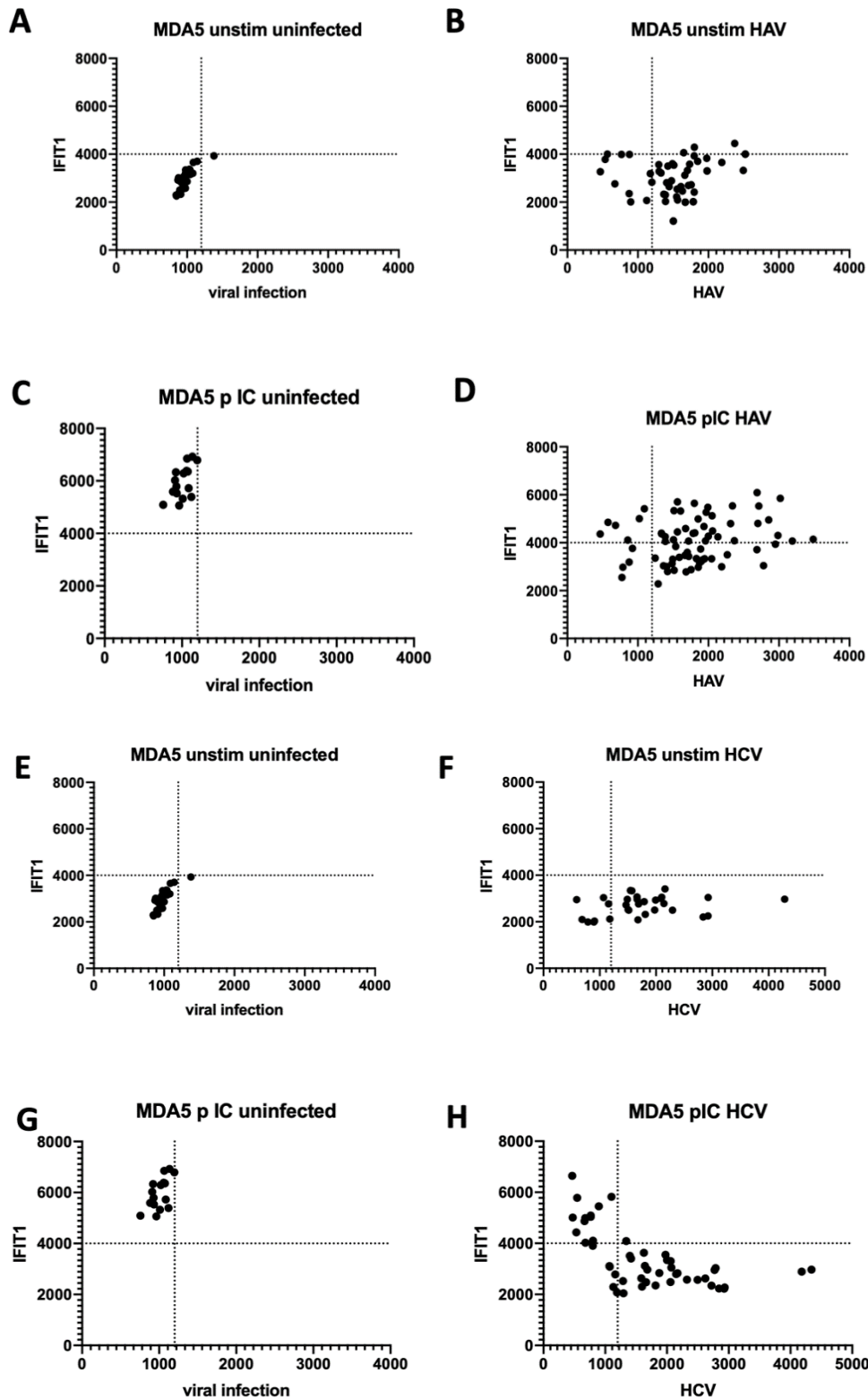


Figure 53. Functional counteraction to the MDA5 pathway by HAV and HCV at single-cell level through immunofluorescence analysis.

(A-H) Huh7.5 cells expressing MDA5 were infected with HCV or HAV. On day 3 and 4, respectively, post infection, cells were re-seeded onto coverslips and transfected with poly(I:C); 6 hours later cells were fixed and stained for viral antigen and IFIT1 (ISG) expression. (A) unstimulated cells (B) HAV infected cells, unstimulated (C) uninfected cells and poly(I:C) -stimulated (D) HAV infected cells stimulated with poly(I:C) (E) unstimulated

cells (F) poly(I:C) HCV infected cells, unstimulated (G) uninfected cells and poly(I:C) -stimulated (H) HCV infected cells stimulated with poly(I:C). Viral antigen and ISGs signals were measured using Fiji in $n \geq 30$ cells basing on IF acquisitions.

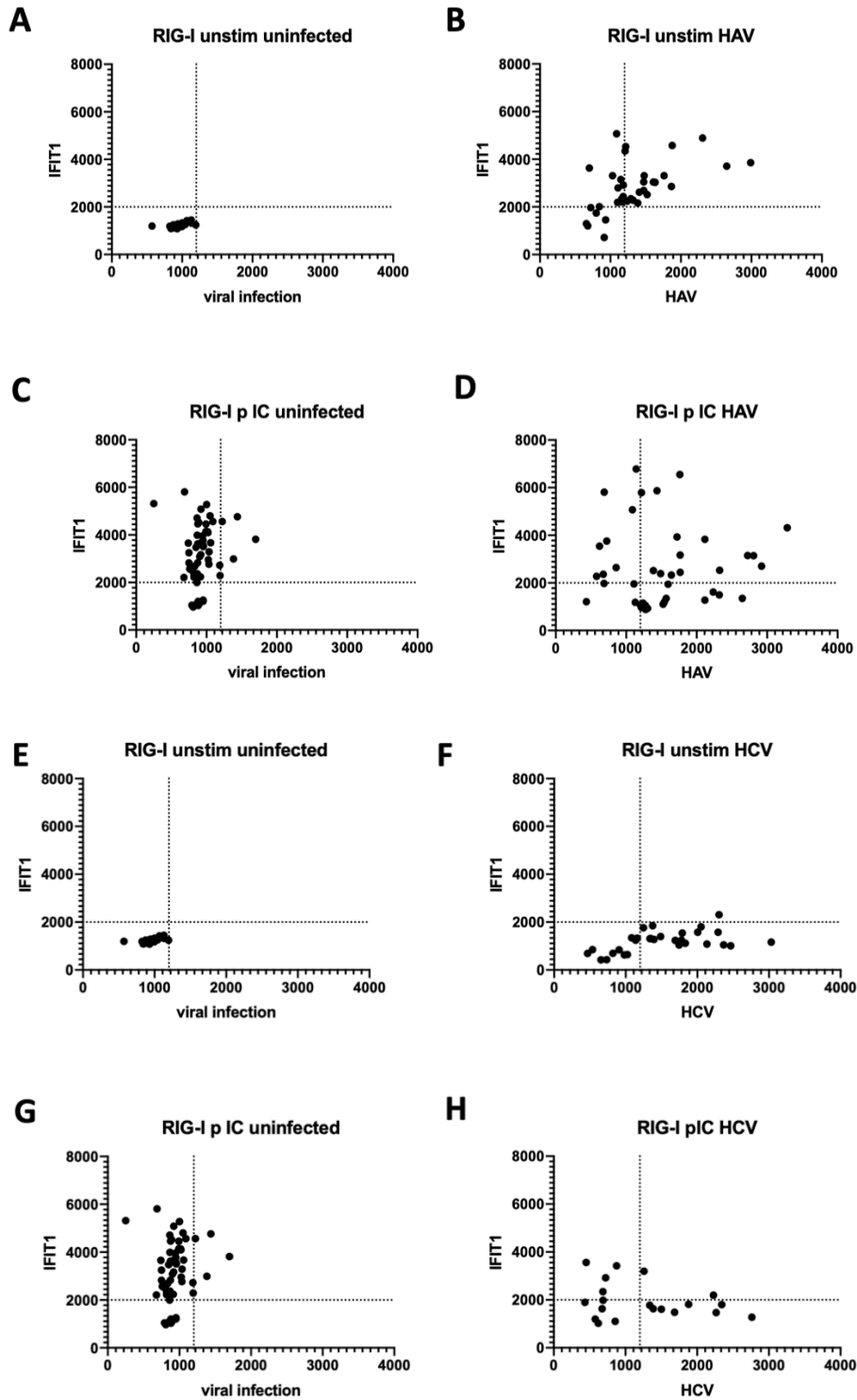


Figure 54. Functional counteraction to the RIG-I pathway by HAV and HCV at single-cell level through immunofluorescence analysis.

(A-H). Huh7.5 cells expressing RIG-I were infected with HCV or HAV. On day 3 and 4, respectively, post infection, cells were re-seeded onto coverslips and transfected with poly(I:C); 6 hours later cells were fixed and stained for viral antigen and IFIT1 (ISG) expression. (A) unstimulated cells (B) HAV infected cells, unstimulated (C) uninfected cells and poly(I:C) -stimulated (D) HAV infected cells stimulated with poly(I:C) (E) unstimulated cells (F) poly(I:C) HCV infected cells, unstimulated (G) uninfected cells and poly(I:C) -stimulated (H) HCV infected cells stimulated with poly(I:C). Viral antigen and ISGs signals were measured using Fiji in $n \geq 30$ cells basing on IF acquisitions.

As expected, all HCV infected cells showed a complete lack of ISG induction upon poly(I:C) stimulation (Figure 53H, 54H). Evaluation of unstimulated, infected cells also showed lack of IFIT1 signal, representing complete abrogation of both RIG-I and MDA5 induction (Figure 53F, 54F). But, for HAV, the cell populations in which the IFIT1 signal overcame the baseline threshold, showing activation upon poly(I:C), contained both uninfected and infected cells (Figure 53D, 54D), hinting again at a lack of strong counteraction by HAV 3ABC or other mechanisms for both RIG-I and MDA5. However, I encountered some technical problems: 1) Among the RIG-I cells upon HAV infection I found several activated cells, also where the viral antigen was low (Figure 54B). 2) the MDA5 cells showed a pre-activation state which rendered correct setting up of the baseline more challenging, and the window of IFIT1 increase upon poly(I:C) was smaller (Figure 54). For the first problem, I decided to move the approach focusing only on infected cells and quantifying their reactivity with Fiji, as done for TLR3. To investigate HAV in MDA5 cells, I decided to attempt a more sensitive approach, based on Fluorescence-Activated Cell Sorting (FACS) analysis (Figure 55).

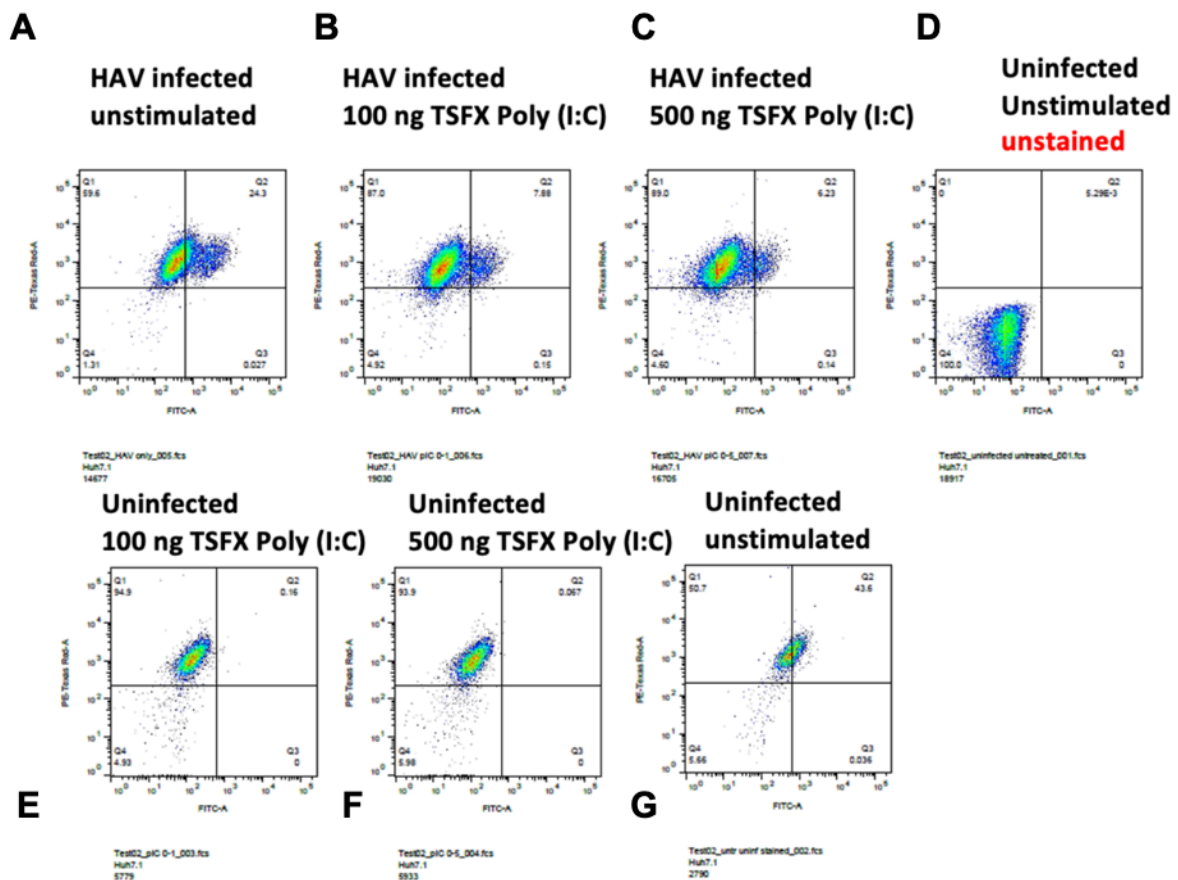


Figure 55. FACS analysis of HAV-mediated interference to MDA5 signaling pathway.

Huh 7.5 MDA5 cells were infected with HAV, reseeded onto coverslips 4 days post infection and subjected to poly(I:C) stimulation at the indicated amounts (B, C, E, F), or left unstimulated for ISGs staining control (A, D, G). Uninfected cells were included as control for viral antigen staining (E-G). 6 hours later, cells were fixed and stained with viral antigen- (HAV Vp3), along with ISGs- (Mx1) specific antibodies. A portion of unstimulated and uninfected cells were left unstained as control (panel D).

As for the IF single cell approach, I aimed at having different conditions based on absence or presence of viral infection / immunostimulant, and being able to quantify the small changes in reactivity to poly(I:C) upon HAV, which I titrated aiming at increasing the visible effect (Figure 55 B,C, E, F). However, here as well I encountered problems: in spite of a good amount of infected cell, and the possibility to discriminate the population, poly(I:C) stimulation did not give a visible outcome in the assay, since the sole antibody staining for Mx1 generated an artefact of pre-activation signal (Figure 55D). Therefore, unfortunately, this approach had to be set aside.

Nonetheless, increasing the poly(I:C) stimulation and focusing only on infected cells in the context of the single-cell IF analysis, I could quantify even in the slightly pre-activated MDA5 cells a sufficient window between mock and stimulated (Figure 56A-D). I could again detect no significant hindering of the pathways by HAV, as opposed as a full blockade by HCV (Figure 56A,B). Despite not significant, I could however detect that the Huh7.5 MDA5 HAV-infected cells had an apparently reduced IFIT1 activation upon poly(I:C). Given the partial cleavage of MAVS by me observed, and the several other HAV-mediated interference mechanisms discussed in literature, I could not entirely exclude that the virus was hindering the pathway. However, the facts that the HAV infected cells were often vacuolized and possibly less viable, together with anyways the vast presence of HAV infected cells which reacted to poly(I:C), and finally the comparison with the full abrogation given by HCV, suggested again that the counteraction might have been only moderate (Figure 56A,B).

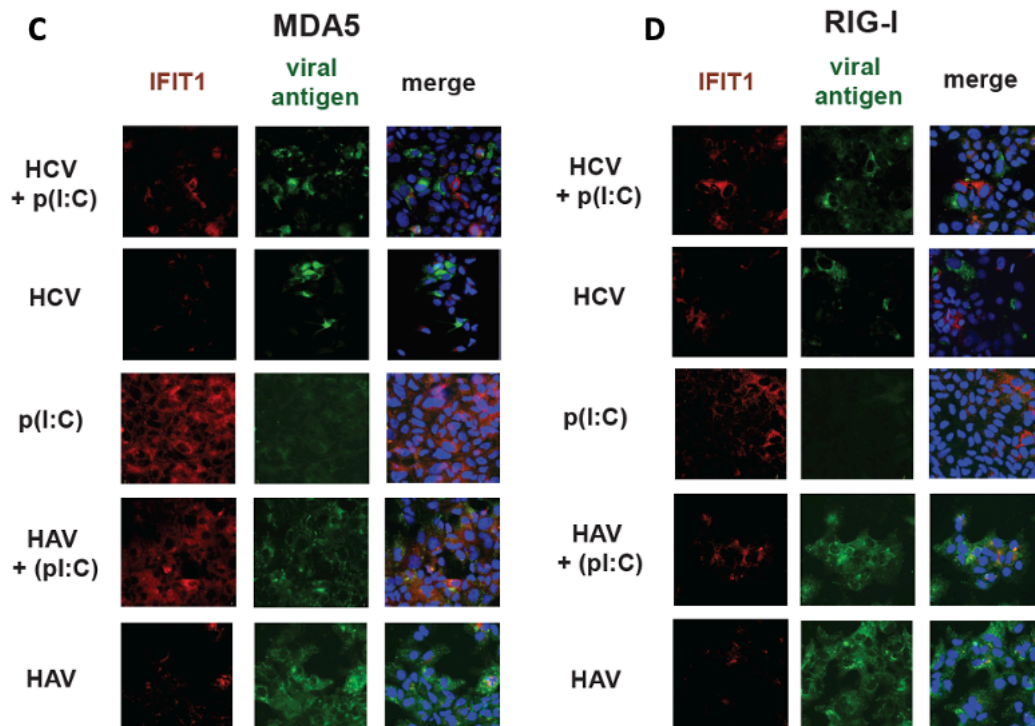
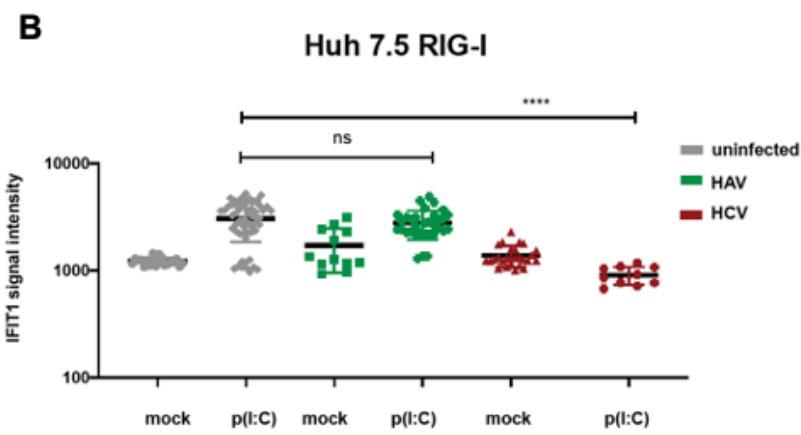
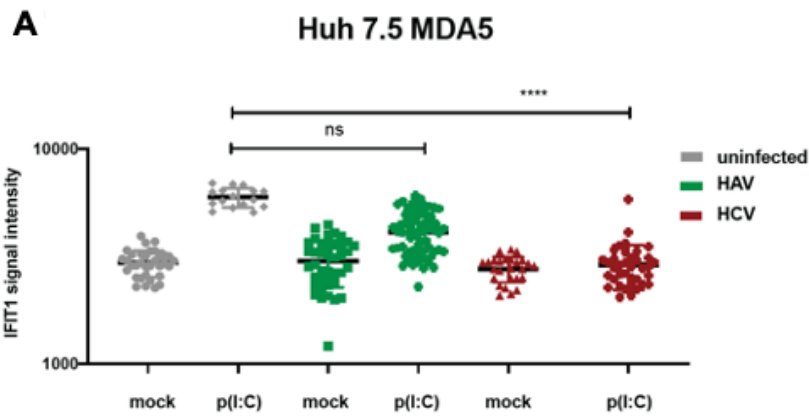


Figure 56. Quantification of RLR functional counteraction through analysis of single Huh7.5 MDA5 and RIG-I infected cells.

Huh7.5 cells stably expressing either RIG-I (E) or MDA5 (F), were infected with HAV HM175/18f, green or HCV (Jc1, red), respectively. Three days after infection, cells were seeded onto coverslips and transfected with 0.5 µg poly(I:C) or mock treated (unstim). Six hours after stimulation, cells were fixed and IF staining was performed using viral antigen- (HAV Vp3 or HCV NS5A) and IFIT1- specific antibodies. Signal intensity for virus and innate immune response was quantified using Fiji and displayed in dot plots, where each dot represents a single cell. Statistical analysis was performed using Welch's *t*-test to compare the innate immune response to poly(I:C) in HAV or HCV infected cells compared to uninfected cells (grey).

In summary, these data showed that the HAV protease 3CD and 3ABC cleave TRIF and MAVS incompletely, and that such cleavage does not suffice in abrogating TLR3 and RLRs pathways. Conversely, my results corroborated that HCV NS3-4A fully degrades MAVS, with consequent disruption of RIG-I and MDA5-mediated innate immune response, whereas no TRIF cleavage was detectable and TLR3 was still functional and induced upon HCV replication.

4.5 Redefining the model: immunocompetence and permissiveness in vitro

My results so far indicated a noticeable absence of interferon-stimulated genes (ISGs) in both Huh7 and Huh7.5 cells upon HAV replication, even when stably reconstituted with pattern recognition receptors (PRRs). While I encountered a few technical issues with MDA5 expression, which led to pre-activation in the cells, the observed phenotype remained consistent across various PRR-expressing cell lines, resembling what has been observed for HCV in cells expressing RLRs. However, in the latter case a striking distinction was observed: potent cleavage activity exerted by NS3-4A, resulting in complete degradation of MAVS. In contrast, the observed cleavage efficiency of HAV 3CD and 3ABC, even under conditions involving the highest and somewhat artificial levels of expressed protease, did not exceed 60%. Consequently, I maintained a degree of skepticism regarding the strong functional counteraction of 3CD and 3ABC claimed by others. Engaging in valuable discussions with colleagues, I began considering the possibility that Huh7 and Huh7.5 cells might exhibit deficiencies in innate immune responses associated with HAV detection. Therefore, I contemplated the utilization of alternative cell culture models that could potentially better mimic innate immune processes. In our lab some alternatives were already available: the immortalized liver-based PH5CH cell line, Upcyte© Human Hepatocytes (UHH)³³⁰, stem-cell derived hepatocyte-like-cells (HLCs), organoid-derived intestinal epithelial cells (IECs) and Primary Human Hepatocytes (PHH) from liver biopsies.

I started with a cell line which was by me used for parallel projects (see *Appendix*), PH5CH, a non-neoplastic human hepatocyte line immortalized with simian virus 40 large T antigen³³¹, in which conveniently all PRRs are expressed. PH5CH were a potentially good choice for their responsiveness through TLR3 and the RLRs, which according to RNAseq data generated for a parallel project (see *Appendix*) was the closest cell line, in terms of innate immune response, to PHH from liver biopsies. My aim, still, was to have an homogeneous cell culture model in which both HAV and HCV could replicate; considering that PH5CH lacked miR122, necessary for HCV replication³³², I decided to try concomitant transfection of viral RNA (Gt2a, JFH1) and miR122 RNA through electroporation. For HAV, instead, having so far obtained always stronger replication upon infection rather than RNA transfection, I infected the cells with HAV HM175/18f directly. For both approaches, unfortunately, there was complete lack of replication (Figure 57A,B) and concluded that PH5CH cells were not suitable for studying innate immune responses by HAV and HCV.

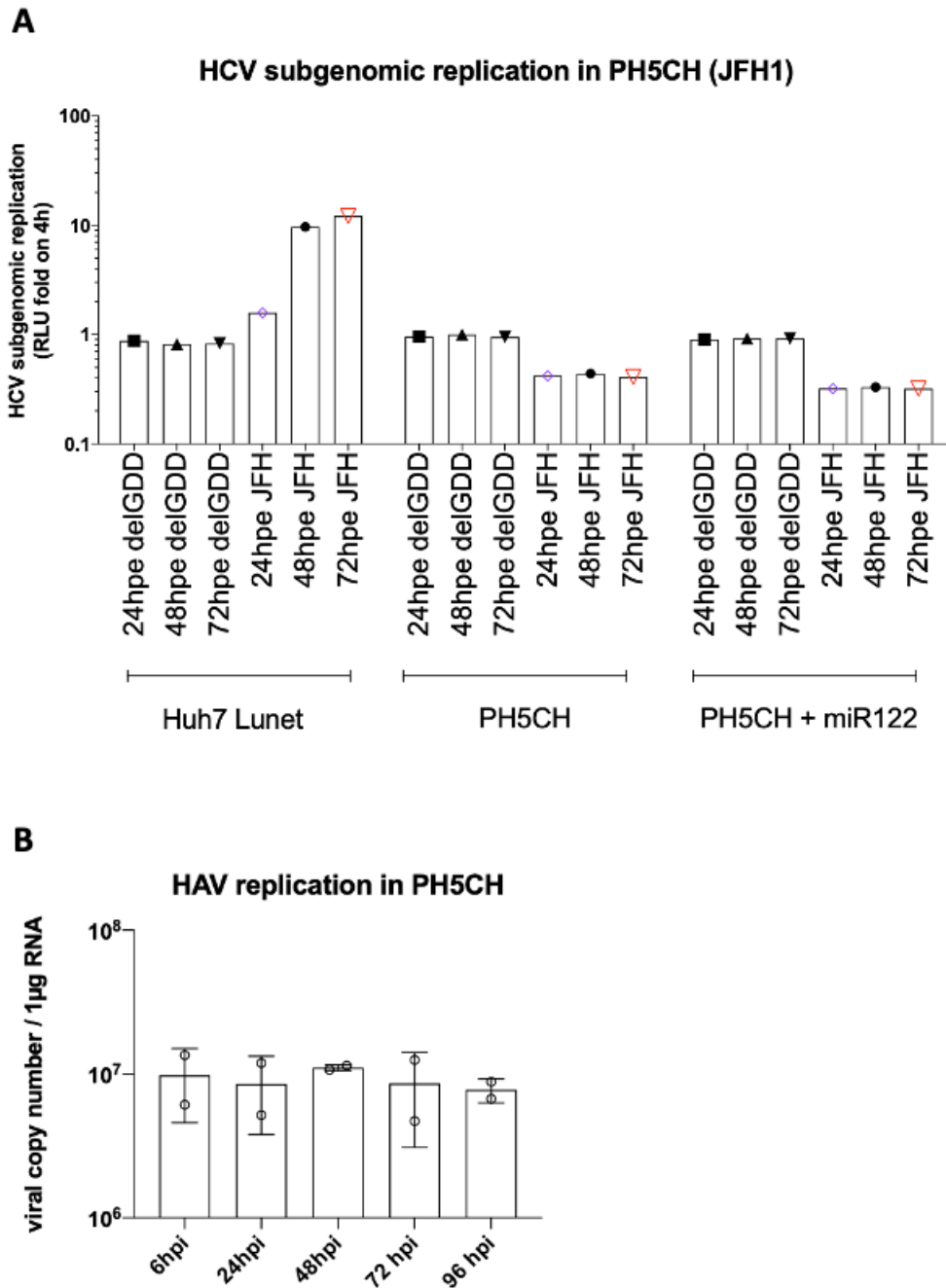


Figure 57. Attempts of HAV and HCV replication in PH5CH immortalized hepatocytes.

(A) Huh7 Lunet (left of the bar graph) and PH5CH cells (middle and right of the bar graph) were electroporated with HCV JFH1 subgenomic replicon, including the GDD replication dead. For PH5CH, co-electroporation of miR122 RNA was attempted. At the indicated time points, cells were harvested and subjected to luciferase assay. Values are indicated normalized on the input Relative Light Unit (RLU) value at 4 hours after electroporation. (B) PH5CH cells were infected with HAV HM175/18f. Cells were harvested at the indicated time points, RNAs were extracted and viral replication was measured through TaqMan RT qPCR. Values are indicated as absolute copy number values basing on a HAV RNA standard curve.

PHH are in principle the most physiological model to study infection of hepatotropic viruses and have been shown to be permissive for HCV^{68,83,239,268,333,334}. Therefore, I tried twice PHH infection only with HAV and once with both HAV and HCV in parallel. Besides the high

fluctuations, probably due to several conditions independent from the infection - the state of the liver, the success of the isolation, which in most cases cannot exclude immune cells³³⁴ and donor-to-donor differences – HAV HM175/18f was in average not able to replicate to the degree reached in Huh7 or Huh7.5 (note that the replication data are expressed in linear scale)(Figure 58A,C). However, interestingly, I observed an IFIT1 response for both donors starting at 24 hours post infection (hpi) for donor#2 (Figure 58C) and for donor#1 (Figure 58A) and, potentially, in donor #2 corresponding to a slight increase of replication (Figure 58C,D). Due to the lack of a specific inhibitor for HAV, which would have been an important control, these data remained hard to interpret.

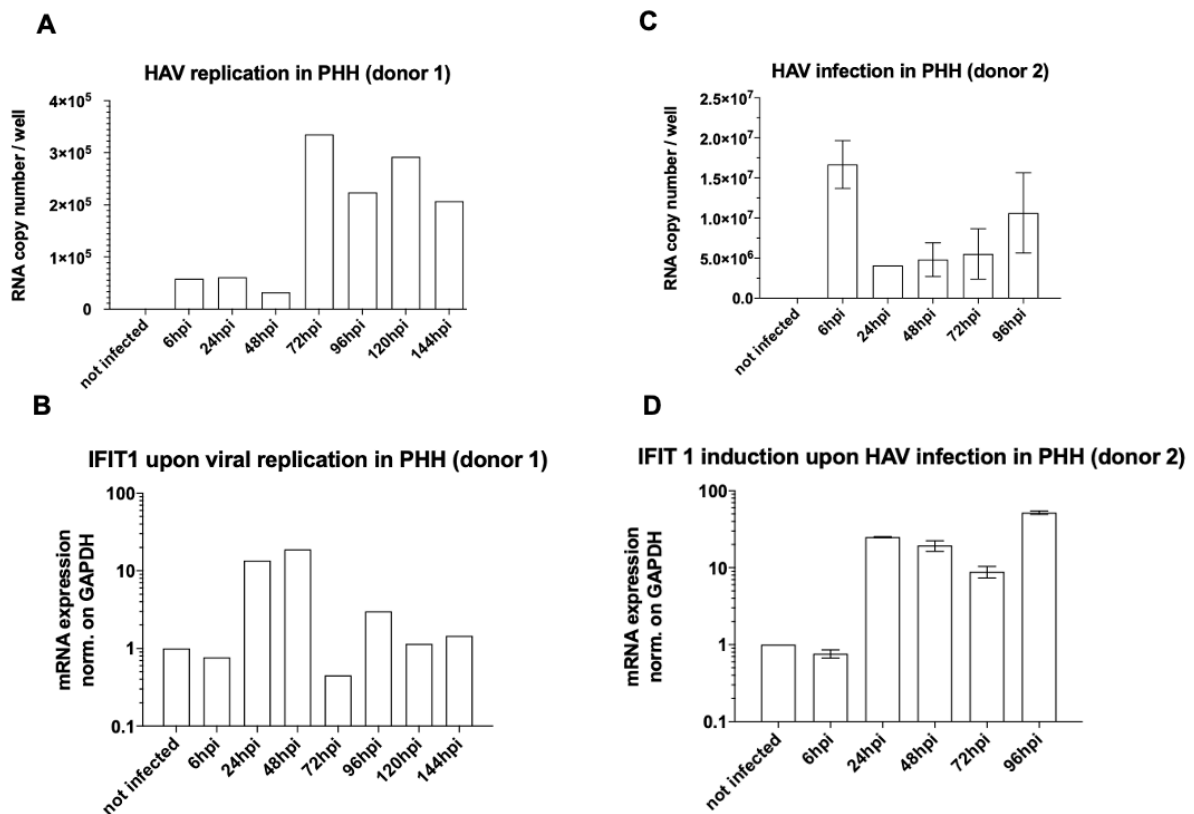


Figure 58. Infection attempts of PHH with HAV. (A-D) Primary Human Hepatocytes (PHHs) were infected with HAV HM175/18f.

At the indicated time points, cells were harvested, total RNA was extracted and viral copy number was assessed through TaqMan RT qPCR (A, C) along with IFIT1 mRNA expression through Sybr RT qPCR (B, D). IFIT1 data are shown as fold expression relative to uninfected cells relative to each time point.

After these attempts with cell-culture adapted HAV HM175/18f, I decided to try with some patient-derived isolate HAV samples. I monitored replication for 4 different patient isolates and detected increase of viral titer only in case of patient #3 (Figure 59).

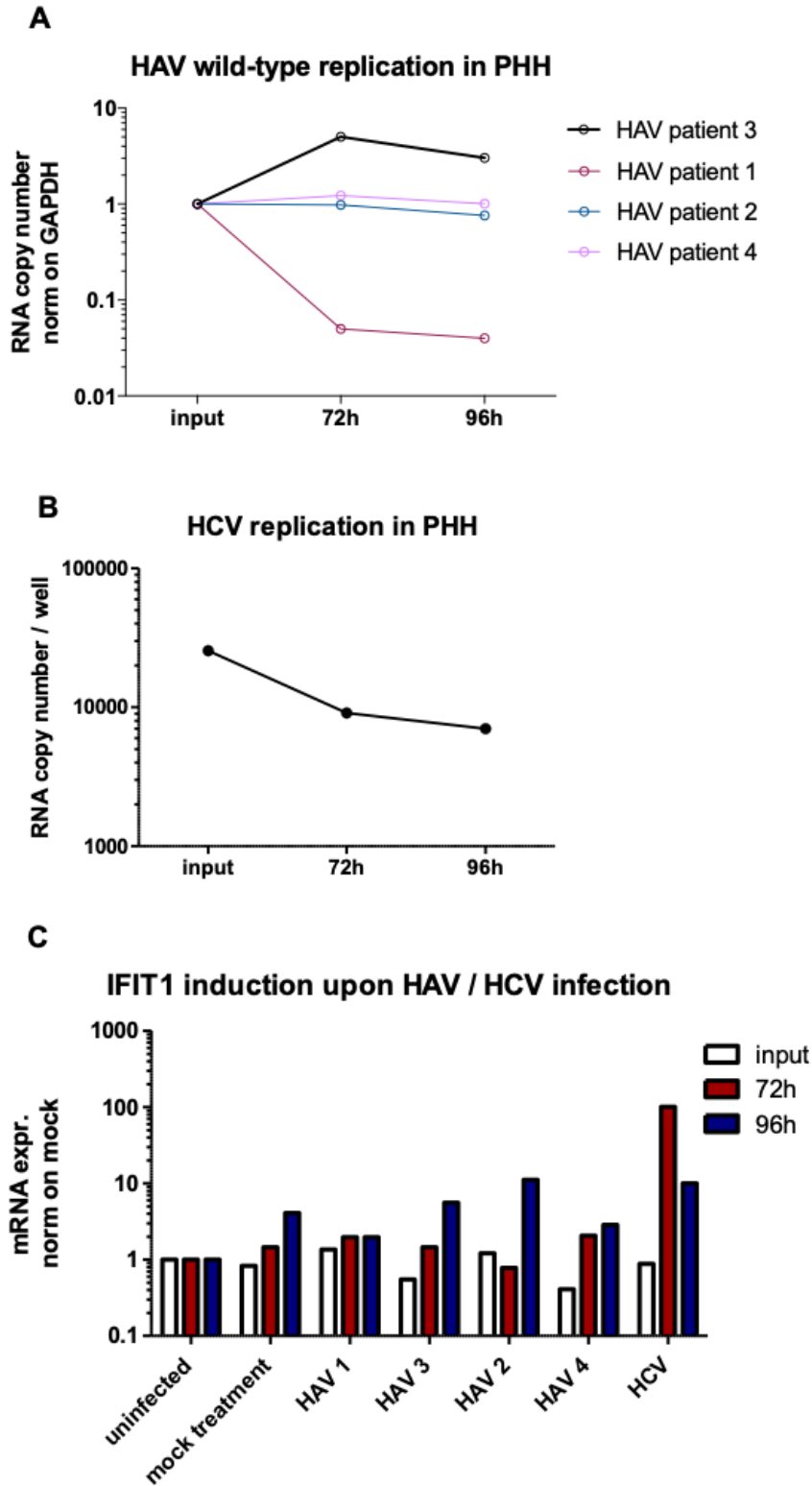


Figure 59. Innate immune response in PHH infected with HAV wild-type virus and HCV Jc1.

Primary Human Hepatocytes (PHHs) were infected with wild-type HAV isolates extracted from four patients' stool (#1, #2, #3, #4) and with HCV Jc1 (JFH1). At the indicated time points, viral titers and IFIT1 mRNA expression levels were measured via TaqMan and Sybr RT qPCR, respectively. IFIT1 data are shown as fold expression relative to uninfected cells relative to each time point.

Nevertheless, differently than for infection with HM175/18f, I could not detect any increase of IFIT1 of a degree significantly higher than the one in mock-treated cells (Figure59C). On the other hand, HCV (Gt2a, Jc1) could not replicate here as well (Figure 59B), but here IFIT1 was robustly increased at 72h (Figure59C), as seen in previous studies^{68,333,334}, suggesting that a strong innate immune response counteracts viral replication in this model.

For my next try in PHH, besides the HAV wild-type patient isolate #3, I decided to try again with the cell-culture adapted HM175/18f, including – besides the non-enveloped virus, termed “naked”, because released from lysed cells - the virus collected from the supernatant of the cells used for virus production as well, which should have acquired a pseudo-envelope through non-lytic release¹⁶⁹. HAV wild-type and HAV HM175/18f “naked” seemed to display a slight increase in viral RNA, while HM175/18f “enveloped” did not replicate (Figure60A). PHH were here infected with HCV Gt2a, Jc1, as well, which did not show an increase in viral RNA levels over time. Interestingly, I could again detect an HCV-specific IFIT1 induction, arguing for active replication, and, despite limited, I could also detect upregulation of IFIT1 upon wild-type HAV infection (Figure60B). To note, HCV activation of innate immune response occurred already at input (=3 hours post infection), hinting at possible extracellular vesicles-mediated secretion of immunostimulant dsRNA rather than replication⁸³.

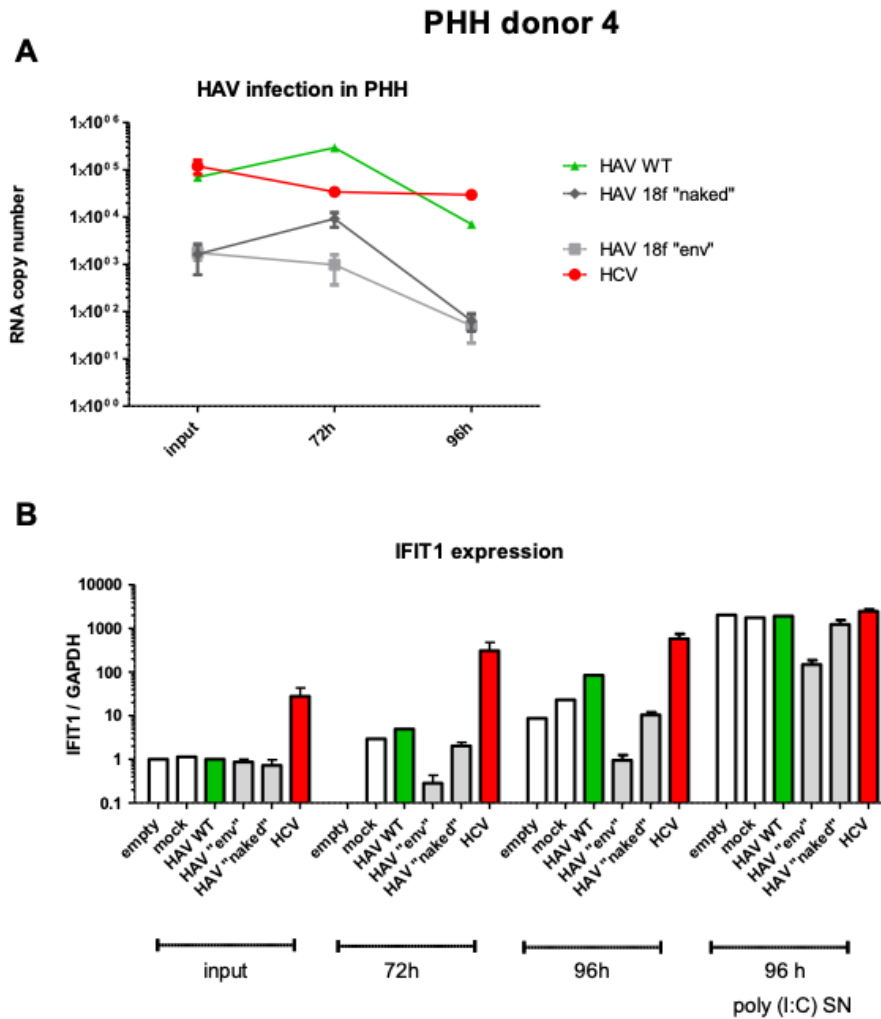


Figure 60. Innate immune response in PHH infected with HAV wild-type virus and HM175/18f “naked” and “enveloped” inoculums.

Primary Human Hepatocytes (PHHs) were infected with wild-type HAV isolate #3 extracted from a HAV-infected patient’s stool; HAV HM175/18f “naked” - obtained through lysis of cells used for viral production - or enveloped (“env”) – obtained through collection of the cells’ supernatant used for viral production; and HCV Jc1 (JFH1). At the indicated time points, viral titers and IFIT1 mRNA expression levels were measured via TaqMan and Sybr RT qPCR, respectively. IFIT1 data are shown as fold expression relative to uninfected cells relative to each time point.

I included a poly(I:C) treatment in presence of virus infection, in the attempt of highlighting the counteraction mechanisms confirmed by HCV towards the RLR pathways. However, the saturating dose of poly(I:C) likely covered any viral impact (Figure 60B).

PHH are generally a challenging model, due to high donor-to-donor differences and limited availability. Therefore, I searched for alternative models which would provide the physiological relevance of PHH with the possibility to be at hand. I had first the opportunity to work in Upcyte® Human Hepatocytes (UHH), primary cells driven into proliferation using a viral gene transfer system³³⁰. Given the pressing discrepancies I observed so far for HAV in my study (no innate immune response in Huh7 cells, but some in PHH) I focused on HAV replication using the cell culture adapted strain HM175/18f (Figure61A). Besides HAV

infection, I tested the cells for TLR3-mediated reactivity to poly(I:C). The cells seem to retain the immunological features of PHH⁸³, reacting to poly(I:C) administered through the supernatant (Figure 61B,C), but at the same time, they seemed to not support HAV replication (Figure 61A).

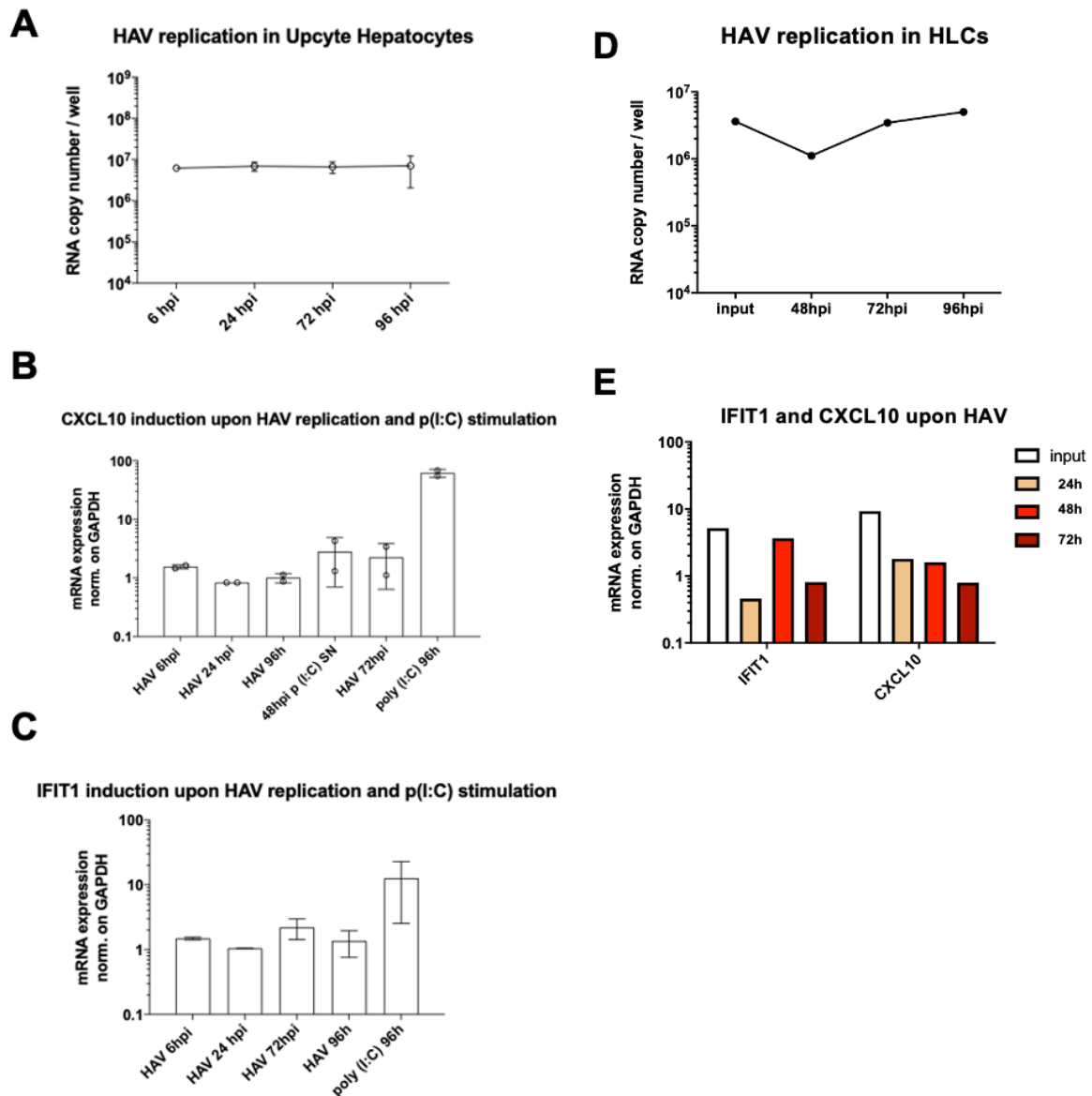


Figure 61. HAV HM175/18f infection of Upcyte® Hepatocytes and Hepatocyte-Like Cells (HLCs).

Upcyte® Hepatocytes (UH) were infected with HAV HM175/18f and Hepatocyte-Like Cells (HLCs) with HAV wild-type #3 extracted from a HAV-infected patient’s stool. At the indicated time points, viral RNA (A, D) and Innate immune response (B, C, E) were assessed through RT qPCR. UH cells were tested for responsiveness upon poly(I:C) at 48h and 96h for CXCL10 (B) and 96h for IFIT1 (C). IFIT1 and CXCL10 data are shown as fold expression relative to uninfected cells relative to each time point. Shown are mean values with SD from two biological duplicates in UH and singlicates in HLCs.

Unfortunately, upon testing of human embryonic or induced pluripotent stem cell (hESC/iPSC)-derived hepatocyte-like cells (“HLCs”)³³⁵, I found the same problem in HAV replication (Figure 61D). Here, the cells were poorly permissive for HAV HM175/18f (Figure

61E), despite having shown full responsiveness upon poly(I:C) stimulation towards all PRRs (Figure 62).

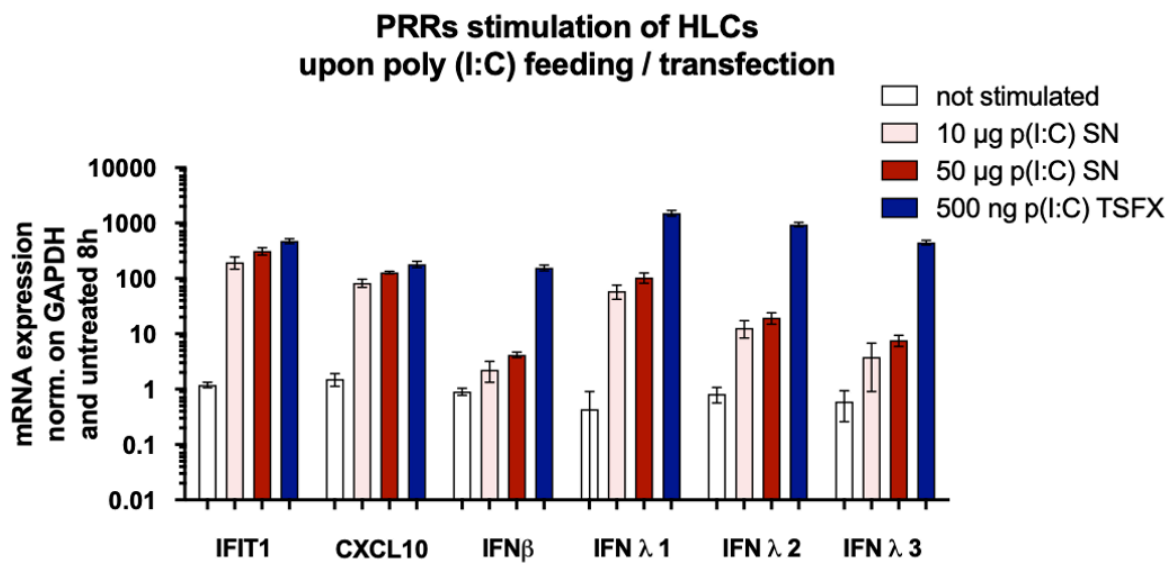


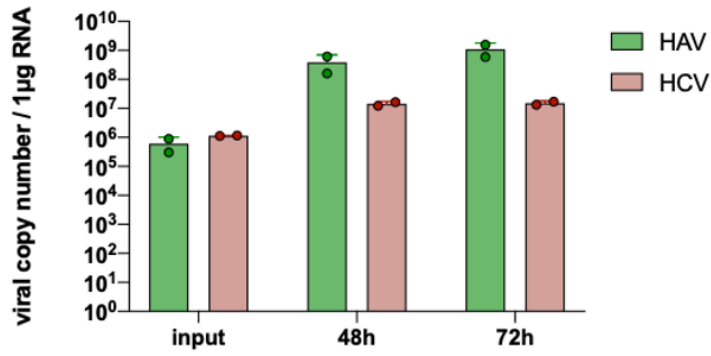
Figure 62. HAV HM175/18f infection of Upcyte® Hepatocytes and Hepatocyte-Like-Cells (HLCs).

Hepatocyte-Like Cells (HLCs) were tested for PRRs responsiveness with supernatant- and transfected-mediated poly(I:C) stimulation. Cells were seeded and fed or transfected for 6 hours; then, total RNA was extracted and mRNA expressions of the indicated target ISGs and IFNs was measured through RT qPCR. ISGs and IFNs data are shown as fold expression relative to GAPDH of untreated cells relative to each time point. Shown are mean values with SD from two biological duplicates.

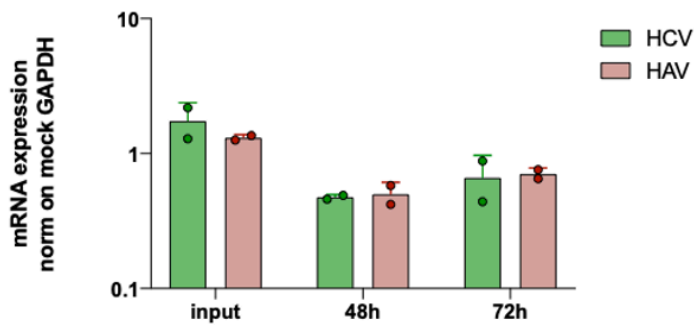
At this point, in line with previous research, I turned to the hepatoma cell lines Hep3B which had been established as effective proxies for primary human hepatocytes (PHH), owing to their endogenous PRR expression²⁶¹, willing to investigate their susceptibility to infection by Hepatitis A and C viruses.

A

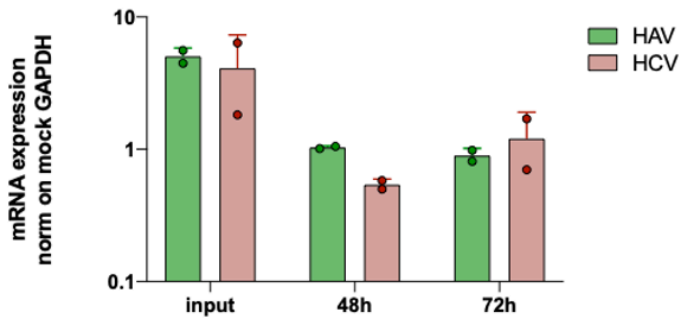
HAV / HCV replication in Hep3B miR122 CD81h

**B**

CXCL10

**C**

IFIT1

**D**

poly(I:C) stimulation in Hep3B

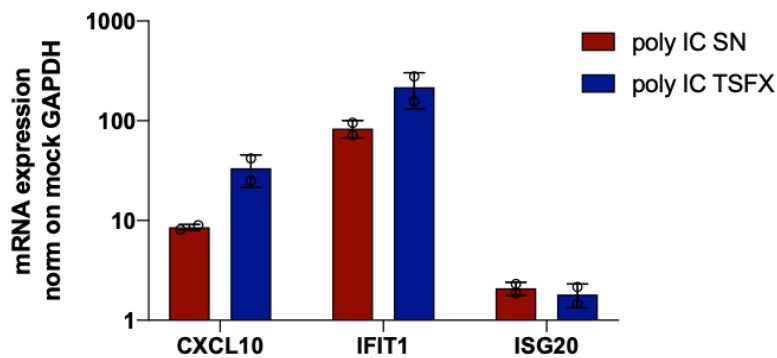


Figure 63. HAV and HCV infection of Hep3B cells.

Hep3B, stably reconstituted with lentiviral particles encoding for miR122 and CD81, were subjected to selection and expansion. Once ready, the cells were infected with HAV HM175/18f and HCV Jc1 (A-C) or tested for PRRs responsiveness with supernatant- and transfected-mediated poly(I:C) stimulation (D). At the indicated time points total RNA was isolated and CXCL10 / IFIT1 mRNA (C), along with viral RNA (B), were quantified via qPCR. ISGs data are shown as fold expression relative to GAPDH of untreated cells relative to each time point. Shown are mean values with SD from two biological duplicates.

Initially, I focused on Hep3B cells, in which I restored miR122 expression through lentiviral transduction, and subsequently selected stable cell lines (Figure63). These Hep3B cells with miR122 demonstrated moderate permissiveness for HCV, supporting replication levels approximately 1 log higher than the input RNA. Notably, the Hep3B cells exhibited a higher susceptibility to HAV infection (Figure63A).

However, upon assessing the innate immune response via quantitative PCR, I observed no upregulation of interferon-stimulated genes (ISGs) (Figure 63B,C). This led me believing that I was once again dealing with an immune-deficient cell line and therefore I checked Hep3B cells for PRRs responsiveness with supernatant feeding- or transfection-based poly(I:C) stimulation (Figure 63D). Both TLR3 and RLRs seemed to be upregulated in the context of IFIT1 but, surprisingly, the breadth of CXCL10's induction, typically one to two log higher than IFIT1 in my previous findings (Figure 20), was here lower. As CXCL10 mediates the downstream signaling of both IRF3 and NFkB pathways, this finding might hint at a reduced NFkB-mediated sensitivity, which would need further assessment. Furthermore, seeing that the supernatant TLR3-specific stimulation upregulated IFIT1 to a high degree, I also tested ISG20, which came up through RNAseq analysis in a parallel project aiming at determining possible candidates to attribute to a TLR3-specific gene signature (see *Appendix*). However, this gene did not result upregulated at all, highlighting once again how different cell lines might present phenotypes not reproducible in others (Figure 63, C).

After observing the upregulation of ISGs in HAV-infected PHH, but neither in Huh7 cells with reconstituted dsRNA receptors, nor in Hep3B, I hypothesized that some of the hepatoma-based cells might have a defect in sensing HAV specifically. It has been reported that LGP2 is a crucial co-factor for MDA5 in triggering an IFN response^{52,336,337}, and MDA5 seemed to be the primary sensor for HAV in a recent study⁶⁵. Therefore, I compared LGP2 mRNA expression levels in liver-based cell lines through RT qPCR and found that Huh7.5 cells lacked LGP2 expression entirely (Figure64A), differently than HepG2 or HepaRG (Figure64A).

The quest for a liver-based cell line that could clarify whether HAV replication would give rise to ISGs, like it seemed to happen in PHH despite hindered replication, reached a turn when I tried HepG2 cells, a model of hepatoblastoma³³⁸ which was also very recently shown to be permissive for HAV by another group⁶⁵, and HepaRG³³⁹ cells, taking advantage of a collaboration with Dr. Nadine Gillich who generated a panel of different KO variants of this cell line³³⁷.

HepG2 cells were more permissive to HAV compared to HepaRG cells, but both cell lines exhibited a clear upregulation of IFIT1 upon HAV infection (Figure 64B,C). However, HepaRG was shown before not to be permissive for HCV, and HepG2 cells, even after restoring miR122 and CD81 expression²⁷², did not support HCV replication either (Figure 65), therefore, I could not compare the HAV data to HCV infection.

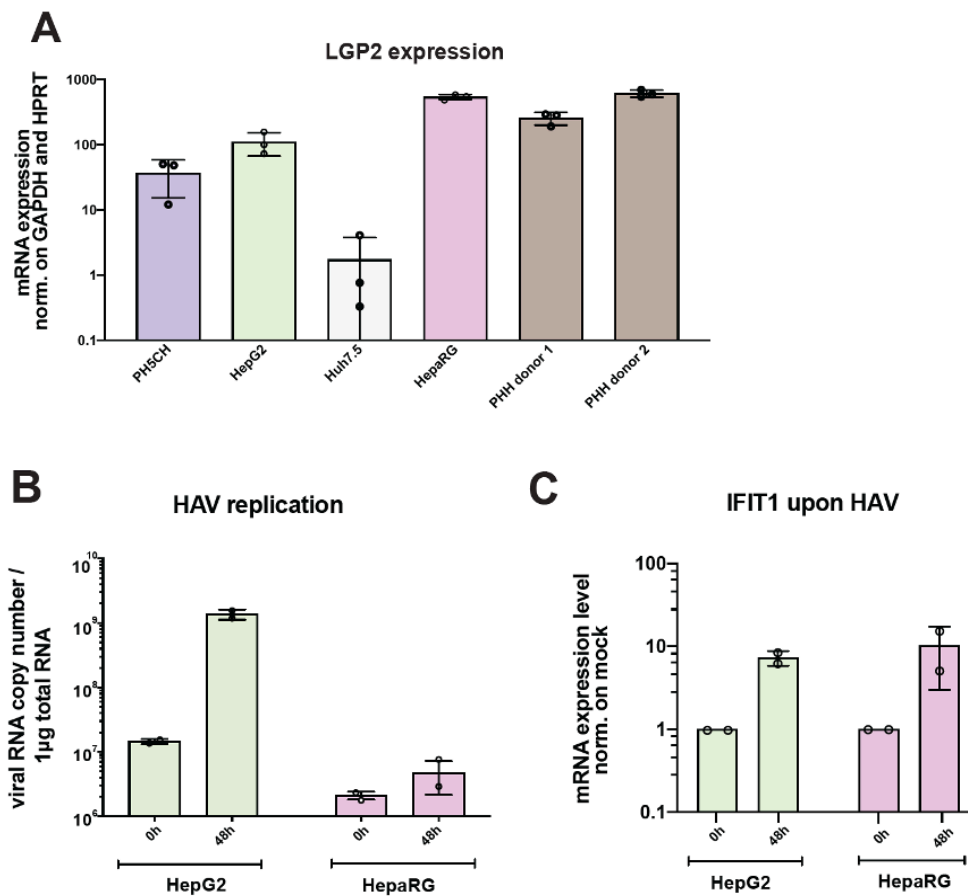


Figure 64. HAV infection of HepG2 and HepaRG cells.

(A) Total RNA was isolated from four different hepatocyte cell lines (PH5CH, HepG2, Huh7.5, and HepaRG) and Primary Human Hepatocytes (PHH) derived from two different donors. LGP2 mRNA levels were quantified by RT qPCR and normalized to GAPDH and HPRT expression. (B) HepG2 and HepaRG cells were infected with HAV HM175/18f. At the indicated time points total RNA was isolated and IFIT1 mRNA (C), and viral RNA (B), were quantified. IFIT1 mRNA levels are shown normalized to GAPDH expression relative to timepoint 0. (D-F) HepaRG cell pools with knockout for LGP2, or mock, were infected with HAV HM175/18f. CXCL10 (D) and IFIT1 (E) mRNA were quantified at the indicated time points, as well as viral RNA (F). IFIT1 and CXCL10 mRNA expression levels were normalized to GAPDH expression relative to infected cells at timepoint 0. All values shown are mean values with SD from biological duplicates.

The used cell line was the same subclone obtained from the laboratory which reported HCV productive infection of HepG2 and had reconstituted expression of miR122 and CD81²⁷². I then tried again, infected the cells with HCV Jc1, but after 72h could not detect any upregulation in neither HCV RNA (Figure65A) nor innate immune response (Figure 65B) – despite avoiding to reconstitute the cells with TLR3, in the hope to keep the immune restriction to a minimum.

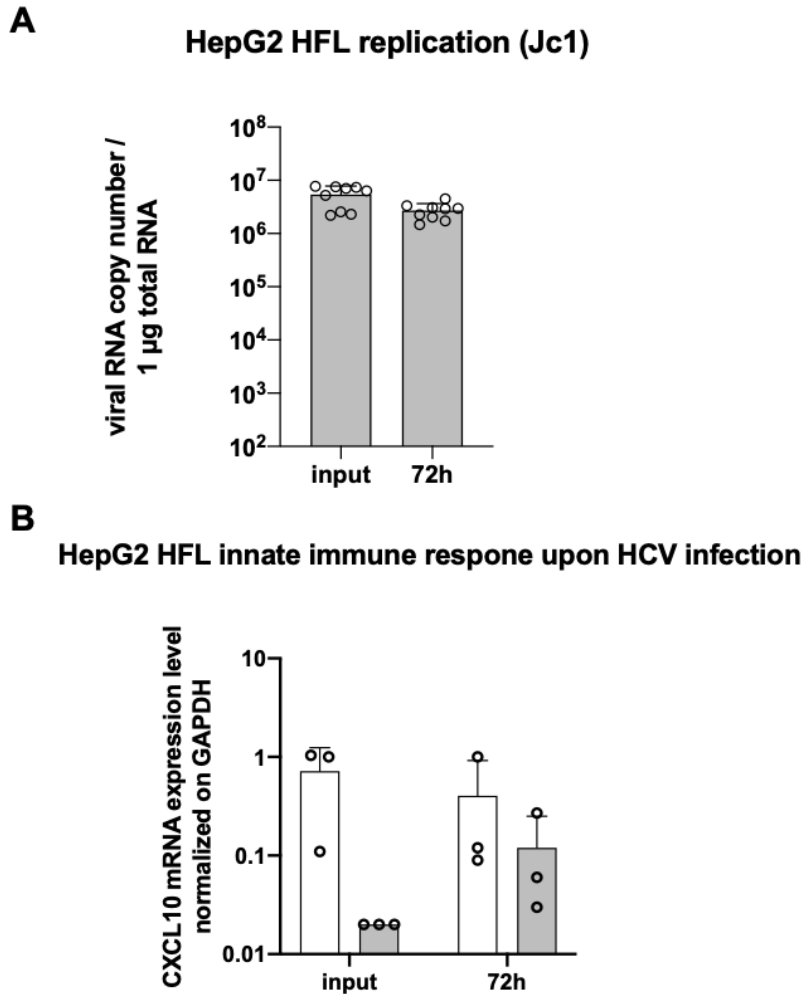


Figure 65. Attempt of HCV infection in HepG2 miR122 CD81h cells (HepG2 HFL).

HepG2 HFL were infected with HCV Jc1 (grey bars) or left untreated (white bars). At the indicated time point total RNA was isolated and CXCL10 mRNA (C), along with viral RNA (B), were quantified through RT qPCR. CXCL10 mRNA levels are shown normalized to GAPDH expression relative to timepoint 0.

In addition, I attempted Jc1 infection increasing the MOI from 1 to 3.5 and under centrifugal incubation of the viral inoculum (*spinoculation*) to increase viral entry³⁴⁰ (Figure 66). I sought at detecting RANTES (Figure 66B) in place of IFIT1 and CXCL10, since it was demonstrated to be upregulated by HCV in exactly this model^{272,273}. In addition, I included HAV infection on the same cell line, to ensure that permissivity and innate immune response were being kept similarly as with HepG2 naïve cells, previously used (Figure 66A). Upon mRNA levels measurement, I could again confirm the predicted ISGs upregulation by HAV replication, even if limited (Figure 66A,B in green), but in the case of HCV the cells did not show any permissivity or response (Figure 66A,B in red).

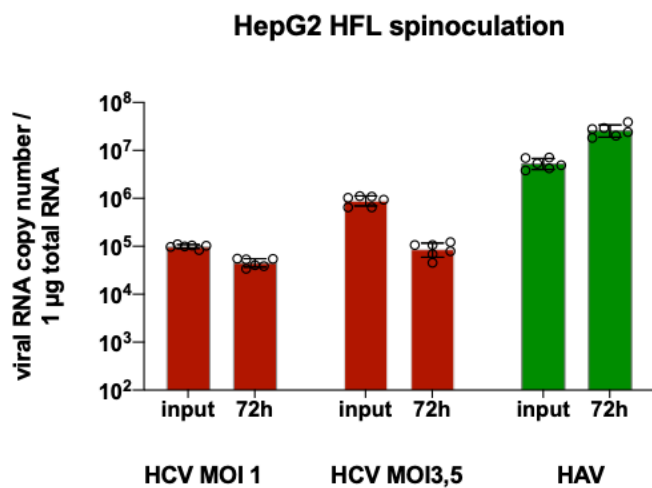
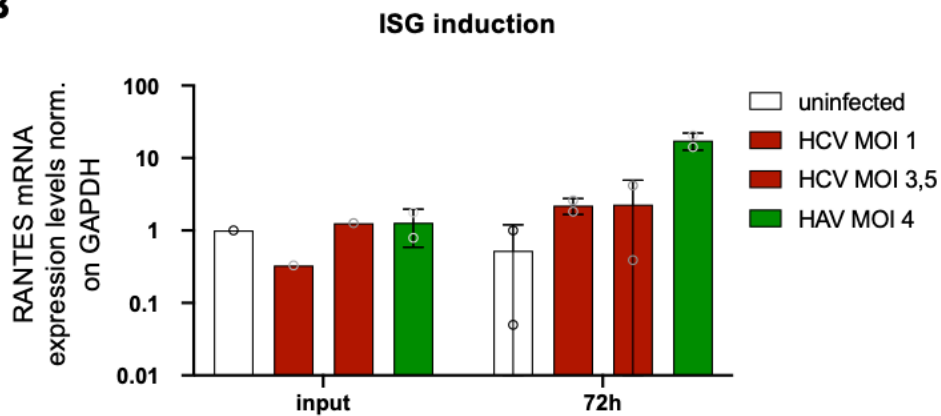
A**B**

Figure 66. Attempt of HCV spinoculation infection in HepG2 miR122 CD81h cells (HepG2 HFL).

HepG2 HFL were infected with HAV HM175/18f and HCV Jc1 at different MOIs. The seeded cells with viral inoculums were subjected to 2 hours centrifugation at 1000 g (spinoculation) to favour viral entry. At the indicated time points total RNA was isolated and RANTES mRNA (C), along with viral RNA (B), were quantified. RANTES mRNA levels are shown normalized to GAPDH expression relative to input time point.

Turning again to HAV, whose replication was instead well supported by HepG2 and HepaRG cells, as proof of concept for the lack of LGP2 in Huh7 cells I tried to rescue the phenotype, stably reconstituting LGP2 expression in Huh7.5 MDA5 cells (Figure 67A) which indeed resulted in increased ISG induction (Figure 67C) upon HAV replication (Figure 67B). However, this reconstitution also led to higher baseline ISG expression in the absence of HAV replication, making it challenging to interpret the data (Figure 67C).

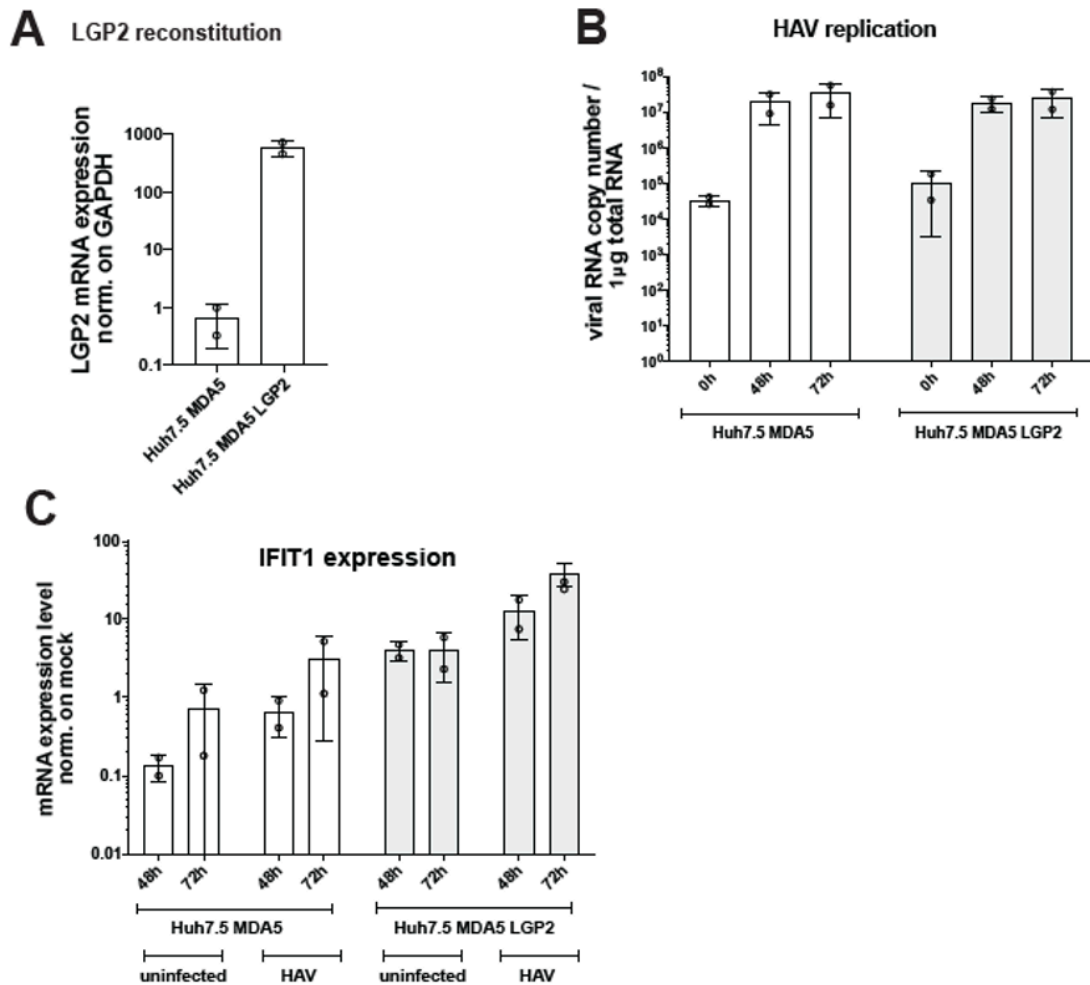


Figure 67. Reconstitution of LGP2 in Huh7.5 MDA5 in the attempt of restoring innate immunity to HAV.

(A) Huh7.5 cells stably expressing MDA5 were transduced with lentiviral vectors encoding LGP2. After selection and passaging, total RNA was isolated from the cells and LGP2 mRNA levels were measured via RT qPCR and normalized to GAPDH expression. Data are shown as fold expression relative to Huh7.5 MDA5 cells without reconstituted LGP2. (B, C) Huh7.5 MDA5 cells, empty or stably expressing LGP2, were infected with HAV HM175/18f using a MOI of 4. At the indicated time points total RNA was isolated and viral RNA (B) along with IFIT1 mRNA expression levels (C) were measured. IFIT1 mRNA levels are shown as fold expression relative to uninfected MDA5 cells without reconstituted LGP2. All values shown are mean values with SD from biological duplicates.

Overall, HepG2 at this point appeared to be the most suitable model to study HAV innate immune response, combining robust viral replication and ISG induction. Since HepG2 cells expressed very low levels of TLR3, I expressed TLR3 ectopically, to study potential sensing of HAV (Figure 68A,B) and tested it functionally with a poly(I:C) TLR3-specific supernatant inhibitory treatment with subsequent inhibitory treatment through Bafilomycin A treatment (Figure 68A). Interestingly, I observed similar levels of IFIT1 induction upon HAV replication with or without TLR3, suggesting a limited role of TLR3 in HAV sensing (Figure 68C,D). Subsequently, I generated knock-out (KO) pools of RIG-I or MDA5 in the HepG2 TLR3 cells (Figure 69). When robust HAV replication occurred (Figure 69A,B), I found that MDA5 was

the only PRR involved in detecting HAV (Figure 69C), since the absence of RIG-I expression did not affect IFIT1 induction (Figure 69D).

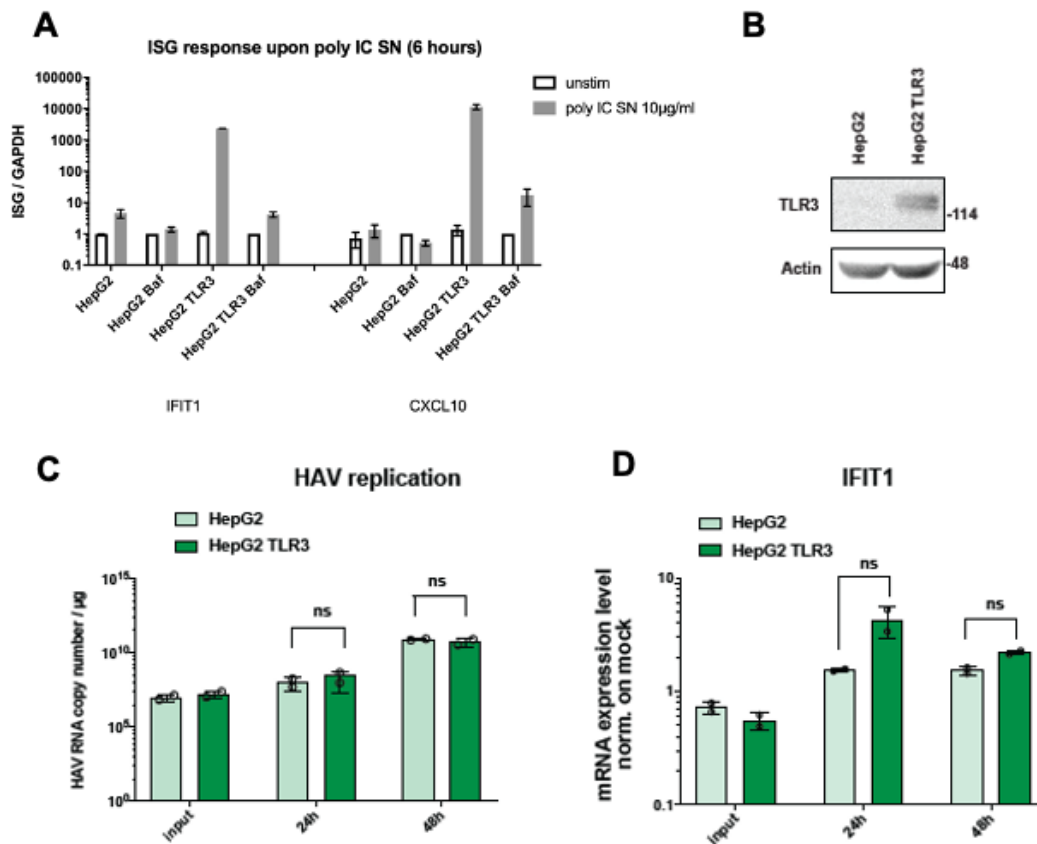


Figure 68. Assessment of the sensing PRR for HAV in HepG2 cells.

(A-D) HepG2 cells were transduced with a lentiviral vector encoding TLR3. After selection and passaging, cells were subjected to poly(I:C) supernatant feeding to exclusively address the TLR3 pathway for 6 hours, including Bafilomycin A treatment as a negative control for the TLR3-specific stimulation. Total RNA was extracted and ISGs mRNA expression levels were assessed through RT qPCR (A). (B) 10 µg of protein lysate were separated by SDS-PAGE and subjected to immunoblotting, using specific antibodies against TLR3 and b-actin (Actin), as indicated. (C-D) HepG2 and HepG2 stable TLR3 cells were infected with HAV HM175/18f for the indicated times. Cells were harvested and total RNA was isolated; viral RNA was measured through TaqMan qPCR (C) and IFIT1 mRNA expression levels were measured by Sybr RT-qPCR. (D). IFIT1 mRNA levels are shown normalized to GAPDH expression. Data are shown as fold expression relative to uninfected cells. All values shown are mean values with SD from biological duplicates (n = 2).

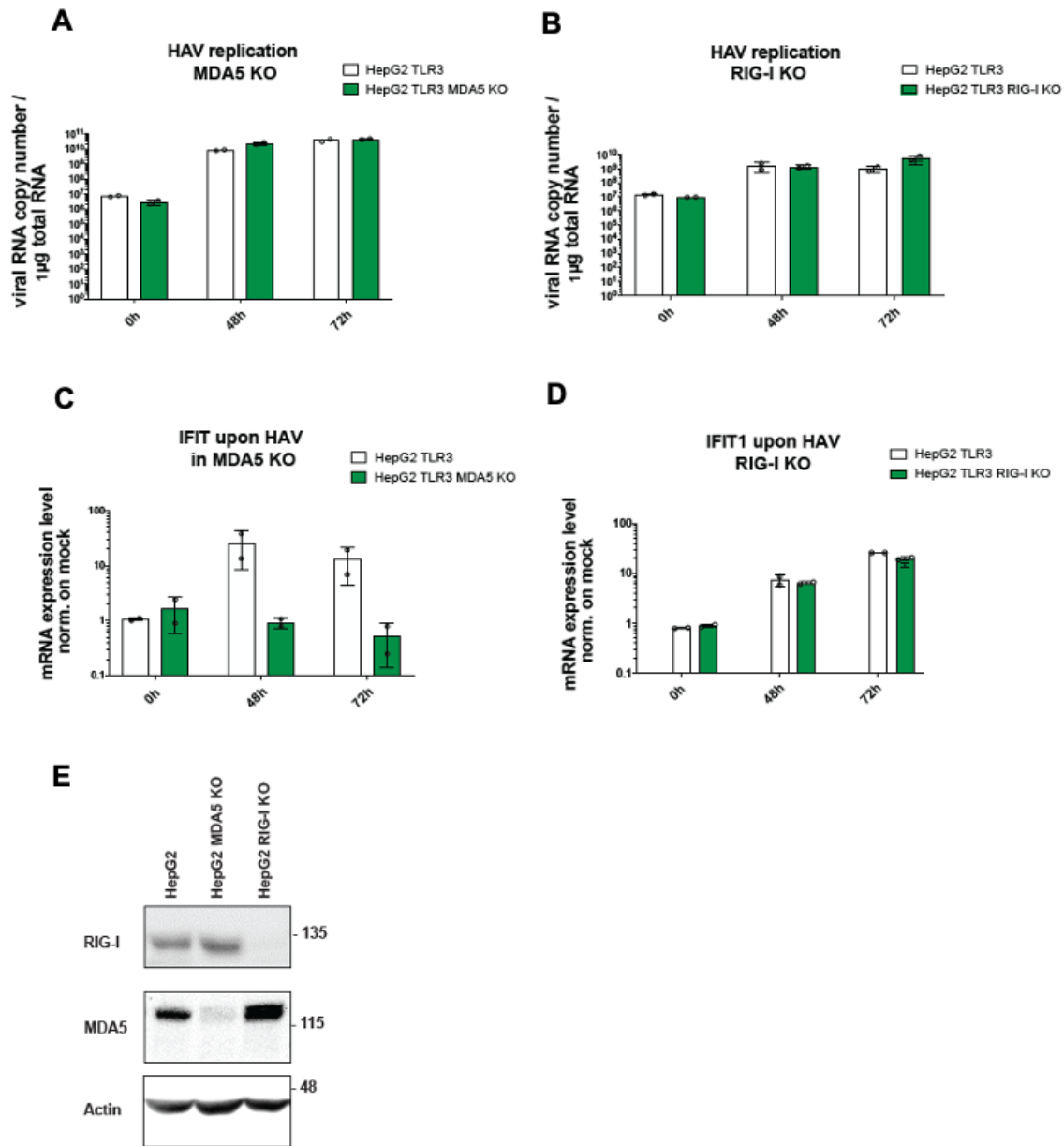


Figure 69. Assessment of the sensing PRR for HAV in HepG2 cells.

(A-D) HepG2 TLR3 cell pools with knockout (KO) of MDA5 (A, C) or RIG-I (B, D), respectively, were infected with HAV and analyzed for IFIT1 mRNA (C, D) and viral RNA (A, B), at the indicated time points. IFIT1 mRNA levels were normalized to GAPDH expression and shown as fold expression relative to uninfected cells. All values shown are mean values with SD from biological replicates (n = 2). (E) HepG2 cells and cell pools with knockout (KO) of RIG-I or MDA5 were analyzed by immunoblotting, using specific antibodies against RIG-I, MDA5 and b-actin (Actin), as indicated.

To then match the phenotype with the role of LGP2, I focused on HepaRG LGP2 KO pool generated by Gillich et al.³³⁷ and infected it with HAV, resulting in similar levels of replication (Figure 70C), but in a significant reduction in CXCL10 (Figure 70A) and IFIT1 (Figure 70B) induction.

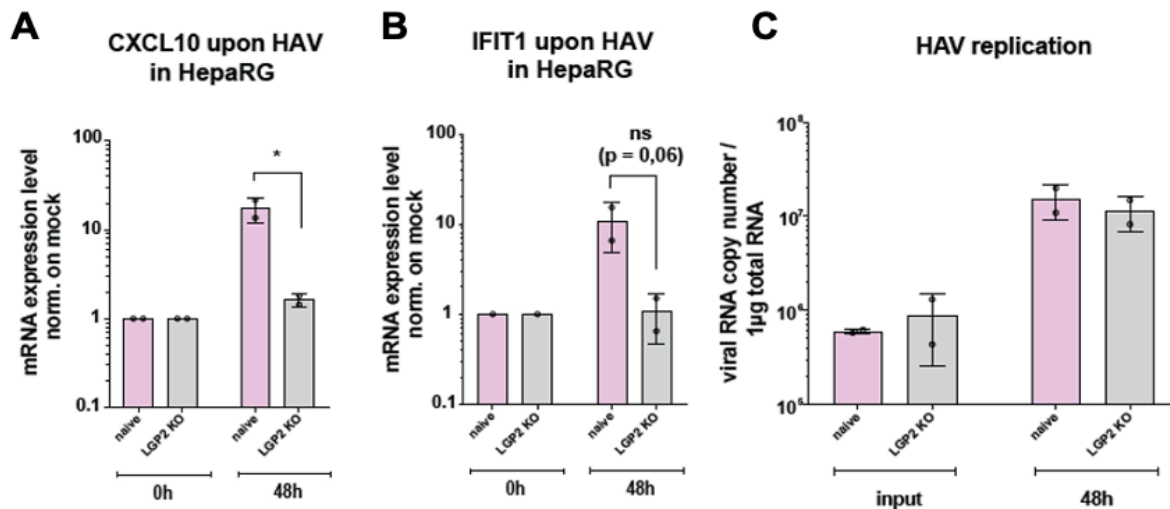


Figure 70. Assessment of the sensing PRR for HAV in HepG2 cells.

(A) (D) HepG2 LGP2 KO cells were generated through LentiCRISPR- mediated transduction and further selection, and infected with HAV. At the indicated time points, RNA was extracted and ISGs (A,B) along with viral RNA (C) were measured through RT qPCR. ISGs values are normalized relative to GAPDH values of uninfected cells. Shown are mean values of two biological replicates.

Hence, knowing from previous research that HepaRG are not permissive for HCV, I shifted my attention to HepG2 cells in attempting HCV infection, as previous reports had indicated their propensity for HCV replication upon expression of miR122 and CD81^{272,273}.

In conclusion, my findings in these three chapters suggest that HAV triggers an innate immune response in human hepatocytes *in vitro*, using permissive models with intact signaling pathways. MDA5 was responsible for sensing HAV replication and LGP2 expression was essential for this process. Despite HAV's moderate proteolytic activity towards MAVS, sensing of HAV was not abolished in HepG2 and HepaRG cells.

Additionally, I determined that HAV sensing did not occur through TLR3, raising questions about the functional significance of partial TRIF cleavage. For HCV, I could not obtain side-by-side information because of lack of a consistent model which would support HAV replication as well.

All of the above pressingly suggested moving to more relevant models, in the hope of clarifying the question, why HAV did not induce an innate immune response in chimpanzees, but in HepG2 and HepaRG cells.

4.6 Moving the perspective towards a small *in vivo* model : Alb/uPa SCID mice with humanized livers

At this point, I reached out for a collaboration with the Meuleman group from the University of Ghent, to address the innate immune response to HAV and HCV *in vivo*, using SCID Alb/uPA mice with humanized liver, which lack functional murine B and T lymphocytes, serving as a permissive *in vivo* model for both HAV and HCV.

These animals are subjected to re-engraftment with human liver tissue upon loss of their own hepatocytes, in consequence of noxious expression of the urokinase plasminogen activator (uPa) in hepatocytes (see *Introduction*), thereby becoming chimeras with a human liver and its own innate immune system, isolated from the murine tissue - with leftovers of adaptive immune cells, but not able to counter-signal to the human hepatocytes. Thereby, this unique model potentially allows for a direct comparison of the innate immune responses to HAV and HCV in human hepatocytes, in the absence of adaptive immunity.

As a first step, I optimized a series of species-specific primers for detection of murine and human tissue, with the aim of evaluating the quality of the individual animals and the potential for successful infection (Figure 71A,B). For the majority of the mice, human GAPDH levels were relatively similar and the ratio murine to human GAPDH was acceptably low (Figure 71A,B).

Therefore, I could proceed with viral infection and innate immune analyses.

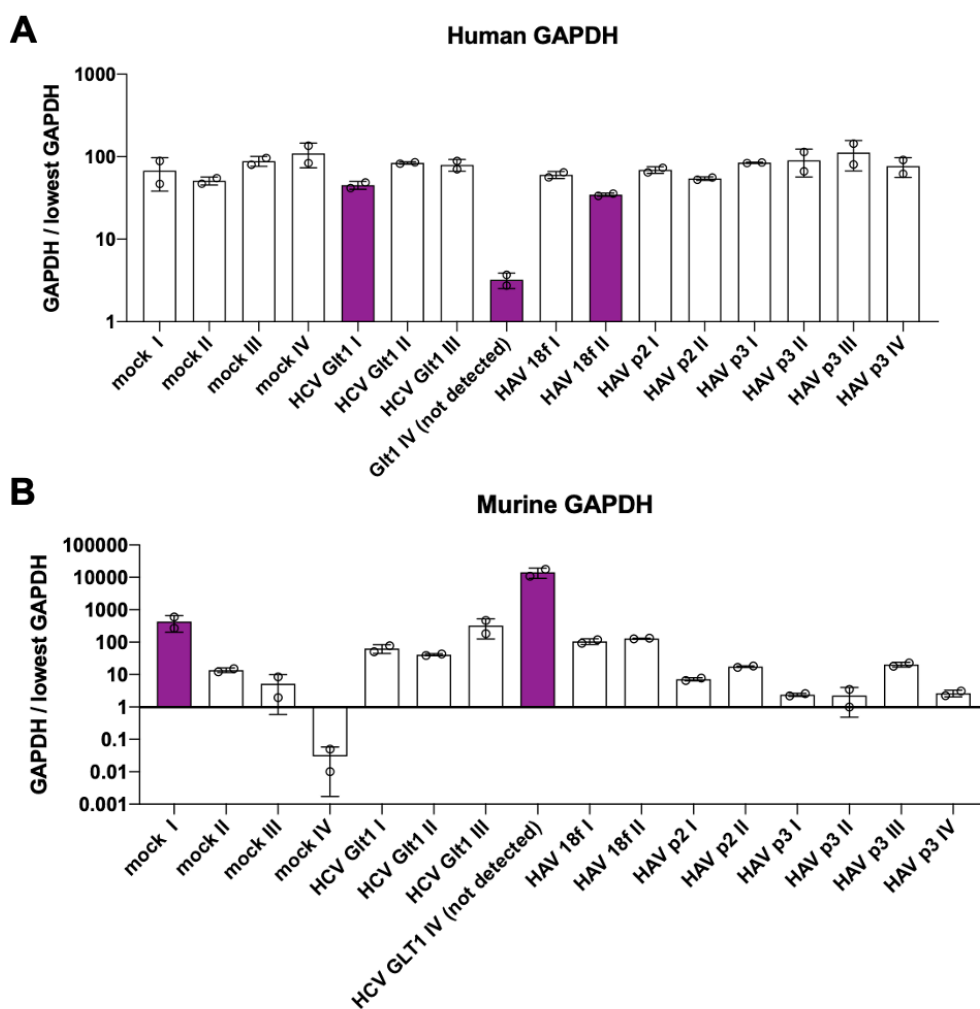


Figure 71. Quantification of human engraftment in SCID alb/uPA chimeric mice with human livers.

Human- and murine-specific qPCR primers were used for a RT-qPCR aiming at measuring mRNA expression of GAPDH to evaluate percentage of human tissue repopulation in the mice used for this study. GAPDH

expression is shown as fold relative expression to the sample with lowest ratio murine / human GAPDH expression. In purple are indicated the mice used further for the IHC studies.

To ensure reliable comparisons, I utilized two different wild-type virus variants for each virus, excluding major strain-specific differences. The prototype strain H77 (gt1a)²⁸⁵ was selected for HCV, along with a high-titer post-transplant serum of the gt1b strain GLT1³⁴¹. Due to the limited availability of well-characterized HAV wild-type strains, I extracted the virus from the stool of two anonymous donors and used cell-cultured HM175/18f as a reference.

First of all, I quantified viral RNA, where my findings demonstrated, on average, higher levels of HAV RNA in the liver compared to HCV (Figure72A), despite similar efficiency in repopulation with human hepatocytes, which was counter-measured through albumin levels expression in serum (Figure72B).

Upon qPCR measurements in bulk, aiming at ISGs detection (always using species-specific primers), at first I did not detect high variations between HAV and HCV infected mice. In addition, I normalized ISGs expression on two housekeeping genes, to increase stability of the analysis, but the mock mouse (infected with mock stool samples) showed in some cases a similar degree of ISGs upregulation as the HAV- or HCV-infected ones (Figure 72C). For these reasons, I decided to normalize the ISG responses on the viral titers, in the hope to lower the high background due to unspecific activations (inflamed tissue, lack of infection in the locally examined lobes, etc.). Surprisingly, using this normalization approach, a very similar ISGs and chemokines upregulation upon both HAV and HCV infection was found, opposite to the response in the infected chimpanzees, lacking of ISG induction upon HAV infection (Figure 72D).

Since the mock infected mouse (not included in the normalized analysis) showed an upregulation of innate immune response, possibly due to LPS present in the stool, I asked our collaborators to perform a stringent gene expression array analysis, including a plethora of ISGs as well as a couple of uninfected (untreated) mice. This analysis confirmed that, for the majority of ISGs, HCV and HAV were triggering a response to very similar degrees (Figure 73,A-H) with few exceptions, possibly associated with a slightly lower replication for HAV HM175/18f (Figure73B,C).

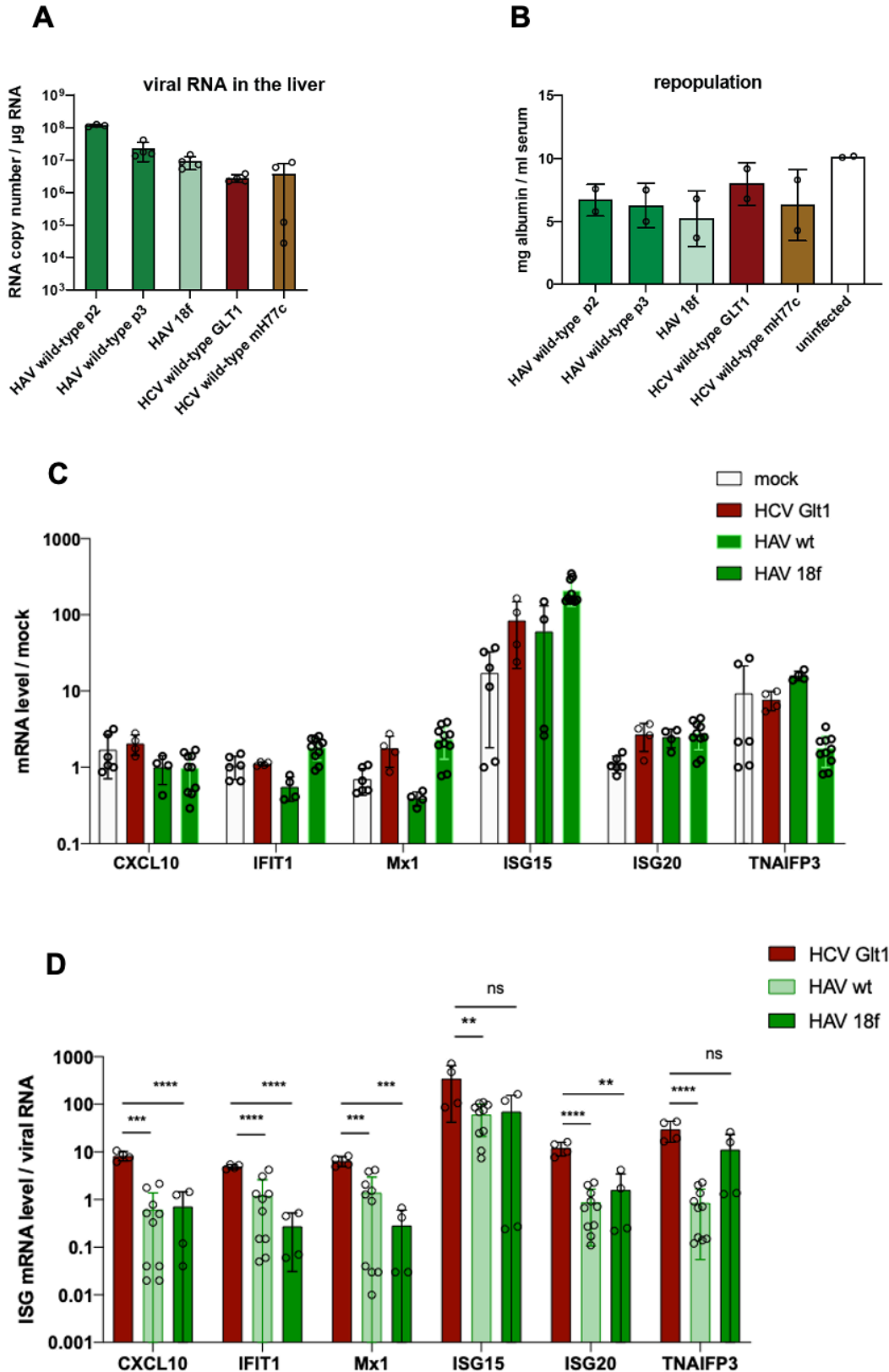


Figure 72. ISGs mRNA expression upon HAV and HCV infection in SCID alb/uPA chimeric mice with human livers.

(A) Viral replication in uPA-SCID mice with humanized liver. Total RNA was isolated from 20 mg of liver of HAV or HCV infected mice ($n \geq 3$) and harvested at the time points indicated in Table XX. Viral RNA was quantified

by RT-qPCR using HAV and HCV specific primers. Note that the high variability in HCV copy numbers in case of mH77c was associated to the variance in repopulation efficiency (B). (B) Human tissue repopulation in uPA-SCID mice with humanized liver. Human albumin was measured in serum of HAV and HCV infected mice as well as in uninfected mice 6 to 8 weeks after engraftment. Adapted from own publication:³⁴²

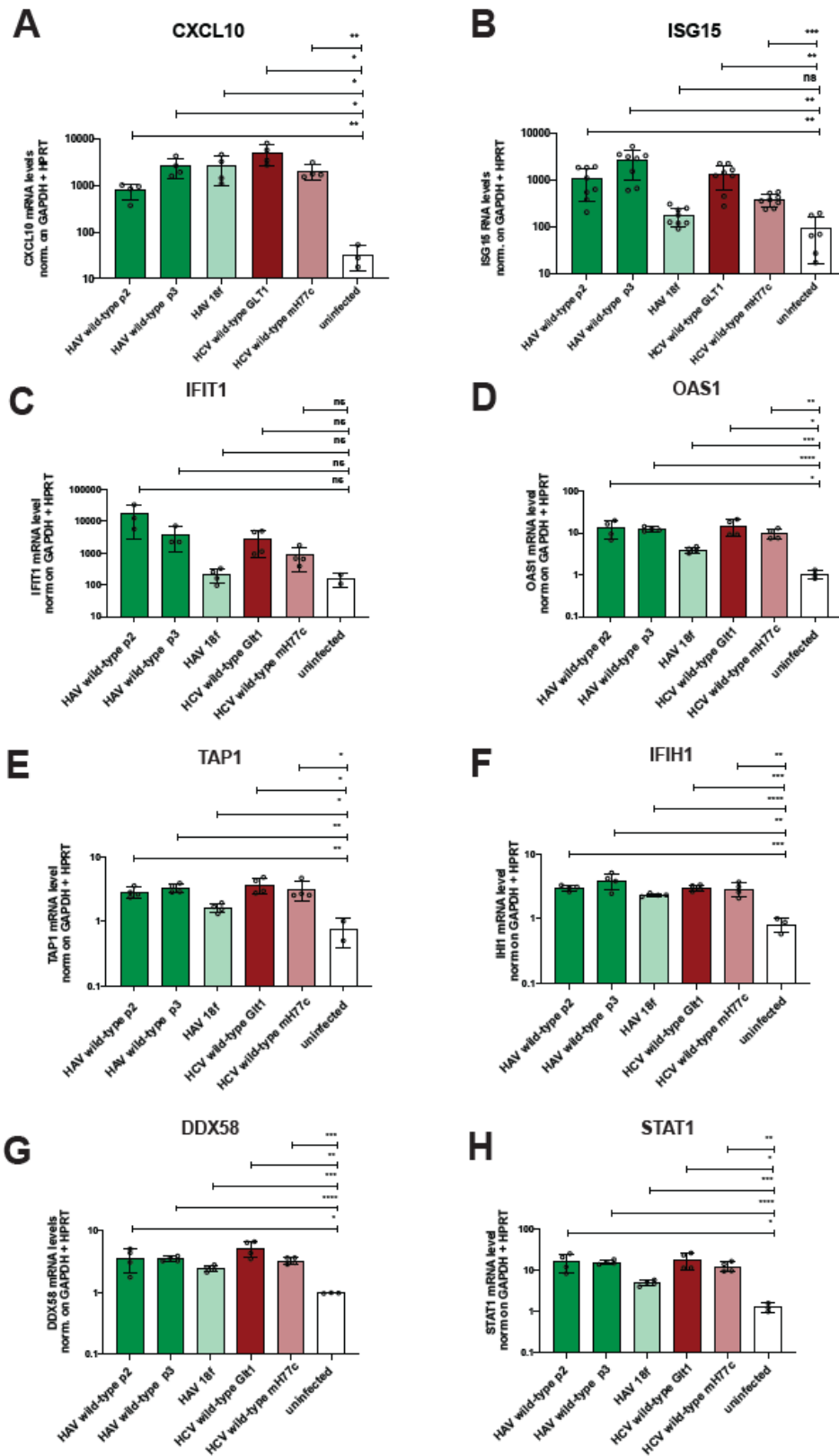


Figure 73. Gene expression array of ISGs upon HAV and HCV infection in SCID alb/uPA chimeric mice with human livers.

(A – H) Total RNA was isolated from 20mg of liver of uninfected mice as well as from HAV or HCV infected mice (n ≥ 3) and mRNA expression levels of a set of ISGs and chemokines were quantified by a Taqman Gene

Expression Array. Gene expression was normalized to GAPDH and HPRT expression. Statistical significance was assessed through Welsch's unpaired *t*-test. Adapted from own publication:³⁴²

At this point, given the high unpredictability given by the choice of areas of the frozen tissues for RNA extraction, which could depict low infection / low human repopulation / high inflammation, it was necessary to investigate at a single cell level to elucidate the viral-specific contribution to the detected innate immune response.

Immunohistochemistry (IHC) analysis was performed in cooperation with Matthias Heikenwalder and revealed the presence of single HAV and HCV positive cells in areas with human hepatocytes, often accompanied by signals of ISGs such as IFIT1 and chemokines like CXCL10, localized to the infected cells (Figures 74,75). To correlate the viral antigen to the innate immune breadth, I measured virus- and ISGs-positive cells in 6 random panels for each mouse, covering around 2 cm, and expressed the number of positive cells on a XY dotplot graph, calculating linear regression (Figures 74, 75 A, B, C, right panels).

Conversely, uninfected mice showed no such signals (Figure 74C). However, in one case of HCV GLT1 infection, I observed lower levels of IFIT1 in HCV-positive human hepatocytes by IHC, along with aggregated clusters of murine cells and CXCL10 positivity surrounding the infected cells, indicating an inflammatory response (Figure75B).

Overall, these data indicate a significant activation of cell-intrinsic innate immune responses during both Hepatitis A and Hepatitis C virus infections in the livers of humanized mice lacking adaptive immunity.

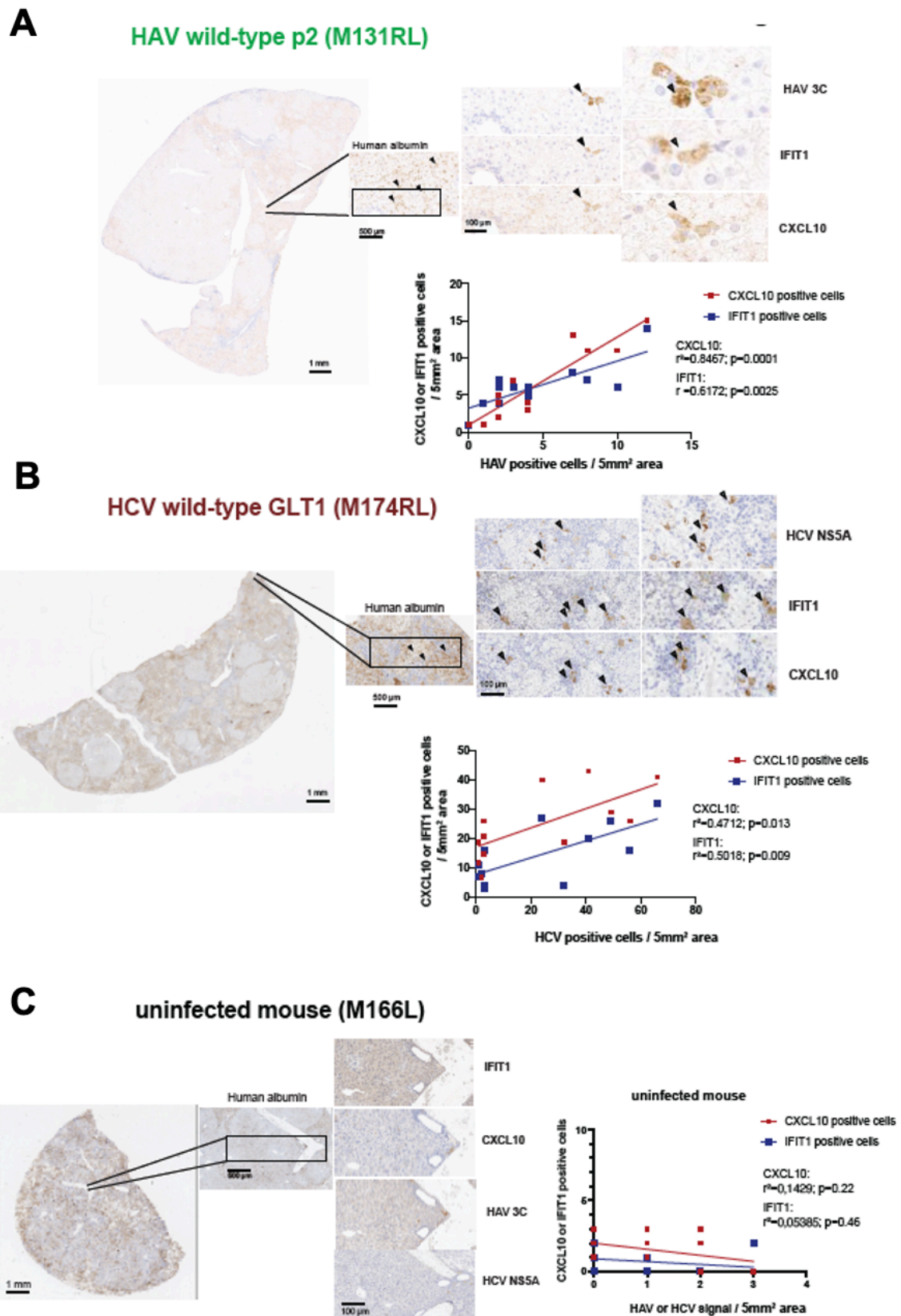


Figure 74. Upregulation of ISGs and chemokines at protein level upon HAV and HCV wild-type infection of SCID alb/uPa mice with humanized livers.

(A, B, C) Sections from the liver of SCID Alb/uPA humanized mice infected with wild-type HAV (A), HCV (B) or uninfected (C), and subjected to IHC, using human albumin, HAV, HCV or ISG specific antibodies, as indicated. Shown are representative examples with abundant albumin signal (A, B, C left and above panels). Consecutive sections from the liver of uPA-SCID mice with humanized liver infected with cell culture adapted HAV strain HM-175/18f (C), serum derived wild-type HCV Gt1b (isolate GLT1) (D) and serum derived wild-type HCV Gt1a (isolate mH77c) (E) were subjected to IHC for human albumin, HAV 3C or HCV NS5A and ISGs (IFIT1 or CXCL10), as indicated. Shown are examples of one repopulated area for each mouse, characterized by abundant human albumin signal, that was chosen for magnification (C, D, E, left and above panels). For each mouse, 6 albumin-rich view fields were quantified by manual counting for viral antigen positive cells as well as ISGs signals. Black arrowheads indicate a triple positive cell. Linear regression analysis was performed on CXCL10 or IFIT1 positive cells and HAV 3C or HCV NS5A positive cells, and statistical significance was assessed through Welsch's unpaired t-test (C, D, E, lower panel). Adapted from own publication:³⁴²

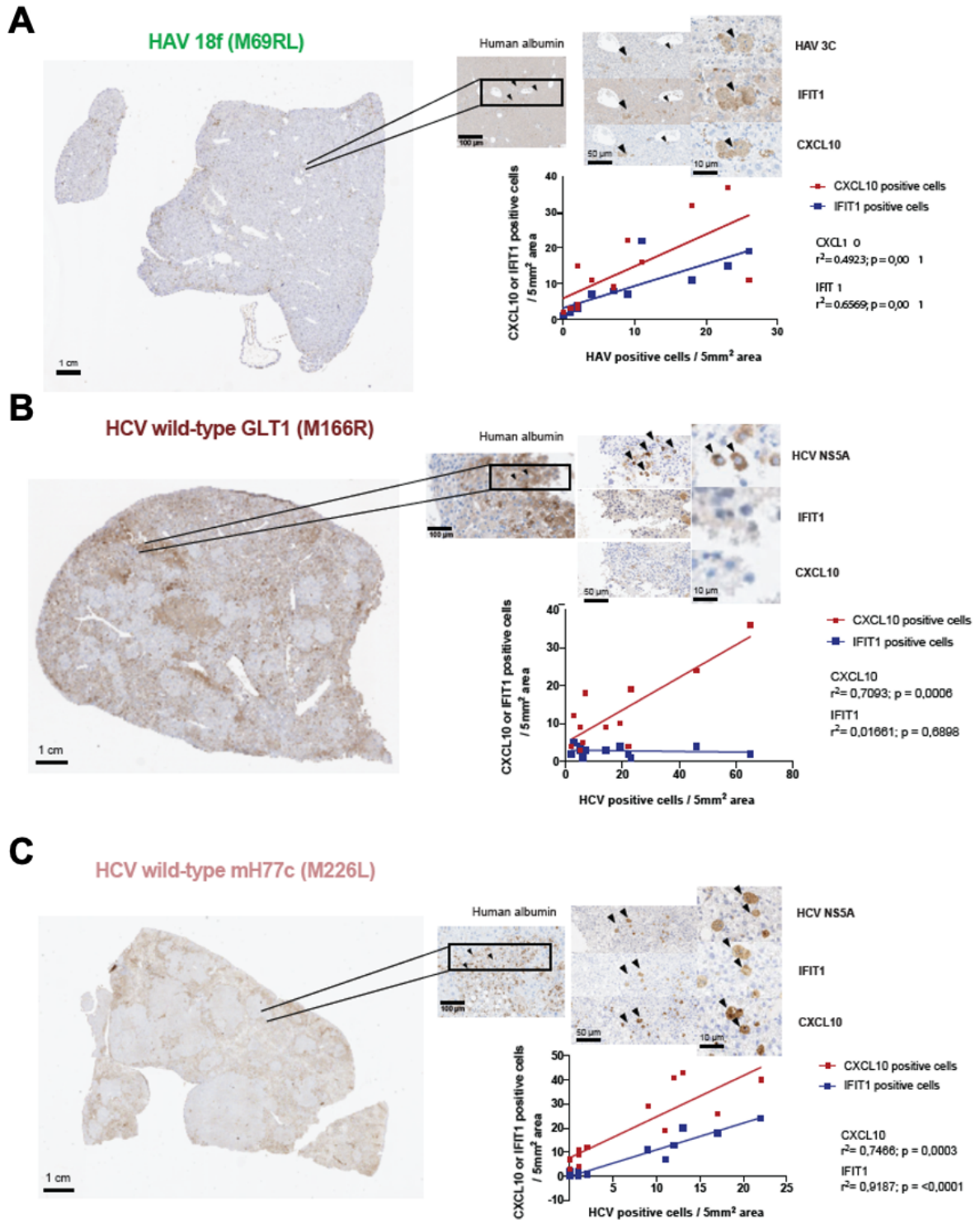


Figure 75. Upregulation of ISGs and chemokines at protein level upon infection with HAV HM175/18f and HCV genotypes 2a and 1a of SCID Alb/uPA mice.

(A, B, C) Consecutive sections from the liver of uPA-SCID mice with humanized liver infected with cell culture adapted HAV strain HM-175/18f (A), serum derived wild-type HCV Gt1b (isolate GLT1) (B) and serum derived wild-type HCV Gt1a (isolate mH77c) (C) were subjected to IHC for human albumin, HAV 3C or HCV NS5A and ISGs (IFIT1 or CXCL10), as indicated. Shown are examples of one repopulated area for each mouse, characterized by abundant human albumin signal, that was chosen for magnification (A, B, C, left and above panels). For each mouse, 6 albumin-rich view fields were quantified by manual counting for viral antigen

positive cells as well as ISGs signals. Black arrowheads indicate a triple positive cell. Linear regression analysis was performed on CXCL10 or IFIT1 positive cells and HAV 3C or HCV NS5A positive cells, and statistical significance was assessed through Welsch's unpaired *t*-test (A, B, C, lower panel). Adapted from own publication:³⁴²

In conclusion, my research, employing various investigative approaches, sheds a novel light on the complex interplay between HAV and HCV and the primary innate immune pathways in human hepatocytes. The findings notably diverge from existing literature, suggesting that HCV's NS3-4A does not cleave TRIF but abrogates RLRs through complete MAVS cleavage, thereby predominantly triggering a TLR3 response. In the case of HAV, my data show incomplete MAVS and TRIF cleavage alongside an ISGs response in immunocompetent models: HepG2 and HepaRG cell cultures *in vitro*, and SCID alb/uPA chimeric mice with humanized livers *in vivo*. The HAV-mediated innate immune response did not originate from TLR3 nor RIG-I, but exclusively from MDA5 with contribution of LGP2.

Altogether, these findings offer new perspectives on understanding immunity against HAV and HCV infections in the liver.

5. Discussion

5.1 Potential role of TLR3 in HAV and HCV infections

The aim of this thesis was elucidating the potential contribution of innate immune induction and counteraction in the context of positive strand-RNA viruses infection with the potential to chronicise, as HCV, in the light of a direct comparison with a similarly structured virus which, however, causes only acute infections of the liver, HAV³⁰⁹.

I started my investigation focusing on TLR3, which stands as a key player among PRRs, significantly contributing to potential acute or chronic developments of liver diseases and inflammation: previous research shows that mice deficient in TLR3 exhibited a lessened production of crucial inflammatory cytokines⁷⁸, underscoring the essential role TLR3 signaling plays in liver injury; at the same time, its pivotal contribution to the infection context in general has been demonstrated by studies which show hepatocyte-TLR3-mediated specific activation of cells bridging innate and immune response, including HSCs³⁴³, monocytes and monocyte-derived dendritic cells³⁰⁷, NK cells³⁴⁴, Kupffer cells and sinusoidal endothelial cells³⁴⁵, among others. Especially, the TLR3 pathway in hepatocytes has been proven to be pivotal in the context of viral hepatitis' infections; for viruses which do not directly trigger the receptor, as for example HBV^{346,347} as well as, importantly, when engaged in direct defense mechanisms, as in the context of HCV^{83,321,329}. However, the specific role of TLR3 in viral hepatitis, as studied in TLR3-deficient mice, still lacks a comprehensive understanding. A limitation in existing research lies in the non-hepatotropic nature of viruses studied so far, which includes EMCV, coxsackievirus B4, poliovirus, and the phlebovirus Punta Toro virus, all of which result in multi-organ pathogenesis, possibly masking liver-exclusive phenotypes³⁴⁸. TLR3-deficient mice have been observed to exhibit increased viral load in the liver and heightened mortality following infections with EMCV90, coxsackievirus B494, and poliovirus³⁴⁹. However, these mice demonstrated increased resilience and less severe liver disease when infected with the hepatotropic Punta Toro virus³⁵⁰. Here, while infection led to similar liver and serum viral loads, TLR3-deficient mice

cleared the virus more rapidly and showed less inflammation, suggesting that the TLR3-mediated response to Punta Toro virus infection might negatively impact on disease outcome. In fact, innate immune activation via TLR3 can dramatically heighten the susceptibility to liver immune-mediated injury³⁵¹, caused by T-cell clusters accumulation³⁵². These opposing examples, highlighting how TLR3 exhibits a complex duality, render increasingly pertinent to elucidate how this sensor might shape the infection processes of HAV and HCV, potentially contributing to their profoundly different outcomes and to the overall clinical picture²⁴², given its robust expression in the liver³⁵³.

Examining existing literature in the context of TLR3 and hepatotropic viruses, it is evident how the study of interactions between HAV and TLR3 remained relatively underexplored. Direct studies on sensing / induction of innate immune response were not conducted for HAV with focus on TLR3⁶⁵, despite several works mentioning the potential recognition of HAV dsRNA by this receptor^{175,208,212,247,354}. More or less hidden hints came from a specific study showing that one of the pivotal ISGs induced by HAV, CXCL10, was expressed independently from IRF3, which in turn would exclude TLR3 activation⁶⁵, opposed to its induction upon HCV infection, directly downstream of the TLR3-NFkB/IRF3 axis³³⁴. To lay down a foundation for the rigorous analysis of HAV-mediated activation of this sensor, I reproduced the work of previous alumni (Esser-Nobis et al., unpublished), transiently expressing TLR3 onto stable replicon cell lines, not detecting upregulation of ISGs for HAV (Figure19); the same was seen by me in the opposite approach, where I infected TLR3 stable cells with HAV (Figure20). Given also that these initial results were all recalling the most important piece of data available in the context of HAV and innate immunity (lack of ISGs in the liver of HAV-infected chimpanzees²¹²), I initially also interpreted them in such a way. But for HCV the scenario was much more elaborated: previously, alumni of our lab showed that knock-down of Rab27a, a factor involved in extracellular vesicles release, led to augmented intracellular HCV viral RNA and increased TLR3 activation, thereby elegantly demonstrating that TLR3 might be target of a peculiar escape mechanisms by HCV, based on secretion of replication intermediates through Extracellular Vesicles (EVs) and thereby a potential balance establishment between replicative breadth and innate immune response⁸³. The described strategy seemed to be HCV-specific and not to be exerted by other Flaviviruses, as DENV, or by HAV⁸³, and therefore potentially representing a specific signature of HCV infections. However, an additional potential interference mechanism towards TLR3, based on efficient virus-mediated cleavage of its adaptor protein TRIF, was reported for both HCV¹³⁸ and HAV¹⁷³, thereby offering the opportunity of a direct, thorough comparative analysis between the two viruses.

Starting from literature analysis, I found discrepancies and fragilities in the way TRIF cleavage was investigated. For HAV¹⁷³, proteolytical cleavage was detected biochemically with evidence of cleavage products in HEK293T, not a relevant model for HAV replication, whereas the evidence of TRIF cleavage in infected Huh7 / Huh7.5 cells as well as in HAV replicon cell lines was scarce; furthermore, TLR3 / TRIF expression was modulated in the hepatic cell lines used for the study (Huh7.5 TLR3, PH5CH8), but only to show a (very modest) effect on HAV replication, and not to elucidate any impact on the innate immune response; lastly, the 3C and 3CD -mediated functional interference was assessed in HeLa cells and Huh7.5 TLR3 cells but only in the context of an IFN Beta promoter-driven Luciferase reporter assay, rather than in the context of endogenous IFNs or ISGs /

chemokines transcribed, or secreted, by the cells. In general, this sharp dissociation between biochemical detection of cleavage and functional importance of the counteraction surely limits a correct assessment of the physiological contribution of viral-host interactions.

Studies were also conducted on analogous protease activities against TRIF in the context of other viruses, often also basing the experimental work on HEK293T cells, HeLa cells and ectopically expressed Luciferase reporters, as in the case of coxsackievirus B³⁵⁵. In other examples, instead, with good supported evidence of the cleavage-derived physiological impact, as for enterovirus 68³⁵⁶, rabbit hemorrhagic disease virus³⁵⁷ and foot-and-mouth-disease-virus³⁵⁸, all members of viral families characterized by the evolutionarily conserved 3C protein¹⁹⁸, shared by *Picornaviridae* members too, as HAV¹⁶⁹.

For what concerned HCV, the research reporting TRIF cleavage by NS3-4A¹³⁸ had its major claim based on *in vitro* translation model in reticulocyte lysates, which is highly artificial, and protease / adaptor expression in HEK293T cells, a non-hepatic cell line with limited physiological relevance for HCV; for the functional data, here as well, only use of IFN β promoter-driven Luciferase reporter assay was employed¹³⁸. Interestingly, shortly after this publication, another group contested it¹³⁸, reporting lack of TRIF cleavage and thereby insufficient counteraction to innate immunity by HCV NS3-4A, this time in appropriate liver-based systems²²².

On the other hand, other members of *Flaviviridae*, whose genomes encode a NS3-4A as well as West-Nile-Virus (WNV), Dengue Virus (DENV) and Yellow Fever Virus (YFW) were reported unable to interfere with TLR3³⁵⁹. The sharp difference between the number of 3C-provided viruses showing ability to interfere with TRIF, and the HCV-NS3-4A protease harboring Flaviviruses which do not cleave TRIF, is also indicative of the potential incompatibility between what was described to be putative TRIF cleavage site for HCV, C372, and the canonical NS3-4A cleavage site³⁶⁰, which will be discussed later in this section.

Taking all this into account, it was important for me to avoid artefacts and work in relevant models. But when I encountered problems with endogenous TRIF detection because of very limited TRIF expression in liver-based cells, and I tried to work with ectopic expression, this led quickly to cell death through a previously described mechanism, in which TRIF's RHIM domain complexes with RIPK1, caspase-8, FADD, and cFLIP to apoptosis (or to RIPK3 to necroptosis)³⁶¹.

Deletion of the RHIM domain rescued cell viability and allowed me to express TRIF to detectable levels. Since the entirety of the biochemical approaches to detect HAV- and HCV-mediated cleavage applied by me had to be based on the use of this deletion mutant, this raised concerns on potential artefacts. However, the delta RHIM construct was previously shown to be fully competent for TLR3 signaling⁸⁰. The RHIM, furthermore, is located at the C-terminal domain and covers the last 56 amino acids on a protein of around 75 kDa. HAV 3CD cleaves at Q554 first and, upon exposure of the folded N-terminal domain, then Q190. Cleavage at Q554 is indispensable for the second cleavage to occur; the first cleavage site, besides being distant from the RHIM domain, belongs to an highly conserved alpha helix stretch which, according to *in silico* models (Figure 76A,B), does not undergo any relevant folding modification, which would potentially interfere with protease cleavage, in absence of RHIM. However, I cannot formally rule out the possibility, especially for HCV NS3-4A

which cleaves at C372 - a much less conserved and characterized region of TRIF which showed a low confidence score in AlphaFold (Figure 76C)³¹⁶⁻³¹⁸ – that the usage of TRIFdelRHIM might have hindered the physiological interaction between the proteinase and the substrate.

Another important limitation in my results was given by the need of keeping HAV 3CD expression to a minimum because of cytotoxicity, due to already well known 3C-mediated mechanisms of ferroptosis³⁶² and vacuolization of lysosomal /endosomal organelles³⁶³. For this reason, in all the approaches based on robust ectopic HAV 3CD expression I cannot formally exclude that the lack of functional counteraction might have been given by an insufficient 3CD expression. On the other hand, in assays based on establishment of robust HAV replication I did not observe cell death, probably due to a physiologically lowly expressed 3C – 3CD; the same held true for persistent HAV subgenomic replication in the stable cell lines, whose low degree of replication and protein expression have been described earlier¹⁹⁰. All in all, it seems that the cell culture-adapted HAV HM175/18f strain might have gained the capacity to modulate the expression level of 3CD to tolerable levels; given the reported highly replicating, inflaming and tissue injuring wild-type HAV strains³⁶⁴, comparing patient isolates and HM175/18f in terms of protein expression and efficient host protein degradation might be highly informative on the 3Cpro potential in disrupting innate immunity *in vivo*.

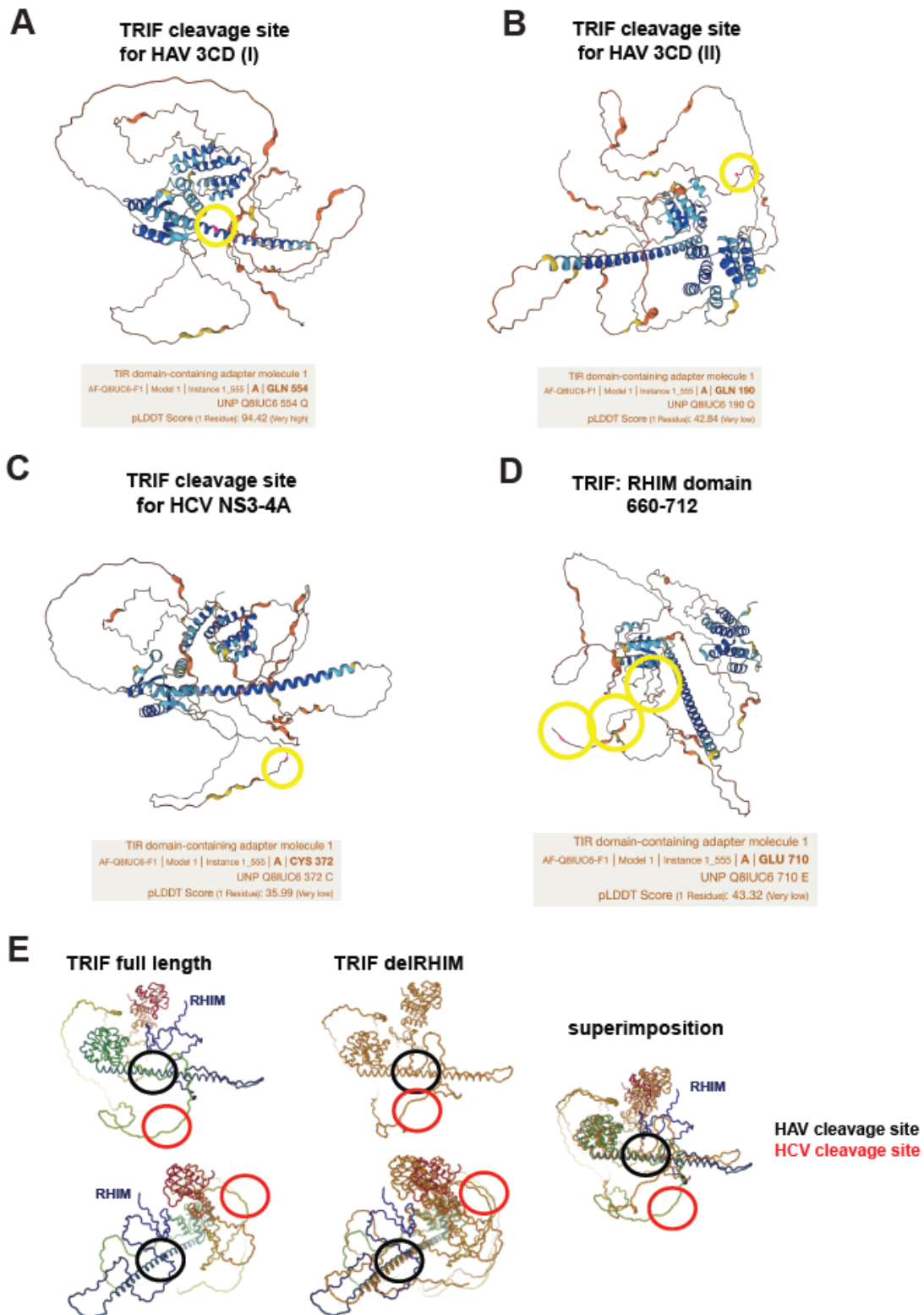


Figure 76. TRIF structure predictions.

(A - D) TRIF *in silico* model, obtained through AlphaFold, with indicated in yellow the two sequential predicted cleavage sites of HAV 3CD (A, B), the one by HCV NS3-4A (C) and the RHIM domain, at the C-terminus (D). (E) TRIF full length (left panel) and TRIF delRHIM (middle panel), compared through ColabFold predictions, with indicated in black the HAV primary cleavage site Q544 (in black) and in red the reported HCV cleavage site C372 (in red). On the right, superimposition of the two predicted structures.

Nevertheless, in all the biochemical detection assays based on 3CD ectopic expression the latter was transient and therefore cytotoxicity could be prevented; here, TRIF cleavage efficiency nonetheless reached at its best 60%, with full length TRIF remaining the most prominent species (Figure 28), allowing me to assume that, similarly as for NS3-4A, the TRIF cleavage site for HAV might not occur at high efficiency, probably due to the TRIF molecule not containing any canonical 3Cpro consensus cleavage sites ((L,V,I)X(S,T)Q↓X, where X is any amino acid³³), but only sites which are partial fits. Qu et al.¹⁷³ claimed that the 3D polymerase might contribute to a “tolerance”, that the 3CD precursor has, to the acidic residues present at the P4 position of cleavage sites in TRIF, which would make the scission possible for 3C+3D (3CD) but not likely for 3C¹⁷³, but the study lacks further evidences: how does the 3D protein re-direct the cleavage preference mechanistically? And most importantly, is HAV dsRNA really sensed by TLR3, and its replication limited by it? If not, what is the significance of the TLR3 pathway disruption by HAV? The capacity of HAV 3CD to partially degrade TRIF might be coincidental, based on an ancestral picornavirus, sensed by TLR3 and necessitating TRIF cleavage. The fact that this cleavage capability is conserved among other picornaviruses might argue in this direction^{170,199}. However, all my data suggest that HAV is rather not sensed by TLR3 and that partial TRIF cleavage therefore appears to have no relevance for HAV replication.

Conversely, robust expression of NS3-4A was confirmed in all my assays to never be associated with cell toxicity (Figures 38, 43, 49, 56) despite previous reports of it inducing stress and apoptosis³⁶⁵. In Huh7.5 TLR3 cells examined through IF, its expression did not suffice to abrogate the response to poly(I:C) when compared with expression of the mutant protease. Initially, statistical analysis showed a significant difference in the IFIT1 mRNA expression upon poly(I:C) in presence of ectopically expressed HCV NS3-4A (Figure 39), which was interestingly reflected in a minimal cleavage detection (6%) of TRIF in Gt1b HCV subgenomic replicon cells (Figure 30). However, tight modulation of the protease expression in stably selected cells, with “low” or “high” NS3-4A, provided evidence on the lack of any functional impact on the TLR3 pathway (Figure 40); and inclusion of the protease inhibitor Simeprevir³²⁷ showed no change on the activity on TRIF (Figure 31B), yet with a minimal reduction of NS3-4A, probably due to the already elevated protease expression due to the features of this specific model, the persistent subgenomic replicon, in which stable genomes are present constantly thereby providing a baseline expression of the non-structural proteins. Drug pre-treatment of cells which are later infected with full-length HCV would, for example, abrogate protein processing at its start. On the other hand, in the Gt1b replicon cell lines a moderate effect was initially also observed on the TLR3 response breadth upon the highest dosage of poly(I:C) (Figure 41). This could have been attributed to the NS4B-induced TRIF degradation by host caspases, claimed by previous researchers³²⁸; however, when TRIF was detected in Gt2a replicon cell lines as well as in HCV infected cells, no trace of degradation was observed (Figures.30,31). The phenotype did not change in the more physiological context of infected hepatocytes (Figure 32), confirming that the TRIF molecule does not undergo a prominent reduction under expression of any of the structural, or nonstructural, HCV proteins. This is in line with previous observations by the group reporting lack of TRIF cleavage by HCV, and in line with the fact that the TRIF molecule does not harbor canonical cleavage sites for a Cys protease like HCV NS3-4A³⁶⁰, as opposed to MAVS, which will be now examined.

5.2 Enhancing the robustness: investigating RLRs upon HAV and HCV infections

In my exploration of RLRs-mediated pathways in HCV and HAV, distinct patterns of innate immune recognition and evasion strategies emerged.

The involvement of RLRs in HCV infection is well-established, with over two decades of research elucidating the interplay between HCV and these pattern recognition receptors. HCV is unambiguously recognized by RIG-I, although the role of MDA5 remains somewhat contentious. HCV NS3-4A protein has been consistently reported to facilitate the proteolytic degradation of MAVS, the pivotal adaptor protein of these cascades³⁶⁶. This cleavage occurs at Cys-508, a canonical site for cysteine proteases, and appears unaffected by the subcellular localization of MAVS (peroxisomal or mitochondrial)²¹³. My research supports these findings, confirming as well the full inhibition of RIG-I and MDA5 signaling pathways in various experimental models.

On the contrary, the role of RLRs in HAV infection and immune evasion in literature is less clear. While some literature suggests that HAV 3ABC protein effectively cleaves MAVS, my findings contradict these claims. In my experiments, MAVS degradation in HAV replicon or infected cells was only moderate. In contrast, the study by Yang et al. reported extensive MAVS cleavage in Huh7 cells transfected with 3ABC, markedly exceeding my observed cleavage levels. This discrepancy extended to functional assays as well: while Yang et al. reported significant IFN- β inhibition using a luciferase reporter, my tests, focusing on endogenous ISG mRNA expression, found no such abrogation. Furthermore, my experiments with a MAVS-GFP-NLS reporter suggest that 3ABC's proteolytic efficiency is greater in infected cells compared to transfected cells: this discrepancy might be explained by the differing stability of the 3C precursors during the HAV replication cycle.

Lastly, it is important to note that for members of the family *Enteroviridae*, which share with HAV a high 3C^{pro} sequence homology¹⁹⁸, it has been demonstrated that the majority of innate immune counteractive events, against PKR, RIG-I, MDA5 and TRAF6, which take place through proteolytic cleavage are due to the 2A protease activity and not to 3C⁹⁹: a following possible reason to uncouple 3C-proteolytic cleavage from innate immune abrogation by HAV. The 2A protein of HAV is indeed very different from that of other Picornaviruses, as the HAV 2A gene lacks identifiable functional motifs, albeit still being essential for virus morphogenesis and virulence³⁶⁷. Although modifications in its central portion don't hinder its function or virus replication, the 2A protein itself doesn't operate as a 2AB precursor³⁶⁸ and, in fact, the cleavage of the 2A/2B junction in the case of HAV is operated by 3C^{pro} and the subsequent cleavage of the mature product VP1/2A is performed by cellular proteinases as trypsin, cathepsin L and Factor Xa^{169,369}. For all these reasons, 2A is considered more as a structural protein in HAV's replication cycle, with its key role in the viral capsids assembly³⁶⁷.

The complex relationship between hepatitis A virus (HAV) and the interferon regulatory factor 3 (IRF3) pathway suggests additional layers of immune evasion that extend beyond the cleavage of the MAVS protein. Work by Fensterl et al. proposed that HAV may impair the phosphorylation of TANK-binding kinase 1 (TBK1) and IKK ϵ in infected FRhK-4 cells, efficiently inhibiting the RIG-I pathway. Furthermore, they suggested that HAV might reduce

the efficiency of TRIF-downstream signaling, cumulatively blocking IRF3 activation²⁴⁵. However, their measurements of innate immune response were based on an IFN-beta enhancer construct, potentially not representing the endogenous pathway activity in hepatocytes accurately.

Additional insights from the same research group, by Paulmann et al., suggested that HAV's counteracting mechanisms could be the result of a concerted effort by HAV proteins 2B and 3ABC affecting TBK1 and MAVS²⁴⁶. Yet, the specifics of this proposed mechanism remain unclear, as the authors did not attempt interaction studies.

Contrastingly, my research, employing various liver-based and immunocompetent HAV-infected cell models, demonstrated fully functional RLR pathways (Figures 41-43). As the HAV infection system used should express all HAV proteins at physiological levels, the absence of significant immune pathway disruption in my study suggests a more nuanced interaction. Rather than fully abrogating the innate immune response, HAV may subtly modulate the cascades; still, I must consider potential model limitations, such as the forementioned potentially inadequate responsiveness, which may hinder a comprehensive exploration of these mechanisms.

I also have to take in consideration an important piece of research, by Hirai-Yuki et al., which reveals that MAVS knockout in wild-type mice allows susceptibility to HAV infection²⁴⁹. The authors suggests that HAV's ability to infect different species depends mainly on its capacity to avoid detection and response through the RLRs-mediated pathway: In doing so, HAV seems to not only evade the body's antiviral defenses but also limits inflammation in the liver, delaying the development of antiviral antibodies, and slowing down the body's ability to clear the virus²⁴⁹. The authors also note an unexpected role of MAVS signaling in contributing to liver injury during HAV infection. The authors propose that both HAV and Hepatitis C Virus (HCV) have evolved to degrade MAVS as a survival strategy. They also note a recent discovery suggesting that IRF3 can be activated in response to stress in the ER, which might represent a shared mechanism for liver injury caused by viruses and toxins, like alcohol²⁴⁹.

This injury occurs through apoptosis in liver cells, which leads to an inflammatory response regulated by IRF3/7 and independent of interferon secretion. Their theories contribute in giving HAV-mediated MAVS cleavage a relevant role; but contrasting this hypothesis, and instead in support of my results, a recent study by Sun et al. shows an intriguing finding. When, in wild-type mice KO for MAVS, murine MAVS was replaced with a „humanized MAVS“ - carrying the specific cleavage site for HAV 3ABC – upon HAV infection cleavage did occur, albeit moderately - yet, not leading to an increased susceptibility to HAV infection, suggesting that the connection between HAV infection and MAVS cleavage might be less crucial than previously discussed in literature³⁵⁴.

Additionally, mice lacking the type I interferon receptor also demonstrate the capacity to support HAV replication. Despite the data suggested by my work would hint at the opposite, this important study suggests a critical role of innate immunity in the context of HAV infection, possibly with MAVS (or IRF3) being directly implicated in it, although not necessarily through proteolytic cleavage²⁴⁹.

To note, these observation might corroborate the hypothesis I brought on throughout the dissertation, that HAV might not be sensed by TLR3 and might cleave TRIF with low efficiency, in support of my experimental data: in fact, TLR3-TRIF can initiate cell death pathways as well, independent of NF- κ B activation⁸⁹. If HAV would evade MAVS-mediated apoptosis through cleavage – given that the cleavage efficiency has been reported comparable between TRIF and MAVS by me, but also by previous findings^{173,175,248} – then TRIF KO mice would have also granted permissivity, while the authors demonstrated that, in lack of a functional TLR3 pathway, HAV infection was not possible. Still, HAV infection in the MAVS / IFNAR KO mice was negatively correlated to inflammatory infiltrates and reduced hepatocellular apoptosis, and while HAV could not establish productive infection in the cleavable, humanized MAVS reconstituted mice, here liver inflammation was shown to be reduced³⁵⁴.; Altogether, a limited cleavage of TRIF and MAVS might contribute to the survival of infected cells and to local reduction of inflammation an aspect I have not addressed in my studies, but which should acquire some attention in future approaches.

Very relevant to the topic of interplay HAV - MAVS is the fact that I confirmed the primary innate immune response source in HAV infections to be originating from MDA5-mediated sensing and not by RIG-I, confirming previous data⁶⁵. Unfortunately, I lacked a homogeneous model in which HAV and HCV would replicate in presence of a fully responsive MDA5-LGP2 axis; but comparing the innate immune response originating by RIG-I in Huh7.5 RIG-I cells infected by HCV, which is very transient and quickly abrogated because of MAVS cleavage (Figure 51), detection of a robust IFIT1 and CXCL10 upregulation in HAV-infected HepG2 cells (Figures 64,65,68,69) strengthens the concept of lack of functional counteraction for what concerns MAVS / IRF3.

Interestingly, an investigation on the role of LGP2 in the context of HAV infection was not conducted so far, despite several pieces of work bringing evidence to its MDA5-boosting role in recognition of several ss(+)RNA viruses, as HDV. Importantly, my data show for the first time, that LGP2 plays an essential role in supporting MDA5 sensing of HAV infection. Lacking LGP2 the CARD domain necessary for MAVS recruitment and further signaling, its direct role in recognition is not intuitive and for long this protein has considered a regulator of RIG-I and MDA5 more than a sensor^{48,54}. However, in the recent study by Gillich and Zhang it was shown how LGP2 can bind directly to HDV RNA, besides promoting stable MDA5-RNA complexes; and that the stability of the latter is increased in case of the Single Nucleotide Polymorphism (SNP) mutation Q425R, which in turn mediate higher IFN responses³³⁷. It would be worth investigating further the direct interaction HAV-LGP2, with potential link between prevalent SNPs in the population and severity of the liver injury observed in AHA patients, which originates by strong T-cell mediated cytotoxicity and therefore might correlate with higher IFN response in the first place.

5.3 HAV induces ISGs in vitro in immunocompetent cell culture models.

Having clarified that TRIF cleavage was incomplete for HAV, and absent in the case of HCV, I aimed at functionally evaluating its functional importance by investigating the TLR3 functionality in the presence of an external stimulus. Given the complexity of the innate immune signaling network - on top of the necessity of using cell lines supportive of viral

replication for both viruses – I initially focused my investigation on the hepatoma cell line Huh7 and its subclone Huh7.5, largely established in the field of hepatology and virology^{256,320}, although with contradictory perspectives on their relevance for assessing innate immunity *in vitro*: previous reports demonstrated how reconstitution of PRRs would trustfully recapitulate the features of innate sensing, for instance for HBV³⁷⁰, HCV^{83,329} and HEV³⁷⁰ infections, while others underpinned how expression of certain host proteins, altered in consequence of the tumor microenvironment which typifies hepatoma cells as Huh7 and Huh7.5, might attenuate the innate immune response, such as micro RNA 122 (miR122)^{371,372}, which might interfere with TLR3³⁷³ and TLR4³⁷⁴, or Glucose regulated protein 78 (GRP78)³⁷⁵, which counteracts TLR3³⁷¹. In my hands, the functionality of TLR3 in the reconstituted Huh7 and Huh7.5 cell lines upon poly(I:C) stimulation seemed to be solid (Figure 21) and associated to ISGs upregulation quite comparably to the liver-based cell lines which have endogenous expression of PRRs, like PHH⁸³ (Figure 56) or HLCs (Figure 62) . Furthermore, the ectopically reconstituted TLR3 in Huh7 and Huh7.5 showed similar subcellular localization, and protein expression levels, to PH5CH (Figure22).

Unfortunately, established cell lines which are considered innate immune competent, with described homogeneous, endogenous expression of all PRRs, were in average either not permissive to HAV or HCV, or not responsive enough through certain PRR axes. Previously, only few groups reported robust infection of PHHs and subsequent production of progeny virions for HCV³⁷⁶ or HAV⁶⁵, which represent a challenge in context of innate immune studies also because of the often impure cell populations, including NK cells, pDCs, macrophages³³⁴, which might strongly alter the baseline immune activation. Consistently to this, I observed strong donor-to-donor differences in terms of morphology, ISGs and, probably in consequence, permissivity for both HCV Jc1 and HAV HM175/18f (Figures 58-60). The many failed attempts with PHH infection of wild-type HAV virus derived from patients' stool, the same virus that later on instead successfully infected the liver of humanized mice repopulated by PHH (Figures 74-75), were by me interpreted as possible requirements for HAV of the cell polarization which typifies the liver 3D structure. Previous findings indeed implied that the primary route of viral entry is through the basolateral plasma membrane, which aligns with the uptake of the virus from the bloodstream following enteric exposure, and suggests that the process of excretion of HAV may depend on the reuptake and transcytosis, requiring hepatocytes polarization³⁷⁷. However, the requirement might be limited to the wild-type strain, as HM175/18f proved capable to establish infection in HepG2 and Huh7 cells (Figures 64, 68, 69).

Another thing to consider in terms of cell permissivity is expression of necessary host factors, with focus on entry, replication and assembly. Here, the requirements for HAV and HCV seem to be profoundly different, with TIM1, one of the HAV entry receptors previously described controversially as either “required” or “non-essential”, respectively^{378,379}. However, TIM1 is ubiquitously expressed in a variety of cells, also not liver-derived^{244,290}. On the contrary, the recently discussed ganglioside GM2A seemed to be pivotal to ensure uncoating, in a proposed model where gangliosides cluster within the endo-lysosomal membrane at the interaction site with the HAV capsid, leading to tunneling of the HAV capsid into the cell and following successful release of the genome^{183,380}. Concerning replication, only lately the host factor TENT4A/B was shown to have a pivotal role in HAV RNA synthesis by promoting the integration of 5-ethynyl uridine into new HAV RNA²⁰⁰. It

would be worth assessing expression of these proteins in PH5CH, HLCs and Upcyte Hepatocytes, where HAV replication seemed completely impaired. Previous literature hinted at PH5CH8 (a clone of PH5CH, potentially permissive for HCV²⁷⁷) being poorly permissive for HAV because of intense innate immune responses, although not related to TLR3, RLRs, IRF3 or STAT1, but specifically to the baseline expression levels of IRF1³⁸¹, which, once abrogated, would rescue HAV replication because of consequent reduced expression of antiviral genes. My data, however, which shows HAV successful replication in alternative immune competent models with enhanced ISGs expression, as HepG2 or HepaRG, seem to contradict this claim, although there I did not delve specifically into IRF1.

In the scenario of HCV, the requirements for entry and replication appear to be less controversial. The idea of using polarized hepatocytes, which simulate the bile canalicular arrangement of hepatocytes *in vivo*, could be here as well highly pertinent: two crucial HCV cell entry factors, claudin-1 and occludin, are tight-junction proteins and unlikely to fully retain their functions in nonpolarized cells^{382,383}. Nevertheless, the Evans group^{272,273} showed that HCV was able to replicate in nonpolarized HepG2 cells with the expression of miR-122, which facilitates efficient HCV RNA replication and stability^{384,385}, with the further addition of the HCV entry factor CD81¹⁴⁶. Since HepG2 cells are innate immune competent, and supportive of HAV replication, I tried to reproduce the results from this study, aiming at using the same line for both viruses; but without success, since in both HepG2 naïve cells, by me reconstituted, and the very same HepG2 HFL cell clone used in this and other studies^{272,273}, HCV could not replicate (Figures 65,66). However, the forementioned research was based on transfection of HCV RNA and this might have represented a bottleneck, with higher initial delivery of RNA and possible higher initial translation compared to viral infection. On the opposite, when I tried to reproduce the work of Kambara et al., obtaining a full HCV replication cycle in Hep3B cells reconstituted with miR122 and CD81³⁸⁶, I succeeded (Figure63A), although with lower replication breadth if compared with Huh7. Here, HAV replication was supported too, potentially hinting at Hep3B being the homogeneous model for HAV and HCV that I was looking for; but upon measurement of ISGs, both upon viral infection and poly(I:C) stimulation, I realized that, similarly to other defective cell lines, the RLRs seemed to be here only partially functional (Figure63C), once again challenging the possibility to compare HAV and HCV infections directly in cell culture. This was especially disappointing, as a recent study pinpointed Hep3B as the liver-derived cell line most accurately recapitulating the PHH innate immune sensing²⁶¹. However, only synthetic immunostimulants, Coronaviruses and Arenaviruses were used in this study, leaving open questions on its relevance in the context of hepatotropic viruses.

Given the intricacies faced so far in the quest of a homogeneous model, and being the uncertainties on innate immunity prevalently concerned on HAV, rather than on HCV, I decided to focus solely on the earlier, aiming at finally confirming the lack of ISGs observed in Huh7 cells. I proceeded with HepG2 cells, which among the functional tests by me conducted showed the highest response, while supporting HAV replication. Furthermore, the forementioned study by Nicolay et al. showed comparable performances, in terms of PRR functionality, of HepG2 and Hep3B as valid surrogates for PHH²⁶¹. In HepG2, having reckoned that TLR3 was not sufficiently expressed (Figure68A,B) I reconstituted this sensor by stable transduction and showed how, upon following supernatant feeding-mediated stimulation with poly(I:C), it was possible to specifically target it and inhibit it) through BafA

treatment (Figure 68A). In such a way, I could finally assess that the ISGs elicited by HAV replication were not induced by TLR3 (Figure 68D), not because of strong counteraction by HAV proteases, but because of lack of sensing, as seen in Huh7 cells (Figures 19,20,21). Nevertheless, I could not identify a cell line harboring endogenous robust TLR3 expression in which HAV could replicate. However, my data do not indicate that TLR3 overexpression might have resulted in altered or reduced functionality for the sensor, since comparison of its protein expression level (Figure 22) and several tests of its functionality (Figure 21A,B) found comparable levels and signaling strength between reconstituted Huh7 / PH5CH / PHH cells (Figures 22, 60). Moreover, the Huh7 and Huh7.5 models proved to be responsive on the TLR3 axes for what concerned HCV, in my data (Figures 19,20,21) as well as in previous work⁸³.

Setting aside other possible explanations for lack of TLR3 sensing by HAV – related to, for example, a possible poor choice of the timepoints, not suited for the asynchronous and delayed replication peak of HAV²⁸⁸; the specific kinetic of TLR3, which has been shown to peak later compared to RLRs⁶⁸; the fact that the infected cells might be only a minority or, even more problematically, undergoing apoptosis upon HAV-induced signaling^{207,363}, making it challenging to draw conclusions, especially in bulk – the most tempting hypothesis is that HAV dsRNA might not reach the endosome, due to HAV's possible replication site being on the outer surface of the induced membranous structures¹⁸⁷, similar to the pattern observed in the case of Poliovirus (PV)^{387,388}. In general, precise knowledge of HAV replicase structure and localization, along with the fate of HAV dsRNA throughout its formation towards the newly formed virions, is not yet entirely gained, not allowing me yet to rigorously exclude possible counteractive impacts on TLR3 by HAV. An approach based on TLR3 exclusive stimulation in HAV-infected HepG2 cells, upon knockout of the MDA5-LGP2 pathway, might prove informative.

In presence of viral counteraction mechanisms, discriminating between absence of innate immune induction and active abrogation strategies can be highly challenging and, since for both HAV and HCV interference mechanisms were described both based on the activity of proteases involved in polyprotein processing and, thus, necessary for viral replication, inactivating them would have automatically precluded the presence of dsRNA triggering an innate immune response. For this reason, I needed to base my assays on the usage of an external stimulus. Here, several previously conducted studies show how different viral triggers can be used, as Sendai Virus (SEV) for RIG-I³⁸⁹, or Mengo for MDA5⁶⁴. This can be advantageous because of the slow kinetic of replication, and consequently the gradual response of the PRRs to amplifying genomes, which recalls physiological events upon infection. However, different problems can be encountered, as, for instance, viruses are provided with direct innate immune counteraction mechanisms which could mask the investigated sensing⁶⁴, or cellular machineries could be exploited by the virus used as immunostimulant, in a way that replication of the virus of choice could be affected, because of lesser resources, or morphological changes, as in the case of lipids employment³⁹⁰, or simply modifying the host cell expression profile³⁹¹. Furthermore, it is very difficult to assign a different virus exclusively to each PRR, as the readout downstream gene expression is often overlapping upon their activation and interplay, as corroborated by the contradictory reports on the exclusive activation of certain receptors over others³⁹². Considering all these, the choice of a synthetic dsRNA analog, like the commercial poly(I:C)

offered a valid alternative, allowing me to have a “clean” stimulus and tightly control the used amounts of immunostimulant. Furthermore, according to the mode of stimulation, the use of poly(I:C) in the supernatant allowed me to exclusively trigger the endosomal TLR3, whereas transfection stimulates TLR3 and the cytoplasmic RLRs³⁹³. Yet, also here, reports which stress the interplay of inflammation with innate immune response are present; for this reason, despite excluding an additional full viral life cycle which would confound my readouts, I have to take into account that even poly(I:C) could lead to, for instance, augmented inflammation and a PRR-independent impact on ISGs expression³⁹⁴.

In view of these difficulties, a proper ISG choice - possibly descriptive of activation of a single, specific pathway - is absolute key. Orientating myself on previous evidence from our lab^{68,83,395}, from a study involving primary human hepatocytes triggered with poly(I:C)³⁹³ and from a study comparing the ISGs transcriptome in HAV- and HCV-infected chimpanzees²¹², I narrowed my choice on IFIT1 and CXCL10. Further data from a parallel project which I supervised (see *Appendix*), later, investigating cleavage of NEMO by HAV, showed that IFIT1 was well reflecting an exclusive TLR3/RLRs/IRFs activation while CXCL10 was indicating an overlapping activation of TLR3/RLRs/IRFs and NFkB pathways (Huang et al., unpublished); therefore, the specific involvement of CXCL10 in NFkB might be a confounder element when evaluating the “pure” RLRs and TLR3 pathways.

5.4 Innate immune responses *in vivo* upon HAV or HCV have a comparable breadth.

So far, I demonstrated for HAV that the 3C^{pro}-cleavage-mediated counteraction of innate immunity did not suffice to block TLR3 and RLRs in Huh7 cells, and that more immunocompetent cell lines, as HepG2 and HepaRG, with an intact MDA5-LGP2 response, upregulate ISGs upon HAV infection. This was in contrast with the study investigating HAV-infected chimpanzees²¹² and from the hypotheses behind it, based on an active counteraction mechanism exerted by the HAV protease 3C and its precursors¹⁷³⁻¹⁷⁵. On the other hand, the *in vivo* infection in human liver chimeric mice in my study clearly showed that HAV (both wild-type and cell culture adapted) was indeed able to induce an innate immune response *in vivo*. This piece of data seems of valuable contribution, as this model offers lack of confounding adaptive immunity as well as a more or less structurally and functionally physiological environment which recalls the hepatotropic infection. But how can we correlate the similar innate immune induction observed in the mice with the different infection outcomes observed in patients?

Reviewing the scientific evidence presented in this dissertation, it is tempting to abide by the adage that “whatever happens early in a viral infection dictates what happens later on”³⁹⁶. Ideally, this would allow us to attribute the divergent outcomes of HAV and HCV infections to specific, distinct innate immune responses and interactions that are characteristic of these two viruses. However, the situation is not so dichotomous, particularly when considering the numerous limitations and potential artefacts I have highlighted throughout this dissertation. These complexities underscore the necessity for employing more relevant and accurate models.

Moving from the endpoint backwards, what is clear is that HAV gets robustly recognized by T cells, specifically with a contribution from CD8+ T³⁹⁷ cells and more significantly from CD4+ T cells^{308,398}. This response, epitope-specific, invariably leads to the spontaneous resolution of infection in more than 99.99% of the cases²⁹⁵. In addition, among the symptomatic HAV infections that can lead to hospitalization, a common outcome is transient liver injury¹⁶¹. This phenomenon has been associated with a reduction in regulatory T cells (T-regs) due to Fas-mediated apoptosis²⁵¹ and direct binding of HAV to TIM1 (a putative entry receptor) on T-regs¹⁶¹. Furthermore, clusters of cytotoxic T cells also infiltrate the liver in severe HepA cases²⁵¹. Additionally, inflammatory cytokines and interferon-stimulated genes (ISGs) like IL-6, IL-8, IL-18, IL-22, CXCL9, and CXCL10 are elevated in HAV patients¹⁶¹. Even genetic variations in host factors, like TIM1 and IL-18 binding protein (IL-18BP), have been associated with the severity of Hepatitis A infection^{399,400}. It's important to note that these mechanisms aren't mutually exclusive; they can operate individually or synergistically to induce liver damage in patients. But what we can notice is that, taken together, these findings paint a picture of a prompt and extremely effective intervention by the adaptive immune response, leading to successful clearance of the virus and, when exacerbated, leading to inflammation and damage²⁵¹. In contrast, with HCV infections, complications in patients arise when the persistent IFN and ISGs responses do not correlate with antigen recognition by T cells^{238,240,241}. This discrepancy results in T cell exhaustion, characterized by diminished proliferation, attenuated cytolytic activities, and curtailed cytokine production^{161,236}, shown also in the context of other virus infections, as LCMV, where continuous type I IFN production has been associated with an absence of initial T cell migration⁴⁰¹. Furthermore, a key mechanisms behind HCV persistence is antigen shift and subsequent lack of T cell recognition. Variability at antigen level is acquired by HCV thanks to the delay showed by T cells^{161,285}. Furthermore, unlike in HAV infections where regulatory T cells (T-regs) display a positive regulatory phenotype, in HCV infections there is an increase in the T-regs population which leads to suppression of T cells, and has been linked to the inability to resolve the infection¹⁶¹. To complicate the already defective defenses in chronic HCV, high basal level of ISGs are also linked to poor response to IFN- α treatment, due to an ISG15-ubiquitin-specific peptidase 18 (USP18)- mediated mechanisms²³⁹.

In addition to the mechanisms of HCV persistence which might be completely unrelated from innate immunity, IFN- λ polymorphisms have been recently shown to be closely tied to disease susceptibility and treatment success. Three major SNPs (*rs12979860*, *rs8099917*, and *rs368234815*) located near the *IFNL3* and *IFNL4* genes are in high linkage disequilibrium (non-randomly occurring in the population) and are linked with the HCV treatment response⁴⁰²⁻⁴⁰⁴. Six additional SNPs (*rs8105790*, *rs11881222*, *rs8103142*, *rs28416813*, *rs4803219*, *rs7248668*) have also been identified to have a significant association with sustained virological response⁴⁰⁵.

However, the mechanisms through which these SNPs influence the treatment outcome are not fully understood. One suggestion is that they might alter the transcriptional regulation of *IFNL3*. For example, the *rs8099917* SNP may influence *IFNL3* mRNA stability⁴⁰⁶, while *rs368234815* SNP could lead to the expression of *IFNL4* in ΔG variant carriers⁴⁰⁷, which results in increased ISGs levels and worsens the treatment outcome.

Moreover, these SNPs are not only important for HCV treatment but are also associated with spontaneous HCV clearance. It's also observed that allele frequencies of certain SNPs vary between individuals with European or African ancestry, with the favorable variants often predominating in the European population, correlating with better HCV clearance rates⁴⁰⁷.

Although the exact mechanisms causing these associations remain largely unknown, the predictive value of these IFNL SNPs extends beyond HCV. They have been described to be associated with various viral infections, including herpes, CMV retinitis, HIV, papilloma virus, HTLV, and RSV-associated bronchiolitis⁴⁰⁸⁻⁴¹⁰ as well as a role in inflammation and allergic responses, like asthma, due to their effect on immune cell behavior, reviewed in⁴¹¹.

As mentioned earlier, during acute HAV infection in chimpanzees, as identified through microarray assay in the only study comparing HAV and HCV-mediated innate immune responses, innate immunity seems to be scarcely activated²¹². With the exception of CXCL10 and Interferon-Stimulated Gene 20 kDa protein (ISG20), both dually regulated by IFN- α/β and IFN- γ , a low-level ISG induction is reported for HAV, limited to the first weeks of infection, subsiding before HAV RNA's peak presence in the liver. The initial Type I IFN response wanes before the liver sees peak HAV replication and the beginning of liver damage, at which point a Type II IFN (IFN- γ) response takes over²¹². Interestingly, in the same study it was noted that pDCs - being "professional" Type I IFN-producers and considered the major contributors to ISGs upregulation in the liver tissue⁹⁹ - were peaking shortly after infection to then disappear from the HAV-positive hepatocytes clusters; we know from literature that pDCs mainly identify viruses through endosomal TLR7 and TLR9, but in theory can also sense viral nucleic acids in the cytosol. But only enveloped virions (eHAV), and not viral RNA exosomes, have been imputed responsible for IFN- α induction¹⁹² and consequent robust ISG induction. Even though membrane envelopment protects HAV from neutralizing antibodies, it allows pDCs to detect HAV infection early, albeit limitedly¹⁹². A reason for this transient and inefficient action of pDCs in chimpanzees is not given²¹². This might represent a bottleneck, as previous research showed that pDCs / NK cells require the establishment of a contacting "synapse" of close contact between the infected hepatocytes and the innate immune cell, in the case of HCV^{412,413}. In the chimpanzee study, for unknown reasons the pDCs were not found close to the infection sites, letting me believe that there might be an important hinderance in the signaling leading to their recruitment, which is also not fully explained nor understood^{192,212}. Furthermore, another publication in recent years pointed out that different innate cell populations (pDCs, NK cells, monocytes) need to activate one another and interact, for a synergistic innate immune response to be robustly established⁴¹⁴; the absence of this mutual activation in the HAV-infected chimpanzees might also contribute to a decreased magnitude of ISGs.

Furthermore, several reports have previously observed that HCV activates, via TLR3, innate immunity in macrophages⁴¹⁵ and hepatic stellate cells⁴¹⁶; such observation have not been referred to HAV, and given the lack of TLR3 sensing evidenced by my results, this might indicate that, in general, in presence of a full set of hepatic cell populations, the HCV-induced ISGs magnitude could be higher compared to HAV *in vivo*.

Opposite to what claimed according to my *in vitro* results, it is worth considering that the humanized mice could show a phenotype which might be less physiological than the one observe in the chimpanzees. Indeed, these animals undergo loss of the murine hepatocytes, and are depleted of B and T cells; but they still harbor murine NK cells, Kupffer cells, NK cells, even if this was not thoroughly assessed (personal communication from the authors generating the model²⁸⁶). Yet, it is known because of an elegant study that signaling between human interferon and murine interferon receptor is extremely poor because of only about 50% sequence homology⁴¹⁷, and that even in “HybNAR mice”, reconstituted with human IFNAR receptors for type I IFNs, upon correct binding of human interferon, the downstream signaling shows a reduced magnitude⁴¹⁷. Nevertheless, this study excluded investigation on the type III IFN receptor, which might be more of relevance for HAV⁶⁵. It would be important to characterize the murine innate immune response using specific markers in the same samples investigated in this study.

In conclusion, my dissertation's findings lead to the proposal of two hypotheses. These hypotheses, while distinct, are not mutually exclusive and both require further exploration for comprehensive understanding.

The first, simpler idea would be that HAV is unable to efficiently abrogate innate immune responses, as illustrated in Figure77, where I recapitulate my findings: a partial adaptor proteins cleavage by HAV still leads to successful ISGs induction through MDA5-LGP2-mediated sensing (left panel), as opposed to HCV innate immune activation which relies on TLR3, given lack of TRIF cleavage, and not on RLRs, because of full MAVS abrogation (right panel). This would thus allow, in the case of HAV, the successful recruitment of adaptive immune cells and further clearance, while HCV would establish persistence through escape mechanisms of adaptive immunity (exacerbated by IFNs continuous flux, which leads to T cells exhaustion²³⁶). This hypothesis would then assume that the observed limited data from *in vivo* chimpanzee studies may not accurately reflect the true condition during HAV infection. Given the typically uncomplicated nature of HAV infection, access to liver biopsies from infected individuals is scarce, resulting in a lack of comprehensive data on this subject. Therefore, understanding the ISGs and IFNs scenarios *in vivo* upon HAV may necessitate further investigations using complex *in vivo* models. According to this model, the reason for HCV's persistence along with the outcome in the individual would solely lie on mechanisms which are distant from innate immune control, as antigen shift, delay in T cell response, T cell exhaustion and occurrence of IFN- λ SNPs in the population^{236,240,402,403,405,410}.

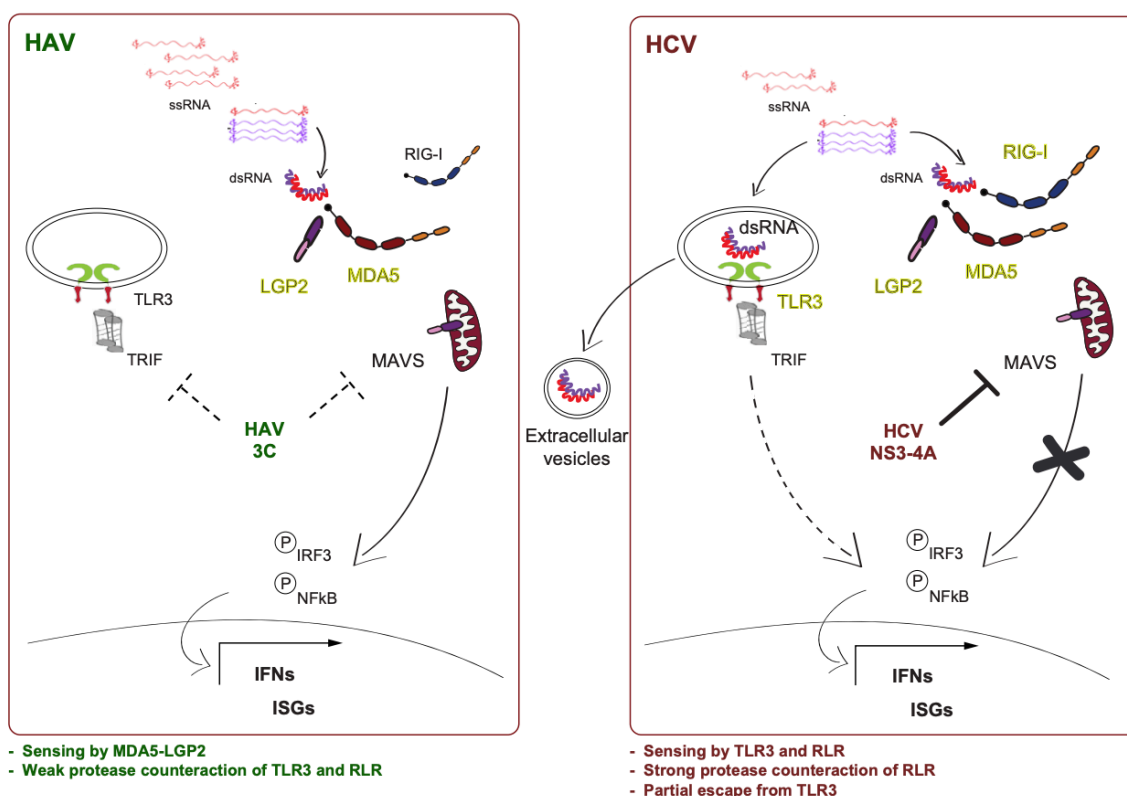


Figure 77. Model of intracellular innate immune induction and counteraction by HAV and HCV.

In my dissertation work I found that HAV induces an innate immune response in hepatocytes via MDA5/LGP2, with limited control of both pathways by proteolytic cleavage. HCV activates Toll-like receptor 3 and lacks TRIF cleavage, suggesting that this pathway mainly contributes to HCV-induced antiviral responses in hepatocytes.

The second hypothesis suggests that HAV may, instead, possess sophisticated mechanisms for innate immunity control, undetected in the models used during my research. These mechanisms could potentially consist of unexplored interactions (as the HAV 2B-IRF3 counteraction^{243,245,246} or the miR146-a5P induction²⁴⁷, which might be assessed in the future; or on the local control of pathways, involving a concentrated sub-cellular expression of proteins that may partially, yet significantly, inhibit innate immunity, as long as it takes for HAV to strongly replicate and shed in the feces for further spread. Altogether, HAV might not “need” to rely on establishing persistent infections; HAV and HCV are both recognized to have ancient origins^{418,419}. This evolutionary longevity brings into question their degree of adaptation, specifically to the liver, and what implications this adaptation holds for counteracting host immunity and facilitating viral dissemination. The underlying drivers of their evolution appear to diverge significantly based on their distinct transmission strategies. HAV, which is primarily spread through fecal contamination, seems to have evolved to gain on acute infection. This is evidenced by its non-lethal nature, which enhances its transmission potential, as a living host with an acute infection excretes more viral particles. Conversely, HCV, which typically relies on direct blood contact for transmission, would seemingly gain no evolutionary advantage from causing an acute infection. Since this transmission route often necessitates an interaction with a living, healthy individual, the virus seems to have evolved towards a more chronic infection strategy, enabling longer periods of potential transmission without rapidly compromising the host's health. These differing “interests” of HAV and HCV underpin the diverse strategies

that viruses have evolved to ensure their propagation, shaped by the balance between infection severity, host survival, and transmission opportunities.

These two ideas reflect the multifaceted nature of our understanding of HAV's interaction with the host immune system, and provide a foundation upon which further approaches can be built.

5.5 Future directions

To further elucidate the processes by which TRIF is cleaved by HAV and HCV, especially considering the limitations highlighted through the use of the RHIM deletion mutant, it may be beneficial to employ caspase knockout cell lines, in which the native form of TRIF would not trigger apoptosis. In addition, controlling the expression of TRIF via an inducible promoter or a weaker promoter such as ROSA26, could potentially moderate the expression level, and thereby decrease cytotoxicity levels, even within caspase-competent cell lines.

The use of caspase knockout cell lines might also be relevant to address the previously discussed phenotype of HCV indirect interference to TRIF, through NS4B induction of caspase activity³²⁸.

Given the discrepancies found in my data relative to the research by Qu et al., regarding the 3CD cleavage of TRIF¹⁷³, it may be worth introducing the TRIF cleavage-resistant mutant, there described, but regulated by a weaker promoter, into TRIF knockout cells. These cells could then be exposed to the HAV 3CD proteases or the HAV full-length virus. Although these experiments have been conducted before (Figure 39), they were either always performed with the delRHIM mutant or probably with a too low expression of TRIF, due to stable selection.

In addition, repeating the alanine scanning analysis could help to accurately identify the exact cleavage site, confirming or not the previous claims on Q554 – Q190. Docking attempts *in silico*, as well as FRET analysis of 3CD and TRIF, might serve to model and quantify the interaction of the 3C catalytic pocket with TRIF, which in absence of the canonical TRIF cleavage site might result inefficient. Additionally, generating an array of mutants for the 3D polymerase, which was believed able to redirect the 3C proteinase towards an uncanonical cleavage site, may provide a clearer understanding of the mechanism. This approach could potentially also highlight the conditions necessary for more efficient cleavage. In the presence of a 3CD „high cleaver” mutant, or TRIF „highly cleavable” mutant, it would be intriguing to then move to functional tests, aiming to, again, link the disruption of TRIF to augmented TLR3 interference. Furthermore, expressing the truncated mutants of TRIF corresponding to the single cleavage products might elucidate whether the molecules suffice to deliver the innate immune signaling. Last but not least, quantifying TRIF

cleavage in relevant samples from *in vivo* infections, as liver biopsies, would be a pivotal reproduction of the phenotypes observed *in cellulo*.

In parallel, one of the most intriguing topics to explore would still be the potential interaction between the endosomal TLR3 and HAV dsRNA which, basing on the data presented in this dissertation, might be absent. This could be obtained through RNAscope analysis, or Fluorescence in situ hybridization (FISH) aiming at labelling HAV dsRNA along with endosomal markers.

Given the concerns raised throughout the dissertation about the limitations of the Huh7 model, particularly its potential insufficiency in eliciting an effective innate immune response upon HAV infection, it would be prudent, and yielding more physiologically relevant insights, to focus efforts on endogenous TRIF detection in HepG2 or HepaRG cells, with endogenous tagging, knock-out and overexpression models.

Further, it may be beneficial to consider additional readouts. While IFIT1 and CXCL10 serve as excellent RLR-TLR3 downstream markers, the measurement of secreted IFN could potentially offer a more accurate depiction of the immune response, despite the challenge of its scarce presence in Huh7, particularly in absence of IRF7 (see *Appendix*). Moreover, other genes might have higher specific relevance for both HCV and HAV infections.

Unraveling the precise role of the PRRs presents another layer of complexity. Potential strategies to approach this might include working towards the identification of PRR-specific gene signatures, which have not yet been conclusively determined. This could be achieved through meticulous knock-out of selected pathways and subsequent RNA sequencing analysis upon stimulation. Such efforts could substantially contribute to our understanding of the intricate interplay between the diverse innate immune arms and their relevance in specifically HAV or HCV infections.

Considering the numerous reports on alternative counteraction mechanisms by HAV which are not based on the protease activity, it should be taken into account that they might prove to be highly relevant if studied in proper models. The hypothesis by Paulmann et al. and Fensterl et al. , built on HAV 2B interfering with IRF3 through potential interaction with MAVS, is not found confirmed through my data, in which I express the whole polyprotein in

infected cells without observing functional abrogation to poly(I:C) response, but might lay its foundation on different mechanisms, for example on the membrane rearrangements which are known to occur upon 2B expression: these might create hinderance for the replicative genomes and decrease of sensing, for instance. Uncovering the HAV dsRNA association with membranes and the formation of the replicase complex, so far understudied, could shed light on further innate immune evasion mechanisms.

Moreover, the authors observed an exacerbation of the 2B effect upon coexpression with 3ABC; expression of several combinations of HAV proteins might be contributing to a synergistic effect in influencing the activity of the RLR pathways, in ways that were by me not verifiable in the chosen readouts.

Moving again the perspective to more complex immune models, in my opinion co-culture studies in which mechanisms of innate immune cell recruitment and activation by HAV would be necessary to elucidate the intriguing phenotype observed in the chimpanzee. Such approach has been attempted, so far, exclusively with HAV subgenomic replicons⁴¹⁴.

Last but not least, and very importantly, matching the skepticism towards the chimpanzee model, the results by me evidenced in the SCID alb/uPA chimeric model used in this study, whose number was kept low for the difficulties bond to generation and maintenance of these mice, would benefit from larger cohorts, given the strong discrepancies in terms of mice health, survival, age at the time of infection and human repopulation success – besides the forementioned problem of great variability in the biopsy-derived PHH cultures, often impure or highly variable. In fact, for the observed infected chimpanzees - in which the main HCV-infected animals show an acute infection course, in which there might be a similar scenario, as with chronic infection, of high ISGs upregulation, but an opposite one in terms of adaptive immune response taking into place - crucially the number of animals is very limited, for obvious ethics- and funding-related reason, leading to evidences highly prone to lack of robustness. In the end, a simple and robust, fully immune competent animal model will be required to unravel the determinants of HAV and HCV clearance and persistence. For HCV, the Norway rat hepacivirus infection in rats and mice might provide some clarity^{420,421}. The HAV infection of mice is so far limited by the necessity to abrogate cell intrinsic

immunity to achieve efficient infection^{249,354}. Once, HAV mediated counteracting mechanisms are full understood, it might be possible to overcome this barrier.

Appendix

Supervised projects

1. Validation of a CRISPR-Cas9 KO library for potential TLR3 interactors

(M. Sc. Santa Olivera, March – June 2018 – Internship)

The aim of this work was testing a library of 50 potential candidates derived from a genome-wide knockout screen (Grünvogel et al., unpublished) targeting 10000 genes enriched by specific TLR3-mediated innate immune response in human hepatocytes. Upon siRNA testing in Huh7 Lunet, the selection of candidates was narrowed down to 4 potential TLR3 interactors.

4. Identification of RBM39 as a novel factor contributing to TLR3 signaling

(Dr. Arthur Lang, October 2018 – March 2020 – MD PhD Thesis)

This research was conducted with the goal of unraveling specific mechanisms of TLR3 induction in hepatocytes, where TLR3-mediated gene induction seems to differ from its cytosolic counterparts. Searching for potential, unique regulators of TLR3 signaling in hepatocytes, Grünvogel et al. conducted a genome-wide knockout screen and identified several candidate genes, which were further explored in this study. The RNA interference-based approach confirmed the role of one of the candidates, RBM39, in TLR3 signaling. Further research on RBM39, an RNA-binding protein, could enhance our understanding of antiviral immunity and offer a potential therapeutic target in viral infections.

5. Impact of HAV 3C proteolytical cleavage of NEMO on the innate immune response in human hepatocytes

(M. Sc. Helen Huang, October 2019 – December 2020 – Internship + Master's Thesis)

This work aimed at investigating how Hepatitis A virus (HAV), despite its high replication rate, causes only limited expression of interferon-stimulated genes (ISGs) by examining the role of the viral protease 3C in cleaving a crucial immune adaptor, NEMO. Methods used included overexpressing HAV 3C to detect NEMO cleavage, measuring mRNA levels of ISGs in liver cells, and determining the effect of NEMO deficiency on the NF- κ B pathway and HAV replication. The findings revealed incomplete cleavage of NEMO and stable ISGs and gene expression levels even with low NEMO expression. The study concludes that HAV may use alternative strategies to evade innate immunity in liver cells, as it doesn't significantly inhibit the NF- κ B pathway, potentially due to inefficient NEMO cleavage or the ability of minimal NEMO expression to trigger a full NF- κ B response.

6. The contribution of IRF3 to innate immune response in human hepatocytes

(Andreas Betz, March 2021 – April 2022, MD PhD Thesis)

This study aimed at determining potential factors impacting on the innate immune system playing a critical role in combating hepatitis virus infections A, C and D. It was found that expression of the human interferon regulatory factor 7 (IRF7) gene can enhance the interferon response to viral infection in hepatoma-based cell lines, Huh7 and Huh7.5, thus making these cells a more physiological model for viral infection. A global gene expression analysis revealed several interferon-stimulated genes dependent on toll-like receptor 3 signaling, and further research into this could provide a deeper understanding of innate immunity's role in hepatitis virus infection. Overall, the study presents a detailed analysis of the response to double-stranded RNA in hepatic cells and provides tools that could benefit future research into hepatitis and innate immunity.

Side projects

1) Secretion of HCV replication intermediates reduces activation of Toll-Like Receptor 3 in Hepatocytes

The project examined HCV's induction of innate immunity with regards to TLR3. The results revealed that HCV-infected cells secrete significant quantities of virus positive- and negative-strand RNAs within extracellular vesicles (EVs). Interestingly, a significant portion of the viral replication complexes and dsRNA was located in the endosomal compartment and multivesicular bodies, suggesting the exosomal pathway's role in the secretion of HCV replication intermediates. Blocking vesicle release in HCV-positive cells led to increased intracellular dsRNA levels, enhancing toll-like receptor 3 activation and suppressing HCV replication. Overall, the findings suggested a novel mechanism where HCV releases dsRNA intermediates in EVs, minimizing toll-like receptor 3 activation, thus potentially aiding in evading host immune responses and promoting viral persistence.⁸³

2) Biochemical and structural characterization of Hepatitis A Virus 2C reveals an unusual ribonuclease activity on single-stranded RNA

The role of the nonstructural protein 2C in Hepatitis A virus (HAV) replication is crucial, yet its specific function is not fully understood. Our collaborators detected an ATPase-independent nuclease function in HAV 2C that favors polyuridylic single-stranded RNAs. The crystal structure of an HAV 2C fragment was resolved to 2.2 Å, including an ATPase domain, a domain resembling enterovirus 2C zinc-finger (ZFER), and a C-terminal amphipathic helix (PBD). The PBD of HAV 2C slots into a hydrophobic pocket (Pocket) on an adjacent 2C, proving the criticality of this PBD-Pocket interaction for 2C operations. Acidic residues pivotal for the ribonuclease function were pinpointed, and my specific contribution was to show that mutations at these locations impede virus replication. Lastly, it was demonstrated that this ribonuclease activity is common among other picornavirus 2Cs. These revelations highlight a previously unrecognized function of picornavirus 2C and provide new insights into virus replication mechanics.

3) Extrahepatic sites of HAV replication

This ongoing research is focused on the exploration of potential extrahepatic sites for HAV replication. Initial insights were drawn from a study that detected HAV negative strand RNA in lymph nodes, tonsils, and salivary gland duct cells of HAV infected-cynomolgus monkeys¹⁹⁶, and another research which identified replication of enteroviruses in salivary gland duct cells, highlighting the possibility of transmission within mammary glands from pups to mothers⁴²². In an attempt to further understand this phenomenon, we initiated in vitro replication experiments using both the HAV HM175/18f strain and HAV wild-type extracted from patient stools, targeting the novel NS-SV-TT-DC human salivary gland cell line. Preliminary observations suggested a lack of permissiveness within these cells, coinciding with a robust innate immune response. Future directions for this project include the generation of knock-outs for the RLRs pathways, aiming to bolster HAV replication. Concurrently, we plan to evaluate mammary cells and conduct a thorough analysis of samples from the previous study¹⁹⁶. This endeavor aims to shed light on the broader replication sites of HAV, enriching our understanding of its pathogenesis and transmission routes.

Acknowledgements

This work would have not existed without a great deal of people who I had the privilege to be surrounded by during my doctoral research time.

First and foremost, my biggest gratitude goes to my mentor, Prof. Volker Lohmann, who took me under his wing and gave me the opportunity to explore innate immunity upon HAV and HCV under his (patient) supervision. Thanks to his decision, I got access to a thrilling environment where my curiosity could be constantly fed with challenges, some of them quite unpredictable and almost “impossible” ;) – exactly as I was wishing for myself when I started.

I am further indebted to Prof. Ralf Bartenschlager, who today I thank not only as my first examiner, but for his constant and insightful input during our department meetings and retreats, which together with his always fair and calm attitude won't by me ever be forgotten.

I would like to thank Dr. Viet Loan Dao Thi and Prof. Friedrich Frischknecht for having participated to my examination. I have great admiration for you and your work and it's an honor and a pleasure to be able to interface myself with you on the topic of my dissertation.

I am deeply indebted to my former supervisor, Dr. Yuri Koussov, who had a crucial role in training me as a virologist and in teaching me to understand and appreciate HAV. On these notes, I also take the occasion to thank the great collaborators I had - all thanks to Volker's vision - who helped us to reach the publication we desired. It was not only productive, but also very enriching from a human point of view! Thanks Suzanne, Tobias, Mathias, Philip, and especially thanks Rani and Laura, for your amazing work and friendship which went beyond sharing protocols and analyzing data.

My deepest gratitude goes further to many special members of our department who maybe do not know how much they did for me and how crucial their help for me was in certain occasions: Pilar, Fredy, Sandra, Ilka, Catherine, for always being there, like a lighthouse in the storm. I am overwhelmed with gratitude if I think at how much every single one of you gave me. Also thanks Sabine, for her smiles that rescued my many bad days, and Marie, for our funny talks about bright colors, coffee and oat milk. Thanks Uli, from the bottom of my heart, for being literally the kindest person I have ever met. Furthermore, I am so thankful to all the colleagues that I encountered daily and decided to share with me a kind word, an advice on difficult techniques and of course also complaints about the Mensa. It was good and very helpful to be immersed in the human variety of our department and to always recognize good virtues in everyone. Thanks AG Ruggieri, AG Bartenschlager, AG Urban and AG Binder, for helping , listening, talking and joking together. Huge gratitude goes also to alumni of the Molecular Virology who I had the privilege to be close to in the previous years, and that contributed strongly to my scientific and personal development: Philipp K., Ji-Young, Nadine, Margara, Chris Dächert, Vera, Julia, Katja, Mirko, Berati: I consider myself fortunate to have you as friends today.

On top of that, I am so blessed to have found in the Lohmann lab a real treasure: thank you Rahel, Cong Si, Helen, Teng-Feng, Arthur, Marit, Paul, Noemi, Philipp S. & Philipp R., Andreas, Christian, Robin and all of the current and former members, for giving unity to the group, for convincing me that my tiramisù is the best in the whole world and for enlightening my sometimes heavy spirit.

Science can be unforgiving and for those difficult moments (amplified by German weather and food dramas that only a Mediterranean soul knows!) I have been overwhelmed by the comforting presence of friends outside of work: my deepest gratitude goes to Eva, Massimiliano, Dolores, Rahel, Thore, Martha, Kim, Julia, Ulrich and Valentina, for having created a family around me when my family was far away. And to my real family who makes me always feel that they're here, standing

behind me and supporting me: my mother Serena, my sister Guenda, my nephew Vinci, my aunt and cousins.

To all my wonderful friends in Bari, Hamburg, Lübeck and Zürich: I owe you so much for keeping me in your lives despite the physical distance! This degree would not exist without your closeness. I would like to extend a heartfelt thank you to my beloved Cesare, for the unwavering support, extraordinary patience, and for truly recognizing and appreciating me just the same whether I hold a doctoral degree or not.

And lastly: it's my desire to dedicate this entire work to my father Davide, whose curiosity for science, selflessness, and zest for life inspire me to this day.

Publications

- 1) Grünvogel, **Colasanti**, Lee, Klöss, Belouzard, Reustle, Esser-Nobis, Hesebeck-Brinckmann, Mutz, Hoffmann, Mehrabi, Koschny, Vondran, Gotthardt, Schnitzler, Neumann-Haefelin, Thimme, Binder, Bartenschlager, Dubuisson, Dalpke, Lohmann. *Secretion of Hepatitis C Virus Replication Intermediates Reduces Activation of Toll Like Receptor 3 in Hepatocytes* – Gastroenterology, March 10th, 2018 – doi.org/10.1053/j.gastro.2018.03.020
- 2) Heuss†, Rothhaar†, Burm, Lee, Haselmann, Ströh, Ralfs, **Colasanti**, Tran, Schäfer, Schnitzler, Merle, Bartenschlager, Patel, Graw, Krey, Laketa, Meuleman, Lohmann. *A Hepatitis C virus genotype 1b post-transplant isolate with high replication efficiency in cell culture and its adaptation to infectious virus production in vitro and in vivo* – PloS Pathogens - June 6th, 2022 – doi.org/10.1371/journal.ppat.1010472 † = Equal contribution
- 3) Chen#, Wojdyla#, **Colasanti**#, Qin#, Wang, Lohmann & Cui. *Biochemical and Structural Characterization of Hepatitis A virus 2C Reveals Unusual Ribonuclease Activity on Single Stranded RNA* – Nucleic Acids Research, August 10th, 2022 – doi.org/10.1093/nar/gkac671 # = Equal contribution
- 4) **Colasanti**, Burm, Huang, Riedl, Traut, Gillich, Li, Corneillie, Faure-Dupuy, Grünvogel, Heide, Lee, Tran, Merle, Chironna, Vondran, Esser-Nobis, Binder, Bartenschlager, Heikenwälder, Meuleman, Lohmann - *Comparison of HAV and HCV infections in vivo and in vitro reveals distinct patterns of innate immune evasion and activation* – Journal of Hepatology, April 28th, 2023 - doi.org/10.1016/j.jhep.2023.04.023
- 5) Tran, Kersten, Diehl, Breinig, Yan, Poth, **Colasanti**, Riedl, Faure-Dupuy, Diehl, Verhoye, Li, Lingemann, Schult, Ahlén, Frelin, Kühnel, Breuhahn, Vondran, Meuleman, Heikenwälder, Schirmacher, Sällberg, Bartenschlager, Laketa, Tschaharganeh, Lohmann - *Phosphatidylinositol 4-kinase III alpha governs cytoskeletal organization for invasiveness of liver cancer cells* – [submitted](#)
- 6) Betz, Huang, Gu, **Colasanti**, Li, Gillich, Gnouamozi, Hesebeck-Brinckmann, Schlesner, Vondran, Bartenschlager, Urban, Binder, Lohmann – *IRF7 expression restores IFN-Beta induction in hepatoma-based cell lines* – [in preparation](#)
- 7) Huang, **Colasanti**, Li, Tran, Binder, Wohlleber, Lohmann. *Limited impact on the function of NF-kB Essential Modulator (NEMO) in Hepatitis A Virus-infected hepatocytes* – [in preparation](#)
- 8) Li, Lang, Traut, Grünvogel, **Colasanti**, Olivera Ugarte, Rothhaar, Willemsen, Springer, Piras, Huang, Willemsen, Stahl, Wohlleber, Pichlmair, Binder, Bartenschlager, Lohmann - *RBM39 orchestrates innate immunity by governing IRF3 and other key innate immune factors on transcription and alternative splicing activity* – [in preparation](#)

Contributions to conferences

1) GASL 2018 (Poster presentation)

Heidelberg, 21-23/02/2018

2) Schauinsland retreat 2018 (Oral presentation)

Oberried, 28-30/5/2018

3) TOLL Meeting 2018 (Poster presentation)

Porto, Portugal 08-11/6/2018

4) GfV 2019 (Poster presentation)

Düsseldorf, 20 – 23/03/2019

5) Schauinsland retreat 2019 (Oral presentation)

Oberried, 2-4/6/2019

6) Positive-Strand RNA Viruses Keystone Symposia (Poster presentation)

Killarney, Irland – 10 – 14/6/2019

7) HCV meeting 2019 (Oral presentation) * (Travel Award)

Seoul, South Korea – 05/10/2019 – 09/10/2019

8) HCV meeting 2021 (Poster presentation)

(Virtual) 6/7/2022 – 9/7/2021

9) GfV 2022 (Short oral presentation)

(Virtual) 27-29/03/2022

10) International TRR179 Symposium “Viral hepatitis and beyond: from basic science to cure” (Oral presentation)

Freiburg, May 29-31, 2022

11) Positive-Strand RNA Viruses Keystone Symposia (Poster presentation) * (NK and Irene Cheung Family Scholar' scholarship) –

Keystone, CO, USA – 18/06/2022 – 22/06/2022

12) HCV meeting 2022 (Poster presentation)

Ghent, Belgium - 05/07/2022 – 08/07/2022

13) Global Hepatitis Summit 2023 (Oral presentation)

Paris, France - 25/04/2023 – 28/04/2023

References

- 1 Piñeiro-Carrero, V. M. & Piñeiro, E. O. Liver. *Pediatrics* **113**, 1097-1106 (2004).
- 2 Cavalcanti de, A. M. A. & Martins, C. History of liver anatomy: Mesopotamian liver clay models. *HPB (Oxford)* **15**, 322-323 (2013). <https://doi.org/10.1111/j.1477-2574.2012.00555.x>
- 3 Orlandi, R., Cianci, N., Invernizzi, P., Cesana, G. & Riva, M. A. "I Miss My Liver." Nonmedical Sources in the History of Hepatocentrism. *Hepatology Communications* **2**, 986-993 (2018). <https://doi.org/https://doi.org/10.1002/hep4.1224>
- 4 Riva, M. A. *et al.* "The city of Hepar": rituals, gastronomy, and politics at the origins of the modern names for the liver. *J Hepatol* **55**, 1132-1136 (2011). <https://doi.org/10.1016/j.jhep.2011.05.011>
- 5 Racanelli, V. & Rehermann, B. The liver as an immunological organ. *Hepatology* **43**, S54-62 (2006). <https://doi.org/10.1002/hep.21060>
- 6 Kubes, P. & Jenne, C. Immune Responses in the Liver. *Annu Rev Immunol* **36**, 247-277 (2018). <https://doi.org/10.1146/annurev-immunol-051116-052415>
- 7 Heymann, F. & Tacke, F. Immunology in the liver--from homeostasis to disease. *Nat Rev Gastroenterol Hepatol* **13**, 88-110 (2016). <https://doi.org/10.1038/nrgastro.2015.200>
- 8 Freitas-Lopes, M. A., Mafra, K., David, B. A., Carvalho-Gontijo, R. & Menezes, G. B. Differential Location and Distribution of Hepatic Immune Cells. *Cells* **6** (2017). <https://doi.org/10.3390/cells6040048>
- 9 Panwar, A., Das, P. & Tan, L. P. 3D Hepatic Organoid-Based Advancements in LIVER Tissue Engineering. *Bioengineering* **8**, 185 (2021).
- 10 Wohlleber, D. & Knolle, P. A. The role of liver sinusoidal cells in local hepatic immune surveillance. *Clin Transl Immunology* **5**, e117 (2016). <https://doi.org/10.1038/cti.2016.74>
- 11 Schenten, D. & Medzhitov, R. The control of adaptive immune responses by the innate immune system. *Adv Immunol* **109**, 87-124 (2011). <https://doi.org/10.1016/b978-0-12-387664-5.00003-0>
- 12 Gao, B., Jeong, W. I. & Tian, Z. Liver: An organ with predominant innate immunity. *Hepatology* **47**, 729-736 (2008). <https://doi.org/10.1002/hep.22034>
- 13 McCaughan, G. W., Bowen, D. G. & Bertolino, P. J. Induction Phase of Spontaneous Liver Transplant Tolerance. *Front Immunol* **11**, 1908 (2020). <https://doi.org/10.3389/fimmu.2020.01908>
- 14 Zheng, M. & Tian, Z. Liver-Mediated Adaptive Immune Tolerance. *Front Immunol* **10**, 2525 (2019). <https://doi.org/10.3389/fimmu.2019.02525>
- 15 Horst, A. K., Neumann, K., Diehl, L. & Tiegs, G. Modulation of liver tolerance by conventional and nonconventional antigen-presenting cells and regulatory immune cells. *Cellular & Molecular Immunology* **13**, 277-292 (2016). <https://doi.org/10.1038/cmi.2015.112>
- 16 Karvellas, C. J. *et al.* HBV-Associated Acute Liver Failure After Immunosuppression and Risk of Death. *Clin Gastroenterol Hepatol* **15**, 113-122 (2017). <https://doi.org/10.1016/j.cgh.2016.06.008>
- 17 Samonakis, D. N., Germani, G. & Burroughs, A. K. Immunosuppression and HCV recurrence after liver transplantation. *J Hepatol* **56**, 973-983 (2012). <https://doi.org/10.1016/j.jhep.2011.06.031>
- 18 Kita, H., Mackay, I. R., Van De Water, J. & Gershwin, M. E. The lymphoid liver: considerations on pathways to autoimmune injury. *Gastroenterology* **120**, 1485-1501 (2001). <https://doi.org/10.1053/gast.2001.22441>
- 19 Kenneth Murphy, C. W. *Janeway's Immunobiology*. (2018).
- 20 Wang, C. *et al.* Macrophage Polarization and Its Role in Liver Disease. *Front Immunol* **12**, 803037 (2021). <https://doi.org/10.3389/fimmu.2021.803037>

- 21 Mikulak, J., Bruni, E., Oriolo, F., Di Vito, C. & Mavilio, D. Hepatic Natural Killer Cells: Organ-Specific Sentinels of Liver Immune Homeostasis and Physiopathology. *Front Immunol* **10**, 946 (2019). <https://doi.org:10.3389/fimmu.2019.00946>
- 22 Knolle, P. A. & Wöhleber, D. Immunological functions of liver sinusoidal endothelial cells. *Cell Mol Immunol* **13**, 347-353 (2016). <https://doi.org:10.1038/cmi.2016.5>
- 23 Zhou, Z., Xu, M. J. & Gao, B. Hepatocytes: a key cell type for innate immunity. *Cell Mol Immunol* **13**, 301-315 (2016). <https://doi.org:10.1038/cmi.2015.97>
- 24 Lung, T. *et al.* The complement system in liver diseases: Evidence-based approach and therapeutic options. *J Transl Autoimmun* **2**, 100017 (2019). <https://doi.org:10.1016/j.jtauto.2019.100017>
- 25 Cheng, M. L., Nakib, D., Perciani, C. T. & MacParland, S. A. The immune niche of the liver. *Clin Sci (Lond)* **135**, 2445-2466 (2021). <https://doi.org:10.1042/cs20190654>
- 26 Goubau, D., Deddouche, S. & Reis e Sousa, C. Cytosolic sensing of viruses. *Immunity* **38**, 855-869 (2013). <https://doi.org:10.1016/j.immuni.2013.05.007>
- 27 Shaw, A. E. *et al.* Fundamental properties of the mammalian innate immune system revealed by multispecies comparison of type I interferon responses. *PLoS Biol* **15**, e2004086 (2017). <https://doi.org:10.1371/journal.pbio.2004086>
- 28 Schoggins, J. W. Interferon-Stimulated Genes: What Do They All Do? *Annu Rev Virol* **6**, 567-584 (2019). <https://doi.org:10.1146/annurev-virology-092818-015756>
- 29 Crosse, K. M., Monson, E. A., Beard, M. R. & Helbig, K. J. Interferon-Stimulated Genes as Enhancers of Antiviral Innate Immune Signaling. *J Innate Immun* **10**, 85-93 (2018). <https://doi.org:10.1159/000484258>
- 30 Boxx, G. M. & Cheng, G. The Roles of Type I Interferon in Bacterial Infection. *Cell Host Microbe* **19**, 760-769 (2016). <https://doi.org:10.1016/j.chom.2016.05.016>
- 31 Suriawinata, A. A. & Thung, S. N. Acute and chronic hepatitis. *Semin Diagn Pathol* **23**, 132-148 (2006). <https://doi.org:10.1053/j.semmp.2006.11.001>
- 32 Younossi, Z. *et al.* Global Perspectives on Nonalcoholic Fatty Liver Disease and Nonalcoholic Steatohepatitis. *Hepatology* **69**, 2672-2682 (2019). <https://doi.org:10.1002/hep.30251>
- 33 EASL Clinical Practice Guidelines: Autoimmune hepatitis. *J Hepatol* **63**, 971-1004 (2015). <https://doi.org:10.1016/j.jhep.2015.06.030>
- 34 Jefferies, M., Rauff, B., Rashid, H., Lam, T. & Rafiq, S. Update on global epidemiology of viral hepatitis and preventive strategies. *World J Clin Cases* **6**, 589-599 (2018). <https://doi.org:10.12998/wjcc.v6.i13.589>
- 35 Wang, R. & Xie, Z. Non-hepatotropic viral hepatitis and its causative pathogens: The ongoing need for monitoring in children with severe acute hepatitis of unknown etiology. *Pediatr Investig* **6**, 151-155 (2022). <https://doi.org:10.1002/ped4.12340>
- 36 Tahaei, S. M., Mohebbi, S. R. & Zali, M. R. Enteric hepatitis viruses. *Gastroenterol Hepatol Bed Bench* **5**, 7-15 (2012).
- 37 Louten, J. in *Essential Human Virology (Second Edition)* (ed Jennifer Louten) 231-253 (Academic Press, 2023).
- 38 Brennan, J. J. & Gilmore, T. D. Evolutionary Origins of Toll-like Receptor Signaling. *Mol Biol Evol* **35**, 1576-1587 (2018). <https://doi.org:10.1093/molbev/msy050>
- 39 Lange, C. *et al.* Defining the origins of the NOD-like receptor system at the base of animal evolution. *Mol Biol Evol* **28**, 1687-1702 (2011). <https://doi.org:10.1093/molbev/msq349>
- 40 Motta, V., Soares, F., Sun, T. & Philpott, D. J. NOD-like receptors: versatile cytosolic sentinels. *Physiol Rev* **95**, 149-178 (2015). <https://doi.org:10.1152/physrev.00009.2014>
- 41 Pisetsky, D. S. The origin and properties of extracellular DNA: from PAMP to DAMP. *Clin Immunol* **144**, 32-40 (2012). <https://doi.org:10.1016/j.clim.2012.04.006>
- 42 Medzhitov, R. & Janeway, C. A., Jr. Innate immunity: the virtues of a nonclonal system of recognition. *Cell* **91**, 295-298 (1997). [https://doi.org:10.1016/s0092-8674\(00\)80412-2](https://doi.org:10.1016/s0092-8674(00)80412-2)
- 43 An, P. *et al.* Hepatocyte mitochondria-derived danger signals directly activate hepatic

- stellate cells and drive progression of liver fibrosis. *Nature Communications* **11**, 2362 (2020). <https://doi.org:10.1038/s41467-020-16092-0>
- 44 O'Neill, L. A. & Bowie, A. G. Sensing and signaling in antiviral innate immunity. *Curr Biol* **20**, R328-333 (2010). <https://doi.org:10.1016/j.cub.2010.01.044>
- 45 Kawai, T. & Akira, S. The roles of TLRs, RLRs and NLRs in pathogen recognition. *Int Immunol* **21**, 317-337 (2009). <https://doi.org:10.1093/intimm/dxp017>
- 46 Hornung, V. *et al.* 5'-Triphosphate RNA is the ligand for RIG-I. *Science* **314**, 994-997 (2006). <https://doi.org:10.1126/science.1132505>
- 47 Kato, H. *et al.* Length-dependent recognition of double-stranded ribonucleic acids by retinoic acid-inducible gene-I and melanoma differentiation-associated gene 5. *J Exp Med* **205**, 1601-1610 (2008). <https://doi.org:10.1084/jem.20080091>
- 48 Komuro, A. & Horvath, C. M. RNA- and virus-independent inhibition of antiviral signaling by RNA helicase LGP2. *J Virol* **80**, 12332-12342 (2006). <https://doi.org:10.1128/jvi.01325-06>
- 49 Pippig, D. A. *et al.* The regulatory domain of the RIG-I family ATPase LGP2 senses double-stranded RNA. *Nucleic Acids Res* **37**, 2014-2025 (2009). <https://doi.org:10.1093/nar/gkp059>
- 50 Takahashi, K. *et al.* Solution structures of cytosolic RNA sensor MDA5 and LGP2 C-terminal domains: identification of the RNA recognition loop in RIG-I-like receptors. *J Biol Chem* **284**, 17465-17474 (2009). <https://doi.org:10.1074/jbc.M109.007179>
- 51 Bamming, D. & Horvath, C. M. Regulation of signal transduction by enzymatically inactive antiviral RNA helicase proteins MDA5, RIG-I, and LGP2. *J Biol Chem* **284**, 9700-9712 (2009). <https://doi.org:10.1074/jbc.M807365200>
- 52 Duic, I. *et al.* Viral RNA recognition by LGP2 and MDA5, and activation of signaling through step-by-step conformational changes. *Nucleic Acids Res* **48**, 11664-11674 (2020). <https://doi.org:10.1093/nar/gkaa935>
- 53 Zhu, Z. *et al.* LGP2 Promotes Type I Interferon Production To Inhibit PRRSV Infection via Enhancing MDA5-Mediated Signaling. *Journal of Virology* **97**, e01843-01822 (2023). <https://doi.org:doi:10.1128/jvi.01843-22>
- 54 Murali, A. *et al.* Structure and Function of LGP2, a DE(D/H) Helicase That Regulates the Innate Immunity Response ^{*}. *Journal of Biological Chemistry* **283**, 15825-15833 (2008). <https://doi.org:10.1074/jbc.M800542200>
- 55 Xie, P. TRAF molecules in cell signaling and in human diseases. *J Mol Signal* **8**, 7 (2013). <https://doi.org:10.1186/1750-2187-8-7>
- 56 Parisien, J.-P. *et al.* RNA sensor LGP2 inhibits TRAF ubiquitin ligase to negatively regulate innate immune signaling. *EMBO reports* **19**, e45176 (2018). <https://doi.org:https://doi.org/10.15252/embr.201745176>
- 57 Ashley, C. L., Abendroth, A., McSharry, B. P. & Slobedman, B. Interferon-Independent Upregulation of Interferon-Stimulated Genes during Human Cytomegalovirus Infection is Dependent on IRF3 Expression. *Viruses* **11** (2019). <https://doi.org:10.3390/v11030246>
- 58 Hartmann, G. Nucleic Acid Immunity. *Adv Immunol* **133**, 121-169 (2017). <https://doi.org:10.1016/bs.ai.2016.11.001>
- 59 Chen, M. *et al.* Targeting nuclear acid-mediated immunity in cancer immune checkpoint inhibitor therapies. *Signal Transduction and Targeted Therapy* **5**, 270 (2020). <https://doi.org:10.1038/s41392-020-00347-9>
- 60 Kawai, T. & Akira, S. The role of pattern-recognition receptors in innate immunity: update on Toll-like receptors. *Nat Immunol* **11**, 373-384 (2010). <https://doi.org:10.1038/ni.1863>
- 61 Faul, E. J. *et al.* Rabies virus infection induces type I interferon production in an IPS-1 dependent manner while dendritic cell activation relies on IFNAR signaling. *PLoS Pathog* **6**, e1001016 (2010). <https://doi.org:10.1371/journal.ppat.1001016>
- 62 Loo, Y. M. *et al.* Distinct RIG-I and MDA5 signaling by RNA viruses in innate immunity. *J Virol* **82**, 335-345 (2008). <https://doi.org:10.1128/jvi.01080-07>
- 63 Sakuragi, S., Liao, H., Yajima, K., Fujiwara, S. & Nakamura, H. Rubella Virus Triggers Type I

- Interferon Antiviral Response in Cultured Human Neural Cells: Involvement in the Control of Viral Gene Expression and Infectious Progeny Production. *International Journal of Molecular Sciences* **23**, 9799 (2022).
- 64 Feng, Q. *et al.* MDA5 detects the double-stranded RNA replicative form in picornavirus-infected cells. *Cell Rep* **2**, 1187-1196 (2012). <https://doi.org:10.1016/j.celrep.2012.10.005>
- 65 Sung, P. S. *et al.* CXCL10 is produced in hepatitis A virus-infected cells in an IRF3-dependent but IFN-independent manner. *Sci Rep* **7**, 6387 (2017). <https://doi.org:10.1038/s41598-017-06784-x>
- 66 McCartney, S. A. *et al.* MDA-5 recognition of a murine norovirus. *PLoS Pathog* **4**, e1000108 (2008). <https://doi.org:10.1371/journal.ppat.1000108>
- 67 Yin, X. *et al.* MDA5 Governs the Innate Immune Response to SARS-CoV-2 in Lung Epithelial Cells. *Cell Rep* **34**, 108628 (2021). <https://doi.org:10.1016/j.celrep.2020.108628>
- 68 Hiet, M. S. *et al.* Control of temporal activation of hepatitis C virus-induced interferon response by domain 2 of nonstructural protein 5A. *J Hepatol* **63**, 829-837 (2015). <https://doi.org:10.1016/j.jhep.2015.04.015>
- 69 Kato, H., Takahasi, K. & Fujita, T. RIG-I-like receptors: cytoplasmic sensors for non-self RNA. *Immunol Rev* **243**, 91-98 (2011). <https://doi.org:10.1111/j.1600-065X.2011.01052.x>
- 70 Chen, Y., Lin, J., Zhao, Y., Ma, X. & Yi, H. Toll-like receptor 3 (TLR3) regulation mechanisms and roles in antiviral innate immune responses. *J Zhejiang Univ Sci B* **22**, 609-632 (2021). <https://doi.org:10.1631/jzus.B2000808>
- 71 Keikha, M. *et al.* HCV genotypes and their determinative role in hepatitis C treatment. *Virusdisease* **31**, 235-240 (2020). <https://doi.org:10.1007/s13337-020-00592-0>
- 72 Wang, Y., Liu, L., Davies, D. R. & Segal, D. M. Dimerization of Toll-like receptor 3 (TLR3) is required for ligand binding. *J Biol Chem* **285**, 36836-36841 (2010). <https://doi.org:10.1074/jbc.M110.167973>
- 73 Seya, T., Matsumoto, M., Ebihara, T. & Oshiumi, H. Functional evolution of the TICAM-1 pathway for extrinsic RNA sensing. *Immunol Rev* **227**, 44-53 (2009). <https://doi.org:10.1111/j.1600-065X.2008.00723.x>
- 74 Levy, D. E., Marié, I. J. & Durbin, J. E. Induction and function of type I and III interferon in response to viral infection. *Curr Opin Virol* **1**, 476-486 (2011). <https://doi.org:10.1016/j.coviro.2011.11.001>
- 75 Sasai, M. *et al.* Direct binding of TRAF2 and TRAF6 to TICAM-1/TRIF adaptor participates in activation of the Toll-like receptor 3/4 pathway. *Mol Immunol* **47**, 1283-1291 (2010). <https://doi.org:10.1016/j.molimm.2009.12.002>
- 76 Sasai, M. *et al.* NAK-associated protein 1 participates in both the TLR3 and the cytoplasmic pathways in type I IFN induction. *J Immunol* **177**, 8676-8683 (2006). <https://doi.org:10.4049/jimmunol.177.12.8676>
- 77 Osterlund, P. I., Pietilä, T. E., Veckman, V., Kotenko, S. V. & Julkunen, I. IFN regulatory factor family members differentially regulate the expression of type III IFN (IFN-lambda) genes. *J Immunol* **179**, 3434-3442 (2007). <https://doi.org:10.4049/jimmunol.179.6.3434>
- 78 Alexopoulou, L., Holt, A. C., Medzhitov, R. & Flavell, R. A. Recognition of double-stranded RNA and activation of NF-kappaB by Toll-like receptor 3. *Nature* **413**, 732-738 (2001). <https://doi.org:10.1038/35099560>
- 79 Han, K. J. *et al.* Mechanisms of the TRIF-induced interferon-stimulated response element and NF-kappaB activation and apoptosis pathways. *J Biol Chem* **279**, 15652-15661 (2004). <https://doi.org:10.1074/jbc.M311629200>
- 80 Kaiser, W. J. & Offermann, M. K. Apoptosis induced by the toll-like receptor adaptor TRIF is dependent on its receptor interacting protein homotypic interaction motif. *J Immunol* **174**, 4942-4952 (2005). <https://doi.org:10.4049/jimmunol.174.8.4942>
- 81 Ruckdeschel, K. *et al.* Signaling of apoptosis through TLRs critically involves toll/IL-1 receptor domain-containing adapter inducing IFN-beta, but not MyD88, in bacteria-infected murine

- macrophages. *J Immunol* **173**, 3320-3328 (2004).
<https://doi.org:10.4049/jimmunol.173.5.3320>
- 82 ViralZone. SIB Swiss Institute of Bioinformatics.
- 83 Grunvogel, O. *et al.* Secretion of Hepatitis C Virus Replication Intermediates Reduces
Activation of Toll-Like Receptor 3 in Hepatocytes. *Gastroenterology* **154**, 2237-2251 e2216
(2018). <https://doi.org:10.1053/j.gastro.2018.03.020>
- 84 Brinton, M. A. Replication cycle and molecular biology of the West Nile virus. *Viruses* **6**, 13-
53 (2013). <https://doi.org:10.3390/v6010013>
- 85 Gagliardi, T. B. *et al.* Rhinovirus C replication is associated with the endoplasmic reticulum
and triggers cytopathic effects in an in vitro model of human airway epithelium. *PLoS Pathog*
18, e1010159 (2022). <https://doi.org:10.1371/journal.ppat.1010159>
- 86 Tissari, J., Sirén, J., Meri, S., Julkunen, I. & Matikainen, S. IFN-alpha enhances TLR3-mediated
antiviral cytokine expression in human endothelial and epithelial cells by up-regulating TLR3
expression. *J Immunol* **174**, 4289-4294 (2005). <https://doi.org:10.4049/jimmunol.174.7.4289>
- 87 Xu, L. *et al.* RIG-I is a key antiviral interferon-stimulated gene against hepatitis E virus
regardless of interferon production. *Hepatology* **65**, 1823-1839 (2017).
<https://doi.org:https://doi.org/10.1002/hep.29105>
- 88 Li, Y. *et al.* MDA5 against enteric viruses through induction of interferon-like response
partially via the JAK-STAT cascade. *Antiviral Research* **176**, 104743 (2020).
<https://doi.org:https://doi.org/10.1016/j.antiviral.2020.104743>
- 89 Vercammen, E., Staal, J. & Beyaert, R. Sensing of viral infection and activation of innate
immunity by toll-like receptor 3. *Clin Microbiol Rev* **21**, 13-25 (2008).
<https://doi.org:10.1128/cmr.00022-07>
- 90 Gal-Ben-Ari, S., Barrera, I., Ehrlich, M. & Rosenblum, K. PKR: A Kinase to Remember. *Front*
Mol Neurosci **11**, 480 (2018). <https://doi.org:10.3389/fnmol.2018.00480>
- 91 McAllister, C. S. & Samuel, C. E. The RNA-activated protein kinase enhances the induction of
interferon-beta and apoptosis mediated by cytoplasmic RNA sensors. *J Biol Chem* **284**, 1644-
1651 (2009). <https://doi.org:10.1074/jbc.M807888200>
- 92 Turton, H. A., Thompson, A. A. R. & Farkas, L. RNA Signaling in Pulmonary Arterial
Hypertension—A Double-Stranded Sword. *International Journal of Molecular Sciences* **21**,
3124 (2020).
- 93 Chow, K. T., Gale Jr, M. & Loo, Y.-M. RIG-I and other RNA sensors in antiviral immunity.
Annual review of immunology **36**, 667-694 (2018).
- 94 Friedman, R. L., Manly, S. P., McMahon, M., Kerr, I. M. & Stark, G. R. Transcriptional and
posttranscriptional regulation of interferon-induced gene expression in human cells. *Cell* **38**,
745-755 (1984). [https://doi.org:10.1016/0092-8674\(84\)90270-8](https://doi.org:10.1016/0092-8674(84)90270-8)
- 95 Paun, A. & Pitha, P. M. The IRF family, revisited. *Biochimie* **89**, 744-753 (2007).
<https://doi.org:10.1016/j.biochi.2007.01.014>
- 96 Lee, A. J. & Ashkar, A. A. The Dual Nature of Type I and Type II Interferons. *Frontiers in*
Immunology **9** (2018). <https://doi.org:10.3389/fimmu.2018.02061>
- 97 Lazear, H. M., Schoggins, J. W. & Diamond, M. S. Shared and Distinct Functions of Type I and
Type III Interferons. *Immunity* **50**, 907-923 (2019).
<https://doi.org:10.1016/j.immuni.2019.03.025>
- 98 Pien, G. C., Satoskar, A. R., Takeda, K., Akira, S. & Biron, C. A. Cutting edge: selective IL-18
requirements for induction of compartmental IFN-gamma responses during viral infection. *J*
Immunol **165**, 4787-4791 (2000). <https://doi.org:10.4049/jimmunol.165.9.4787>
- 99 Bencze, D., Fekete, T. & Pázmándi, K. Type I Interferon Production of Plasmacytoid Dendritic
Cells under Control. *Int J Mol Sci* **22** (2021). <https://doi.org:10.3390/ijms22084190>
- 100 de Weerd, N. A., Samarajiwa, S. A. & Hertzog, P. J. Type I interferon receptors: biochemistry
and biological functions. *J Biol Chem* **282**, 20053-20057 (2007).
<https://doi.org:10.1074/jbc.R700006200>

- 101 Levy, D. E. Whence interferon? Variety in the production of interferon in response to viral
infection. *J Exp Med* **195**, F15-18 (2002). <https://doi.org:10.1084/jem.20020075>
- 102 Doyle, S. E. *et al.* Interleukin-29 uses a type 1 interferon-like program to promote antiviral
responses in human hepatocytes. *Hepatology* **44**, 896-906 (2006).
<https://doi.org:10.1002/hep.21312>
- 103 Kotenko, S. V. *et al.* IFN-lambdas mediate antiviral protection through a distinct class II
cytokine receptor complex. *Nat Immunol* **4**, 69-77 (2003). <https://doi.org:10.1038/ni875>
- 104 Bustamante, J. *et al.* Novel primary immunodeficiencies revealed by the investigation of
paediatric infectious diseases. *Curr Opin Immunol* **20**, 39-48 (2008).
<https://doi.org:10.1016/j.coi.2007.10.005>
- 105 Dupuis, S. *et al.* Impaired response to interferon-alpha/beta and lethal viral disease in
human STAT1 deficiency. *Nat Genet* **33**, 388-391 (2003). <https://doi.org:10.1038/ng1097>
- 106 Ito, T. *et al.* Differential regulation of human blood dendritic cell subsets by IFNs. *J Immunol*
166, 2961-2969 (2001). <https://doi.org:10.4049/jimmunol.166.5.2961>
- 107 Thomas, E. & Saito, T. Special Issue "IFN-Independent ISG Expression and its Role in Antiviral
Cell-Intrinsic Innate Immunity". *Viruses* **11** (2019). <https://doi.org:10.3390/v11110981>
- 108 Ohmori, Y. & Hamilton, T. A. Cooperative interaction between interferon (IFN) stimulus
response element and kappa B sequence motifs controls IFN gamma- and
lipopolysaccharide-stimulated transcription from the murine IP-10 promoter. *J Biol Chem*
268, 6677-6688 (1993).
- 109 Imaizumi, T. *et al.* Involvement of retinoic acid-inducible gene-I in the IFN- γ /STAT1
signalling pathway in BEAS-2B cells. *Eur Respir J* **25**, 1077-1083 (2005).
<https://doi.org:10.1183/09031936.05.00102104>
- 110 Oslund, K. L. *et al.* Synergistic up-regulation of CXCL10 by virus and IFN γ in human airway
epithelial cells. *PLoS One* **9**, e100978 (2014). <https://doi.org:10.1371/journal.pone.0100978>
- 111 Pichlmair, A. *et al.* IFIT1 is an antiviral protein that recognizes 5'-triphosphate RNA. *Nat*
Immunol **12**, 624-630 (2011). <https://doi.org:10.1038/ni.2048>
- 112 Fleith, R. C. *et al.* IFIT3 and IFIT2/3 promote IFIT1-mediated translation inhibition by
enhancing binding to non-self RNA. *Nucleic Acids Research* **46**, 5269-5285 (2018).
<https://doi.org:10.1093/nar/gky191>
- 113 Abbas, Y. M., Pichlmair, A., Gónna, M. W., Superti-Furga, G. & Nagar, B. Structural basis for
viral 5'-PPP-RNA recognition by human IFIT proteins. *Nature* **494**, 60-64 (2013).
<https://doi.org:10.1038/nature11783>
- 114 Cole, A. M. *et al.* Cutting edge: IFN-inducible ELR- CXC chemokines display defensin-like
antimicrobial activity. *J Immunol* **167**, 623-627 (2001).
<https://doi.org:10.4049/jimmunol.167.2.623>
- 115 Kubo, Y. *et al.* A cDNA fragment of hepatitis C virus isolated from an implicated donor of
post-transfusion non-A, non-B hepatitis in Japan. *Nucleic Acids Res* **17**, 10367-10372 (1989).
<https://doi.org:10.1093/nar/17.24.10367>
- 116 Robinson, W. S. The Enigma of Non-A, Non-B Hepatitis. *The Journal of Infectious Diseases*
145, 387-395 (1982).
- 117 Schlaak, J. F. Current Therapy of Chronic Viral Hepatitis B, C and D. *J Pers Med* **13** (2023).
<https://doi.org:10.3390/jpm13060964>
- 118 Dore, G. J. & Bajis, S. Hepatitis C virus elimination: laying the foundation for achieving 2030
targets. *Nature Reviews Gastroenterology & Hepatology* **18**, 91-92 (2021).
<https://doi.org:10.1038/s41575-020-00392-3>
- 119 Axley, P., Ahmed, Z., Ravi, S. & Singal, A. K. Hepatitis C Virus and Hepatocellular Carcinoma: A
Narrative Review. *J Clin Transl Hepatol* **6**, 79-84 (2018).
<https://doi.org:10.14218/jcth.2017.00067>
- 120 Global prevalence and genotype distribution of hepatitis C virus infection in 2015: a
modelling study. *Lancet Gastroenterol Hepatol* **2**, 161-176 (2017).

- [https://doi.org/10.1016/s2468-1253\(16\)30181-9](https://doi.org/10.1016/s2468-1253(16)30181-9)
- 121 Martell, M. *et al.* Hepatitis C virus (HCV) circulates as a population of different but closely related genomes: quasispecies nature of HCV genome distribution. *J Virol* **66**, 3225-3229 (1992). <https://doi.org/10.1128/jvi.66.5.3225-3229.1992>
- 122 Zeng, H. *et al.* Direct-acting Antiviral in the Treatment of Chronic Hepatitis C: Bonuses and Challenges. *Int J Med Sci* **17**, 892-902 (2020). <https://doi.org/10.7150/ijms.43079>
- 123 Tsubota, A., Fujise, K., Namiki, Y. & Tada, N. Peginterferon and ribavirin treatment for hepatitis C virus infection. *World J Gastroenterol* **17**, 419-432 (2011). <https://doi.org/10.3748/wjg.v17.i4.419>
- 124 Kish, T., Aziz, A. & Sorio, M. Hepatitis C in a New Era: A Review of Current Therapies. *P t* **42**, 316-329 (2017).
- 125 Heidelberg, U. GEOGRAPHIC PATTERN OF HCV PREVALENCE. (2023).
- 126 Prentoe, J. *et al.* Antigenic and immunogenic evaluation of permutations of soluble hepatitis C virus envelope protein E2 and E1 antigens. *PLOS ONE* **16**, e0255336 (2021). <https://doi.org/10.1371/journal.pone.0255336>
- 127 Lindenbach, B. D. Virion assembly and release. *Curr Top Microbiol Immunol* **369**, 199-218 (2013). https://doi.org/10.1007/978-3-642-27340-7_8
- 128 Murray, C. L., Jones, C. T. & Rice, C. M. Architects of assembly: roles of Flaviviridae non-structural proteins in virion morphogenesis. *Nat Rev Microbiol* **6**, 699-708 (2008). <https://doi.org/10.1038/nrmicro1928>
- 129 Griffin, S. D. C. *et al.* A conserved basic loop in hepatitis C virus p7 protein is required for amantadine-sensitive ion channel activity in mammalian cells but is dispensable for localization to mitochondria. *J Gen Virol* **85**, 451-461 (2004). <https://doi.org/10.1099/vir.0.19634-0>
- 130 Pallaoro, M. *et al.* Characterization of the hepatitis C virus NS2/3 processing reaction by using a purified precursor protein. *J Virol* **75**, 9939-9946 (2001). <https://doi.org/10.1128/jvi.75.20.9939-9946.2001>
- 131 Waxman, L., Whitney, M., Pollok, B. A., Kuo, L. C. & Darke, P. L. Host cell factor requirement for hepatitis C virus enzyme maturation. *Proc Natl Acad Sci U S A* **98**, 13931-13935 (2001). <https://doi.org/10.1073/pnas.241510898>
- 132 Bartenschlager, R., Penin, F., Lohmann, V. & André, P. Assembly of infectious hepatitis C virus particles. *Trends in Microbiology* **19**, 95-103 (2011). <https://doi.org/10.1016/j.tim.2010.11.005>
- 133 Paul, D., Hoppe, S., Saher, G., Krijnse-Locker, J. & Bartenschlager, R. Morphological and biochemical characterization of the membranous hepatitis C virus replication compartment. *J Virol* **87**, 10612-10627 (2013). <https://doi.org/10.1128/jvi.01370-13>
- 134 Moradpour, D., Penin, F. & Rice, C. M. Replication of hepatitis C virus. *Nat Rev Microbiol* **5**, 453-463 (2007). <https://doi.org/10.1038/nrmicro1645>
- 135 Anggakusuma *et al.* Hepacivirus NS3/4A Proteases Interfere with MAVS Signaling in both Their Cognate Animal Hosts and Humans: Implications for Zoonotic Transmission. *J Virol* **90**, 10670-10681 (2016). <https://doi.org/10.1128/JVI.01634-16>
- 136 Bartenschlager, R., Ahlborn-Laake, L., Mous, J. & Jacobsen, H. Kinetic and structural analyses of hepatitis C virus polyprotein processing. *J Virol* **68**, 5045-5055 (1994). <https://doi.org/10.1128/jvi.68.8.5045-5055.1994>
- 137 Ferreira, A. R. *et al.* Hepatitis C virus NS3-4A inhibits the peroxisomal MAVS-dependent antiviral signalling response. *J Cell Mol Med* **20**, 750-757 (2016). <https://doi.org/10.1111/jcmm.12801>
- 138 Li, K. *et al.* Immune evasion by hepatitis C virus NS3/4A protease-mediated cleavage of the Toll-like receptor 3 adaptor protein TRIF. *Proc Natl Acad Sci U S A* **102**, 2992-2997 (2005). <https://doi.org/10.1073/pnas.0408824102>
- 139 Egger, D. *et al.* Expression of hepatitis C virus proteins induces distinct membrane alterations

- including a candidate viral replication complex. *J Virol* **76**, 5974-5984 (2002).
<https://doi.org:10.1128/jvi.76.12.5974-5984.2002>
- 140 Moradpour, D., Penin, F. & Rice, C. M. Replication of hepatitis C virus. *Nature Reviews*
Microbiology **5**, 453-463 (2007). <https://doi.org:10.1038/nrmicro1645>
- 141 Lohmann, V. Hepatitis C virus cell culture models: an encomium on basic research paving the
road to therapy development. *Medical Microbiology and Immunology* **208**, 3-24 (2019).
<https://doi.org:10.1007/s00430-018-0566-x>
- 142 Albecka, A. *et al.* Role of low-density lipoprotein receptor in the hepatitis C virus life cycle.
Hepatology **55**, 998-1007 (2012). <https://doi.org:10.1002/hep.25501>
- 143 Zeisel, M. B., Felmlee, D. J. & Baumert, T. F. Hepatitis C virus entry. *Curr Top Microbiol*
Immunol **369**, 87-112 (2013). https://doi.org:10.1007/978-3-642-27340-7_4
- 144 Chang, K.-S., Jiang, J., Cai, Z. & Luo, G. Human Apolipoprotein E Is Required for Infectivity and
Production of Hepatitis C Virus in Cell Culture. *Journal of Virology* **81**, 13783-13793 (2007).
<https://doi.org:doi:10.1128/jvi.01091-07>
- 145 Evans, M. J. *et al.* Claudin-1 is a hepatitis C virus co-receptor required for a late step in entry.
Nature **446**, 801-805 (2007). <https://doi.org:10.1038/nature05654>
- 146 Pileri, P. *et al.* Binding of hepatitis C virus to CD81. *Science* **282**, 938-941 (1998).
<https://doi.org:10.1126/science.282.5390.938>
- 147 Ploss, A. & Evans, M. J. Hepatitis C virus host cell entry. *Curr Opin Virol* **2**, 14-19 (2012).
<https://doi.org:10.1016/j.coviro.2011.12.007>
- 148 Heo, T. H., Lee, S. M., Bartosch, B., Cosset, F. L. & Kang, C. Y. Hepatitis C virus E2 links soluble
human CD81 and SR-B1 protein. *Virus Res* **121**, 58-64 (2006).
<https://doi.org:10.1016/j.virusres.2006.04.002>
- 149 Penin, F., Dubuisson, J., Rey, F. A., Moradpour, D. & Pawlotsky, J. M. Structural biology of
hepatitis C virus. *Hepatology* **39**, 5-19 (2004). <https://doi.org:10.1002/hep.20032>
- 150 Twu, W. I. *et al.* Contribution of autophagy machinery factors to HCV and SARS-CoV-2
replication organelle formation. *Cell Rep* **37**, 110049 (2021).
<https://doi.org:10.1016/j.celrep.2021.110049>
- 151 Romero-Brey, I. *et al.* Three-Dimensional Architecture and Biogenesis of Membrane
Structures Associated with Hepatitis C Virus Replication. *PLOS Pathogens* **8**, e1003056
(2012). <https://doi.org:10.1371/journal.ppat.1003056>
- 152 Vieyres, G. & Pietschmann, T. HCV Pit Stop at the Lipid Droplet: Refuel Lipids and Put on a
Lipoprotein Coat before Exit. *Cells* **8** (2019).
- 153 Saeed, M. *et al.* SEC14L2 enables pan-genotype HCV replication in cell culture. *Nature* **524**,
471-475 (2015). <https://doi.org:10.1038/nature14899>
- 154 Berger, K. L., Kelly, S. M., Jordan, T. X., Tartell, M. A. & Randall, G. Hepatitis C virus stimulates
the phosphatidylinositol 4-kinase III alpha-dependent phosphatidylinositol 4-phosphate
production that is essential for its replication. *J Virol* **85**, 8870-8883 (2011).
<https://doi.org:10.1128/jvi.00059-11>
- 155 Germain, M.-A. *et al.* Elucidating novel hepatitis C virus–host interactions using combined
mass spectrometry and functional genomics approaches. *Molecular & Cellular Proteomics*
13, 184-203 (2014).
- 156 Tellinghuisen, T. L., Foss, K. L. & Treadaway, J. Regulation of hepatitis C virion production via
phosphorylation of the NS5A protein. *PLoS Pathog* **4**, e1000032 (2008).
<https://doi.org:10.1371/journal.ppat.1000032>
- 157 Grassi, G. *et al.* Hepatitis C virus relies on lipoproteins for its life cycle. *World J Gastroenterol*
22, 1953-1965 (2016). <https://doi.org:10.3748/wjg.v22.i6.1953>
- 158 Shrivastava, S. *et al.* Knockdown of Autophagy Inhibits Infectious Hepatitis C Virus Release by
the Exosomal Pathway. *J Virol* **90**, 1387-1396 (2016). <https://doi.org:10.1128/jvi.02383-15>
- 159 Ariumi, Y. *et al.* The ESCRT system is required for hepatitis C virus production. *PLoS One* **6**,
e14517 (2011). <https://doi.org:10.1371/journal.pone.0014517>

- 160 Gerold, G. & Pietschmann, T. The HCV Life Cycle: In vitro Tissue Culture Systems and Therapeutic Targets. *Digestive Diseases* **32**, 525-537 (2014).
<https://doi.org:10.1159/000360830>
- 161 Shin, E. C., Sung, P. S. & Park, S. H. Immune responses and immunopathology in acute and chronic viral hepatitis. *Nat Rev Immunol* **16**, 509-523 (2016).
<https://doi.org:10.1038/nri.2016.69>
- 162 Foster, M. A. *et al.* Widespread Hepatitis A Outbreaks Associated with Person-to-Person Transmission - United States, 2016-2020. *MMWR Morb Mortal Wkly Rep* **71**, 1229-1234 (2022). <https://doi.org:10.15585/mmwr.mm7139a1>
- 163 Hepatitis A Outbreaks in Developed Countries: Detection, Control, and Prevention. *Foodborne Pathogens and Disease* **17**, 166-171 (2020).
<https://doi.org:10.1089/fpd.2019.2648>
- 164 Kroneman, A. *et al.* Usability of the international HAVNet hepatitis A virus database for geographical annotation, backtracing and outbreak detection. *Eurosurveillance* **23**, 1700802 (2018). <https://doi.org:https://doi.org/10.2807/1560-7917.ES.2018.23.37.1700802>
- 165 Organization, W. H. World Health Organization 2021. Global progress report on HIV, viral hepatitis and sexually transmitted infections. . (2021).
- 166 Wells, R., Fisher, D., Fenaughty, A., Cagle, H. & Jaffe, A. Hepatitis A prevalence among injection drug users. *Clin Lab Sci* **19**, 12-17 (2006).
- 167 Scholz, E., Heinricy, U. & Flehmig, B. Acid stability of hepatitis A virus. *J Gen Virol* **70 (Pt 9)**, 2481-2485 (1989). <https://doi.org:10.1099/0022-1317-70-9-2481>
- 168 Zhu, L. & Zhang, X. Hepatitis A virus exhibits a structure unique among picornaviruses. *Protein Cell* **6**, 79-80 (2015). <https://doi.org:10.1007/s13238-014-0103-7>
- 169 McKnight, K. L. & Lemon, S. M. Hepatitis A Virus Genome Organization and Replication Strategy. *Cold Spring Harb Perspect Med* **8** (2018).
<https://doi.org:10.1101/cshperspect.a033480>
- 170 Seipelt, J. *et al.* The structures of picornaviral proteinases. *Virus Res* **62**, 159-168 (1999).
[https://doi.org:10.1016/s0168-1702\(99\)00043-x](https://doi.org:10.1016/s0168-1702(99)00043-x)
- 171 Kusov, Y. Y. & Gauss-Müller, V. In vitro RNA binding of the hepatitis A virus proteinase 3C (HAV 3Cpro) to secondary structure elements within the 5' terminus of the HAV genome. *Rna* **3**, 291-302 (1997).
- 172 Kusov, Y. & Gauss-Müller, V. Improving Proteolytic Cleavage at the 3A/3B Site of the Hepatitis A Virus Polyprotein Impairs Processing and Particle Formation, and the Impairment Can Be Complemented in<i>trans</i> by 3AB and 3ABC. *Journal of Virology* **73**, 9867-9878 (1999). <https://doi.org:doi:10.1128/jvi.73.12.9867-9878.1999>
- 173 Qu, L. *et al.* Disruption of TLR3 signaling due to cleavage of TRIF by the hepatitis A virus protease-polymerase processing intermediate, 3CD. *PLoS Pathog* **7**, e1002169 (2011).
<https://doi.org:10.1371/journal.ppat.1002169>
- 174 Wang, D. *et al.* Hepatitis A Virus 3C Protease Cleaves NEMO To Impair Induction of Beta Interferon. *Journal of Virology* **88**, 10252-10258 (2014).
<https://doi.org:doi:10.1128/JVI.00869-14>
- 175 Yang, Y. *et al.* Disruption of innate immunity due to mitochondrial targeting of a picornaviral protease precursor. *Proc Natl Acad Sci U S A* **104**, 7253-7258 (2007).
<https://doi.org:10.1073/pnas.0611506104>
- 176 Kusov, Y. Y., Morace, G., Probst, C. & Gauss-Müller, V. Interaction of hepatitis A virus (HAV) precursor proteins 3AB and 3ABC with the 5' and 3' termini of the HAV RNA. *Virus Research* **51**, 151-157 (1997). [https://doi.org:https://doi.org/10.1016/S0168-1702\(97\)00089-0](https://doi.org:https://doi.org/10.1016/S0168-1702(97)00089-0)
- 177 Vijay Kumar, S. D., Shahid Jameel. The biology and pathogenesis of hepatitis viruses. *Current Science* **98(3):312-325** (2010).
- 178 Jecht, M., Probst, C. & Gauss-Müller, V. Membrane permeability induced by hepatitis A virus proteins 2B and 2BC and proteolytic processing of HAV 2BC. *Virology* **252**, 218-227 (1998).

- <https://doi.org:10.1006/viro.1998.9451>
179 Zhang, X. *et al.* T-Cell Immunoglobulin and Mucin Domain 1 (TIM-1) Is a Functional Entry Factor for Tick-Borne Encephalitis Virus. *mBio* **13**, e0286021 (2022).
<https://doi.org:10.1128/mbio.02860-21>
- 180 Brunton, B. *et al.* TIM-1 serves as a receptor for Ebola virus in vivo, enhancing viremia and pathogenesis. *PLoS Negl Trop Dis* **13**, e0006983 (2019).
<https://doi.org:10.1371/journal.pntd.0006983>
- 181 Costafreda, M. I. & Kaplan, G. HAVCR1 (CD365) and Its Mouse Ortholog Are Functional Hepatitis A Virus (HAV) Cellular Receptors That Mediate HAV Infection. *J Virol* **92** (2018).
<https://doi.org:10.1128/jvi.02065-17>
- 182 Das, A., Maury, W. & Lemon, S. M. TIM1 (HAVCR1): an Essential "Receptor" or an "Accessory Attachment Factor" for Hepatitis A Virus? *J Virol* **93** (2019).
<https://doi.org:10.1128/jvi.01793-18>
- 183 Das, A. *et al.* Gangliosides are essential endosomal receptors for quasi-enveloped and naked hepatitis A virus. *Nat Microbiol* **5**, 1069-1078 (2020). <https://doi.org:10.1038/s41564-020-0727-8>
- 184 Pintó, R. M. *et al.* Hepatitis A Virus Codon Usage: Implications for Translation Kinetics and Capsid Folding. *Cold Spring Harb Perspect Med* **8** (2018).
<https://doi.org:10.1101/cshperspect.a031781>
- 185 Schultz, D. E., Hardin, C. C. & Lemon, S. M. Specific Interaction of Glyceraldehyde 3-Phosphate Dehydrogenase with the 5'-Nontranslated RNA of Hepatitis A Virus*. *Journal of Biological Chemistry* **271**, 14134-14142 (1996).
<https://doi.org:https://doi.org/10.1074/jbc.271.24.14134>
- 186 Yin, J. & Bergmann, E. M. Hepatitis A Virus Picornain 3C.
187 Teterina, N. L., Bienz, K., Egger, D., Gorbalenya, A. E. & Ehrenfeld, E. Induction of intracellular membrane rearrangements by HAV proteins 2C and 2BC. *Virology* **237**, 66-77 (1997).
<https://doi.org:10.1006/viro.1997.8775>
- 188 Baggen, J., Thibaut, H. J., Strating, J. R. P. M. & van Kuppeveld, F. J. M. The life cycle of non-polio enteroviruses and how to target it. *Nature Reviews Microbiology* **16**, 368-381 (2018).
<https://doi.org:10.1038/s41579-018-0005-4>
- 189 Li, Y. *et al.* The ZCCHC14/TENT4 complex is required for hepatitis A virus RNA synthesis. *Proceedings of the National Academy of Sciences* **119**, e2204511119 (2022).
<https://doi.org:10.1073/pnas.2204511119>
- 190 Esser-Nobis, K., Harak, C., Schult, P., Kusov, Y. & Lohmann, V. Novel perspectives for hepatitis A virus therapy revealed by comparative analysis of hepatitis C virus and hepatitis A virus RNA replication. *Hepatology* **62**, 397-408 (2015). <https://doi.org:10.1002/hep.27847>
- 191 Rivera-Serrano, E. E., González-López, O., Das, A. & Lemon, S. M. Cellular entry and uncoating of naked and quasi-enveloped human hepatoviruses. *eLife* **8**, e43983 (2019).
<https://doi.org:10.7554/eLife.43983>
- 192 Feng, Z. *et al.* Human pDCs preferentially sense enveloped hepatitis A virions. *J Clin Invest* **125**, 169-176 (2015). <https://doi.org:10.1172/jci77527>
- 193 Jiang, W. *et al.* Hepatitis A virus structural protein pX interacts with ALIX and promotes the secretion of virions and foreign proteins through exosome-like vesicles. *J Extracell Vesicles* **9**, 1716513 (2020). <https://doi.org:10.1080/20013078.2020.1716513>
- 194 La Bella, G. *et al.* Food-Borne Viruses in Shellfish: Investigation on Norovirus and HAV Presence in Apulia (SE Italy). *Food Environ Virol* **9**, 179-186 (2017).
<https://doi.org:10.1007/s12560-016-9273-1>
- 195 Jacobsen, K. H. Globalization and the Changing Epidemiology of Hepatitis A Virus. *Cold Spring Harb Perspect Med* **8** (2018). <https://doi.org:10.1101/cshperspect.a031716>
- 196 Amado, L. A. *et al.* Experimental hepatitis A virus (HAV) infection in cynomolgus monkeys (*Macaca fascicularis*): evidence of active extrahepatic site of HAV replication. *Int J Exp Pathol*

- 91, 87-97 (2010). <https://doi.org:10.1111/j.1365-2613.2009.00699.x>
- 197 Asher, L. V. *et al.* Pathogenesis of hepatitis A in orally inoculated owl monkeys (*Aotus*
trivirgatus). *J Med Virol* **47**, 260-268 (1995). <https://doi.org:10.1002/jmv.1890470312>
- 198 Kim, Y. *et al.* Broad-spectrum antivirals against 3C or 3C-like proteases of picornaviruses,
noroviruses, and coronaviruses. *J Virol* **86**, 11754-11762 (2012).
<https://doi.org:10.1128/jvi.01348-12>
- 199 Tan, J. *et al.* 3C protease of enterovirus 68: structure-based design of Michael acceptor
inhibitors and their broad-spectrum antiviral effects against picornaviruses. *J Virol* **87**, 4339-
4351 (2013). <https://doi.org:10.1128/jvi.01123-12>
- 200 Li, Y. *et al.* The ZCCHC14/TENT4 complex is required for hepatitis A virus RNA synthesis. *Proc*
Natl Acad Sci U S A **119**, e2204511119 (2022). <https://doi.org:10.1073/pnas.2204511119>
- 201 Kanda, T. *et al.* Cell Culture Systems and Drug Targets for Hepatitis A Virus Infection. *Viruses*
12 (2020). <https://doi.org:10.3390/v12050533>
- 202 Lemon, S. Hepatitis A virus: current concepts of the molecular virology, immunobiology and
approaches to vaccine development. *Reviews in Medical Virology* **2**, 73-87 (1992).
- 203 Melgaco, J. G. *et al.* A single dose of inactivated hepatitis A vaccine promotes HAV-specific
memory cellular response similar to that induced by a natural infection. *Vaccine* **33**, 3813-
3820 (2015). <https://doi.org:10.1016/j.vaccine.2015.06.099>
- 204 Sung, J. J. Epidemiology of hepatitis A in Asia and experience with the HAV vaccine in Hong
Kong. *J Viral Hepat* **7 Suppl 1**, 27-28 (2000). [https://doi.org:10.1046/j.1365-
2893.2000.00012.x](https://doi.org:10.1046/j.1365-2893.2000.00012.x)
- 205 Cao, X. *et al.* MDA5 plays a critical role in interferon response during hepatitis C virus
infection. *J Hepatol* **62**, 771-778 (2015). <https://doi.org:10.1016/j.jhep.2014.11.007>
- 206 Saito, T. *et al.* Regulation of innate antiviral defenses through a shared repressor domain in
RIG-I and LGP2. *Proc Natl Acad Sci U S A* **104**, 582-587 (2007).
<https://doi.org:10.1073/pnas.0606699104>
- 207 Khvalevsky, E., Rivkin, L., Rachmilewitz, J., Galun, E. & Giladi, H. TLR3 signaling in a hepatoma
cell line is skewed towards apoptosis. *J Cell Biochem* **100**, 1301-1312 (2007).
<https://doi.org:10.1002/jcb.21119>
- 208 Qu, L. & Lemon, S. M. Hepatitis A and hepatitis C viruses: divergent infection outcomes
marked by similarities in induction and evasion of interferon responses. *Semin Liver Dis* **30**,
319-332 (2010). <https://doi.org:10.1055/s-0030-1267534>
- 209 Schöbel, A., Rösch, K. & Herker, E. Functional innate immunity restricts Hepatitis C Virus
infection in induced pluripotent stem cell-derived hepatocytes. *Sci Rep* **8**, 3893 (2018).
<https://doi.org:10.1038/s41598-018-22243-7>
- 210 Wieland, S. *et al.* Simultaneous detection of hepatitis C virus and interferon stimulated gene
expression in infected human liver. *Hepatology* **59**, 2121-2130 (2014).
<https://doi.org:10.1002/hep.26770>
- 211 Lanford, R. E., Bigger, C., Bassett, S. & Klimpel, G. The Chimpanzee Model of Hepatitis C Virus
Infections. *ILAR Journal* **42**, 117-126 (2001). <https://doi.org:10.1093/ilar.42.2.117>
- 212 Lanford, R. E. *et al.* Acute hepatitis A virus infection is associated with a limited type I
interferon response and persistence of intrahepatic viral RNA. *Proc Natl Acad Sci U S A* **108**,
11223-11228 (2011). <https://doi.org:10.1073/pnas.1101939108>
- 213 Bender, S. *et al.* Activation of Type I and III Interferon Response by Mitochondrial and
Peroxisomal MAVS and Inhibition by Hepatitis C Virus. *PLoS Pathog* **11**, e1005264 (2015).
<https://doi.org:10.1371/journal.ppat.1005264>
- 214 Ferreira, A. R., Ramos, B., Nunes, A. & Ribeiro, D. Hepatitis C Virus: Evading the Intracellular
Innate Immunity. *Journal of Clinical Medicine* **9**, 790 (2020).
- 215 Brass, V. *et al.* Structural determinants for membrane association and dynamic organization
of the hepatitis C virus NS3-4A complex. *Proc Natl Acad Sci U S A* **105**, 14545-14550 (2008).
<https://doi.org:10.1073/pnas.0807298105>

- 216 Horner, S. M., Liu, H. M., Park, H. S., Briley, J. & Gale, M., Jr. Mitochondrial-associated endoplasmic reticulum membranes (MAM) form innate immune synapses and are targeted by hepatitis C virus. *Proc Natl Acad Sci U S A* **108**, 14590-14595 (2011). <https://doi.org/10.1073/pnas.1110133108>
- 217 Kolykhalov, A. A., Agapov, E. V. & Rice, C. M. Specificity of the hepatitis C virus NS3 serine protease: effects of substitutions at the 3/4A, 4A/4B, 4B/5A, and 5A/5B cleavage sites on polyprotein processing. *J Virol* **68**, 7525-7533 (1994). <https://doi.org/10.1128/jvi.68.11.7525-7533.1994>
- 218 Li, X. D., Sun, L., Seth, R. B., Pineda, G. & Chen, Z. J. Hepatitis C virus protease NS3/4A cleaves mitochondrial antiviral signaling protein off the mitochondria to evade innate immunity. *Proc Natl Acad Sci U S A* **102**, 17717-17722 (2005). <https://doi.org/10.1073/pnas.0508531102>
- 219 Loo, Y. M. *et al.* Viral and therapeutic control of IFN-beta promoter stimulator 1 during hepatitis C virus infection. *Proc Natl Acad Sci U S A* **103**, 6001-6006 (2006). <https://doi.org/10.1073/pnas.0601523103>
- 220 Meylan, E. *et al.* Cardif is an adaptor protein in the RIG-I antiviral pathway and is targeted by hepatitis C virus. *Nature* **437**, 1167-1172 (2005). <https://doi.org/10.1038/nature04193>
- 221 Ferreon, J. C., Ferreon, A. C. M., Li, K. & Lemon, S. M. Molecular Determinants of TRIF Proteolysis Mediated by the Hepatitis C Virus NS3/4A Protease*. *Journal of Biological Chemistry* **280**, 20483-20492 (2005). <https://doi.org/https://doi.org/10.1074/jbc.M500422200>
- 222 Dansako, H., Ikeda, M. & Kato, N. Limited suppression of the interferon-beta production by hepatitis C virus serine protease in cultured human hepatocytes. *FEBS J* **274**, 4161-4176 (2007). <https://doi.org/10.1111/j.1742-4658.2007.05942.x>
- 223 Jones, C. T. *et al.* Real-time imaging of hepatitis C virus infection using a fluorescent cell-based reporter system. *Nat Biotechnol* **28**, 167-171 (2010). <https://doi.org/10.1038/nbt.1604>
- 224 Otsuka, M. *et al.* Interaction between the HCV NS3 protein and the host TBK1 protein leads to inhibition of cellular antiviral responses. *Hepatology* **41**, 1004-1012 (2005). <https://doi.org/10.1002/hep.20666>
- 225 Oshiumi, H., Miyashita, M., Matsumoto, M. & Seya, T. A Distinct Role of Riplet-Mediated K63-Linked Polyubiquitination of the RIG-I Repressor Domain in Human Antiviral Innate Immune Responses. *PLOS Pathogens* **9**, e1003533 (2013). <https://doi.org/10.1371/journal.ppat.1003533>
- 226 Taylor, D. R., Shi, S. T., Romano, P. R., Barber, G. N. & Lai, M. M. C. Inhibition of the Interferon- Inducible Protein Kinase PKR by HCV E2 Protein. *Science* **285**, 107-110 (1999). <https://doi.org/doi:10.1126/science.285.5424.107>
- 227 Gale, M., Jr. *et al.* Control of PKR protein kinase by hepatitis C virus nonstructural 5A protein: molecular mechanisms of kinase regulation. *Mol Cell Biol* **18**, 5208-5218 (1998). <https://doi.org/10.1128/mcb.18.9.5208>
- 228 Çevik, R. E. *et al.* Hepatitis C Virus NS5A Targets Nucleosome Assembly Protein NAP1L1 To Control the Innate Cellular Response. *J Virol* **91** (2017). <https://doi.org/10.1128/jvi.00880-17>
- 229 Joo, M. *et al.* Hepatitis C virus core protein suppresses NF-kappaB activation and cyclooxygenase-2 expression by direct interaction with IkappaB kinase beta. *J Virol* **79**, 7648-7657 (2005). <https://doi.org/10.1128/jvi.79.12.7648-7657.2005>
- 230 Liao, Q. J. *et al.* Hepatitis C virus non-structural 5A protein can enhance full-length core protein-induced nuclear factor-kappaB activation. *World J Gastroenterol* **11**, 6433-6439 (2005). <https://doi.org/10.3748/wjg.v11.i41.6433>
- 231 Dolganiuc, A. *et al.* Hepatitis C Virus Core and Nonstructural Protein 3 Proteins Induce Pro- and Anti-inflammatory Cytokines and Inhibit Dendritic Cell Differentiation1. *The Journal of Immunology* **170**, 5615-5624 (2003). <https://doi.org/10.4049/jimmunol.170.11.5615>
- 232 Qi, H. *et al.* Systematic identification of anti-interferon function on hepatitis C virus genome

- reveals p7 as an immune evasion protein. *Proceedings of the National Academy of Sciences* **114**, 2018-2023 (2017). <https://doi.org/doi:10.1073/pnas.1614623114>
- 233 Jarret, A. *et al.* Hepatitis-C-virus-induced microRNAs dampen interferon-mediated antiviral signaling. *Nat Med* **22**, 1475-1481 (2016). <https://doi.org/10.1038/nm.4211>
- 234 Murai, K. *et al.* Induction of Selenoprotein P mRNA during Hepatitis C Virus Infection Inhibits RIG-I-Mediated Antiviral Immunity. *Cell Host Microbe* **25**, 588-601.e587 (2019). <https://doi.org/10.1016/j.chom.2019.02.015>
- 235 Holz, L. & Rehmann, B. T cell responses in hepatitis C virus infection: historical overview and goals for future research. *Antiviral Res* **114**, 96-105 (2015). <https://doi.org/10.1016/j.antiviral.2014.11.009>
- 236 Hofmann, M., Tauber, C., Hensel, N. & Thimme, R. CD8(+) T Cell Responses during HCV Infection and HCC. *J Clin Med* **10** (2021). <https://doi.org/10.3390/jcm10050991>
- 237 Jo, J. *et al.* Analysis of CD8+ T-cell-mediated inhibition of hepatitis C virus replication using a novel immunological model. *Gastroenterology* **136**, 1391-1401 (2009). <https://doi.org/10.1053/j.gastro.2008.12.034>
- 238 Sarasin-Filipowicz, M. *et al.* Interferon signaling and treatment outcome in chronic hepatitis C. *Proc Natl Acad Sci U S A* **105**, 7034-7039 (2008). <https://doi.org/10.1073/pnas.0707882105>
- 239 Sung, P. S. *et al.* IFN- λ 4 potently blocks IFN- α signalling by ISG15 and USP18 in hepatitis C virus infection. *Scientific Reports* **7**, 3821 (2017). <https://doi.org/10.1038/s41598-017-04186-7>
- 240 Chen, Q. *et al.* Interferon lambda 4 impairs hepatitis C viral antigen presentation and attenuates T cell responses. *Nat Commun* **12**, 4882 (2021). <https://doi.org/10.1038/s41467-021-25218-x>
- 241 Terczynska-Dyla, E. *et al.* Reduced IFNlambda4 activity is associated with improved HCV clearance and reduced expression of interferon-stimulated genes. *Nat Commun* **5**, 5699 (2014). <https://doi.org/10.1038/ncomms6699>
- 242 Xu, C., Chen, J. & Chen, X. Host Innate Immunity Against Hepatitis Viruses and Viral Immune Evasion. *Frontiers in Microbiology* **12** (2021). <https://doi.org/10.3389/fmicb.2021.740464>
- 243 Brack, K. *et al.* Hepatitis A virus inhibits cellular antiviral defense mechanisms induced by double-stranded RNA. *J Virol* **76**, 11920-11930 (2002). <https://doi.org/10.1128/jvi.76.23.11920-11930.2002>
- 244 Dotzauer, A., Feinstone, S. M. & Kaplan, G. Susceptibility of nonprimate cell lines to hepatitis A virus infection. *J Virol* **68**, 6064-6068 (1994). <https://doi.org/10.1128/jvi.68.9.6064-6068.1994>
- 245 Fensterl, V. *et al.* Hepatitis A virus suppresses RIG-I-mediated IRF-3 activation to block induction of beta interferon. *J Virol* **79**, 10968-10977 (2005). <https://doi.org/10.1128/JVI.79.17.10968-10977.2005>
- 246 Paulmann, D. *et al.* Hepatitis A virus protein 2B suppresses beta interferon (IFN) gene transcription by interfering with IFN regulatory factor 3 activation. *J Gen Virol* **89**, 1593-1604 (2008). <https://doi.org/10.1099/vir.0.83521-0>
- 247 Mo, L. *et al.* Hepatitis A virus-induced hsa-miR-146a-5p attenuates IFN- β signaling by targeting adaptor protein TRAF6. *Archives of Virology* **166**, 789-799 (2021). <https://doi.org/10.1007/s00705-021-04952-z>
- 248 Feng, H. *et al.* Hepatovirus 3ABC proteases and evolution of mitochondrial antiviral signaling protein (MAVS). *J Hepatol* **71**, 25-34 (2019). <https://doi.org/10.1016/j.jhep.2019.02.020>
- 249 Hirai-Yuki, A. *et al.* MAVS-dependent host species range and pathogenicity of human hepatitis A virus. *Science* **353**, 1541-1545 (2016). <https://doi.org/10.1126/science.aaf8325>
- 250 Bolen, C. R., Ding, S., Robek, M. D. & Kleinstein, S. H. Dynamic expression profiling of type I and type III interferon-stimulated hepatocytes reveals a stable hierarchy of gene expression. *Hepatology* **59**, 1262-1272 (2014). <https://doi.org/10.1002/hep.26657>

- 251 Choi, Y. S. *et al.* Liver injury in acute hepatitis A is associated with decreased frequency of regulatory T cells caused by Fas-mediated apoptosis. *Gut* **64**, 1303-1313 (2015).
<https://doi.org:10.1136/gutjnl-2013-306213>
- 252 Kim, J. *et al.* Innate-like Cytotoxic Function of Bystander-Activated CD8(+) T Cells Is Associated with Liver Injury in Acute Hepatitis A. *Immunity* **48**, 161-173 e165 (2018).
<https://doi.org:10.1016/j.immuni.2017.11.025>
- 253 Lohmann, V. *et al.* Replication of subgenomic hepatitis C virus RNAs in a hepatoma cell line. *Science* **285**, 110-113 (1999). <https://doi.org:10.1126/science.285.5424.110>
- 254 Yanagi, M., Purcell, R. H., Emerson, S. U. & Bukh, J. Transcripts from a single full-length cDNA clone of hepatitis C virus are infectious when directly transfected into the liver of a chimpanzee. *Proc Natl Acad Sci U S A* **94**, 8738-8743 (1997).
<https://doi.org:10.1073/pnas.94.16.8738>
- 255 Bukh, J. *et al.* Mutations that permit efficient replication of hepatitis C virus RNA in Huh-7 cells prevent productive replication in chimpanzees. *Proc Natl Acad Sci U S A* **99**, 14416-14421 (2002). <https://doi.org:10.1073/pnas.212532699>
- 256 Nakabayashi, H., Taketa, K., Miyano, K., Yamane, T. & Sato, J. Growth of human hepatoma cells lines with differentiated functions in chemically defined medium. *Cancer Res* **42**, 3858-3863 (1982).
- 257 Friebe, P., Boudet, J., Simorre, J. P. & Bartenschlager, R. Kissing-loop interaction in the 3' end of the hepatitis C virus genome essential for RNA replication. *J Virol* **79**, 380-392 (2005).
<https://doi.org:10.1128/jvi.79.1.380-392.2005>
- 258 Blight, K. J., McKeating, J. A. & Rice, C. M. Highly permissive cell lines for subgenomic and genomic hepatitis C virus RNA replication. *J Virol* **76**, 13001-13014 (2002).
<https://doi.org:10.1128/jvi.76.24.13001-13014.2002>
- 259 Sainz, B., Jr., Barretto, N. & Uprichard, S. L. Hepatitis C Virus Infection in Phenotypically Distinct Huh7 Cell Lines. *PLOS ONE* **4**, e6561 (2009).
<https://doi.org:10.1371/journal.pone.0006561>
- 260 Koutsoudakis, G., Herrmann, E., Kallis, S., Bartenschlager, R. & Pietschmann, T. The level of CD81 cell surface expression is a key determinant for productive entry of hepatitis C virus into host cells. *J Virol* **81**, 588-598 (2007). <https://doi.org:10.1128/jvi.01534-06>
- 261 Nicolay, W. *et al.* Characterization of RNA Sensing Pathways in Hepatoma Cell Lines and Primary Human Hepatocytes. *Cells* **10** (2021). <https://doi.org:10.3390/cells10113019>
- 262 Sumpter, R., Jr. *et al.* Regulating intracellular antiviral defense and permissiveness to hepatitis C virus RNA replication through a cellular RNA helicase, RIG-I. *J Virol* **79**, 2689-2699 (2005). <https://doi.org:10.1128/JVI.79.5.2689-2699.2005>
- 263 Binder, M., Kochs, G., Bartenschlager, R. & Lohmann, V. Hepatitis C virus escape from the interferon regulatory factor 3 pathway by a passive and active evasion strategy. *Hepatology* **46**, 1365-1374 (2007). <https://doi.org:10.1002/hep.21829>
- 264 Harak, C. *et al.* Tuning a cellular lipid kinase activity adapts hepatitis C virus to replication in cell culture. *Nat Microbiol* **2**, 16247 (2016). <https://doi.org:10.1038/nmicrobiol.2016.247>
- 265 Kato, T. *et al.* Sequence analysis of hepatitis C virus isolated from a fulminant hepatitis patient. *J Med Virol* **64**, 334-339 (2001). <https://doi.org:10.1002/jmv.1055>
- 266 Date, T. *et al.* Novel cell culture-adapted genotype 2a hepatitis C virus infectious clone. *J Virol* **86**, 10805-10820 (2012). <https://doi.org:10.1128/jvi.07235-11>
- 267 Pietschmann, T. *et al.* Construction and characterization of infectious intragenotypic and intergenotypic hepatitis C virus chimeras. *Proc Natl Acad Sci U S A* **103**, 7408-7413 (2006).
<https://doi.org:10.1073/pnas.0504877103>
- 268 Gondeau, C. *et al.* In vitro infection of primary human hepatocytes by HCV-positive sera: insights on a highly relevant model. *Gut* **63**, 1490-1500 (2014).
<https://doi.org:10.1136/gutjnl-2013-304623>
- 269 Mutz, P. *et al.* HBV Bypasses the Innate Immune Response and Does Not Protect HCV From

- Antiviral Activity of Interferon. *Gastroenterology* **154**, 1791-1804.e1722 (2018).
<https://doi.org:10.1053/j.gastro.2018.01.044>
- 270 Su, S. *et al.* Long-term culture and characterization of patient-derived primary hepatocytes using conditional reprogramming. *Exp Biol Med (Maywood)* **244**, 857-864 (2019).
<https://doi.org:10.1177/1535370219855398>
- 271 Kegel, V. *et al.* Protocol for Isolation of Primary Human Hepatocytes and Corresponding Major Populations of Non-parenchymal Liver Cells. *J Vis Exp*, e53069 (2016).
<https://doi.org:10.3791/53069>
- 272 Israelow, B., Narbus, C. M., Sourisseau, M. & Evans, M. J. HepG2 cells mount an effective antiviral interferon-lambda based innate immune response to hepatitis C virus infection. *Hepatology* **60**, 1170-1179 (2014). <https://doi.org:https://doi.org/10.1002/hep.27227>
- 273 Narbus, C. M. *et al.* HepG2 cells expressing microRNA miR-122 support the entire hepatitis C virus life cycle. *J Virol* **85**, 12087-12092 (2011). <https://doi.org:10.1128/jvi.05843-11>
- 274 De Tomassi, A., Pizzuti, M. & Traboni, C. Hep3B human hepatoma cells support replication of the wild-type and a 5'-end deletion mutant GB virus B replicon. *J Virol* **77**, 11875-11881 (2003). <https://doi.org:10.1128/jvi.77.22.11875-11881.2003>
- 275 Thibault, P. A., Huys, A., Dhillon, P. & Wilson, J. A. MicroRNA-122-dependent and -independent replication of Hepatitis C Virus in Hep3B human hepatoma cells. *Virology* **436**, 179-190 (2013). <https://doi.org:10.1016/j.virol.2012.11.007>
- 276 Luangsay, S. *et al.* Expression and functionality of Toll- and RIG-like receptors in HepaRG cells. *Journal of Hepatology* **63**, 1077-1085 (2015).
<https://doi.org:10.1016/j.jhep.2015.06.022>
- 277 Ikeda, M. *et al.* Human hepatocyte clonal cell lines that support persistent replication of hepatitis C virus. *Virus Res* **56**, 157-167 (1998). [https://doi.org:10.1016/s0168-1702\(98\)00063-x](https://doi.org:10.1016/s0168-1702(98)00063-x)
- 278 Martin, A. *et al.* Chronic hepatitis associated with GB virus B persistence in a tamarin after intrahepatic inoculation of synthetic viral RNA. *Proc Natl Acad Sci U S A* **100**, 9962-9967 (2003). <https://doi.org:10.1073/pnas.1731505100>
- 279 Burbelo Peter, D. *et al.* Serology-Enabled Discovery of Genetically Diverse Hepaciviruses in a New Host. *Journal of Virology* **86**, 6171-6178 (2012). <https://doi.org:10.1128/jvi.00250-12>
- 280 Zou, J., Chang, M., Nie, P. & Secombes, C. J. Origin and evolution of the RIG-I like RNA helicase gene family. *BMC Evolutionary Biology* **9**, 85 (2009). <https://doi.org:10.1186/1471-2148-9-85>
- 281 Vercauteren, K., de Jong, Y. P. & Meuleman, P. Animal models for the study of HCV. *Current Opinion in Virology* **13**, 67-74 (2015).
<https://doi.org:https://doi.org/10.1016/j.coviro.2015.04.009>
- 282 Li, D. *et al.* Altered Glycosylation Patterns Increase Immunogenicity of a Subunit Hepatitis C Virus Vaccine, Inducing Neutralizing Antibodies Which Confer Protection in Mice. *J Virol* **90**, 10486-10498 (2016). <https://doi.org:10.1128/jvi.01462-16>
- 283 Allweiss, L. *et al.* Human liver chimeric mice as a new model of chronic hepatitis E virus infection and preclinical drug evaluation. *Journal of Hepatology* **64**, 1033-1040 (2016).
<https://doi.org:https://doi.org/10.1016/j.jhep.2016.01.011>
- 284 Mercer, D. F. *et al.* Hepatitis C virus replication in mice with chimeric human livers. *Nat Med* **7**, 927-933 (2001). <https://doi.org:10.1038/90968>
- 285 Meuleman, P. *et al.* In vivo evaluation of the cross-genotype neutralizing activity of polyclonal antibodies against hepatitis C virus. *Hepatology* **53**, 755-762 (2011).
<https://doi.org:10.1002/hep.24171>
- 286 Meuleman, P. *et al.* Morphological and biochemical characterization of a human liver in a uPA-SCID mouse chimera. *Hepatology* **41**, 847-856 (2005).
<https://doi.org:10.1002/hep.20657>
- 287 Walters, K. A. *et al.* Host-specific response to HCV infection in the chimeric SCID-beige/Alb-

- uPA mouse model: role of the innate antiviral immune response. *PLoS Pathog* **2**, e59 (2006).
<https://doi.org:10.1371/journal.ppat.0020059>
- 288 Cromeans, T., Fields, H. A. & Sobsey, M. D. Replication Kinetics and Cytopathic Effect of Hepatitis A Virus. *Journal of General Virology* **70**, 2051-2062 (1989).
<https://doi.org:https://doi.org/10.1099/0022-1317-70-8-2051>
- 289 Flehmig, B. Hepatitis A-virus in cell culture: I. Propagation of different hepatitis A-virus isolates in a fetal rhesus monkey kidney cell line (Frhk-4). *Medical Microbiology and Immunology* **168**, 239-248 (1980). <https://doi.org:10.1007/BF02121807>
- 290 Flehmig, B., Vallbracht, A. & Wurster, G. Hepatitis A virus in cell culture. III. Propagation of hepatitis A virus in human embryo kidney cells and human embryo fibroblast strains. *Med Microbiol Immunol* **170**, 83-89 (1981). <https://doi.org:10.1007/bf02122672>
- 291 Konduru, K. & Kaplan, G. G. Stable growth of wild-type hepatitis A virus in cell culture. *J Virol* **80**, 1352-1360 (2006). <https://doi.org:10.1128/jvi.80.3.1352-1360.2006>
- 292 Gauss-Müller, V. & Kusov, Y. Y. Replication of a hepatitis A virus replicon detected by genetic recombination in vivo. *J Gen Virol* **83**, 2183-2192 (2002). <https://doi.org:10.1099/0022-1317-83-9-2183>
- 293 Yi, M. & Lemon, S. M. Replication of subgenomic hepatitis A virus RNAs expressing firefly luciferase is enhanced by mutations associated with adaptation of virus to growth in cultured cells. *J Virol* **76**, 1171-1180 (2002). <https://doi.org:10.1128/jvi.76.3.1171-1180.2002>
- 294 Kozak, R. A. *et al.* Development and Evaluation of a Molecular Hepatitis A Virus Assay for Serum and Stool Specimens. *Viruses* **14**, 159 (2022).
- 295 Shin, E. C. & Jeong, S. H. Natural History, Clinical Manifestations, and Pathogenesis of Hepatitis A. *Cold Spring Harb Perspect Med* **8** (2018).
<https://doi.org:10.1101/cshperspect.a031708>
- 296 Ross, B. C., Anderson, B. N., Edwards, P. C. & Gust, I. D. Nucleotide Sequence of High-passage Hepatitis A Virus Strain HM175: Comparison with Wild-type and Cell Culture-adapted Strains. *Journal of General Virology* **70**, 2805-2810 (1989).
<https://doi.org:https://doi.org/10.1099/0022-1317-70-10-2805>
- 297 Brown, E. A., Day, S. P., Jansen, R. W. & Lemon, S. M. The 5' nontranslated region of hepatitis A virus RNA: secondary structure and elements required for translation in vitro. *J Virol* **65**, 5828-5838 (1991). <https://doi.org:10.1128/jvi.65.11.5828-5838.1991>
- 298 Sasaki-Tanaka, R. *et al.* Masitinib Inhibits Hepatitis A Virus Replication. *Int J Mol Sci* **24** (2023). <https://doi.org:10.3390/ijms24119708>
- 299 Win, N. N. *et al.* Inhibitory effect of Japanese rice-koji miso extracts on hepatitis A virus replication in association with the elevation of glucose-regulated protein 78 expression. *Int J Med Sci* **15**, 1153-1159 (2018). <https://doi.org:10.7150/ijms.27489>
- 300 Park, E., Yoo, Y., Park, S., Choi, C. & Yoon, Y. siRNAs to Knockdown Antiviral Chemokine-related Genes in FRhK-4 Cells. *Journal of Food Protection* **86**, 100076 (2023).
<https://doi.org:https://doi.org/10.1016/j.jfp.2023.100076>
- 301 Sakuma, R., Mael, A. A. & Ikeda, Y. Alpha interferon enhances TRIM5alpha-mediated antiviral activities in human and rhesus monkey cells. *J Virol* **81**, 10201-10206 (2007).
<https://doi.org:10.1128/jvi.00419-07>
- 302 Nosaka, T. *et al.* Regulatory function of interferon-inducible 44-like for hepatitis B virus covalently closed circular DNA in primary human hepatocytes. *Hepatology Research* **52**, 141-152 (2022). <https://doi.org:https://doi.org/10.1111/hepr.13722>
- 303 Purcell, R. H. & Emerson, S. U. Animal models of hepatitis A and E. *Ilar j* **42**, 161-177 (2001).
<https://doi.org:10.1093/ilar.42.2.161>
- 304 Song, Y. J. *et al.* Experimental evidence of hepatitis A virus infection in pigs. *J Med Virol* **88**, 631-638 (2016). <https://doi.org:10.1002/jmv.24386>
- 305 Kayesh, M. E. H., Sanada, T., Kohara, M. & Tsukiyama-Kohara, K. Tree Shrew as an Emerging Small Animal Model for Human Viral Infection: A Recent Overview. *Viruses* **13** (2021).

- <https://doi.org:10.3390/v13081641>
- 306 Pang, D. To HAV or not to HAV: Novel hepatitis A virus (HAV) infection in a chimeric mouse model. (2013).
- 307 Perrin-Cocon, L. *et al.* Th1 disabled function in response to TLR4 stimulation of monocyte-derived DC from patients chronically-infected by hepatitis C virus. *PLoS One* **3**, e2260 (2008).
<https://doi.org:10.1371/journal.pone.0002260>
- 308 Zhou, Y. *et al.* Dominance of the CD4(+) T helper cell response during acute resolving hepatitis A virus infection. *J Exp Med* **209**, 1481-1492 (2012).
<https://doi.org:10.1084/jem.20111906>
- 309 Misumi, I. *et al.* T cells protect against hepatitis A virus infection and limit infection-induced liver injury. *J Hepatol* **75**, 1323-1334 (2021). <https://doi.org:10.1016/j.jhep.2021.07.019>
- 310 van den Hoff, M. J., Moorman, A. F. & Lamers, W. H. Electroporation in 'intracellular' buffer increases cell survival. *Nucleic Acids Res* **20**, 2902 (1992).
<https://doi.org:10.1093/nar/20.11.2902>
- 311 Backes, P. *et al.* Role of Annexin A2 in the Production of Infectious Hepatitis C Virus Particles. *Journal of Virology* **84**, 5775-5789 (2010). <https://doi.org:doi:10.1128/JVI.02343-09>
- 312 Wallenstein, E. J., Barminko, J., Schloss, R. S. & Yarmush, M. L. Serum starvation improves transient transfection efficiency in differentiating embryonic stem cells. *Biotechnol Prog* **26**, 1714-1723 (2010). <https://doi.org:10.1002/btpr.472>
- 313 Lohmann, V., Korner, F., Dobierzewska, A. & Bartenschlager, R. Mutations in hepatitis C virus RNAs conferring cell culture adaptation. *J Virol* **75**, 1437-1449 (2001).
<https://doi.org:10.1128/JVI.75.3.1437-1449.2001>
- 314 Rosenberg, A. H. *et al.* Vectors for selective expression of cloned DNAs by T7 RNA polymerase. *Gene* **56**, 125-135 (1987). [https://doi.org:10.1016/0378-1119\(87\)90165-x](https://doi.org:10.1016/0378-1119(87)90165-x)
- 315 Lohmann, V., Hoffmann, S., Herian, U., Penin, F. & Bartenschlager, R. Viral and cellular determinants of hepatitis C virus RNA replication in cell culture. *J Virol* **77**, 3007-3019 (2003).
<https://doi.org:10.1128/jvi.77.5.3007-3019.2003>
- 316 Jumper, J. *et al.* Highly accurate protein structure prediction with AlphaFold. *Nature* **596**, 583-589 (2021). <https://doi.org:10.1038/s41586-021-03819-2>
- 317 Varadi, M. *et al.* AlphaFold Protein Structure Database: massively expanding the structural coverage of protein-sequence space with high-accuracy models. *Nucleic Acids Research* **50**, D439-D444 (2021). <https://doi.org:10.1093/nar/gkab1061>
- 318 Mirdita, M. *et al.* ColabFold: making protein folding accessible to all. *Nature Methods* **19**, 679-682 (2022). <https://doi.org:10.1038/s41592-022-01488-1>
- 319 Hajarizadeh, B., Grebely, J. & Dore, G. J. Epidemiology and natural history of HCV infection. *Nature Reviews Gastroenterology & Hepatology* **10**, 553-562 (2013).
<https://doi.org:10.1038/nrgastro.2013.107>
- 320 Blight, K. J., McKeating, J. A. & Rice, C. M. Highly Permissive Cell Lines for Subgenomic and Genomic Hepatitis C Virus RNA Replication. *Journal of Virology* **76**, 13001-13014 (2002).
<https://doi.org:doi:10.1128/jvi.76.24.13001-13014.2002>
- 321 Li, K. *et al.* Activation of chemokine and inflammatory cytokine response in hepatitis C virus-infected hepatocytes depends on Toll-like receptor 3 sensing of hepatitis C virus double-stranded RNA intermediates. *Hepatology* **55**, 666-675 (2012).
<https://doi.org:10.1002/hep.24763>
- 322 Tabata, K., Neufeldt, C. J. & Bartenschlager, R. Hepatitis C Virus Replication. *Cold Spring Harb Perspect Med* **10** (2020). <https://doi.org:10.1101/cshperspect.a037093>
- 323 Uhlen, M. *et al.* Proteomics. Tissue-based map of the human proteome. *Science* **347**, 1260419 (2015). <https://doi.org:10.1126/science.1260419>
- 324 Zambrowicz, B. P. *et al.* Disruption of overlapping transcripts in the ROSA beta geo 26 gene trap strain leads to widespread expression of beta-galactosidase in mouse embryos and hematopoietic cells. *Proc Natl Acad Sci U S A* **94**, 3789-3794 (1997).

- <https://doi.org:10.1073/pnas.94.8.3789>
- 325 Neufeldt, C. J. *et al.* SARS-CoV-2 infection induces a pro-inflammatory cytokine response through cGAS-STING and NF- κ B. *Commun Biol* **5**, 45 (2022). <https://doi.org:10.1038/s42003-021-02983-5>
- 326 Hopp, T. P. *et al.* A Short Polypeptide Marker Sequence Useful for Recombinant Protein Identification and Purification. *Bio/Technology* **6**, 1204-1210 (1988). <https://doi.org:10.1038/nbt1088-1204>
- 327 Kim, S. *et al.* PubChem 2023 update. *Nucleic Acids Research* **51**, D1373-D1380 (2022). <https://doi.org:10.1093/nar/gkac956>
- 328 Liang, Y. *et al.* Hepatitis C virus NS4B induces the degradation of TRIF to inhibit TLR3-mediated interferon signaling pathway. *PLoS Pathog* **14**, e1007075 (2018). <https://doi.org:10.1371/journal.ppat.1007075>
- 329 Wang, N. *et al.* Toll-like receptor 3 mediates establishment of an antiviral state against hepatitis C virus in hepatoma cells. *J Virol* **83**, 9824-9834 (2009). <https://doi.org:10.1128/jvi.01125-09>
- 330 Schaefer, M., Schänzle, G., Bischoff, D. & Süßmuth, R. D. Upcyte Human Hepatocytes: a Potent In Vitro Tool for the Prediction of Hepatic Clearance of Metabolically Stable Compounds. *Drug Metab Dispos* **44**, 435-444 (2016). <https://doi.org:10.1124/dmd.115.067348>
- 331 Ikeda, M. *et al.* Analysis of the cell tropism of HCV by using in vitro HCV-infected human lymphocytes and hepatocytes. *J Hepatol* **27**, 445-454 (1997). [https://doi.org:10.1016/s0168-8278\(97\)80347-9](https://doi.org:10.1016/s0168-8278(97)80347-9)
- 332 Schult, P. *et al.* microRNA-122 amplifies hepatitis C virus translation by shaping the structure of the internal ribosomal entry site. *Nature Communications* **9**, 2613 (2018). <https://doi.org:10.1038/s41467-018-05053-3>
- 333 Sheahan, T. *et al.* Interferon lambda alleles predict innate antiviral immune responses and hepatitis C virus permissiveness. *Cell Host Microbe* **15**, 190-202 (2014). <https://doi.org:10.1016/j.chom.2014.01.007>
- 334 Brownell, J. *et al.* Independent, parallel pathways to CXCL10 induction in HCV-infected hepatocytes. *J Hepatol* **59**, 701-708 (2013). <https://doi.org:10.1016/j.jhep.2013.06.001>
- 335 Dao Thi, V. L. *et al.* Stem cell-derived polarized hepatocytes. *Nat Commun* **11**, 1677 (2020). <https://doi.org:10.1038/s41467-020-15337-2>
- 336 Bruns, A. M., Leser, G. P., Lamb, R. A. & Horvath, C. M. The innate immune sensor LGP2 activates antiviral signaling by regulating MDA5-RNA interaction and filament assembly. *Mol Cell* **55**, 771-781 (2014). <https://doi.org:10.1016/j.molcel.2014.07.003>
- 337 Gillich, N., Zhang, Z., Binder, M., Urban, S. & Bartenschlager, R. Effect of variants in LGP2 on MDA5-mediated activation of interferon response and suppression of hepatitis D virus replication. *J Hepatol* (2022). <https://doi.org:10.1016/j.jhep.2022.08.041>
- 338 Donato, M. T., Tolosa, L. & Gómez-Lechón, M. J. Culture and Functional Characterization of Human Hepatoma HepG2 Cells. *Methods Mol Biol* **1250**, 77-93 (2015). https://doi.org:10.1007/978-1-4939-2074-7_5
- 339 Parent, R., Marion, M. J., Furio, L., Trépo, C. & Petit, M. A. Origin and characterization of a human bipotent liver progenitor cell line. *Gastroenterology* **126**, 1147-1156 (2004). <https://doi.org:10.1053/j.gastro.2004.01.002>
- 340 Fukuhara, T. *et al.* Intracellular delivery of serum-derived hepatitis C virus. *Microbes Infect* **13**, 405-412 (2011). <https://doi.org:10.1016/j.micinf.2011.01.005>
- 341 Heuss, C. *et al.* A Hepatitis C virus genotype 1b post-transplant isolate with high replication efficiency in cell culture and its adaptation to infectious virus production in vitro and in vivo. *PLoS Pathog* **18**, e1010472 (2022). <https://doi.org:10.1371/journal.ppat.1010472>
- 342 Colasanti, O. *et al.* Comparison of HAV and HCV infections *in vivo* and *in vitro* reveals distinct patterns of innate immune evasion and activation.

- Journal of Hepatology* <https://doi.org:10.1016/j.jhep.2023.04.023>
- 343 Wang, B. *et al.* Toll-like receptor activated human and murine hepatic stellate cells are potent regulators of hepatitis C virus replication. *J Hepatol* **51**, 1037-1045 (2009).
<https://doi.org:10.1016/j.jhep.2009.06.020>
- 344 Duluc, D. *et al.* PolyI:C plus IL-2 or IL-12 induce IFN-gamma production by human NK cells via autocrine IFN-beta. *Eur J Immunol* **39**, 2877-2884 (2009).
<https://doi.org:10.1002/eji.200838610>
- 345 Wu, J. *et al.* Toll-like receptor-mediated control of HBV replication by nonparenchymal liver cells in mice. *Hepatology* **46**, 1769-1778 (2007). <https://doi.org:10.1002/hep.21897>
- 346 Fischer, J. *et al.* Polymorphisms in the Toll-like receptor 3 (TLR3) gene are associated with the natural course of hepatitis B virus infection in Caucasian population. *Scientific Reports* **8**, 12737 (2018). <https://doi.org:10.1038/s41598-018-31065-6>
- 347 Zhang, B. *et al.* TLR3 Activation of Hepatic Stellate Cell Line Suppresses HBV Replication in HepG2 Cells. *Front Immunol* **9**, 2921 (2018). <https://doi.org:10.3389/fimmu.2018.02921>
- 348 Mendenhall, M., Wong, M. H., Skirpstunas, R., Morrey, J. D. & Gowen, B. B. Punta Toro virus (Bunyaviridae, Phlebovirus) infection in mice: strain differences in pathogenesis and host interferon response. *Virology* **395**, 143-151 (2009).
<https://doi.org:10.1016/j.virol.2009.09.003>
- 349 Abe, Y. *et al.* The toll-like receptor 3-mediated antiviral response is important for protection against poliovirus infection in poliovirus receptor transgenic mice. *J Virol* **86**, 185-194 (2012).
<https://doi.org:10.1128/jvi.05245-11>
- 350 Gowen, B. B. *et al.* TLR3 deletion limits mortality and disease severity due to Phlebovirus infection. *J Immunol* **177**, 6301-6307 (2006). <https://doi.org:10.4049/jimmunol.177.9.6301>
- 351 Lang, K. S. *et al.* Immunoprivileged status of the liver is controlled by Toll-like receptor 3 signaling. *J Clin Invest* **116**, 2456-2463 (2006). <https://doi.org:10.1172/jci28349>
- 352 Siegl, G. & Weitz, M. Pathogenesis of hepatitis A: persistent viral infection as basis of an acute disease? *Microbial Pathogenesis* **14**, 1-8 (1993).
<https://doi.org:https://doi.org/10.1006/mpat.1993.1001>
- 353 Uhlén, M. *et al.* Tissue-based map of the human proteome. *Science* **347**, 1260419 (2015).
<https://doi.org:doi:10.1126/science.1260419>
- 354 Sun, L. *et al.* Viral protease cleavage of MAVS in genetically modified mice with hepatitis A virus infection. *J Hepatol* (2022). <https://doi.org:10.1016/j.jhep.2022.09.013>
- 355 Mukherjee, A. *et al.* The coxsackievirus B 3C protease cleaves MAVS and TRIF to attenuate host type I interferon and apoptotic signaling. *PLoS Pathog* **7**, e1001311 (2011).
<https://doi.org:10.1371/journal.ppat.1001311>
- 356 Cortez, K. J. *et al.* Infections Caused by *Scedosporium* spp. *Clinical Microbiology Reviews* **21**, 157-197 (2008). <https://doi.org:doi:10.1128/cmr.00039-07>
- 357 Men, Y. *et al.* RHDV 3C protein antagonizes type I interferon signaling by cleaving interferon promoter stimulated 1 protein. *Virus Genes* **59**, 215-222 (2023).
<https://doi.org:10.1007/s11262-022-01958-w>
- 358 Du, Y. *et al.* 3Cpro of foot-and-mouth disease virus antagonizes the interferon signaling pathway by blocking STAT1/STAT2 nuclear translocation. *J Virol* **88**, 4908-4920 (2014).
<https://doi.org:10.1128/JVI.03668-13>
- 359 Baronti, C., Sire, J., de Lamballerie, X. & Quérat, G. Nonstructural NS1 proteins of several mosquito-borne Flavivirus do not inhibit TLR3 signaling. *Virology* **404**, 319-330 (2010).
<https://doi.org:10.1016/j.virol.2010.05.020>
- 360 Ferreon, J. C., Ferreon, A. C., Li, K. & Lemon, S. M. Molecular determinants of TRIF proteolysis mediated by the hepatitis C virus NS3/4A protease. *J Biol Chem* **280**, 20483-20492 (2005). <https://doi.org:10.1074/jbc.M500422200>
- 361 Riebeling, T., Kundendorf, U. & Krautwald, S. The role of RHIM in necroptosis. *Biochem Soc Trans* **50**, 1197-1205 (2022). <https://doi.org:10.1042/bst20220535>

- 362 Komissarov, A. A. *et al.* Individual Expression of Hepatitis A Virus 3C Protease Induces Ferroptosis in Human Cells In Vitro. *Int J Mol Sci* **22** (2021).
<https://doi.org/10.3390/ijms22157906>
- 363 Shubin, A. V. *et al.* Protease 3C of hepatitis A virus induces vacuolization of lysosomal/endosomal organelles and caspase-independent cell death. *BMC Cell Biology* **16**, 4 (2015). <https://doi.org/10.1186/s12860-015-0050-z>
- 364 Fujiwara, K. *et al.* Association between severity of type A hepatitis and nucleotide variations in the 5' non-translated region of hepatitis A virus RNA: strains from fulminant hepatitis have fewer nucleotide substitutions. *Gut* **51**, 82 (2002). <https://doi.org/10.1136/gut.51.1.82>
- 365 Ríos-Ocampo, W. A. *et al.* Hepatitis C virus core or NS3/4A protein expression preconditions hepatocytes against oxidative stress and endoplasmic reticulum stress. *Redox Rep* **24**, 17-26 (2019). <https://doi.org/10.1080/13510002.2019.1596431>
- 366 Seth, R. B., Sun, L., Ea, C.-K. & Chen, Z. J. Identification and Characterization of MAVS, a Mitochondrial Antiviral Signaling Protein that Activates NF- κ B and IRF3. *Cell* **122**, 669-682 (2005). <https://doi.org/10.1016/j.cell.2005.08.012>
- 367 Emerson, S. U. *et al.* Identification of VP1/2A and 2C as Virulence Genes of Hepatitis A Virus and Demonstration of Genetic Instability of 2C. *Journal of Virology* **76**, 8551-8559 (2002). <https://doi.org/doi:10.1128/jvi.76.17.8551-8559.2002>
- 368 Beard, M. R., Cohen, L., Lemon, S. M. & Martin, A. Characterization of Recombinant Hepatitis A Virus Genomes Containing Exogenous Sequences at the 2A/2B Junction. *Journal of Virology* **75**, 1414-1426 (2001). <https://doi.org/doi:10.1128/jvi.75.3.1414-1426.2001>
- 369 Rachow, A., Gauss-Müller, V. & Probst, C. Homogenous Hepatitis A Virus Particles: PROTEOLYTIC RELEASE OF THE ASSEMBLY SIGNAL 2A FROM PROCAPSIDS BY FACTOR Xa *. *Journal of Biological Chemistry* **278**, 29744-29751 (2003).
<https://doi.org/10.1074/jbc.M300454200>
- 370 Devhare, P. B., Desai, S. & Lole, K. S. Innate immune responses in human hepatocyte-derived cell lines alter genotype 1 hepatitis E virus replication efficiencies. *Sci Rep* **6**, 26827 (2016).
<https://doi.org/10.1038/srep26827>
- 371 Wei, D. *et al.* The Molecular Chaperone GRP78 Contributes to Toll-like Receptor 3-mediated Innate Immune Response to Hepatitis C Virus in Hepatocytes*. *Journal of Biological Chemistry* **291**, 12294-12309 (2016).
<https://doi.org/https://doi.org/10.1074/jbc.M115.711598>
- 372 Jopling, C. Liver-specific microRNA-122: Biogenesis and function. *RNA Biol* **9**, 137-142 (2012).
<https://doi.org/10.4161/rna.18827>
- 373 Zheng, W., Chang, R., Luo, Q., Liu, G. & Xu, T. The long noncoding RNA MIR122HG is a precursor for miR-122-5p and negatively regulates the TAK1-induced innate immune response in teleost fish. *Journal of Biological Chemistry* **298** (2022).
<https://doi.org/10.1016/j.jbc.2022.101773>
- 374 Shi, L. *et al.* The contribution of miR-122 to the innate immunity by regulating toll-like receptor 4 in hepatoma cells. *BMC Gastroenterology* **19**, 130 (2019).
<https://doi.org/10.1186/s12876-019-1048-3>
- 375 Luo, C. *et al.* GRP78 Promotes Hepatocellular Carcinoma proliferation by increasing FAT10 expression through the NF- κ B pathway. *Exp Cell Res* **365**, 1-11 (2018).
<https://doi.org/10.1016/j.yexcr.2018.02.007>
- 376 Podevin, P. *et al.* Production of Infectious Hepatitis C Virus in Primary Cultures of Human Adult Hepatocytes. *Gastroenterology* **139**, 1355-1364.e1356 (2010).
<https://doi.org/10.1053/j.gastro.2010.06.058>
- 377 Snooks, M. J. *et al.* Vectorial Entry and Release of Hepatitis A Virus in Polarized Human Hepatocytes. *Journal of Virology* **82**, 8733-8742 (2008).
<https://doi.org/doi:10.1128/jvi.00219-08>
- 378 Silberstein, E., Konduru, K. & Kaplan, G. G. The interaction of hepatitis A virus (HAV) with

- soluble forms of its cellular receptor 1 (HAVCR1) share the physiological requirements of infectivity in cell culture. *Virology Journal* **6**, 175 (2009). <https://doi.org:10.1186/1743-422X-6-175>
- 379 Das, A., Maury, W. & Lemon, S. M. TIM1 (HAVCR1): an Essential “Receptor” or an “Accessory Attachment Factor” for Hepatitis A Virus? *Journal of Virology* **93**, 10.1128/jvi.01793-01718 (2019). <https://doi.org:doi:10.1128/jvi.01793-18>
- 380 Misumi, I. *et al.* Iminosugar Glucosidase Inhibitors Reduce Hepatic Inflammation in Hepatitis A Virus-Infected Ifnar1(-/-) Mice. *J Virol* **95**, e0005821 (2021). <https://doi.org:10.1128/jvi.00058-21>
- 381 Yamane, D. *et al.* Basal expression of interferon regulatory factor 1 drives intrinsic hepatocyte resistance to multiple RNA viruses. *Nat Microbiol* **4**, 1096-1104 (2019). <https://doi.org:10.1038/s41564-019-0425-6>
- 382 Liu, S. *et al.* Tight junction proteins claudin-1 and occludin control hepatitis C virus entry and are downregulated during infection to prevent superinfection. *J Virol* **83**, 2011-2014 (2009). <https://doi.org:10.1128/jvi.01888-08>
- 383 Ploss, A. *et al.* Human occludin is a hepatitis C virus entry factor required for infection of mouse cells. *Nature* **457**, 882-886 (2009). <https://doi.org:10.1038/nature07684>
- 384 Jopling, C. L., Yi, M., Lancaster, A. M., Lemon, S. M. & Sarnow, P. Modulation of hepatitis C virus RNA abundance by a liver-specific MicroRNA. *Science* **309**, 1577-1581 (2005). <https://doi.org:10.1126/science.1113329>
- 385 Kunden, R. D., Ghezelbash, S., Khan, J. Q. & Wilson, J. A. Location specific annealing of miR-122 and other small RNAs defines an Hepatitis C Virus 5' UTR regulatory element with distinct impacts on virus translation and genome stability. *Nucleic Acids Res* **48**, 9235-9249 (2020). <https://doi.org:10.1093/nar/gkaa664>
- 386 Kambara, H. *et al.* Establishment of a Novel Permissive Cell Line for the Propagation of Hepatitis C Virus by Expression of MicroRNA miR122. *Journal of Virology* **86**, 1382-1393 (2012). <https://doi.org:doi:10.1128/jvi.06242-11>
- 387 Harak, C. & Lohmann, V. Ultrastructure of the replication sites of positive-strand RNA viruses. *Virology* **479-480**, 418-433 (2015). <https://doi.org:https://doi.org/10.1016/j.virol.2015.02.029>
- 388 Dales, S., Eggers, H. J., Tamm, I. & Palade, G. E. Electron microscopic study of the formation of poliovirus. *Virology* **26**, 379-389 (1965).
- 389 Bruni, D. *et al.* Viral entry route determines how human plasmacytoid dendritic cells produce type I interferons. *Science Signaling* **8**, ra25-ra25 (2015). <https://doi.org:doi:10.1126/scisignal.aaa1552>
- 390 Monson, E. A., Crosse, K. M., Das, M. & Helbig, K. J. Lipid droplet density alters the early innate immune response to viral infection. *PLOS ONE* **13**, e0190597 (2018). <https://doi.org:10.1371/journal.pone.0190597>
- 391 Roli, M. & Curt, M. H. Sendai Virus Infection Induces Expression of Novel RNAs in Human Cells. *bioRxiv*, 451369 (2018). <https://doi.org:10.1101/451369>
- 392 Runge, S. *et al.* In vivo ligands of MDA5 and RIG-I in measles virus-infected cells. *PLoS Pathog* **10**, e1004081 (2014). <https://doi.org:10.1371/journal.ppat.1004081>
- 393 Jouan, L. *et al.* Distinct antiviral signaling pathways in primary human hepatocytes and their differential disruption by HCV NS3 protease. *Journal of Hepatology* **52**, 167-175 (2010). <https://doi.org:10.1016/j.jhep.2009.11.011>
- 394 Sales Conniff, A. *et al.* Poly(I:C) transfection induces a pro-inflammatory cascade in murine mammary carcinoma and fibrosarcoma cells. *RNA Biol* **19**, 841-851 (2022). <https://doi.org:10.1080/15476286.2022.2084861>
- 395 Grunvogel, O. *et al.* DDX60L Is an Interferon-Stimulated Gene Product Restricting Hepatitis C Virus Replication in Cell Culture. *J Virol* **89**, 10548-10568 (2015). <https://doi.org:10.1128/JVI.01297-15>

- 396 Flint, E., Racaniello, Skalka. Principles of Virology. **II**, 140 (2009).
- 397 Schulte, I. *et al.* Characterization of CD8+ T-cell response in acute and resolved hepatitis A virus infection. *J Hepatol* **54**, 201-208 (2011). <https://doi.org:10.1016/j.jhep.2010.07.010>
- 398 Kervecan, J. & Chakrabarti, L. A. Role of CD4+ T Cells in the Control of Viral Infections: Recent Advances and Open Questions. *Int J Mol Sci* **22** (2021). <https://doi.org:10.3390/ijms22020523>
- 399 Wang, M. & Feng, Z. Mechanisms of Hepatocellular Injury in Hepatitis A. *Viruses* **13** (2021). <https://doi.org:10.3390/v13050861>
- 400 Belkaya, S. *et al.* Inherited IL-18BP deficiency in human fulminant viral hepatitis. *J Exp Med* **216**, 1777-1790 (2019). <https://doi.org:10.1084/jem.20190669>
- 401 Althaus, C. L., Ganusov, V. V. & De Boer, R. J. Dynamics of CD8+ T Cell Responses during Acute and Chronic Lymphocytic Choriomeningitis Virus Infection1. *The Journal of Immunology* **179**, 2944-2951 (2007). <https://doi.org:10.4049/jimmunol.179.5.2944>
- 402 Rauch, A. *et al.* Genetic variation in IL28B is associated with chronic hepatitis C and treatment failure: a genome-wide association study. *Gastroenterology* **138**, 1338-1345, 1345.e1331-1337 (2010). <https://doi.org:10.1053/j.gastro.2009.12.056>
- 403 Duggal, P. *et al.* Genome-wide association study of spontaneous resolution of hepatitis C virus infection: data from multiple cohorts. *Ann Intern Med* **158**, 235-245 (2013). <https://doi.org:10.7326/0003-4819-158-4-201302190-00003>
- 404 Antaki, N. *et al.* IL28B polymorphisms predict response to therapy among chronic hepatitis C patients with HCV genotype 4. *J Viral Hepat* **20**, 59-64 (2013). <https://doi.org:10.1111/j.1365-2893.2012.01621.x>
- 405 Tanaka, Y. *et al.* Genome-wide association of IL28B with response to pegylated interferon-alpha and ribavirin therapy for chronic hepatitis C. *Nat Genet* **41**, 1105-1109 (2009). <https://doi.org:10.1038/ng.449>
- 406 McFarland, A. P. *et al.* The favorable IFNL3 genotype escapes mRNA decay mediated by AU-rich elements and hepatitis C virus-induced microRNAs. *Nat Immunol* **15**, 72-79 (2014). <https://doi.org:10.1038/ni.2758>
- 407 Prokunina-Olsson, L. *et al.* A variant upstream of IFNL3 (IL28B) creating a new interferon gene IFNL4 is associated with impaired clearance of hepatitis C virus. *Nat Genet* **45**, 164-171 (2013). <https://doi.org:10.1038/ng.2521>
- 408 Griffiths, S. J. *et al.* A systematic analysis of host factors reveals a Med23-interferon- λ regulatory axis against herpes simplex virus type 1 replication. *PLoS Pathog* **9**, e1003514 (2013). <https://doi.org:10.1371/journal.ppat.1003514>
- 409 Bibert, S. *et al.* The IFNL3/4 Δ G variant increases susceptibility to cytomegalovirus retinitis among HIV-infected patients. *Aids* **28**, 1885-1889 (2014). <https://doi.org:10.1097/qad.0000000000000379>
- 410 Machmach, K. *et al.* IL28B single-nucleotide polymorphism rs12979860 is associated with spontaneous HIV control in white subjects. *J Infect Dis* **207**, 651-655 (2013). <https://doi.org:10.1093/infdis/jis717>
- 411 Chinnaswamy, S. Gene-disease association with human IFNL locus polymorphisms extends beyond hepatitis C virus infections. *Genes Immun* **17**, 265-275 (2016). <https://doi.org:10.1038/gene.2016.24>
- 412 Assil, S. *et al.* Plasmacytoid Dendritic Cells and Infected Cells Form an Interferogenic Synapse Required for Antiviral Responses. *Cell Host Microbe* **25**, 730-745.e736 (2019). <https://doi.org:10.1016/j.chom.2019.03.005>
- 413 Dreux, M. *et al.* Short-range exosomal transfer of viral RNA from infected cells to plasmacytoid dendritic cells triggers innate immunity. *Cell Host Microbe* **12**, 558-570 (2012). <https://doi.org:10.1016/j.chom.2012.08.010>
- 414 Klöss, V. *et al.* Interaction and Mutual Activation of Different Innate Immune Cells Is Necessary to Kill and Clear Hepatitis C Virus-Infected Cells. *Front Immunol* **8**, 1238 (2017).

- <https://doi.org:10.3389/fimmu.2017.01238>
- 415 Zhou, Y. *et al.* Toll-like receptor 3-activated macrophages confer anti-HCV activity to hepatocytes through exosomes. *Faseb j* **30**, 4132-4140 (2016).
<https://doi.org:10.1096/fj.201600696R>
- 416 Wang, Y., Li, J., Wang, X., Sang, M. & Ho, W. Hepatic stellate cells, liver innate immunity, and hepatitis C virus. *J Gastroenterol Hepatol* **28 Suppl 1**, 112-115 (2013).
<https://doi.org:10.1111/jgh.12023>
- 417 Harari, D. *et al.* Bridging the species divide: transgenic mice humanized for type-I interferon response. *PLoS One* **9**, e84259 (2014). <https://doi.org:10.1371/journal.pone.0084259>
- 418 Forni, D. *et al.* Evolutionary Analysis Provides Insight Into the Origin and Adaptation of HCV. *Front Microbiol* **9**, 854 (2018). <https://doi.org:10.3389/fmicb.2018.00854>
- 419 Drexler, J. F. *et al.* Evolutionary origins of hepatitis A virus in small mammals. *Proceedings of the National Academy of Sciences* **112**, 15190-15195 (2015).
<https://doi.org:doi:10.1073/pnas.1516992112>
- 420 Dorner, M. *et al.* A genetically humanized mouse model for hepatitis C virus infection. *Nature* **474**, 208-211 (2011). <https://doi.org:10.1038/nature10168>
- 421 Kapoor, A. *et al.* Identification of rodent homologs of hepatitis C virus and pegiviruses. *mBio* **4**, e00216-00213 (2013). <https://doi.org:10.1128/mBio.00216-13>
- 422 Ghosh, S. *et al.* Enteric viruses replicate in salivary glands and infect through saliva. *Nature* **607**, 345-350 (2022). <https://doi.org:10.1038/s41586-022-04895-8>